

**Whey protein / polysaccharide coacervates:
structure and dynamics**

Fanny Weinbreck

Whey protein / gum arabic coacervates: structure and dynamics

Thesis Utrecht University, The Netherlands

Photography and cover design: Cornelia van Dijk - Heuker of Hoek

Printing house: Ponsen & Looijen, Wageningen

Whey protein / polysaccharide coacervates:
structure and dynamics

Wei-eiwit / polysaccharide coacervaten:
structuur en dynamica

(met een samenvatting in het Nederlands)

Coacervats de protéines du lactosérum / polysaccharide:
structure et dynamique

(avec un résumé en français)

Proefschrift ter verkrijging van de graad van doctor

aan de Universiteit Utrecht

op gezag van de Rector Magnificus, Prof.dr. W.H. Gispen,

ingevolge het besluit van het College voor Promoties

in het openbaar te verdedigen

op vrijdag 7 mei 2004 des middags te 2.30 uur

door

Fanny Chantal Jacqueline Weinbreck

geboren in Saint-Quentin (Frankrijk) op 22 februari 1977



Universiteit Utrecht

Supervisor: Prof. Dr. C. G. de Kruif

Physical and Colloid Chemistry, Utrecht University, The Netherlands

NIZO food research, Ede, The Netherlands



This doctoral dissertation was produced with the financial support of Friesland Coberco Dairy Foods (FCDF), Deventer and NIZO food research, Ede.

ISBN 90-393-3672-5

On fait la science avec des faits, comme on fait une maison avec des pierres: mais une accumulation de faits n'est pas plus une science qu'un tas de pierres n'est une maison.
[Henri Poincaré]

Learning is a treasure that will follow its owner everywhere.
[Chinese Proverb]

To Rui Paulo

TABLE OF CONTENTS

Table of contents		VII
List of abbreviations		IX
Chapter 1	General introduction	1
Chapter 2	Complex coacervation of whey protein and gum arabic	27
Chapter 3	Complex formation of whey protein / exocellular polysaccharide EPS B40	53
Chapter 4	Complexation of whey protein with carrageenan	73
Chapter 5	Composition and structure of whey protein / gum arabic coacervates	87
Chapter 6	Rheological properties of whey protein / gum arabic coacervates	109
Chapter 7	Diffusivity of whey protein and gum arabic in their coacervates	127
Chapter 8	Microencapsulation of oils using whey protein / gum arabic coacervates	149
References		165
Summary		175
Samenvatting		181
Résumé		187
Acknowledgements		193
Curriculum vitae		196
List of publications		197

LIST OF ABBREVIATIONS

BSA	bovine serum albumin
CG	carrageenan
CMC	carboxymethylcellulose
Cp	total biopolymer concentration
CSLM	confocal scanning laser microscopy
D	diffusion coefficient
D _{GA}	diffusion coefficient of gum arabic
DLS	dynamic light scattering
DOSY	diffusion ordered spectroscopy
DWS	diffusing wave spectroscopy
D ₂ O	deuterium oxide, heavy water
EEP	electrical equivalence pH
EPS B40	exocellular polysaccharide B40
FAM-SE	5- (and 6-) carboxylfluorescein succinimidyl ester
FCDF	Friesland Coberco Dairy Foods
FITC	fluorescein-5-isothiocyanate
FRAP	fluorescence recovery after photobleaching
G'	elastic or storage modulus
G''	viscous or loss modulus
GA	gum arabic
GDL	glucono- δ -lactone
g ₁ (t)	field autocorrelation function
g ₂ (t)	intensity autocorrelation function
HPLC	high-performance liquid chromatography
I	ionic strength
I _{0.1}	scattering intensity at $Q = 0.1 \text{ nm}^{-1}$
I(Q)	scattering intensity
l*	transport mean free path of a photon
l _K	Kuhn segment length
MS	mass spectrophotometer
M _w	molar mass
[NaCl]	concentration of sodium chloride
NMR	nuclear magnetic resonance

List of abbreviations

O/W	oil in water emulsion
PDADMAC	poly(dimethyldiallylammonium chloride)
pH _c	pH at which soluble complexes are formed
pH _{Cp-max}	pH at which the biopolymer concentration in the coacervate phase is the largest
pl	iso-electric pH
pH _{ini}	initial pH
pH _{opt}	optimum pH
pH _{Vol-max}	pH at which the maximum volume of coacervate is obtained
P(Q)	particle scattering form factor
Pr:Ps	protein to polysaccharide ratio
(Pr:Ps) _{ini}	initial protein to polysaccharide mixing ratio
pH _φ or pH _{Ö1}	pH below which macroscopic phase separation occurs
pH _{Ö2}	pH below which complex coacervation is suppressed
Q	scattering wave vector
R _g	radius of gyration
s	velocity of creaming
s ₀	creaming velocity at pH 7.0
SAXS	small angle X-ray scattering
SEC MALLS	size exclusion chromatography followed by multiangle laser light scattering
SLS	static light scattering
S(Q)	structure factor
T	transmission
WP	whey proteins
Z _{GA}	zeta potential of the gum arabic
Z _{WP}	zeta potential of the whey proteins
α-la	α-lactalbumin
â-Ig	â-lactoglobulin
κ ⁻¹	Debye length
λ	wavelength
η	viscosity
ó	charge density
τ	turbidity or fluorescence recovery time

CHAPTER 1

General Introduction

Proteins and polysaccharides are biopolymers widely present in living organisms. They were even reported as being at the origin of life [Oparin, 1953]. They can be naturally associated in order to maintain cell integrity (membranes, organelles) or induce cell division (histones / DNA complexes, enzyme catalysis) [Menger, 2002], but they can also be incompatible, participating in cell partition [Turgeon *et al.*, 2003]. Food products are widely composed of ingredients like proteins and polysaccharides. Mixtures of biopolymers are often unstable, which leads to a separation of the mixture into two phases, as illustrated in Figure 1.1 [Tolstoguzov, 1991].

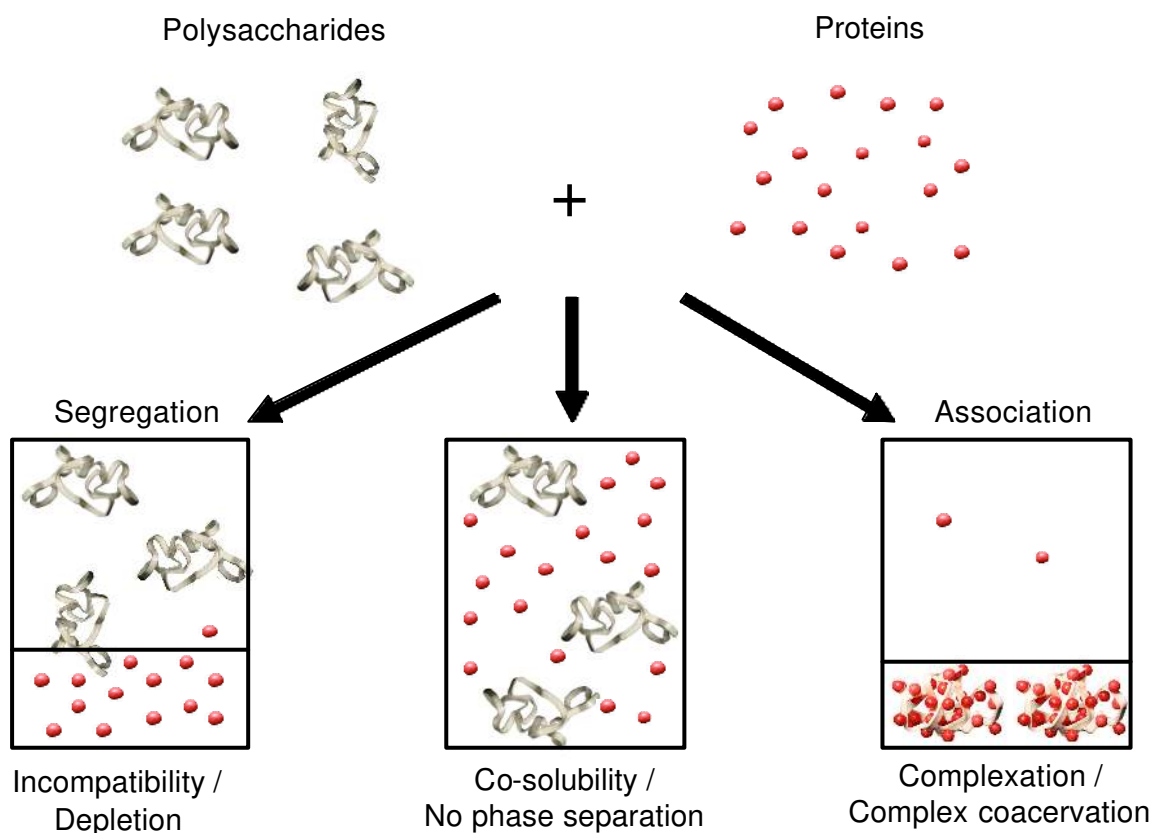


Figure 1.1: Main trends in the behavior of protein / polysaccharide mixtures.

A diluted non-interactive biopolymer mixture of proteins and polysaccharides may be co-soluble. If the biopolymers are incompatible, *i.e.* they repel each other, thermodynamic phase separation occurs, also called segregation or depletion interaction. After phase separation, the mixture exhibits two phases: one rich in protein and the other one rich in polysaccharide. On the other hand, if proteins and polysaccharides show net attraction, usually through electrostatic interactions (when they have oppositely charged groups), complex coacervation or associative phase separation occurs, giving rise to the formation of protein/polysaccharide complexes

[Bungenberg de Jong, 1949a]. The mixture separates into two phases: the lower phase containing the protein/polysaccharide complex and the upper phase containing mainly the solvent. The work reported in this thesis focuses on the associative phase separation of charged biopolymers.

Terminology

The term associative phase separation encompasses both complex coacervation, which is a liquid/liquid type phase separation, and precipitation, a solid/liquid type phase separation. The driving force is similar in both cases, but in the case of complex coacervation, the concentrated polymer phase is liquid, whereas the precipitate phase is more solid or “glass” like. In this chapter, a greater emphasis will be put on complex coacervation, although some references on protein / polysaccharide precipitation will also be reported. The polymers used in this study are of biological origin and are thus referred to as biopolymers. Polysaccharides belong to the biopolymer family. When a polymer (natural or synthetic) is homogeneously charged, it can be called a polyelectrolyte or a polyion. A biopolymer such as a protein usually carries both positively and negatively charged groups and is called a polyampholyte. All these terminologies will be used in this thesis.

WHAT IS COMPLEX COACERVATION?

When two polymers are oppositely charged, an electrostatic complex can be formed. The electrostatically bound complexes can be either soluble or “insoluble”. The “insoluble” complexes concentrate in liquid coacervate droplets, that further coalesce and phase separate to form a separate coacervate layer. As a result, one phase of the mixture is concentrated in the two polymers and the other phase contains mainly the solvent. A schematic picture of the complex coacervation mechanism is given in Figure 1.2.

Complex coacervation between oppositely charged proteins and polysaccharides was discovered by Tiebackx in 1911 [Tiebackx, 1911]. By mixing gelatin and gum arabic (GA) in an acetic acid solution, he observed opalescence or precipitation. This type of phase separation of gelatin / GA mixtures was extensively studied by the Dutch chemists Bungenberg de Jong and Kruyt in the 1920's and 1940's [Bungenberg de

Jong and Kruyt, 1929; Bungenberg de Jong, 1949a, 1949b, 1949c] and most of our present knowledge stems from their studies. The word “coacervation” was introduced by Bungenberg de Jong and Kruyt [Bungenberg de Jong and Kruyt, 1929] and derives from Latin “acervus”, which means aggregation (a heap), and the prefix “co”, which means together. “Coacervation” signifies the union of the colloidal particles. By colloidal particles, one understands liquid droplets, called coacervates, primarily induced by demixing (Figure 1.3). Bungenberg de Jong described the conditions under which complex coacervation of gelatin / GA occurred, such as pH, ionic strength, polymer concentration, polymer ratio, and temperature [Bungenberg de Jong, 1949a].

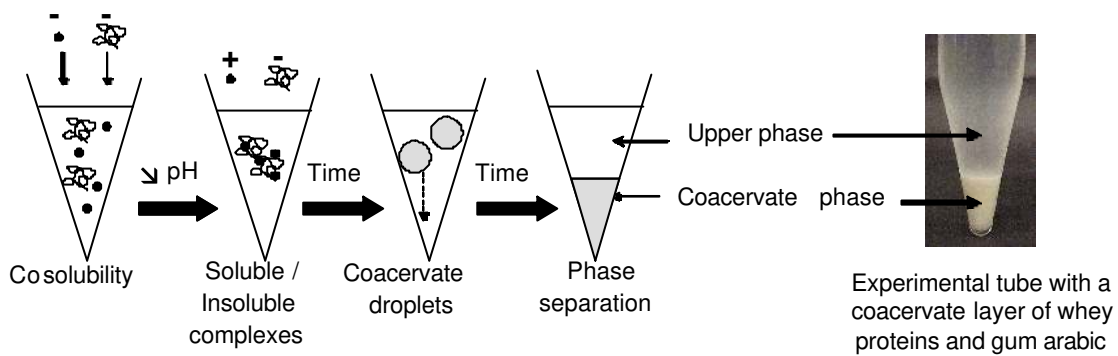


Figure 1.2: Schematic representation of the phase separation by complex coacervation.

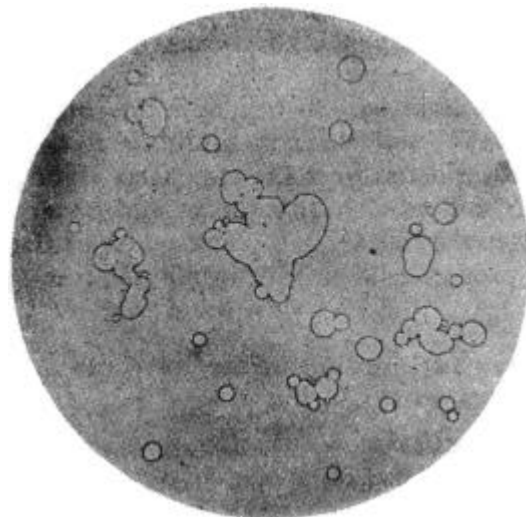


Figure 1.3: Microscopic picture of complex coacervation of bovine serum albumin and GA (120x). The coacervate droplets have partially spread over the surface of the microslide and so coalesced with each other. Picture reproduced from [Bungenberg de Jong and Kruyt, 1929] with the courtesy of Edita KNAW .

Bungenberg de Jong gathered an impressive amount of data on which the first theoretical model of complex coacervation was developed by Overbeek and Voorn [Overbeek and Voorn, 1957]. A typical phase diagram of complex coacervation is shown in Figure 1.4. A large number of reviews is available on the status of associative phase separation, and complex coacervation in particular [see for example: Dickinson, 1998; Doublier *et al.*, 2000; de Kruif and Tuinier, 2001; Nairn, 1995; Schmitt *et al.*, 1998; Tolstoguzov, 2002, 2003; Turgeon *et al.*, 2003].

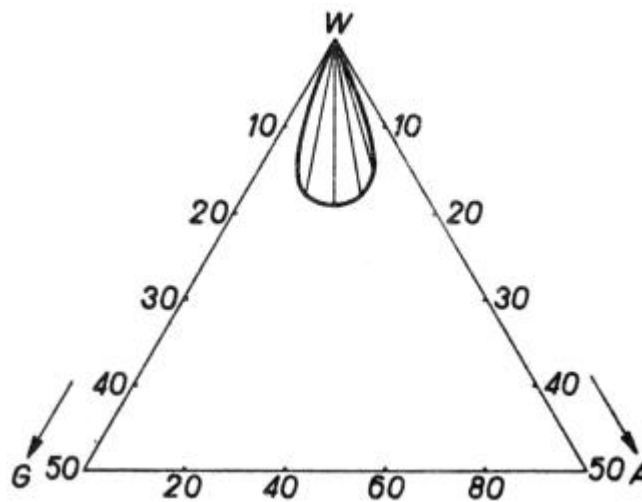


Figure 1.4: Schematic phase diagram of a water (W) / gum arabic (A) / gelatin (G) system at such a pH that G is positively charged and A is negatively charged. The coacervates are both rich in A and G and are to be found on the arched branch of the curve in the plane of the triangle. The equilibrium liquid which is poor in G and A lies on a branch of the curve close to the water corner of the triangle. Figure reproduced from [Bungenberg de Jong, 1949a].

The coacervation phenomenon can sometimes be defined as simple when it involves only one biopolymer. If the biopolymer is mixed with an incompatible or poor solvent, phase separation can also occur [Bungenberg de Jong, 1949a]. The phase separation by a poor solvent was not studied in this thesis.

RELEVANCE OF COMPLEX COACERVATION

Complex coacervation is an interesting phenomenon from a fundamental point of view, since the detailed formation and structure of the complex coacervates can help to understand the mechanism of complex biological processes. Additionally, certain properties of protein / polysaccharides coacervates were found to be better than the

material properties of the pure protein or the pure polysaccharide. Thus, besides the fundamental interest for biological phenomena, complex coacervation is pragmatically used in foods, cosmetics, pharmaceutical and medicine, as extensively described in the review of Schmitt *et al.* [Schmitt *et al.*, 1998].

Biological processes

Bungenberg de Jong already mentioned in his pioneering work that protoplasm had some properties in common with coacervates [Bungenberg de Jong and Kruyt, 1929]. Like the coacervate droplets, the protoplasm was often considered as an isotropic, liquid, concentrated colloid water system itself [Lepeschkin, 1924] and often presented a tendency to vacuolization [Heilbrunn, 1928]. However, Bungenberg de Jong only reported the points of resemblance but could not prove that coacervates have played a part in living matter. Later, Oparin suggested that coacervates could play a role in the appearance of life on earth [Oparin, 1953]. Indeed, he wrote: “The formation of coacervates [sic] was a most important event in the evolution of the primary organic substance and in the process of autogeneration of life”. However, six decades later, despite much research effort, coacervates remain among the most esoteric of the colloidal systems [Menger *et al.*, 2000]. The knowledge of biopolymer interactions is of fundamental importance in biological systems, as in the case of DNA and replication enzymes, immunoglobulins and exocellular proteins, or polysaccharides, virus and bacterial membranes [Albertsson, 1971]. Condensation (such as DNA and F-actin filaments) can be promoted by complexation with oppositely charged species [de Vries, 2001]. For instance, a novel system for gene delivery, based on the use of DNA-gelatin nanoparticles formed by salt-induced complex coacervation of gelatin and plasmid DNA, has been developed [Truong-Le *et al.*, 1998].

Purification of macromolecules

The use of attractive interactions in the purification of proteins has already been developed on a lab scale. A negatively charged polymer can be added to a protein medium, and after pH adjustment, precipitation of the protein / polymer complexes occurs and the proteins are reclaimed through centrifugation and filtration. This method is not yet used on an industrial scale, but various studies have shown the good selectivity and efficiency of this method by controlling the environmental conditions

(e.g. pH, nature of the polymer, salt) [Hidalgo and Hansen, 1971; Serov *et al.*, 1985; Strege *et al.*, 1990; Wang *et al.*, 1996].

Microencapsulation

One of the most important industrial applications of complex coacervation is microencapsulation. The microcapsules are widely used in many industries such as printing, food, aerospace, agriculture, cosmetics, and especially pharmaceuticals [Nairn, 1995]. Microencapsulation is a means of protecting sensitive materials

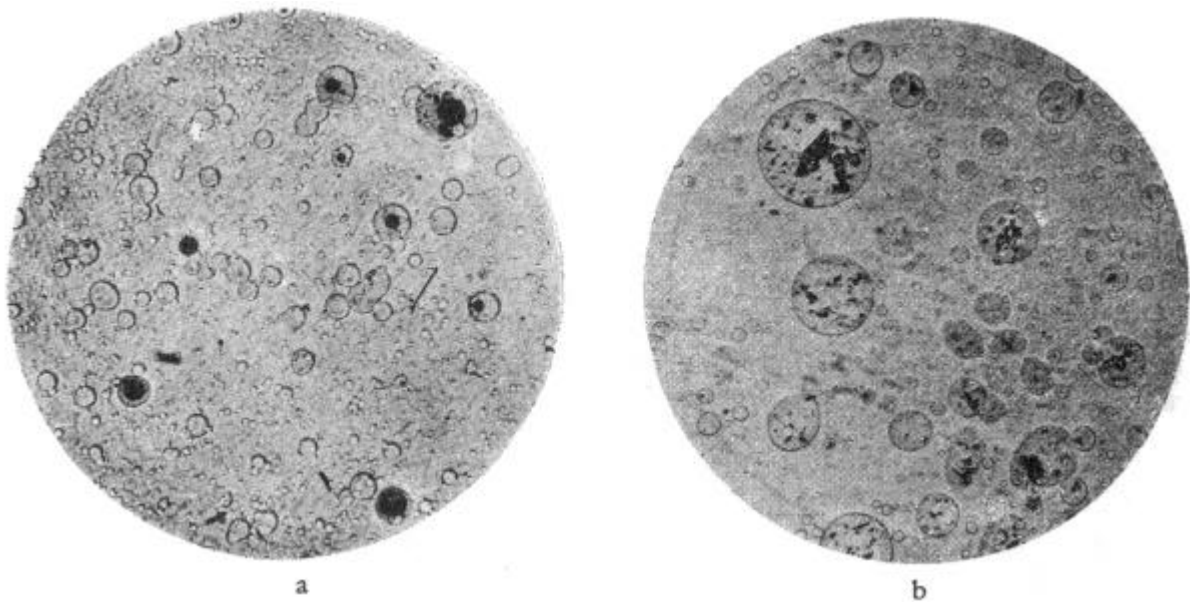


Figure 1.5: Micrographs of complex coacervate droplets with encapsulated carbon particles. (a): encapsulated tetrahydro-naphtalene droplets with ink. (b): magnified approx. 75 x Figures reproduced from [Bungenberg de Jong, 1949c]

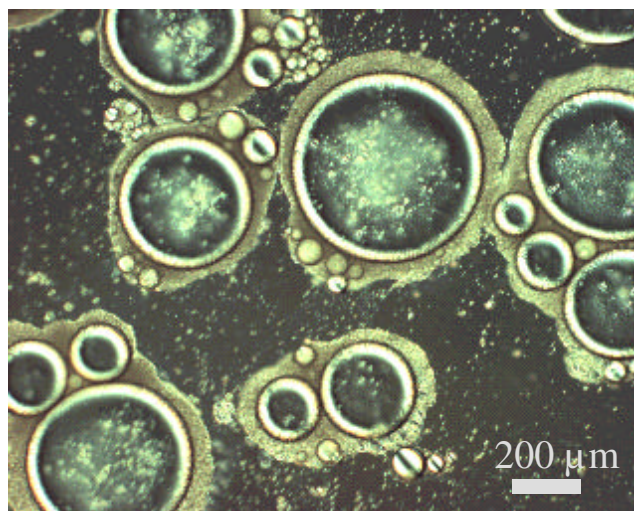


Figure 1.6: Microcapsules of orange flavor before drying. Figure reproduced from Chapter 8.

(volatiles, enzymes, dyes, drugs, etc) from the environment but also of controlling and targeting the release. The potential of encapsulation by coacervates was first recognized by Bungenberg de Jong, who observed the entrapment of solid particles and organic liquids in coacervate systems (Figure 1.5) [Bungenberg de Jong, 1949c]. Microcapsules prepared by complex coacervation result from the ability of the coacervate to form a coating around sensitive materials [see for example: Burgess, 1994; Daniels and Mittermaier, 1995; Luzzi, 1970]. Indeed, when coacervate droplets are formed, they usually coalesce and sediment as a separate (coacervate) phase. If an insoluble material (such as a drug particle or an oil droplet containing flavors) is present in the mixture, the coacervates will deposit at the surface of this material and, if sufficient stirring is applied to prevent sedimentation of the coacervate droplets, the compound to be encapsulated will be homogeneously coated by a layer of coacervate. A prerequisite is that the coacervate phase wets the particles or oil droplets. An example of encapsulated oil droplets is given in Figure 1.6. In 1954, the National Cash Register Company was the first to use gelatin / GA coacervates for the manufacture of carbonless copy paper [Green and Schleicher, 1956, 1957]. Since then, the gelatin / GA system has been used in many investigations (Table 1.1) [see for example: Flores *et al.*, 1992; Ijichi *et al.*, 1997; Jizomoto *et al.*, 1993; Lamprecht *et al.*, 2000a, 2000b, 2001; Luzzi and Gerraughty, 1964, 1967; Madan *et al.*, 1972, 1974; Newton *et al.*, 1977; Nixon and Nouh, 1978; Palmieri *et al.*, 1996, 1999; Takeda *et al.*, 1981; Takenaka *et al.*, 1980, 1981]. However, nowadays, other protein / polysaccharide systems are replacing the traditional gelatin / GA coacervates [Schmitt *et al.*, 1998].

Table 1.1: Some examples using gelatin / gum arabic coacervation for encapsulation purposes.

REFERENCES	ENCAPSULATED PRODUCT	FIELD OF APPLICATION	PARAMETERS STUDIED
Bungenberg de Jong, 1949c	Tetrahydro naphthalene Carbon particles	-	Mixing ratio of protein to polysaccharide (Pr:Ps), wetting phenomena, morphology of coacervate droplets and vacuoles
Daniels and Mittermaier 1995	Indomethacin	Pharmacy	Addition of different acids, pH
Flores <i>et al.</i> , 1992	Prototype fragrances	Cosmetic	Water solubility, fragrance volatility
Green and Schleicher, 1956, 1957	Oil containing dyes like Sudan III or nigrosine	Carbonless copy paper	-

Ijichi <i>et al.</i> , 1997	Biphenyl	Biotechnology, Pharmacy	Biopolymer concentration (Cp), capsule size, mechanism of encapsulation, multi layers, affinity of coacervate to a core material
Jizomoto <i>et al.</i> , 1993	Lipophilic drug (ProbucoI, S-312-d)	Pharmacy	Oral bioavailability, rehydration of the capsules, preservation test
Lamprecht <i>et al.</i> , 2000a	Fish oil	Pharmacy	Visualization of capsules using CSLM, distribution of the compounds in the wall, addition of casein, labeling efficiency
Lamprecht <i>et al.</i> , 2000b	Oil (Eicosapentaenoic acid ethyl ester or neutral oil)	Pharmacy	pH, visualization of the capsules with CSLM and light microscopy, labeling efficiency, addition of casein
Lamprecht <i>et al.</i> , 2001	Eicosapentaenoic acid ethyl ester (EPA-EE) = $\dot{U} - 3$ unsaturated fatty acid ethyl esters	Food ingredients	Oil / polymer ratio, homogenization time, hardening techniques, particle structure (with CSLM), yield, encapsulation rate, spray-drying of the coacervates, storage stability, oxidation rate
Luzzi and Gerraugthy, 1964	Oil (light liquid petrolatum mixed with coconut oil)	Pharmacy	Range of saponification values, effect of acid value, effect of surfactants
Luzzi and Gerraugthy, 1967	Solid (pentobarbituric acid)	Pharmacy	Starting pH, starting temperature, ratio of solid to encapsulating materials, quantity of denaturant, pH, simulation of gastrointestinal fluids
Madan <i>et al.</i> , 1972	Stearyl alcohol (waxy solid)	Pharmacy	Cp, Particle size
Madan <i>et al.</i> , 1974	Stearyl alcohol (waxy solid)	Pharmacy	Cp, total solid content, particle size, wall thickness, surface of the capsules
Newton <i>et al.</i> , 1977	Drug (sulfamerazine)	Pharmacy	pH, Pr:Ps ratio, Cp, cross-linking, stirring rate, drug to polymer ratio
Nixon and Nouh, 1978	Benzaldehyde	Pharmacy	Size of microcapsules, oxidation of benzaldehyde, pH
Palmieri <i>et al.</i> , 1996	Ketoprofen	Pharmacy	Different drying techniques, yield, moisture content, encapsulation percentage, morphology of solid particles, particle size, dissolution behavior
Palmieri <i>et al.</i> , 1999	Methoxybutropate	Pharmacy	Different drying techniques, yield, moisture content, encapsulation percentage, morphology of solid particles, particle size
Takeda <i>et al.</i> , 1981	Indomethacin suspended in soybean	Pharmacy	<i>In vitro</i> dissolution of indomethacin, bioavailability
Takenaka <i>et al.</i> , 1980	Micronized sulfamethoxazole	Pharmacy	pH, amount of formaldehyde, particle size, wall thickness and porosity, capsule surface topography, drug content, remaining amounts of hardening agents
Takenaka <i>et al.</i> , 1981	Micronized sulfamethoxazole	Pharmacy	Electrophoretic properties, pH, amount of formaldehyde

Food ingredients and biomaterials

Since proteins and polysaccharides are of biological origin, they can be used in products that are directly in contact with the living organism with more limited allergic risks than products with synthetic polymers [Schmitt *et al.*, 1998]. Thus, the use of protein / polysaccharide complexes in the food and cosmetics industries is not surprising. The textural properties of the coacervates allowed their use as new food ingredients, *e.g.* fat substitutes and meat replacers. In 1989, Chen *et al.* patented the use of milk protein / xanthan gum complexes to be used as fat replacers [Chen *et al.*, 1989]. Bakker *et al.* (1994) proposed as a fat substitute the use of gelatin / GA coacervates with a spherical shape of 11 μm diameter and a melting point of about 31.5°C, so that the mouthfeel was supposed to mimic that of fat. Analogues of meat textures were also obtained with protein / polysaccharide complexes. Tolstoguzov *et al.* (1974) used mainly caseins with addition of alginates, pectates, and low-ester pectins to prepare foodstuffs that resembled minced meat. Fibrous protein / xanthan gum complexes can also be used in the formulation of low-fat meat products [Soucie and Chen, 1986]. The biodegradability of the biopolymers complexes is a great advantage when they are used as biopackaging or edible food packages based on the film formation properties of biopolymers such as proteins and polysaccharides [Kester and Fennema, 1986]. The formation of a complex between soy isolate / sodium alginate / propylene glycol was found to have beneficial effects on the solubility and emulsifying properties of the polymers, resulting in better film properties [Shih, 1994]. Another study reported the formation of edible films based on a blend of sodium caseinate and wheat or corn starch in water [Arvanitoyannis *et al.*, 1996]. Most of the films with less than 15 wt % of water displayed good strength and gas barrier properties. Some recent research found that chitosan / alginate polyelectrolyte complexes (PEC) films could be prepared by casting and drying suspensions of chitosan / alginate coacervates [Yan *et al.*, 2001]. The PEC films exhibited good *in vitro* biocompatibility with mouse and human fibroblasts, suggesting that they can be further explored for biomedical applications. In the past 20 years, protein / polysaccharide complexes have received increased attention as biomaterials in medicine, *e.g.* for wound dressings, sutures, blood substitutes, articular prostheses, artificial grafts, or vessels [Easton *et al.*, 1986; Ellis and Yannas, 1996; O'Brien *et al.*, 2004; Prouchayret *et al.*, 1992; Samuel *et al.*, 2002; Stupp and Braun, 1997; Taravel and Domard, 1995, 1996; Yannas, 1990, 1994, 1997; Zaleskas *et al.*, 2001].

THEORETICAL DESCRIPTION OF COMPLEX COACERVATION

Bungenberg de Jong (1929 and 1949)

The first theoretical explanation of the coacervation phenomenon by Bungenberg de Jong and Kruyt (1929) is based on the stability of hydrophilic colloids, which is characterized by two stability factors: capillary electric charge and hydration. Coacervation would be the consequence of the removal of the two stability factors, *i.e.* charge and hydration. As desolvation sets in, there would be shrinkage of the solvent layer (“solvate mantle”) around the colloidal particles, which then would merge through their “concrete solvate mantles” (concrete = after desolvation) (Figure 1.7).

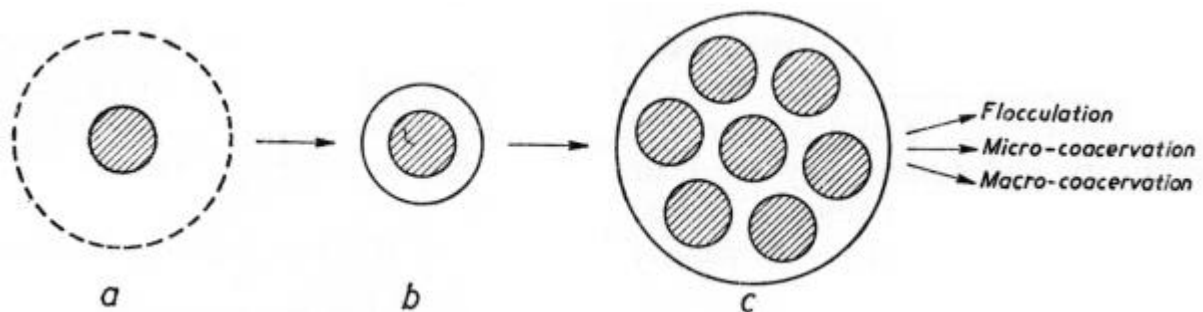


Figure 1.7: Schematic representation of the mechanism of phase separation by coacervation. (a): particle with a “diffuse solvate mantle” (dotted periphery). (b): particle with a “concrete solvate mantle”. (c): fusion of the particles to a coacervate with their “concrete solvate mantle”. Figure reproduced from [Bungenberg de Jong, 1949a].

Coacervates could be regarded as a liquid which had lost its free mobility to a certain degree. This explanation was mainly of the simple coacervation phenomenon, but when coacervation was brought about by a decrease of charge (complex coacervation), Bungenberg de Jong needed more research. He came up with a theory for complex coacervation in 1949 based on a large amount of experimental data on the gelatin / GA system [Bungenberg de Jong, 1949a]. The negative GA and the positive gelatin interact to form a complex. The role of experimental parameters, such as salt and pH, on the coacervation highlighted that the coacervation was a consequence of electrostatic interactions.

Voorn-Overbeek (1957)

Based on the experimental results of Bungenberg de Jong, Overbeek and Voorn developed the first quantitative theory on complex coacervation, in which they considered gelatin / GA coacervation as a spontaneous phenomenon [Overbeek and Voorn, 1957]. They interpreted coacervation as a competition between electrostatic forces which tend to accumulate the charged molecules and entropic effects which tend to disperse them. The oppositely charged molecules are associated together to form a coacervate phase entrapping solvent molecules. The presence of solvent in the coacervate phase contributed to the increase of entropy of the system, as it allowed a number of possible rearrangements of the molecules. For this reason, the coacervates were liquid in nature and the coacervation is fully reversible. The theory was based on several assumptions: (1) the molecules have a random chain configuration, (2) solvent – solute interactions are negligible, (3) the interactive forces are distributive in nature, with the system behaving as though the charges are free to move, and (4) there is no site specific interaction between the molecules. The theoretical treatment of complex coacervation was put on a quantitative basis by using the Debye-Hückel equations for the electrical interactions and the Flory-Huggins theory for the entropy term. According to this theory, for a two component system consisting of a polyion salt and water, the critical conditions for coacervation are met when $\delta^3 r \geq 0.53$, that is to say when the charge density (δ) or the molar mass (r) are sufficiently large. This model was extended to three- or four-component systems. Overbeek and Voorn explained that the suppression of coacervation by a salt excess was due to an increase of the solubility of the polyions, a decrease of the amount of polyions in the coacervate, and a decrease of charge density through charge screening by counterions (Figure 1.8).

It was also shown that not only polymers but also small ions were accumulated in the coacervate. Other systems than gelatin / GA seemed to follow this model under optimum conditions [Burgess *et al.*, 1991]. However, complex coacervation was also found when the above conditions were not met [Burgess and Carless, 1985]. Thus, various adaptations of the theory were developed later, since it seemed that the assumption that the Huggins interaction parameter was negligible was insufficient.

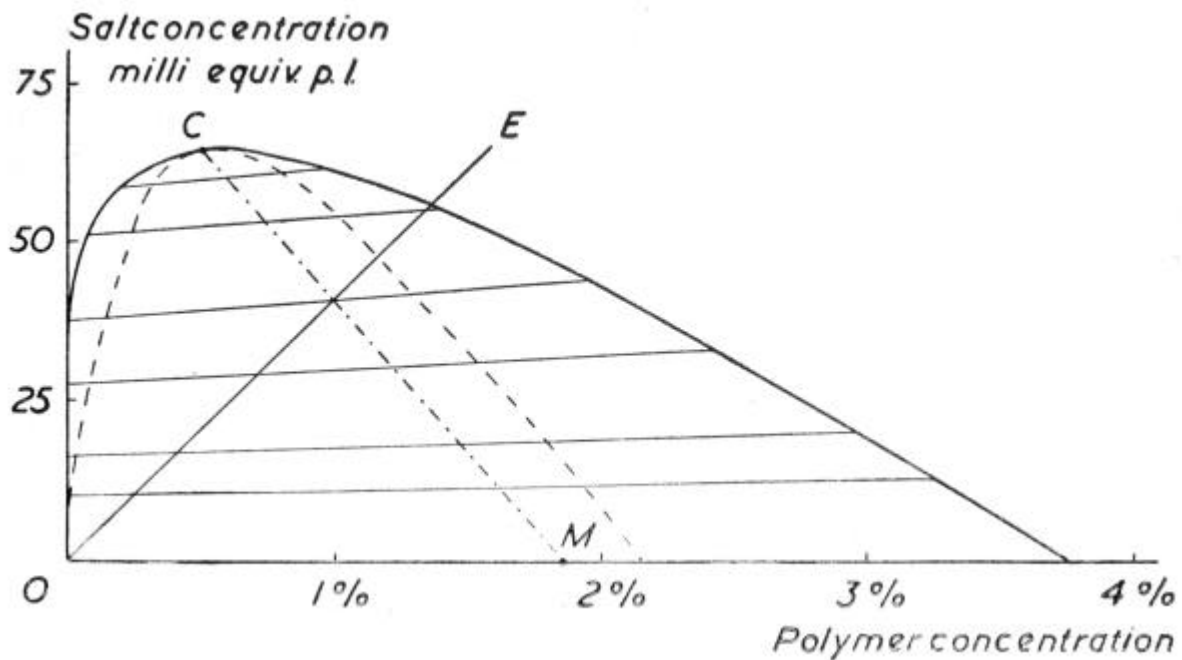


Figure 1.8: Theoretical phase diagram for complex coacervation in the system solvent / polymer PQ / univalent salt KA. The figure has been constructed for $r = 1000$, $\delta = 0.15$. The dotted line is the spinodal, C is the critical point, CM is positioned at the middle of the node lines and OE gives the equivalent polyelectrolyte / salt composition. Figure reproduced from J. T. G. Overbeek and M. J. Voorn, *Phase separation in polyelectrolyte solutions. Theory of Complex Coacervation*, J. Cell. Comp. Physiol., 1957 [Overbeek and Voorn, 1957], Copyright © 1970 Wiley-Liss, Inc., a subsidiary of John Wiley & Sons, Inc. Reprinted with permission of John Wiley & Sons, Inc.

Veis-Aranyi (1960 - 1970)

Veis and Aranyi developed a theory at conditions where $\delta^3 r < 0.53$, *i.e.* when the Voorn-Overbeek theory was not applicable [Veis and Aranyi, 1960; Veis, 1961, 1963; Veis *et al.*, 1967]. This theory was based on a practical case of coacervation upon temperature reduction between two oppositely charged gelatins. Veis modified the Voorn – Overbeek theory, including the Huggins interaction parameter, corresponding to the solvent – solute interaction; this parameter increases significantly on temperature reduction. In the Veis – Aranyi theory, coacervation is considered as a two-step process rather than a spontaneous one. First the gelatins spontaneously aggregate by electrostatic interaction to form neutral aggregates of low configurational entropy, and then, these aggregates slowly rearrange to form the coacervate phase. The mechanism is driven by the gain in configurational entropy resulting from the formation of a randomly mixed coacervate phase. Veis – Aranyi considered that the molecules were not randomly distributed in both phases, but that ion-paired aggregates are present in the dilute phase. Moreover, the electrostatic term of the Voorn – Overbeek

model was replaced by a term which is a function of concentration and charge density of the polymers. The differences between the Voorn – Overbeek and the Veis - Aranyi theories come from the fact that they explain different coacervation conditions: Voorn – Overbeek theory was based on the spontaneous coacervation of gelatin / GA, whereas Veis – Aranyi was developed for coacervation between two oppositely charged gelatins.

Nakajima – Sato (1972)

Nakajima and Sato studied an equivalent mixture of sulphated polyvinyl alcohol and aminoacetylated polyvinyl alcohol in microsalt aqueous solution [Nakajima and Sato, 1972]. They adapted the Voorn – Overbeek theory by including the Huggins parameter and changing the electrostatic term. Nevertheless, they agreed with Overbeek and Voorn that the charges should be treated as uniformly distributed in both dilute and concentrated phases. The experimental and theoretical results were in good agreement with each other, and the study showed that for specific systems the Overbeek– Voorn model could still be used.

Tainaka (1979 – 1980)

The Tainaka theory is the most recent model developed for complex coacervation, and is an adaptation of the Veis – Aranyi theory. The main difference from the Veis – Aranyi model is that the aggregates, present in both the dilute and concentrated phase, are formed without specific ion pairing [Tainaka, 1979, 1980]. The biopolymer aggregates present in the initial phase condense to form a coacervate. According to Tainaka, the driving forces for phase separation are the electrostatic and the attractive force between the aggregates, which become stronger when the molar mass and the charge density of the polymers increase. Charge density and molar mass of the polymers should fall within a critical range for coacervation to occur. If the charge density or molar mass of the polymer becomes higher than the critical range, then a concentrated gel or a precipitate, induced by the long-range attractive forces among the aggregates, will be formed. On the other hand, for charge densities or molar mass below the range, short range repulsive forces will stabilize the dilute solution and coacervation will not occur. The Tainaka theory is more general than all the previous theories and is applicable to both high and low charge density systems. It provides an adequate explanation of the complex coacervation process for a large number of systems.

Comparison with experimental results

Burgess and co-workers described four different coacervation systems (gelatin / GA, albumin / gelatin, gelatin / gelatin, and albumin / alginic acid) [Burgess and Carless, 1985, 1986; Burgess, 1990; Singh and Burgess, 1989]. Spontaneous coacervation as described by Overbeek and Voorn was observed upon mixing oppositely charged polymers only under specific conditions. The limiting conditions are that the average molecular mass of the polymers and their charge densities must fall within a specific range, the polymers should be in a random coil configuration, Flory-Huggins type interactions should be negligible and the charge interaction between the molecules should be distributive in nature. When deviation from these conditions occurs, coacervation may still take place, as described by Veis – Aranyi and by Tainaka. A large number of studies also reported the presence of primary complexes prior to complex coacervation, supporting the theories of Veis and Tainaka [see for example Kaibara *et al.*, 2000; Wang *et al.*, 2000]. Considering thermodynamic parameters, knowledge is still lacking and some results are contradictory. Some authors write and show that electrostatic complexation between protein and polysaccharide is mainly enthalpically driven, due to the decrease of the electrostatic free energy of the system [Girard *et al.*, 2003; de Kruif and Tuinier, 2001]. Others indicate that complexation is mainly entropically driven owing to the liberation of counterions and water molecules [Ball *et al.*, 2002; Dautzenberg, 2001].

CURRENT STATUS OF RESEARCH

Most of the references given above dealt mainly with the liquid / liquid complex coacervation phenomenon. The following section aims to report more broadly on the research made on protein / polysaccharide (Table 1.2) and protein / synthetic polyelectrolyte (Table 1.3) and their ability to form electrostatic complexes (coacervates or precipitates). More extensive information is available in the review of Schmitt *et al.* (1998) and in a recent review by Turgeon *et al.* (2003).

Complex formation

When a protein and a polyelectrolyte are oppositely charged, they can form a complex through electrostatic interactions. Various physico-chemical parameters can influence the electrostatic interactions and thus the complex formation. Some important

Table 1.2: Factors studied for some protein / polysaccharide systems.

REFERENCES	SYSTEMS	EXPERIMENTAL TECHNIQUES	PARAMETERS
Bungenberg de Jong, 1949	Gelatin / GA	Light microscopy, Viscosity, Turbidity, Phase diagrams	pH, Pr:Ps, Cp, ionic strength, types of ions.
Burgess and Carless, 1984	Gelatin / GA	Microelectrophoretic mobility	pH, Pr:Ps, pl of gelatin, ionic strength
Burgess and Carless, 1985	Gelatin / Gelatin	Microelectrophoretic mobility Preparation of gelatin microcapsules	pH, ionic strength, temperature, gelatine concentration, Pr:Ps, time, drug content
Burgess and Carless, 1986	Gelatin / Gelatin	Microelectrophoretic mobility Coacervate yield determination Photon correlation spectroscopy	pH, ionic strength, temperature, time, treatment of gelatin solutions
Burgess, 1990	Gelatin / GA BSA / GA	Microelectrophoretic mobility Dry coacervate yield determination	pH, ionic strength, Cp, time
Burgess, 1991	BSA / GA	Microelectrophoretic mobility Dry coacervate yield determination	pH, ionic strength, Cp
Burgess, 1994	Gelatin / GA BSA / GA	Microcapsule production Particle size stability Scanning electron microscopy	pH, Pr:Ps, stirring speed, time,
Girard <i>et al.</i> , 2002	β -Ig / Pectin (low- and high-methylated)	Potentiometric titrations Determination of the quantity of $\hat{\alpha}$ -Ig complexed to pectin (ultrafiltration)	Pr:Ps, pH, NaCl, urea, temperature
Girard <i>et al.</i> , 2003	β -Ig / Pectin (low- and high-methylated)	Isothermal titration calorimetry (binding constant, stoichiometry, enthalpy, entropy) Overlapping binding site model	Pr:Ps, time
Plashchina <i>et al.</i> , 2001	Faba bean legumin / chitosan	Ultraviolet spectroscopy, Viscometry, Calorimetry, Turbidimetric titration, Surface tension, Emulsion stability	Pr:Ps, ionic strength, pH
Sanchez <i>et al.</i> , 2002a	β -Ig / GA	Confocal scanning laser microscopy, Small angle static light scattering (SASLS), Time-resolved SASLS, Turbidity	Time, Pr:Ps = 1:1 and 2:1
Schmitt <i>et al.</i> , 2001a	β -Ig / GA	Confocal scanning laser microscopy Diffusing wave spectroscopy	Pr:Ps, $\hat{\alpha}$ -Ig with or without aggregates, time, Cp = 1% or 5%, pH 4.2 or 4.5
Schmitt <i>et al.</i> , 2001b	β -Ig / GA	Fourier transform infrared spectroscopy Circular dichroism Front face fluorescence	pH, Pr:Ps, Cp, $\hat{\alpha}$ -Ig with or without aggregates
Singh and Burgess, 1989	BSA / Alginate acid	Microelectrophoresis Dry coacervate yield determination	pH, ionic strength, Cp
Tuinier <i>et al.</i> , 2002	Casein micelles / pectin	Dynamic light scattering Adsorption measurements Renneting experiments	Time, concentration in GDL, pectin concentration, percentage of renneting

Table 1.3: Factors studied for some protein / synthetic polyelectrolyte systems.

REFERENCES	SYSTEMS	EXPERIMENTAL TECHNIQUES	PARAMETERS
Dubin <i>et al.</i> , 1994	Review on various systems		Molar mass of polymers, polyelectrolyte charge density, Cp, ionic strength
Kaibara <i>et al.</i> , 2000	BSA / PDADMAC BSA / PMETAC	Titration, Spectroscopic measurements, Microscopic observations	pH, temperature, ionic strength, protein to polyelectrolyte ratio
Leisner and Imae, 2003	Sodium poly(L-glutamate) / poly(amido amine) dendrimer	Static and dynamic light scattering Small angle X-ray scattering	pH, Cp, ratio
Mattison <i>et al.</i> , 1995	BSA / PDMDAAC	Turbidimetric titrations using colorimetry and dynamic light scattering, pH titration for determining macromolecular charge	pH, Ionic strength, Cp, protein to polyelectrolyte ratio, polyelectrolyte molecular weight, polyelectrolyte and protein charge
Mattison <i>et al.</i> , 1998	BSA / PDADMAC BSA / PMAPTAC BSA / PAMPS	Turbidimetric titrations using colorimetry, spectrophotometry, and light scattering, Potentiometric titrations, Protein surface modeling	Polyelectrolytes with various linear charge density, charge spacing and persistence length, pH, protein charge density, ionic strength
Mattison <i>et al.</i> , 1999	BSA / PDADMAC BSA / PMAPTAC BSA / PAMPS	Turbidimetric titrations, Dynamic light scattering, Electrophoretic mobility, Composition of the coacervates in BSA and water	pH, protein and polymer charge density, protein to polymer ratio, Cp, ionic strength
Menger <i>et al.</i> , 2000	Zwitterionic Gemini surfactant AOT/NaCl/water	Light microscopy Cryo-high resolution scanning electron microscopy	Coacervate droplets, fractured coacervate droplets, and coacervate layer
Menger, 2002	Branched Gemini	Discussion on the success, problems and potential of supramolecular systems	
Park <i>et al.</i> , 1992	BSA, Lysozyme, RNase + PSS1, PVS, NVP-AMPS, PSS2, PAMPS, LBN52b, PDMDAAC, LBN66	Turbidimetric titrations Quasielastic light scattering	pH, protein charge density
Wang <i>et al.</i> , 1996	BSA / PDADMAC β -Ig / PDADMAC γ -globulin / PDADMAC ribonuclease A / PDADMAC	Turbidimetry Separation and analysis Size exclusion chromatography UV measurements Dynamic light scattering	Protein type, pH, ionic strength, polyelectrolyte molar mass, protein to polyelectrolyte ratio
Wen and Dubin, 1997	BSA / PDADMAC	Potentiometric titrations Turbidimetric titrations	pH, Cp, protein to polymer ratio
Xia <i>et al.</i> , 1999	Bovine ferrihemoglobin + PDADMAC, PAMPS, AMPS	Quasi-elastic light scattering Electrophoretic light scattering CD spectroscopy Azide binding titrations	Polyelectrolyte charge density and sign, protein and polymer concentrations

parameters are reported in this section. It is well known that pH plays a key role in the strength of electrostatic interaction since it determines the charge density of the protein. The formation of electrostatic complexes is extensively reported in the literature for protein / synthetic polyelectrolyte systems [see for example: Dubin *et al.*, 1994; Kaibara *et al.*, 2000; Mattison *et al.*, 1995, 1998, 1999; Park *et al.*, 1992; Wang *et al.*, 1996; Wen and Dubin, 1997; Xia *et al.*, 1999]. These studies revealed that the complexation appeared as a two-step process upon pH change. Indeed, two pH-induced structural transitions (pH_c and pH_ϕ) were identified. At pH_c , the formation of soluble complexes was initiated, and below pH_ϕ visual phase separation occurred. Soluble complexes were often formed at pH values above the isoelectric point (pI) of the protein, *i.e.* at a pH where the protein is negatively charged overall, like the polyelectrolyte [Dubin *et al.*, 1994; de Vries *et al.*, 2003; Wen and Dubin, 1997]. Recently, de Vries *et al.* (2003) proposed a model for the formation of soluble protein-polysaccharide complexes incorporating the non homogeneous charge distribution along the protein backbone. They were able to predict the complexation above the protein pI, due to the presence of (randomly) charged patches on the surface of the proteins. The existence of two major structural transitions in the mechanism of complexation was also shown for α -lactoglobulin (α -lg) / pectin [Girard *et al.*, 2002]. Thus, for all systems studied, the process of complex formation can be explained by the formation of (i) intrapolymeric soluble complexes at pH_c , (ii) interpolymeric soluble and insoluble complexes, (iii) insoluble complexes and macroscopic phase separation at pH_ϕ (coacervation or precipitation) (Figure 1.9).

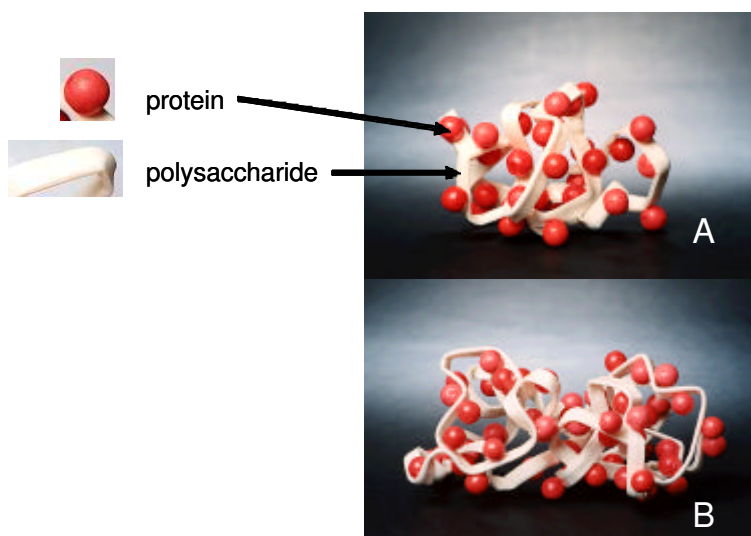


Figure 1.9: Intrapolymer (A) and interpolymer (B) complexes.

Furthermore, the ionic strength of the system should be carefully controlled, since the presence of salt can suppress the complexation, depending on the nature and the concentration of the salt [Bungenberg de Jong, 1949a; Overbeek and Voorn, 1957; Schmitt *et al.*, 1998]. The polymer concentration is also a critical parameter, since above a critical concentration, self suppression of the coacervation occurs as described in the Voorn-Overbeek theory [Overbeek and Voorn, 1957]. Moreover, an optimum mixing polymer ratio exists which corresponds to an electrically equivalent amount of each polymer [Burgess and Carless, 1984]. When one of the polymers is in excess, coacervation does not occur because of the low energetic interest of concentrating the polymers in one phase if the concentration is already high. Other parameters (*i.e.* molar mass, temperature, shear, pressure, etc.) also influence the complexation of polymers, but were hardly addressed.

Kinetics of phase separation

A first attempt to describe the kinetics of complex coacervation was made on a system composed of $\hat{\alpha}$ -lg and GA using diffusing wave spectroscopy (DWS) and confocal scanning laser microscopy (CSLM) [Schmitt *et al.*, 2001a]. Phase separation depended on the $\hat{\alpha}$ -lg / GA mixing ratio and the DWS patterns were difficult to interpret because coalescence and sedimentation of the coacervate droplets occurred at the same time. Kinetics studies were continued with the same system [Sanchez *et al.*, 2002a]. No definite conclusions on the occurrence of spinodal decomposition or nucleation and growth phenomena could be proposed, probably because the system was already at the late stage of phase separation. Thus, to overcome this drawback, acidification can be done *in situ* using glucono-delta-lactone (GDL), and the pH can be decreased slowly from a value at which no interaction takes place to a value at which phase separation occurs [Tuinier *et al.*, 2002].

Structure of the coacervates

The structure of the soluble complexes, coacervate droplets and coacervate phase remain poorly known and only very few references are available on this aspect. On the molecular level, it was found that complex coacervation between $\hat{\alpha}$ -lg and GA induces a conformational change of the protein with a loss in α -helix content [Schmitt *et al.*, 2001b]. The fact that the conformation of the protein changes when a protein is bound to a polysaccharide by electrostatic interactions was also reported for faba bean

legumin / chitosan system [Plashchina *et al.*, 2001]. Some studies also show that complexation of the protein with a polysaccharide can preserve the functionality of the protein and prevent denaturation [Burova *et al.*, 2002; Ivinova *et al.*, 2003]. However, it remains difficult to understand exactly what the structure of soluble protein / polysaccharide complexes is. Most of the information on that subject is available from molecular simulations [Akinchina and Linse, 2002; Hayashi *et al.*, 2003; Skepö and Linse, 2003; Stoll and Chodanowski, 2002]. Depending on the ionic strength, the polyelectrolyte chain length, flexibility, charge density, and radius of charged spheres, a large number of interesting complex structures emerges, ranging from collapsed polyelectrolyte wrapping the sphere to “rosette”, “tennis ball”, solenoid or multiloop-like conformations [Turgeon *et al.*, 2003]. Recent work from Leisner and Imae (2003) describes for the first time the structure of complexes and coacervates in a poly(glutamic acid) / dendrimer system. The transition from interpolymeric soluble electrostatic complex to coacervates can be explained by the aggregation of intermolecular clusters giving rise to intramolecular microgels, then intermolecular microgels coagulate to form coacervates. Leisner and Imae report that coacervates are randomly branched gels with a sponge-like morphology and compact and smooth microgel inhomogeneities larger than 20 nm. The structure of α -lg / GA coacervate droplets was studied by CSLM, and it appears that their internal structure exhibits spherical inclusions of water more or less numerous depending on the initial protein to polysaccharide mixing ratio [Schmitt *et al.*, 2001a]. A light micrograph picture of a coacervate droplet is shown in Figure 1.10. Sanchez *et al.* (2002a) explain that the presence of vacuoles is induced by the presence of residual uncharged GA at the interface, which facilitates the entrapment of water. In time, rearrangement of the coacervates occurs and the vacuoles disappear.



Figure 1.10: Whey protein / GA coacervate droplets with vacuoles. [Weinbreck, internal report].

In a purely synthetic system of zwitterionic Gemini surfactant in water, Menger *et al.* (2000) reported the structure of the obtained coacervates as sponge-like vesicles (Figure 1.11). In another family of Gemini the authors showed that adding only one carbon atom in the surfactant chain led to the formation of either a transparent gel or a coacervate [Menger, 2002].

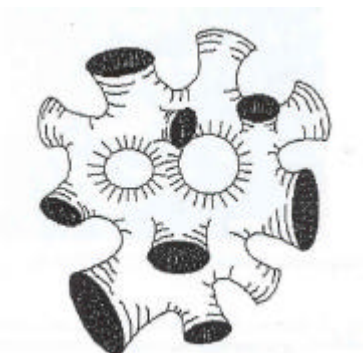


Figure 1.11: Schematic drawing of the sponge phase. Reprinted with permission from [Menger, 2000]. Copyright 2000 American Chemical Society.

AIM OF THE THESIS

The main goal of this thesis is to get more insights into complex coacervation, and more generally electrostatic interactions, between proteins and polysaccharides. The main motivation is to be able to better control the interactions of ingredients within food products, and also to use complex coacervation as a tool of encapsulation.

Choice of biopolymers

Traditionally, complex coacervation of gelatin and GA was studied and used industrially. But, today, there is a need to replace gelatin for health and religious reasons. Thus, the proteins used in this study are whey proteins (WP, mainly composed of β -lg). WP is very often used as a food ingredient due to its emulsifying and texturizing properties. Its molecular structure is nowadays very well known. Various polysaccharides were used in this thesis and the one that received most of the attention was GA, also called acacia gum. GA is also widely used as a food ingredient especially because of its low viscosity and its remarkable interfacial properties. GA was traditionally studied for complex coacervation with gelatin by Bungenberg de Jong [Bungenberg de Jong and Kruyt, 1929; Bungenberg de Jong, 1949a, 1949b, 1949c] and from an industrial point of view, GA is the main polysaccharide used for

encapsulation using complex coacervation. It is a weak polyelectrolyte that carries carboxylic groups. However, many polysaccharides used in food systems are more strongly charged than GA. Since it is well known that electrostatic interactions depend on the charge density of the polyelectrolyte, two other (more strongly charged) polysaccharides were also investigated: the exopolysaccharide EPS B40 and carrageenan (CG). EPS B40 is naturally excreted from *Lactococcus lactis* subsp. *cremoris* during fermentation and thus acts as a natural thickener in acidified milk products. EPS B40 carries phosphate groups and its structure and behavior are well known since it has been extensively studied at NIZO food research. CG is a sulfated polysaccharide extracted from red algae and it is mainly used as a thickener in food products. Two CG batches were used in this study: a pure λ -CG and a commercial hybrid CG. Both batches do not gel. For systems of WP/GA, complex coacervates were formed, and for WP/EPS B40 and WP/CG, precipitates were obtained.

Characteristics of whey proteins

WP are the proteins present in the whey obtained from cheesemaking. WP are globular proteins present in milk and are mainly composed of β -lactoglobulin (β -lg), α -lactalbumin (α -la), bovine serum albumin (BSA), immunoglobulin (IMG), and several minor proteins and enzymes. In whey, about 52% of the protein is β -lg and 20% is α -la. Native β -lg has an isoelectric point of 5.2. At room temperature and physiological pH (pH 6.7) β -lg exists mainly as a dimer which consists of an ellipsoid of length 6.45 nm and width 3.6 nm. The β -lg monomer has a molar mass of 18.3 kDa and comprises 162 amino acids. The α -la molecule in milk is a compact, low molar mass (14.2 kDa) globular protein. The pI of α -la is 4.1 [Vasbinder, 2002]. In this thesis, denatured proteins arising from drying of the powder were removed by acidification and centrifugation. The final powder contains 75% β -lg and 15% α -la.

Characteristics of GA

GA is a complex polysaccharide exuded from the African tree *Acacia Senegal*. It is an arabinogalactan composed of three distinct fractions with different protein contents and different molar masses [Osman *et al.*, 1993; Randall *et al.*, 1989]. GA has a 'wattle blossom'-type structure with a number of polysaccharide units linked to a common polypeptide chain. The composition analysis of GA revealed the presence of a main galactan chain carrying heavily branched galactose/arabinose side chains (Figure

1.12). The carbohydrate moiety is composed of D-galactose (40% of the residues), L-arabinose (24%), L-rhamnose (13%), and 2 uronic acids, responsible for the polyanionic character of the gum, the D-glucuronic acid (21%) and 4-O-methyl-D-glucuronic acid (2%). The structure of GA is complex and poorly known. GA is negatively charged above pH 2.2, since at low pH (< 2.2) the dissociation of the carboxyl groups is suppressed. GA displays good emulsifying properties and its viscosity is low compared to other polysaccharides of similar molar mass [Sanchez *et al.*, 2002b]. The GA sample used in this study has a weight-averaged radius of gyration (R_g) of 24 nm and a molar mass (M_w) of 520 kDa [see Chapter 2].

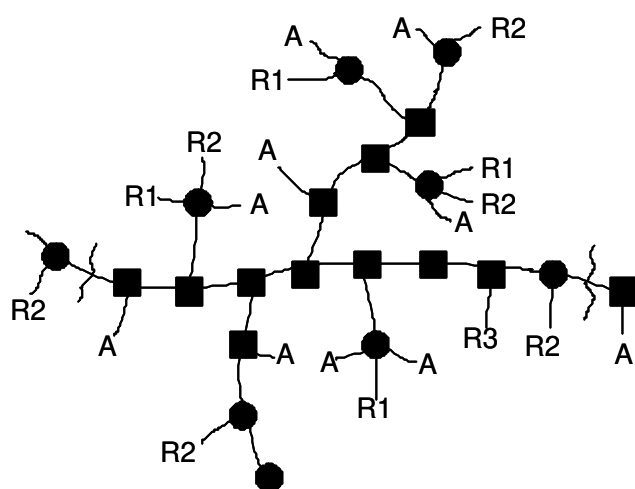


Figure 1.12: Putative molecular structure of GA; A = arabinosyl; \square = 3-linked Galp; \square = 6-linked Galp (Galp or Glcp attached), or end group; R1 = Rha 4GlcA (Rha occasionally absent, or replaced by Me, or by Ara f); R2 = Gal 3Ara; R3 = Ara 3Ara 3Ara Adapted from [Islam *et al.*, 1997].

Characteristics of EPS B40

The EPS B40 is excreted by the lactic acid bacterium *Lactococcus lactis* subsp. *cremoris* NIZO B40 during fermentation. The structure of the repeating unit consists of a backbone in which the repeating unit contains three α (1-4)-linked monosaccharides, namely two D-glucose residues and one D-galactose unit (Figure 1.13). The galactose residue carries two side groups. Carbon atom C3 is linked to a phosphoric acid group of which one oxygen atom is bound to the C1 of an α -D-galactose. The backbone galactose also has a covalent bond with an α -L-rhamnose residue through a (1-2) bond. EPS B40 has already been extensively studied at NIZO food research from a genetic point of view [van Kranenburg, 1999]; the physical properties of the EPS and its role in fermented milks have been studied by van Marle *et al.* (1999) and Ruas-

Madiedo *et al.* (2002), and the segregative phase separation between EPS B40 and dairy proteins at neutral pH was studied by Tuinier *et al.* (1999, 2000). The EPS B40 has a weight-averaged $R_g = 86$ nm and $M_w = 1620$ kDa [see Chapter 3].

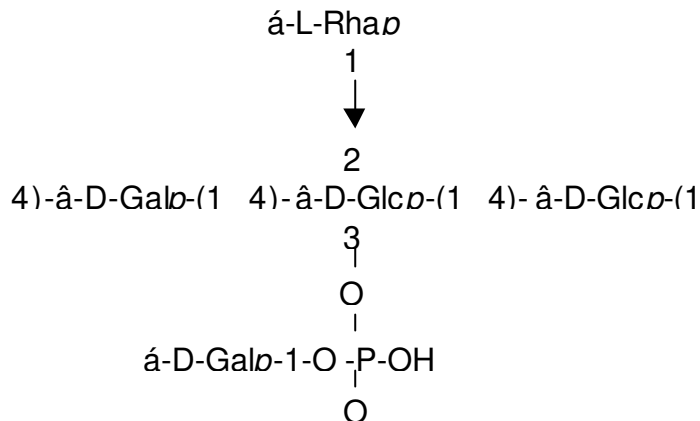


Figure 1.13: Chemical structure of EPS B40.

Characteristics of CG

Carrageenan (CG) is often not a single biopolymer but a mixture of water-soluble, linear, sulphated galactans. They are composed of alternating 3-linked α -D-galactopyranose (G-units) and 4-linked β -D-galactopyranose (D-units) or 4-linked 3,6-anhydrogalactose (A-units), forming the disaccharide-repeating unit of CG (see Figure 1.14) [van de Velde *et al.*, 2002]. The most common types of CG are traditionally identified by a Greek prefix. The three commercially most important carrageenans are called κ , ι , and λ -CG. κ -CG and ι -CG are gel-forming carrageenans, whereas λ -CG is a thickener/viscosity builder. The two CG batches used in this study are a non-gelling CG, a pure λ -CG sample and a hybrid of various CG types with a $R_g = 49$ nm and $M_w = 774$ kDa [see Chapter 4].

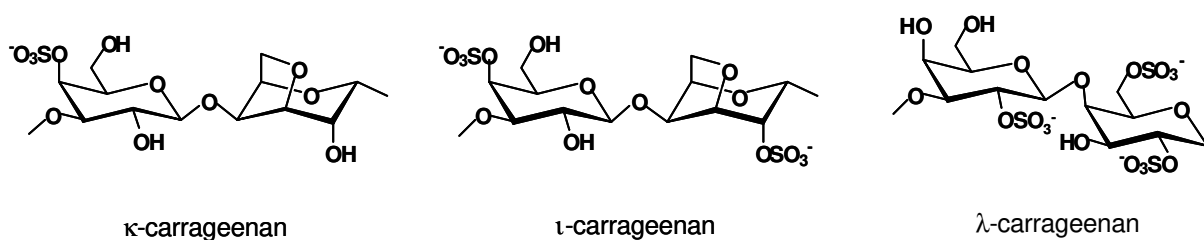


Figure 1.14: Schematic representation of the repeating units of three types of carrageenan. Figure adapted from [van de Velde *et al.*, 2002].

Outline of the thesis

This thesis consists of three parts. In the first part, the interactions between oppositely charged biopolymers and the influence of various physico-chemical parameters (*e.g.* pH, ionic strength, biopolymer concentration) on the complex formation are investigated (Chapters 2, 3 and 4). An attempt is made to compare all the results of the three different systems (WP/GA, WP/EPS B40 and WP/CG) and to highlight the system-specific or generic properties of the complexes. Chapter 2 deals with the complex coacervation of WP and GA. The aim of this chapter is to investigate the influence of pH on the formation of WP/GA complexes and coacervates and whether pH-transitions (pH_c and pH_ϕ) can also be obtained for this system as for synthetic polymers (see above). For that purpose, the mixtures were subjected to a gradual pH decrease *in situ* by the use of GDL. A state diagram and a phase diagram summarize the effect of pH, ionic strength and biopolymer concentration. Chapter 3 describes the same type of experiments as in chapter 2, but for a system of WP/EPS B40. A more detailed investigation of the structure of the soluble complexes on the molecular level was performed by light scattering and viscosity measurements. The influence of protein to polysaccharide mixing ratio and mixing order gave new insights into the structure and rearrangement of soluble complexes. Chapter 4 describes studies on the electrostatic interactions between WP and CG as a function of pH and ionic strength. New experiments on the addition of calcium ions, instead of sodium ions, and on the influence of temperature are also reported. The behavior of these complexes as an ion trap is finally discussed. In the following chapters, the system WP/GA was further investigated.

In the second part of the thesis, the main objective is the characterization of the coacervate phase (chapters 5, 6, and 7). In chapter 5 the parameters defined in chapter 2 are used to study the kinetics of sedimentation of the coacervate phase. The composition of the coacervate phase was determined after complete phase separation for various pH values and protein to polysaccharide ratios. These results are used to explain the structure of the coacervate phase by small angle X-ray scattering. Taken together, the results of chapter 5 highlight that, at a defined protein to polysaccharide ratio, there is a specific pH at which complex coacervation is maximal. In chapter 6, the visco-elastic properties of the coacervate are reported for one specific protein to polysaccharide ratio. Once again, the results confirm those previously found in chapter 5, since at the pH of maximum coacervation, the viscosity of the coacervate was also

maximum. The effect of the coacervate composition and the electrostatic force are decoupled to highlight that the high viscosity is mainly due to the strong electrostatic interactions. Finally, the diffusion properties of the biopolymers in the WP/GA coacervate phase are presented in chapter 7. With the help of three different techniques (nuclear magnetic resonance, fluorescence recovery after photobleaching, and diffusing wave spectroscopy), the diffusion of the two biopolymers, and the diffusion of each specific biopolymer, were measured. The conclusion is that WP and GA diffuse independently in the coacervate phase.

Finally, the third part (chapter 8) shows a direct application of the WP/GA coacervates used for microencapsulation of oils and flavors. This chapter is based on a patent application and it shows that the traditional gelatin / GA system can be replaced by WP/GA coacervates.

CHAPTER 2

Complex Coacervation of Whey Protein and Gum Arabic*

ABSTRACT

Mixtures of gum arabic (GA) and whey protein (whey protein isolate - WP) form an electrostatic complex in a specific pH-range. Three phase boundaries (pH_c , pH_{ϕ_1} , pH_{ϕ_2}) have been determined using an original titration method, newly applied to complex coacervation. It consists of monitoring the turbidity and light scattering intensity under slow acidification in situ with glucono- δ -lactone. Furthermore, the particle size could also be measured in parallel by dynamic light scattering. When the pH is lowered, WP and GA first form soluble complexes, this boundary is designated as pH_c . When the interaction is stronger (at lower pH), phase separation takes place (at pH_{ϕ_1}). Finally, at pH_{ϕ_2} complexation was suppressed by the charge reduction of the GA. The major constituent of the WP preparation used was β -lactoglobulin (β -lg) and it was shown that β -lg was indeed the main complex forming protein. Moreover, an increase of the ionic strength shifted the pH boundaries to lower pH values, which was summarized in a state diagram. The experimental pH_c values were compared to a newly developed theory for polyelectrolyte adsorption on heterogeneous surfaces. Finally, the influence of the total biopolymer concentration (0-20% w/w) was represented in a phase diagram. For concentrations below 12%, the results are reminiscent to the theory on complex coacervation developed by Overbeek and Voorn. However, for concentrations above 12% phase diagrams surprisingly revealed a "metastable" region delimited by a percolation line. Overall, a strong similarity is seen between the behavior of this system and a colloidal gas-liquid phase separation.

*F. Weinbreck, R. de Vries, P. Schrooyen, C. G. de Kruif, *Biomacromolecules* **2003**, 4 (2), 293-303.

INTRODUCTION

The study of the attractive interactions between proteins and polysaccharides has relevance for many biological systems (*e.g.* organization of living cells), and also for pharmaceutical products and processed food (*e.g.* purification of macromolecules, microencapsulation of ingredients or cosmetics, fat substitutes, meat analogues, films, coatings, packaging, ...) [Dickinson, 1998; Doublier *et al.*, 2000; de Kruif and Tuinier, 2001; Sanchez and Paquin, 1997; Tolstoguzov, 1996]. For instance, macromolecular interaction between biopolymers may affect the properties of food products (such as yogurts, acidified milk, yogurt drinks, juices, where *e.g.* added pectin and carrageenan form electrostatic complexes with casein micelles). Indeed, arising from electrostatic interaction, the two - weak or strong – oppositely charged polyelectrolytes form a complex, thereby releasing counterions and water molecules, contributing to an entropy gain in the system. The electrostatically bound complexes can be either soluble or insoluble. The insoluble complexes concentrate in liquid coacervate drops, leading to a phase separation of the mixture into two liquid layers. As a result, one phase is concentrated in the two polymers and the other phase contains mainly the solvent. This phenomenon has been studied since 1911, starting with the work of Tiebackx (1991), followed in 1929 by Bungenberg de Jong and Kruyt (1929) on mixtures of GA and gelatin; the term complex coacervation was then introduced to describe this phenomenon.

To gain more insights into the formation of these complexes, a number of studies have identified the influence of various parameters. It is now well known that the electrostatic interaction is determined by the physicochemical characteristics of each polymer (*e.g.* charge density and molar mass), their concentration and ratio, the solution conditions (*e.g.* pH, ionic strength, type of ions) [Schmitt *et al.*, 1998]. Furthermore, temperature, shear and pressure can affect the formation and the stability of complexes. Overbeek and Voorn (1957) proposed a theoretical treatment based on the results of Bungenberg de Jong (1949a, 1949b) and explain the spontaneous coacervation which occurred between gelatin and GA as a competition between the electrostatic attractive forces which tend to accumulate charged polyions and entropy effects which tend to disperse them [Overbeek and Voorn, 1957]. Later, Veis *et al.* (1960) suggested a modification of this theory, where they considered the formation of soluble complexes prior to

coacervation. The charge density of weak polyelectrolytes is governed mainly by the pH, which is, therefore, a significant parameter for complex coacervation. Furthermore, the addition of salt can reduce and even suppress complexation owing to a screening of the charged groups of the polymers [Bungenberg de Jong, 1949b]. However, as shown by Burgess (1990), coacervation can also be suppressed at low salt concentrations.

Some previous studies of the interactions between carboxymethylcellulose (CMC) and proteins (whey proteins, gelatin, ...) showed that the formation of the complexes could be monitored by measuring the viscosity, the turbidity, or the coacervate volume [Ganz, 1974; Koh and Tucker, 1988a, 1988b]. Synthetic polymers in combination with bovine serum albumin (BSA) were studied in detail for protein purification using turbidity measurement and pH titration. The pH-induced structural transitions (pH transitions) were used to parameterize the phenomenological results and were determined as a function of several parameters (*e. g.* ionic strength). Two specific pH values, pH_c and pH_{ϕ_1} , were identified. The formation of soluble protein-polyelectrolyte complexes was initiated at pH_c , which preceded the pH of visual phase separation called pH_{ϕ_1} [Dubin *et al.*, 1994; Kaibara *et al.*, 2000; Mattison *et al.*, 1995, 1999; Wang *et al.*, 1996; Wen and Dubin, 1997].

Former studies were made with synthetic polyelectrolytes, and systems with biopolymers currently used in food products have been poorly investigated so far. The novelty of this study lies in the use of a complex mixture of whey proteins (WP, whey protein isolate) together with a complex polysaccharide, GA. The acid-titration of the biopolymer mixtures is carried out in order to see whether pH-transitions found for synthetic polymers could also be detected for biopolymers, and for a weak polyelectrolyte like GA. The “standard” parameters influencing complex coacervation are studied (*e.g.* pH, ionic strength). However, an original titration method is used. With the classical titration method (*i.e.* addition of HCl solution), a dilution effect has to be considered, but in this study an *in situ* titration technique avoids the external perturbation of the system. The biopolymer mixtures are slowly acidified with glucono- δ -lactone (GDL) and their turbidity, scattering intensity, and particle size are monitored in parallel and reveal the formation of soluble and insoluble complexes. The determination of a state diagram – different from the one found with strong

polyelectrolytes – summarizes the effect of ionic strength and pH. Also, recently developed analytical estimates for pH_c that include the important effects of protein surface charge heterogeneity are applied to our experimental results [de Vries *et al.*, 2003]. This work aims to clarify whether pH-transitions and soluble complexes are formed for biopolymers just as for synthetic systems. Furthermore, the effect of using a weak polyelectrolyte is outlined. And finally, the study of the total biopolymer concentration is summarized in a phase diagram, which - to our opinion – was never done for such a large range of concentration (0.05% - 20% w/w).

The biomacromolecules used in this study are WP and GA. GA is a complex polysaccharide exuded from the African tree *Acacia Senegal*. It is an arabinogalactan-type polysaccharide composed of six carbohydrates moieties and a protein fraction. It was suggested that this polysaccharide has a “wattle blossom”-type structure with a number of polysaccharide units linked to a common polypeptide chain [Islam *et al.*, 1997]. This polysaccharide presents good emulsifying properties and a remarkable low viscosity. GA is a weak polyelectrolyte that carries carboxyl groups, and microelectrophoretic measurements showed that GA is negatively charged above pH 2.2, since at low pH (<2.2) the dissociation of the carboxyl groups is suppressed (with a minimum value at $-2.2 \text{ m}^2\text{s}^{-1}\text{V}^{-1}$ for the pH range 5-10) [Burgess and Carless, 1984]. From the molecular structure of the GA, one can estimate the charge density of the polyelectrolyte as one carboxylic group per 5 nm [Islam *et al.*, 1997]. The WP isolate used is comprised of 75% of β -lactoglobulin (β -lg) and 15% of α -lactalbumin (α -la). Native β -lg has an isoelectric point (pI) at pH 5.2 and native α -la at pH 4.1 and they are thus positively charged below their pI. Since the pI of β -lg is higher than the pI of α -la and because β -lg is present in a much larger quantity than α -la, one can presume that the interaction between the WP and GA is dominated by the β -lg. As a result, complexation between WP and GA takes place in the pH range where they carry opposite charges. Schmitt *et al.* have already performed extensive work on this system and pointed out the large influence of WP aggregates on complex coacervation [Schmitt *et al.*, 1999, 2000a; Schmitt, 2000b]. Therefore, aggregates from our protein mixtures were removed.

THEORY

Primary soluble complexes between protein and polyelectrolyte are formed at a specific pH, called pH_c , which varies with the ionic strength. In a number of cases it was found that at low ionic strength, soluble complexes also form at pH values for which the proteins and polyelectrolytes carry the same net charge. This is also observed for the system WP/GA. The phenomenon has been ascribed to the attraction between polyelectrolyte charges and oppositely charged “patches” on the protein surface [Dubin *et al.*, 1994; Wen *et al.*, 1997]. A number of recent theoretical papers deal with the complexation of homogeneously charged spheres and oppositely charged polyelectrolytes [see for example: Netz and Joanny, 1999; Nguyen and Shklovskii, 2001]. These could be applied to complexation between oppositely charged proteins and polyelectrolytes. However, complexation between similarly charged proteins and polyelectrolytes cannot be explained by these theories. Ellis *et al.* (2000) performed Monte Carlo simulations of polyelectrolyte adsorption on randomly charged surfaces and found complexation for polyelectrolytes and surfaces of the same net charge. Carlsson *et al.* (2001) performed Monte Carlo simulations of polyelectrolytes complexing with heterogeneously charged spheres (with a surface charge distribution mimicking that of lysozyme). These authors found that it was necessary to include a small nonelectrostatic protein-polyelectrolyte attraction in order to account for complexation of similarly charged proteins and polyelectrolytes. Finally, Grymonpré *et al.* (2001) used computer modeling of protein electrostatics to identify a “charge patch” on serum albumin that could act as an electrostatic binding site.

Recently, de Vries *et al.* (2003) have developed analytical estimates for pH_c , that include the effects of charge patches, or more generally, the protein surface charge heterogeneity. The theory gives simple expressions for the dependence of the measurable quantity pH_c on the ionic strength and the linear charge density of the flexible polyelectrolyte. However, these are obtained at the expense of neglecting many protein and polyelectrolyte structural details. Therefore, at best, this theory can be expected to give correct order-of-magnitude estimates. In the Results section, we compare our own experimental data for pH_c to these analytical estimates. Below, we outline the essential ingredients of the theory.

A first crucial observation is that there is virtually no correlation in the sign of neighboring charges on the surface of globular proteins. This was demonstrated

through a statistical analysis of the surface charge distribution for β -lg. A continuous (but heterogeneous) protein surface charge density is introduced by coarse-graining the discrete protein surface charge distribution at the level of the Kuhn segment length l_K of the flexible polyelectrolyte. Roughly speaking, the protein surface is divided into “sites” of area l_K^2 having a statistically independent random surface charge density that may vary between $\sigma - \Delta\sigma$ and $\sigma + \Delta\sigma$, where σ is the average protein surface charge density and $\Delta\sigma$ are the root-mean-square variations of the local protein surface charge density. Each of these sites is large enough to accommodate one segment of the flexible polyelectrolyte. Note that in such a model, there is a finite probability of finding charged patches of various sizes that have a charge opposite to the net protein charge. Hence, this model is not inconsistent with the idea of charged patches, but rather tries to approximate the statistics of how often these charge patches typically occur.

Existing approaches for polymer adsorption on randomly interacting surfaces were used to estimate critical adsorption conditions [Odijk, 1990; Andelman and Joanny, 1991]. The electrostatic interaction potential between polymer segments and the protein surface is approximated by a “random square well” potential. The width of the well, *i.e.* the range of the interaction, is the Debye length κ^{-1} (which is a function of the ionic strength). This approximation leads to expressions for the polyelectrolyte adsorption that are only accurate up to a numerical factor of order unity, but do retain the correct dependence on the salt concentration. The average depth V of the well (in units of the thermal energy $k_B T$) is proportional to the product of the polymer linear charge density ν (number of elementary charges e per Kuhn segment length l_K) and the average protein surface charge density σ (number of elementary charges e per unit area):

$$V = 4\pi l_B \kappa^{-1} \sigma \nu, \quad (\text{Eq. 1})$$

where $l_B = e^2/\epsilon k_B T$ is the Bjerrum length and ϵ is the solvent dielectric constant. In aqueous solutions, and at room temperature, $l_B \approx 0.7$ nm. In terms of the concentration c_s of added monovalent electrolyte, the Debye length is given by $\kappa^{-1} = (8\pi l_B c_s)^{-1/2}$. The root-mean-square fluctuation of the well depth due to the variations of the local protein surface charge density is ΔV . It is proportional to the polymer linear charge density and to the root-mean-square variation $\Delta\sigma$ of the (local) protein surface charge density. In units of the thermal energy $k_B T$:

$$\Delta V = 4\pi l_B \kappa^{-1} \Delta\sigma \nu \quad (\text{Eq. 2})$$

In the interesting limit of strong fluctuations ($\Delta V^2 \gg V$), the random square well model predicts polymer adsorption for

$$V - 0.5\Delta V^2 < 0.95(\kappa_K)^2 \quad (\text{Eq. 3})$$

In the general case, the critical conditions ($V, \Delta V^2, \kappa_K$) for the onset of polymer adsorption follow from the full analytical solution of the random square well model [de Vries *et al.*, 2003].

To estimate values of V and ΔV for globular proteins around the isoelectric point pI , we set:

$$\sigma \approx \left. \frac{\partial \sigma}{\partial pH} \right|_{pH=pI} (pH - pI) \quad (\text{Eq. 4})$$

The derivative can be deduced from titration data, assuming some reasonable estimate for the protein surface area. The magnitude of the root-mean-square variations of the local surface charge density is roughly pH independent around the isoelectric point and is left as an adjustable parameter [de Vries *et al.*, 2003]:

$$\Delta \sigma^2 \approx \frac{\mu}{\pi_K^2} \left. \frac{\partial \sigma}{\partial pH} \right|_{pH=pI} \quad (\text{Eq. 5})$$

for some numerical constant μ of order 1. Estimates for the critical pH for the formation of soluble complexes are deduced by finding the pH for which the random square well model predicts the onset of polymer adsorption.

EXPERIMENTAL SECTION

Materials

Bipro is a whey protein isolate (WP) comprised mainly of α -lactoglobulin (α -lg), and α -lactalbumin (α -la) - from Davisco Foods International (Le Sueur, USA). The WP aggregates were removed by acidification (at $pH = 4.75$) and centrifugation (1h at 33000 rpm with a Beckman L8-70M ultracentrifuge, Beckman instruments, The Netherlands). The supernatant was then freeze-dried (in a Modulo 4K freeze-dryer from Edwards High Vacuum International, UK). Finally, the resulting powder was stored at 5°C . The final powder contained (w/w) 88.1% protein (N x 6.38), 9.89% moisture, 0.3% fat and 1.84% ash (0.66% Na^+ , 0.075% K^+ , 0.0086% Mg^{2+} , and 0.094% Ca^{2+}). The protein content of the treated Bipro is: 14.92% α -la, 1.46% BSA, 74.86% β -lg, and 3.21% immunoglobuline (IMG).

Batches of > 90% pure β -lg and > 90% pure α -la were provided by NIZO food research (Ede, The Netherlands). The powder of β -lg contained (w/w) 92% β -lg, 2% α -la, 2% of nonprotein nitrogen compounds, and 2.1% ash (including 0.75% Na^+ , 0.02% K^+ , 0.008% Mg^{2+} , and 0.12% Ca^{2+}) on a dry basis. The amount of moisture was 4.0%. The composition of α -la powder is not exactly known but contains 93.8% of α -la (determined by reverse HPLC).

GA (IRX 40693) was a gift from the Colloides Naturels International Company (Rouen, France). The powder contained (w/w) 90.17% dry solid, 3.44% moisture, 0.338% nitrogen, and 3.39% ash (0.044% Na^+ , 0.76% K^+ , 0.200% Mg^{2+} , and 0.666% Ca^{2+}). Its weight average molar mass ($M_w = 520\,000\text{ g/mol}$) and its average radius of gyration ($R_g = 24.4\text{ nm}$) were determined by size exclusion chromatography followed by multiangle laser light scattering (SEC MALLS). SEC MALLS was performed using TSK-Gel[®] 6000 PW + 5000 PW column (Tosoh Corporation, Tokyo, Japan) in combination with a precolumn Guard PW 11. The separation was carried out at 30°C with 0.1 M NaNO_3 as eluent at a flow rate of 1.0 mL min⁻¹.

Stock solutions were prepared by dissolving the powder in deionized water (concentrations were varied from 0.5% - 25% w/w). For concentrations of 1% and below, the mixtures were stirred for 2 h at room temperature and the resting time was one night at 5°C. For concentrations of 5% and more, the mixtures were stirred 24h (5h at room temperature and overnight at 5°C).

Preparation of the mixtures

Various concentrations of WP and GA mixtures were obtained by diluting the stock solutions in deionized water at the desired pH and ionic strength. The concentration of the total biopolymer (C_p) varied from 0.05% to 25% and the ratio of WP to GA (Pr:Ps) was set at 2:1 (w/w). The mixtures were slowly acidified using glucono- δ -lactone (GDL) powder, which is an internal ester. Once added to the mixture, the GDL dissolves and hydrolyses slowly to form gluconic acid (GH), a weak acid, and further dissociation leads to the formation of G^- and H^+ [de Kruif, 1997]. To cover the desired pH range, 0.07% to 0.16% (w/w) of GDL was added to the mixture. Occasionally the mixtures were also acidified using 1 M HCl. Comparisons of acidification with GDL and HCl showed no difference in the experimental pH_c and $\text{pH}_{\phi 1}$ values. After mixing proteins

and polysaccharides, the ionic strength was adjusted using NaCl, and finally the pH was brought to the desired initial value ($\text{pH} = 7.0 \pm 0.5$) with 0.5 M NaOH. Then, the sample was put in a water bath at 25°C. Next, GDL powder was added and the mixture was stirred for 1 min to allow a homogeneous dissolution of the GDL. A sample was subsequently taken out for pH measurements, another one for turbidity measurements and another for static light scattering measurements. Of the same sample, pH, turbidity, and scattering intensity were followed in time. The measurements were repeated at least three times at each condition. The values of the pH_c and $\text{pH}_{\phi 1}$ had a variation within the accuracy of the pH-meter (± 0.05 pH-units). Controls with only WP and only GA were systematically performed in the same conditions as those for the mixtures of biopolymers.

Turbidity measurement

Turbidity measurements were carried out with a Cary 1E spectrophotometer (Varian, USA) at a wavelength of 514.5 nm (*i.e.* similar to the laser light wavelength used for static light scattering measurements). The samples were put in a 1 cm path length cuvette and the turbidity was then measured as a function of time at 25°C. The turbidity (τ) was defined as:

$\tau = -\ln(I/I_0)$, with I the light intensity that passes through a volume of solution in 1 cm cube and I_0 the incident light intensity.

Static and dynamic light scattering measurement

The static and dynamic light scattering experiments were performed on mixtures of 0.05% - 1% w/w biopolymer concentration, using a Spectra Physics 275 mW Argon laser with a wavelength of 514.5 nm. The light beam was focused on the axis of the goniometer using a lens. The sample was initially filtered with a 0.45 μm filter and centrifuged for 30 seconds to remove all impurities and air bubbles. The sample was placed in the cuvette housing, which was kept at a temperature 25°C in a toluene bath. The goniometer was set at 45° (90° for Figure 2.1b). The detected intensity was processed by a digital ALV-5000 correlator. Finally, the scattered light intensity was measured and its average was recorded every minute. The second order cumulant fit was used for the determination of the particle size and the averaged intensity was used as the scattering intensity value each minute.

The filtration was performed at pH values higher than pH_c to avoid any removal of material. Experiments performed with and without filtration showed that the pH-transitions were found at the same value, proving that the filtration step did not spoil the results.

Building the phase diagrams

Addition and removal of salt

For each total concentration of biopolymer (C_p) in the range (0.05% - 25%), the concentration of NaCl was varied. By slowly adding NaCl to a mixture of WP and GA (Pr:Ps = 2:1) at pH 3.5, one could see at which concentration of NaCl, or/and at which conductivity, the turbidity of the mixture started to decrease. Then, by adding ion exchange resins (mixed bed) into the solution, one could remove the salt without varying the pH and measure the increase of turbidity. This measurement was done for high C_p values (from 12% to 20%). However, one cannot exclude the possibility of protein adsorption on the ion-exchange resins, therefore another method of building phase diagram was used, *i.e.* the dilution method.

Dilution method

The concentration of NaCl was maintained constant and the concentration of biopolymer was varied. A mixture of WP and GA (Pr:Ps = 2:1) was prepared at pH 3.5, at a defined [NaCl], and at a high biopolymer concentration (C_p around 25%). This mixture was then diluted slowly with water of the same pH and ionic strength and the turbidity was measured as the mixture was diluted. Finally, the concentration of biopolymer could be calculated for each measurement. As a result, the C_p of phase separation was determined. This measurement was repeated for all added [NaCl] in the range 0 mM-150 mM.

Conductivity measurement

The conductivity of the mixtures was measured at $T=25^\circ\text{C}$ with a conductivity handheld meter LF 340 and a standard conductivity cell TetraCon[®] 325 (Wissenschaftlich – Technische Werkstätten GmbH, Germany).

RESULTS AND DISCUSSION

The strength of complexation depends on the charge density of both biopolymers. Therefore pH and ionic strength play a fundamental role in the formation of complexes between WP and GA. We determined under which conditions complexation occurs using turbidity and static light scattering measurements as a function of pH and salt concentration. The complexity of the protein mixture has been investigated as well, by titrating mixtures of > 90% pure β -lg/GA and > 90% pure α -la/GA. Furthermore, the total biopolymer concentration and the ratio of the two biopolymers also influence complexation. The effect of each parameter will be systematically discussed.

Effect of the pH

By adding GDL to a mixture of WP and GA, complexation of biopolymers could be studied in the pH range 7.0 – 4.0. Controls with only WP or GA were measured as a background measurement. During acidification, the turbidity of the mixtures was monitored simultaneously by spectrophotometry and static light scattering. The latter technique is more sensitive to the detection of small particles than the turbidity measurement, especially in highly transparent systems. Dynamic light scattering experiments performed in parallel allowed the size evolution of the particles to be followed as a function of pH. Initially, measurements were carried out on mixtures containing a total biopolymer concentration (C_p) of 0.1% and 0.3% with a ratio of protein to polysaccharide (Pr:Ps) of 2:1 (w/w) at $[\text{NaCl}] = 12.5 \text{ mM}$ and $[\text{NaCl}] = 0 \text{ mM}$. The initial pH of the mixture was set at 7.0 and, by adding 0.07(w/w)% GDL, it decreased slowly to pH 4.0 in approximately 1.5 h.

As illustrated in Figure 2.1a, the increase of scattering intensity of the biopolymer mixture reveals three phases (A, B, C) as compared to the blanks with only WP or GA, which intensity remains almost constant over the whole pH-range. The turbidity curve corresponding to the mixture of biopolymers presents only one strong increase. The scattering intensity of the WP/GA mixture is almost constant and low at a pH above a critical pH value (pH_c) (region A). The second phase is comprised between pH_c and a pH of phase separation (called pH_{δ_1}) where the scattering intensity increases slightly with decreasing pH (region B). This small increase is clearly perceptible with the light scattering but the turbidity value remains low. Then at pH_{δ_1} (and below), the scattering intensity increases abruptly as shown by both the static light scattering measurement

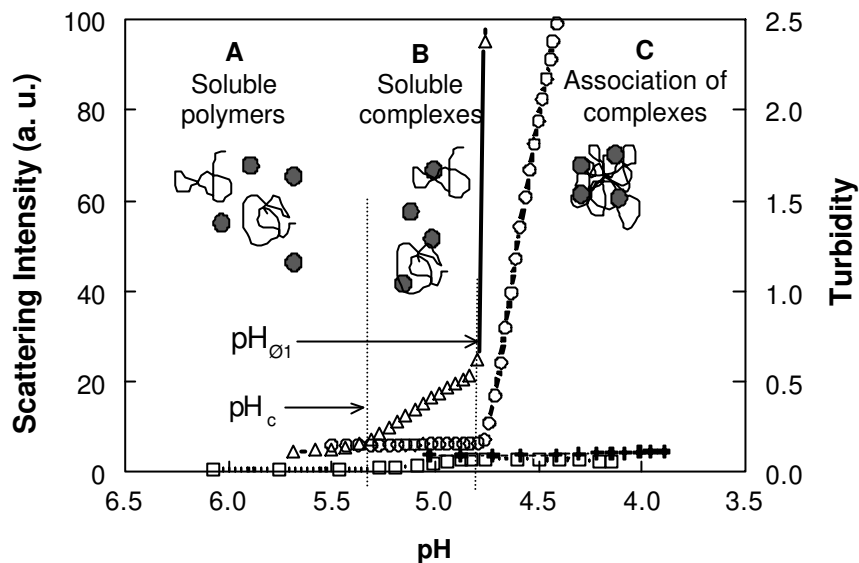


Figure 2.1a: Stability and instability regions (A, B, C) as a function of pH. (○): Scattering intensity and (○): Turbidity of a mixture of WP and GA ($C_p = 0.1\%$ and Pr:Ps = 2:1). (○): Scattering intensity of WP ($C_p = 0.07\%$). (+): Scattering intensity of GA ($C_p = 0.03\%$). [NaCl] = 12.5 mM, [GDL] = 0.07%.

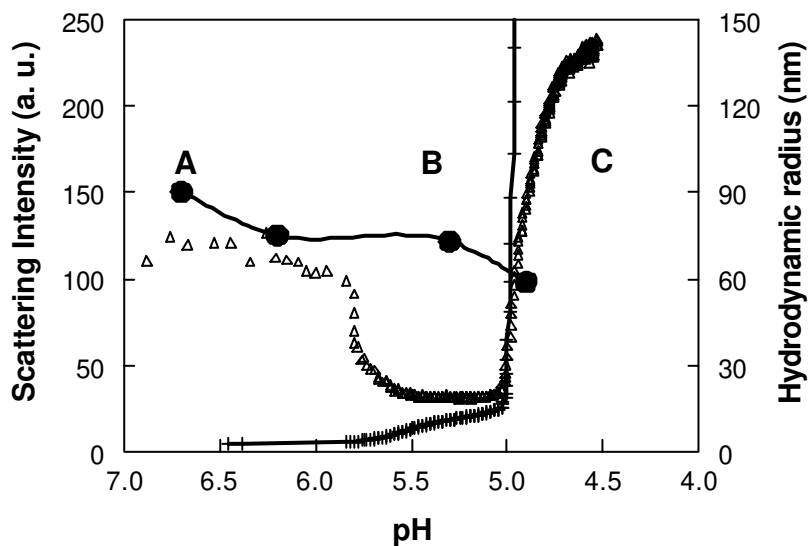


Figure 2.1b: Stability and instability regions (A, B, C) as a function of pH. (+): Scattering intensity at 90° and (○) Hydrodynamic radius of a mixture of WP and GA ($C_p = 0.3\%$, [NaCl] = 0 mM, and Pr:Ps = 2:1, [GDL] = 0.07%). (○): Hydrodynamic radius of GA ($C_p = 0.1\%$, [NaCl] = 0 mM).

and the turbidity measurement (region C). The values of pH_c and $\text{pH}_{\hat{0}1}$ were measured graphically as the intersection point of two tangents to the curve. In Figure 2.1a, the values are $\text{pH}_c = 5.3$ and $\text{pH}_{\hat{0}1} = 4.8$. Figure 2.1a illustrates that in the presence of only one biopolymer (WP or GA), the scattering intensity remains flat compared to the one of the WP/GA mixtures. This result proves that a pH-dependent two-step increase of scattering intensity in the biopolymer mixture is due to an electrostatic interaction between the GA and the WP. No aggregation of GA takes place, and a very limited protein-protein association is visible at pH 4.75. This slight aggregation of protein could be induced by the freeze-drying step or by some residual aggregates that were not removed.

In Figure 2.1b, the evolution of the scattering intensity and the hydrodynamic radius of the particles are plotted as a function of the pH for a mixture of WP and GA with a $C_p = 0.3\%$, $\text{Pr:Ps} = 2:1$, and a $[\text{NaCl}] = 0 \text{ mM}$. A blank of 0.1% GA shows the size evolution of the polysaccharide alone as a function of pH ($[\text{NaCl}] = 0 \text{ mM}$). This result illustrates that at a $\text{pH} > \text{pH}_c$ (region A), the initial radius of the complex is similar to the radius of the GA alone. At pH_c , when the scattering intensity increases, the radius of the complex strongly decreases to a value close to 20 nm, whereas the radius of the GA alone remains between 90 and 60 nm on the whole pH range. The particle size of the complexes is constant from pH_c until $\text{pH}_{\hat{0}1}$ (region B), and increases abruptly at $\text{pH}_{\hat{0}1}$ together with the scattering intensity (region C).

The presence of the pH transitions (pH_c and $\text{pH}_{\hat{0}1}$) is comparable to the results of Mattison *et al.* (1995) for a system of BSA-poly(dimethyldiallylammonium chloride) (PDADMAC). However, the difference is that PDADMAC is a highly charged cationic polyelectrolyte. At $\text{pH} > \text{pH}_c$ (region A in Figure 2.1a and 2.1b) proteins and polysaccharides are both negatively charged and then repulsive Coulombic forces prevent the complexation. This means that biopolymers are soluble in the aqueous solvent, and consequently the scattering intensity measured is low and constant. In this region, the particle size in the WP/GA mixture - determined by the DLS - (region A Figure 2.1b) corresponds to the size of the GA measured in the blank. (The proteins are very small ($\sim 3 \text{ nm}$) and, therefore, they do not contribute to the measurement of the hydrodynamic radius.) This result gives us an indication of the size range of the polymer, but cannot be taken as the absolute value of the polymer radius, since the measurements were only performed at one angle (90° in this case) in view of the polydispersity of the sample. The apparent hydrodynamic radius of the GA blank and

the initial radius of the mixture (region A) is high compared to the radius of gyration determined with the SEC MALLS ($R_g = 24.4$ nm). This result is attributed to the fact that the mixtures were prepared without adding any salt. The GA being negatively charged, the polymer will be in an expanded form due to intramolecular electrostatic repulsions. In a pH window between pH_c and $pH_{\hat{O}1}$, the scattering intensity increases but the radius of the particles in the solution decreases strongly compared to the blank of GA (region B Figure 2.1b). If the particle size decreases in the presence of WP, the increase of the scattering intensity is induced by an increase in molecular mass of the particles. The result can be explained by the formation of soluble complexes of WP and GA. The decrease of the GA radius could be due to the shrinkage of the molecule, which becomes less expanded when WP interacts with the carboxylic groups of the polysaccharide, leading to a reduced intramolecular repulsion. The blank of GA does not show such a strong decrease of its radius, the slight decrease of the radius of GA alone can be explained by the addition of microions induced by the acidification. Between pH_c and $pH_{\hat{O}1}$ (region B), the soluble complexes still carry a net negative charge, and are thus soluble in the solvent [Kaibara *et al.*, 2000]. Furthermore, at low ionic strengths, pH_c appears at a pH above the isoelectric point of the protein (5.2 in the case of native \hat{a} -lg). Here, it is proposed that soluble complexes are formed by the attraction between some positively charged protein “patches” and the negatively charged polysaccharide [Dubin *et al.*, 1994; Wen and Dubin, 1997]. Finally, macroscopic phase separation is reached in the third region (C), where $pH < pH_{\hat{O}1}$. The primary complexes tend towards electroneutrality, which allows their association, and phase separation takes place, as illustrated by the strong increase in scattering intensity, turbidity and particle size.

Comparison with pure β -lactoglobulin and \hat{a} -lactalbumin

The proteins used in this system are WP isolate and their main compound is β -lg, but some molecules of \hat{a} -la are also present in the powder. It is more likely that the β -lg will mostly determine the complexation with GA. This hypothesis was checked by comparing the behavior of WP with >90% pure β -lg and >90% pure \hat{a} -la. Figure 2.2 represents the turbidity as a function of pH for WP/GA, β -lg/GA, and \hat{a} -la/GA. The turbidity of the mixture of WP/GA and the mixture of pure β -lg/GA strongly increases at the same $pH_{\hat{O}1}$ ($pH_{\hat{O}1} = 4.7$). However, the $pH_{\hat{O}1}$ of \hat{a} -la/GA shifts to $pH_{\hat{O}1} = 4.1$. This result confirms that the interaction between WP/GA is mainly driven by the interaction

of β -lg with GA, and especially concerning the pH_c and pH_{ϕ_1} values. The difference between the pH_{ϕ_1} of β -lg/GA and α -la/GA is easily understandable since the pI of α -la is 4.1 and the pI of β -lg is 5.2.

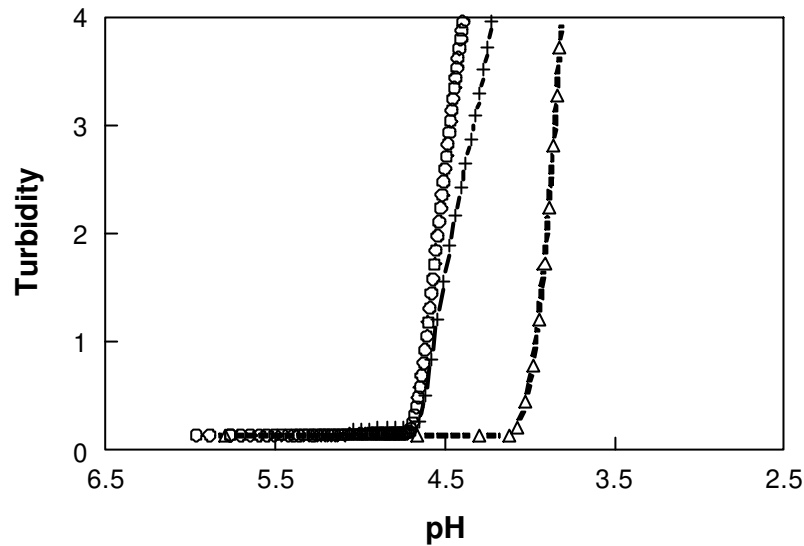


Figure 2.2: Mixture of proteins and gum arabic, $C_p = 0.1\%$, Pr:Ps ratio = 2:1, $[\text{NaCl}] = 7 \text{ mM}$, $[\text{GDL}] = 0.13\%$, Temperature = 25°C , (\circ): WP/GA, (+) β -lg/GA; (Δ): α -la/GA.

Therefore, one can conclude that the pH boundaries pH_c (not shown here) and pH_{ϕ_1} are due to the formation of a complex between the β -lg and the GA mainly. Of course α -la might form coacervates with the GA as well at lower pH values ($\text{pH} < 4.1$) where the β -lg/GA coacervates are already formed. Then the structure of the coacervates, in the two phase region, might be changed or at least influenced by the presence of other proteins in the WP isolate. Furthermore, the β -lg molecule is mainly present as a dimer in solution. However, if some monomers are present, their pI being lower, they might also interact with the GA at lower pH values. However, all this will not influence the main results of this paper.

The values of pH_c and pH_{ϕ_1} depend on several parameters such as the pI of the protein, the biopolymer ratio (for the pH_{ϕ_1} only), the ionic strength, the molar masses of the biopolymers, but does not depend – or very little - on total biopolymer concentration [Mattison *et al.*, 1995, 1999]. Some previous experiments (not reported here) showed that pH_{ϕ_1} is influenced by the Pr:Ps ratio (by increasing the Pr:Ps, the pH_{ϕ_1} shifts to

higher pH values, since more proteins are available per polysaccharide chain). In this work the Pr:Ps ratio was kept constant at 2:1, since the pH window where complexation occurs was easily reachable with GDL titration. In the present study, special attention was given to the influence of the ionic strength and the total biopolymer concentration on the phase boundaries. The temperature was kept constant at 25°C.

Effect of the ionic strength

The influence of the ionic strength was studied by adding various amounts of microions (NaCl) to a mixture of 0.1% WP and GA ($C_p = 0.1\%$, Pr:Ps = 2:1). Similarly to the previous experiment, the turbidity and the scattering intensity of the mixtures were monitored during acidification. Figure 2.3a highlights the strong effect of salt concentration on complex formation, since the addition of NaCl causes a significant decrease of the pH_{δ_1} to lower values. Besides, with increasing ionic strength, the intensity corresponding to the soluble complexes phase decreases.

The effect of ionic strength on complex coacervation is a well-known phenomenon. The microions present in the solution screen the charges of the polymers and thus reduce the range of their associative interactions [Bungenberg de Jong, 1949b; Schmitt *et al.*, 1998; Overbeek and Voorn, 1957]. As a result, the polymers interact at a lower pH, where the protein carries more positive charges. The screening of the charges reduces also the number and the stoichiometry of soluble complexes formed, and the scattering intensity between pH_c and pH_{δ_1} is therefore lower.

However, it should be noticed here that complexation is influenced by salt concentration above a certain value only. Indeed, as displayed in Figure 2.3a, pH_{δ_1} has the same values between $I=7.6$ mM and $I=20.3$ mM. The addition of small amounts of microions even slightly enhances the coacervation by promoting the solubility of the polymers (coiling of the molecule); the access to the charge is then favored, and so is the electrostatic attraction [Burgess, 1990]. On the other hand, a high salt concentration inhibits complexation by total screening of the charges.

The interaction between GA and WP is a function of their charge density. This charge density is dependent on the pH for the WP but also for the GA since it is a weak (pH-dependent) polyelectrolyte. The electrophoretic mobility measurements made by Schmitt *et al.* (1999) showed that GA tended to electroneutrality at pH 3.5. This method was previously used by Burgess and Carless (1984) for the same polysaccharide and they measured a zero mobility at pH = 2.2. Schmitt *et al.* (1999) explained the

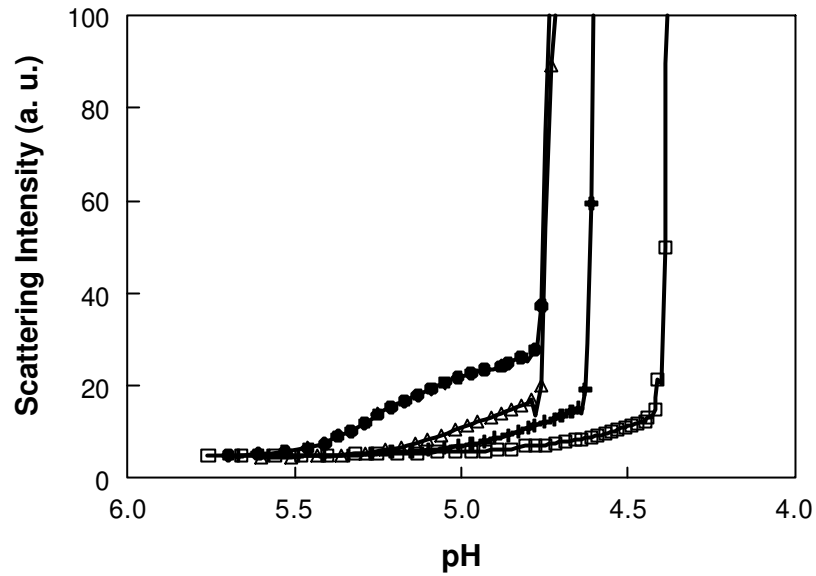


Figure 2.3a: Influence of salt on a mixture of WP/GA, total biopolymer concentration = 0.1%, Pr:Ps ratio = 2:1, [GDL] = 0.07%, Temperature = 25°C, (●): $I_{ni} = 4$ mM, $I_{fin} = 8$ mM; (▲): $I_{ni} = 17$ mM, $I_{fin} = 20$ mM; (■): $I_{ni} = 26$ mM, $I_{fin} = 30$ mM; (◻): $I_{ni} = 35$ mM, $I_{fin} = 39$ mM.

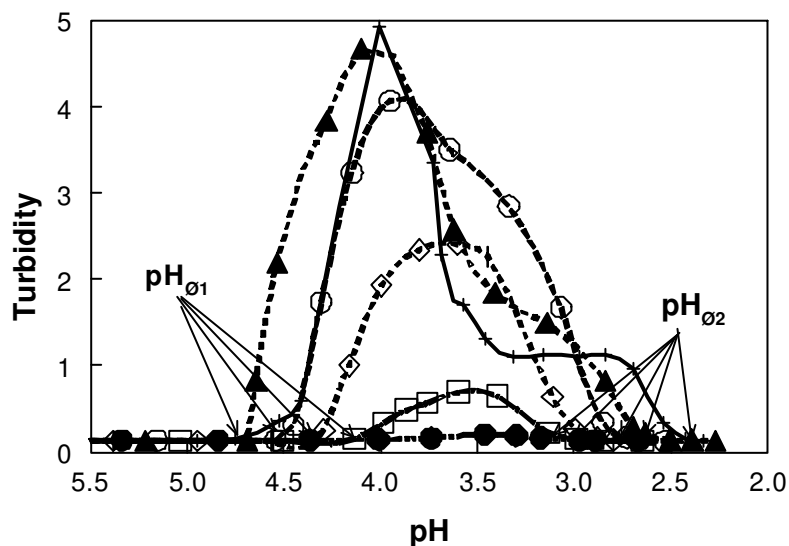


Figure 2.3b: Titration with HCl at different ionic strengths of a mixture of WP/GA, total biopolymer concentration = 0.1%, Pr:Ps ratio = 2:1, Temperature = 25°C; (●): $I_{ni} = 0$ mM; (▲): $I_{ni} = 17$ mM; (■): $I_{ni} = 30$ mM; (◻): $I_{ni} = 40$ mM; (●): $I_{ni} = 50$ mM; (▲): $I_{ni} = 60$ mM.

difference by the probable polydispersity and the origin of the GA sample. From our following results, a zero mobility measurement at pH 2.2 seems more probable, since complexation was observed until pH 2.5.

The behavior of the mixture ($C_p = 0.1\%$, Pr:Ps = 2:1) was followed across the pH range 6.0 – 2.0 by HCl titration (this experiment could not be performed with GDL down to this low pH). Examining the $pH_{\hat{O}1}$ determined with the GDL acidification method gave results identical with those determined by HCl acidification. The influence of ionic strength on the turbidity of the system was studied in a broader pH range. As illustrated in Figure 2.3b, below a certain pH (<3.0), the biopolymer mixture exhibits a loss of turbidity, indicating that phase separation is suppressed at $pH_{\hat{O}2}$. A maximum in turbidity and two limiting pH values of complexation ($pH_{\hat{O}1}$ and $pH_{\hat{O}2}$) are observed, and the region between $pH_{\hat{O}1}$ and $pH_{\hat{O}2}$ narrows when the ionic strength is increased. The erratic shape of the curves is due to a phase separation of the sample during the measurement, since at these pH values the mixtures are highly unstable.

By plotting the pH_c , $pH_{\hat{O}1}$ and $pH_{\hat{O}2}$ as a function of the ionic strength, the phase boundaries of the 0.1% mixture of WP and GA are identified (Figure 2.4). This resulting state diagram is consistent with the three phases already explained in Figure 2.1, and depends on the main parameters influencing charge density (*i.e.* pH and ionic strength). Above pH_c the large overall negative charges of the biopolymers provide stable mixtures, whereas between pH_c and $pH_{\hat{O}1}$, the electrostatic associations are becoming favorable to the formation of soluble complexes but the mixture does not demix (region B in Figures 2.1 and 2.3). A further decrease in pH, between $pH_{\hat{O}1}$ and $pH_{\hat{O}2}$, leads to phase separation between insoluble complexes of oppositely charged biopolymers and the solvent. As outlined previously, the ionic strength is the other relevant parameter reported on the state diagram. The shrinking of the pH window (between $pH_{\hat{O}1}$ and $pH_{\hat{O}2}$) - from low to high NaCl concentration - is due to the screening by microions of the biopolymer charges. Plotting the turbidity value (within the two-phase region) as a function of ionic strength allows us to determine the point of salt resistance. This term was introduced by Bungenberg de Jong (1949b), and is the amount of added salt necessary to prevent coacervation. Here, a high concentration of salt (>54 mM) causes sufficient charge compensation and screening to prevent complexation of the biopolymers.

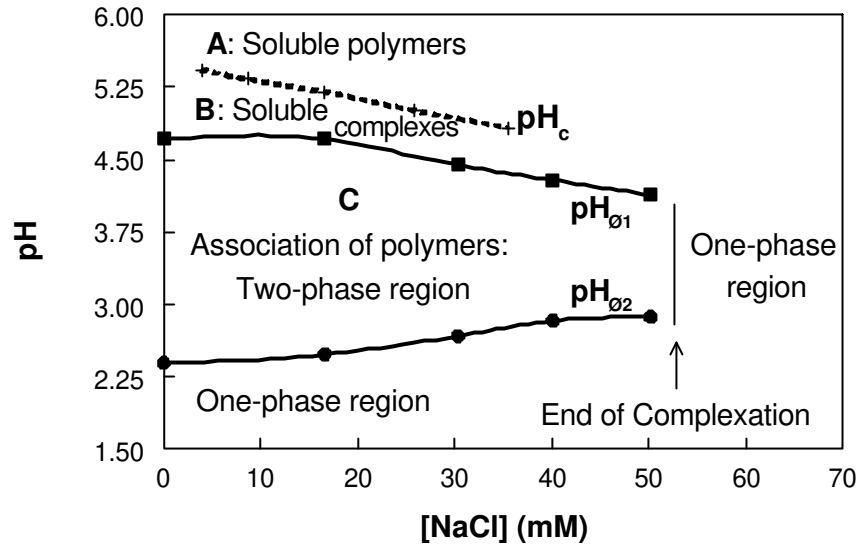


Figure 2.4: State diagram of a mixture of WP/GA, total biopolymer concentration = 0.1%, Pr:Ps ratio = 2:1, Temperature = 25°C, (+) pH_c , () pH_{θ_1} , () pH_{θ_2} .

The existence of a symmetric phase of soluble complexes was studied under highly acidic conditions (below pH_{θ_2}) using static light scattering, but soluble complexes were not observed at this low pH. The transition between the unstable and the stable region seems to be very sharp owing to the neutrality of GA, which suppresses complexation completely. Below pH_{θ_1} the attraction takes place between a fully negatively charged GA and slightly positively charged proteins. Maybe no soluble complexes can be found between highly positively charged proteins and almost neutral GA. The shape of the GA might be changed so that the interaction is not favorable anymore. However, these ideas should be checked.

Turbidity measurement, while slowly acidifying a mixture of oppositely charged biopolymers such as GA and WP, permits identification of its phase boundaries of demixing. Analytical estimates for pH_c , as discussed in the Theory section, were calculated for our system from the full solution of the random square well model and compared to the experimental data [de Vries *et al.*, 2003]. The Kuhn segment length (l_k) of the polymer was set to $l_k = 3\text{nm}$. Assuming a protein surface area of $2\pi R_p^2$ with a radius $R_p \approx 2.5\text{nm}$ gives $\partial\sigma/\partial pH \approx -0.25\text{nm}^2$ at the isoelectric point of $pI = 5.2$ for the β -lg dimer, as deduced from titration data for β -lg [Fogolari *et al.*, 2000]. Note that around

the isoelectric point there is considerable self-association of β -lg [Verheul *et al.*, 1999]. This might result in a lower protein surface area available for complexation, but this effect is not taken into account here. Comparing the experimental data with the analytical estimates gives an estimated polyelectrolyte charge density of one elementary charge per 3 nm, which is of the right order of magnitude. Indeed, one can estimate the charge density from the structure of the GA of one carboxylic group per 5 nm [Islam *et al.*, 1997]. The estimate for the proportionality constant μ for the magnitude of the surface charge density variations deduced from the experimental data is $\mu=0.35$, which is of order 1, as it should be.

Figure 2.5 shows that with these parameter values, the analytical estimates can indeed account for the experimental data. Note that for low ionic strengths complexation is predicted at pH values above the isoelectric point of the protein, as observed experimentally. The parameters values are perfectly reasonable, which further supports the interpretation of complexation above the isoelectric point as being due to strong variations of the local protein surface charge density, or, in other words, due to positively charged patches on the protein surface.

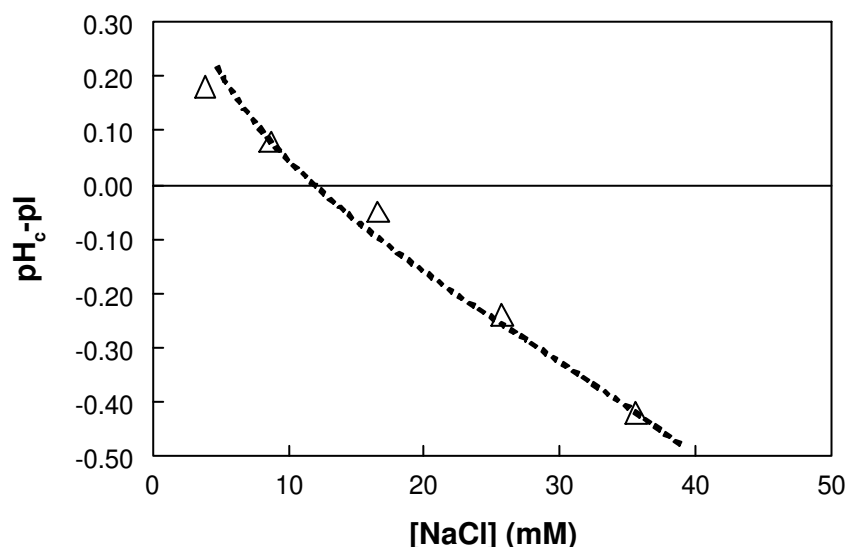


Figure 2.5: Comparison of theoretical model and experimental data of pH_c (for a mixture with $C_p = 0.1\%$, Pr:Ps ratio = 2:1, Temperature = 25°C). (Δ): experimental points and dashed line: theoretical model by de Vries *et al.* (2003) which estimates pH_c at which weakly charged polyelectrolytes and globular proteins start forming soluble complexes.

Effect of the total biopolymer concentration

The determination of the transition pH, previously described for $C_p = 0.1\%$, was performed for other biopolymer concentrations (in the range $0.05\% - 1\%$), and the results are presented in Figure 2.6. Although the general trend is that by increasing C_p (from 0.05% to 1%) the $pH_{\hat{O}1}$ shifts to higher values, the investigation shows slightly less profound effects at low ionic strengths. Indeed, for $C_p = 0.05\%$ and 1% and $[NaCl] < 20$ mM, the $pH_{\hat{O}1}$ is initially constant and then decreases with increasing $[NaCl]$, whereas for a C_p of 0.5% and 1% , no significant difference in $pH_{\hat{O}1}$ is noticeable. Owing to experimental limitations, the pH_c was difficult to determine for all ionic strengths, especially for $C_p < 0.1\%$ and $C_p > 1\%$. However, when no NaCl was added to the mixtures, the pH_c had the same value ($pH_c \sim 5.5$) for all the total biopolymer concentration.

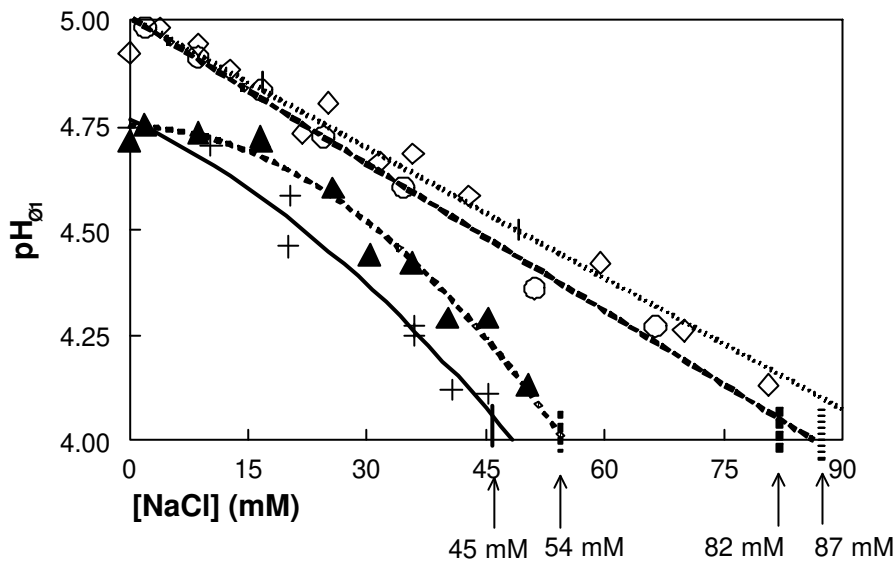


Figure 2.6: State diagram ($pH_{\hat{O}1}$) of a mixture of WP/GA at various total biopolymer concentrations (C_p), Pr:Ps ratio = 2:1, Temperature = 25°C , (+): $C_p = 0.05\%$; (o): $C_p = 0.10\%$; (x): $C_p = 0.50\%$; (Δ): $C_p = 1.00\%$

Examining the stable values of pH_c for various C_p supports the hypothesis that soluble complexes are formed between a single polysaccharide and a given amount of proteins, therefore independently of the total amount of biopolymers. This result is in good agreement with the particle size results (Figure 2.1b) that shows that the size of

the soluble complex shrinks upon addition of WP and remains constant between pH_c and $\text{pH}_{\delta 1}$. The independence of the pH_c value of concentration was already reported by Mattison *et al.* (1995, 1999) for a system of BSA-PDADMAC, where the total solute concentration, at constant Pr:Ps ratio, had no effect on either pH_c or $\text{pH}_{\delta 1}$. These results are consistent with ours on pH_c but not on $\text{pH}_{\delta 1}$, probably due to our use of biopolymers at higher concentrations. Indeed Mattison *et al.* reported no mass-action law on his system in a C_p window 0.01% - 0.3%, whereas the C_p window in this study is broader and higher (0.05% - 1%). Besides, biopolymers were used instead of synthetic polymers. For a similar system ($\hat{\alpha}$ -lg and GA), Schmitt (2000b) found that increasing biopolymer concentration reduces the influence of pH on complex coacervation, which is in accordance with our study. At $C_p = 0.5\%$ and 1% , the shift in the $\text{pH}_{\delta 1}$ values is not as significant as for lower concentrations.

The binary phase diagram, obtained at pH 3.5, provides information on the influence of the concentration of microions as a function of total biopolymer concentration. Here, higher values of C_p were measured (up to 20%). In Figure 2.7, the phase diagram built with various methods clearly illustrates the boundaries above which the biopolymer mixture remains stable. Conductivity measurements indicate the amount of salt present in the mixture and are another measure of the ionic strength. In the main graph, the conductivity due to the presence of the biopolymers itself was subtracted and only the influence of NaCl was plotted. However, the conductivity due to the presence of all ions is reported in the inset of Figure 2.7. The shift of the phase line to higher conductivity values is due to the presence of the counterions.

Using the “adding salt” method, the salt concentration ($[\text{NaCl}]$) at which the complexes dissociated was determined. A high ionic strength inhibits complex coacervation and this critical $[\text{NaCl}]$, also called salt resistance, varies with C_p . Indeed, as C_p increases up to 1%, a larger increment of NaCl is required to reach the point of salt resistance, but for $C_p > 1\%$ the critical $[\text{NaCl}]$ decreases finally to zero for $C_p = 15\%$. An optimum C_p could then be determined at $C_p = 1\%$. And at $C_p = 15\%$, the loss of turbidity is indicative of a stable mixture, phase separation does not take place (with the “adding salt” method).

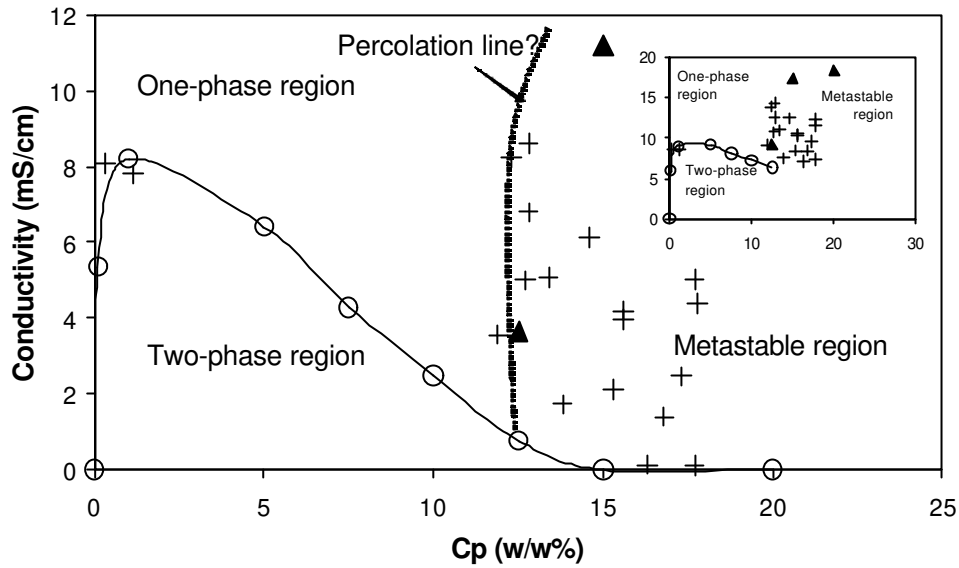


Figure 2.7: Phase diagram of mixtures of WP/GA, Pr:Ps ratio = 2:1, pH 3.5, Temperature = 25°C, with the “adding salt method” (○), “removing salt method” (△), and the “dilution method” (+). In the inset, the conductivity due to the presence of all ions is plotted.

These results are in agreement with the previous results shown in Figure 2.6, where a pH_{01} shifts to higher values as the C_p increases to 1%. Furthermore, at low C_p and for a conductivity of 6 mS/cm, the system is in the one-phase region, since the microions are screening the charges of the biopolymers. If one increases the C_p to 0.5%, there are not enough microions to screen the additional biopolymer added; the system is moved to the two-phase region.

The effect of the total biopolymer concentration is not extensively reported in the literature, and it varies depending on the polyelectrolytes used. As discussed by Burgess (1990) for a system of gelatin-BSA, the salt resistance of a mixture varies with the total polymer concentration (the amount of microions required for suppression of complexation increases with increasing the concentration, until the maximum intensity is reached, and then decreases). Our results are in agreement with hers. Moreover, an optimum C_p of 2%, was already observed for a pectin-gelatin system by McMullen *et al.* (1982), who explained it in terms of a mass action effect. Then, above this optimum C_p , the efficiency of coacervation is decreased, as illustrated in the phase diagram (Figure 2.7). Indeed, increasing the total biopolymer concentration favors the release of more counterions in solution, which screen the charges of the biopolymers, suppressing coacervation, and increasing the solubility of the coacervates. The phase

diagram built by the “adding salt” method (Figure 2.7) points out the characteristic features of complex coacervation as described in the theory of Overbeek and Voorn (1957). Below a critical salt concentration and a critical polymer concentration, the mixture demixes in a polymer rich phase and an aqueous phase poor in polymers. The composition of the two phases becomes closer when the concentration of microions is increased, and finally reaches a critical point, beyond which phase separation no longer occurs.

The phase diagram was also built using different methods at high C_p , by using a second method (“removing salt”). For $C_p > 12.5\%$ the mixtures become much more unstable and exhibit a high turbidity even at high concentration of microions. Since one cannot exclude the possibility of protein adsorption of the resins, a third method was used. This “dilution method” provides further evidence for this unstable region. It seems that above 12.5% of biopolymers the system is in a “metastable” state. Indeed, the measurements were difficult to duplicate (they were unstable at different C_p values) but they all show instability in these regions for the “dilution method” and the “removing salt method”. However, this region was not found using the “adding salt” method, which means that it is path-dependent. Furthermore, this instability occurs only when both biopolymers are in solution. Controls with only WP and only GA stayed clear, refuting the hypothesis that this high turbidity would be induced by the aggregation of one of the biopolymer.

Our tentative and imaginative explanation of the results is as follows. As shown in Figure 2.7 WP/GA form complexes, which can be viewed as new and separate entities. These new particles are dynamic in nature; *i.e.* the WP and the microions can be exchanged. On a time average scale these “WP/GA particles” have an effective interaction potential (not to be confused by the potential between the WP and the GA). The interaction potential is probably repulsive just below pH_c but is strongly attractive at pH_{ϕ_1} . In the two-phase region (*e.g.* at pH 3.5) the interaction potential between the WP/GA complexes is also a function of salt concentration.

Now, the shape of the phase diagram in Figure 2.7 is reminiscent of a gas-liquid demixing of a polymer or colloid in solution, where salt concentration here would play the role of temperature in a gas-liquid demixing [Poon *et al.*, 1996]. Therefore, Figure

2.7 can be understood as the coexistence of two phases: a dilute phase and a concentrated phase of WP / GA complexes. The analogy goes even further. Just as in gas-liquid demixing, a solid (crystal) phase appears at high concentrations. For colloid mixtures, this phase is usually hidden under a glass phase delimited by a percolation line. The position of the percolation line depends very much on the range of the colloidal attractions [Poon *et al.*, 1996]. Short-ranged interactions tend to shift the glass transition to lower concentrations. Possibly therefore complexes of strong polyelectrolytes form “precipitates”. For the WP/GA system interactions seem to be relatively weak (low charge density and screening by uncharged polymer) and then the glass transition would be expected at a higher concentration. The unpredictable behavior in the glass state region shows similarities to systems that show delayed creaming or delayed phase separation. The dynamics of the system are time and preparation path dependent. It is therefore suggested that much of the phase behavior can easily be understood by considering the WP/GA complexes as separate entities and the strength of their attractive interactions depends on salt concentration. Sure enough the description is speculative, but the parallels with colloidal demixing are striking.

CONCLUSIONS

The in situ titration method – using GDL – combined to light scattering, turbidity and particle size measurement allowed us to follow the formation of soluble and insoluble complexes. The complexation of WP and GA seems to be mainly driven by the interaction of β -lg (main component of the WP) and GA. The effect of various parameters on the complex coacervation between WP and GA has been investigated. A state diagram was built, where the two main parameters influencing complex coacervation are taken into account (*i.e.* pH and ionic strength). It revealed the region of stability and instability of the system. Below a certain pH_c , WP and GA form electrostatic (stoichiometric) complexes as predicted by a theoretical model. A lower boundary ($\text{pH}\phi_2$) was found due to the neutrality of the GA. The pH window where complex coacervation occurs shrinks with increasing ionic strength, due to the screening of the charges by the microions. Although the effect of total biopolymer concentration is certainly less evident than the influence of pH and ionic strength, it is, however, relevant, since an optimum concentration exists, where complex coacervation

is maximum. The complexes can be viewed as separate entities, where interaction depends on salt concentration. At low salt concentration, the complexes demix into a complex rich and a complex poor phase, just as in a gas-liquid coexistence. At high concentrations, a glassy state with poorly defined kinetics is formed. Future work includes a further experimental confirmation and a better understanding of the formation of the soluble complexes and the structure of the coacervate phase. Other polysaccharides will be tested as well.

ACKNOWLEDGEMENTS

The authors wish to express their gratitude to Friesland Coberco Dairy Foods (FCDF) for sponsoring this work. We thank the Colloides Naturels International Company and in particular T. Kravtchenko for giving us GA. Professor Martien Cohen Stuart and Professor Erik van den Linden are thanked for encouraging discussions. Dr. Remco Tuinier is acknowledged for a critical reading of this manuscript.

CHAPTER 3

Complex Formation of Whey Protein / Exocellular Polysaccharide EPS B40*

ABSTRACT

Whey proteins (WP) and the exopolysaccharide B40 (EPS B40) form electrostatic complexes under specific conditions. EPS B40 is a natural thickener in yogurt-like products. It is a phosphated polysaccharide and thus has a strong polyelectrolyte character. When the WP and the EPS B40 were mixed at pH values near or below the isoelectric point (pI) of the protein, soluble complexes were formed at pH_c and phase separation took place below pH_ϕ . The formation and the structure of those complexes were studied by various methods, including turbidity, dynamic and static light scattering (DLS and SLS), and viscosity measurements. The results showed that the strength of the interaction was strongly pH- and salt-dependent. The zeta-potential of the protein at pH_c and pH_ϕ was linearly dependent on the square root of the ionic strength (\sqrt{I}), showing the electrostatic nature of the interaction. Light scattering and viscosity measurements provided new results on the behavior of the complexes at the molecular level. In the region where the complexes were still soluble and at low ionic strength, the DLS radius measured in the WP/EPS B40 mixture was smaller than the coil size in the EPS B40 solution but the apparent molar mass was increased. The increase of the molecular mass was attributed to the complexation of WP on the EPS B40 chain, which, at low salt, induced a reduction of the intramolecular repulsion and led to the compaction of the polysaccharide. Also, the ratio of protein to polysaccharide was varied in order to get more insights into the dynamics, the structure and the apparent stoichiometry of the EPS B40/WP complexes. The results illustrated that phase separation was a consequence of charge neutralization of the complexes and that the apparent stoichiometry of the complexes depends on the order of mixing of the compounds. In time, the complexes rearranged to form neutralized complexes and free EPS B40. The concept of cooperative binding was highlighted in the case studied.

*F. Weinbreck, H. Nieuwenhuijse, G. W. Robijn, C. G. de Kruif
Langmuir **2003**, *19*, 9404-9410.

INTRODUCTION

Associative interactions between proteins and polysaccharides, *i.e.* between amphiphiles and strong polyelectrolytes, are of relevance for many products in both food and pharmaceutical science [Dickinson, 1998; Doublier *et al.*, 2000; Sanchez and Paquin, 1997; Tolstoguzov, 2002]. The interactions between proteins and polysaccharides can be either repulsive, or attractive. The last induces interbiopolymer complexing, which almost always arises from electrostatic interactions between opposite charges on the biopolymers. At pH values below their isoelectric point (pI), proteins carry positive charges and can interact with polysaccharides bearing carboxylic, phosphate or sulfate groups. The first empirical experimental studies were made by Bungenberg de Jong in the 1940's (1949a, 1949b, 1949c), studying the complex coacervation of gelatin and gum arabic. The theoretical work on complexing oppositely charged polymers was initialized by Overbeek and Voorn (1957). They extended the Flory-Huggins theory with an extra term accounting for electrostatic interactions, for which they used the Debye-Hückel approximation. Later theories on complex coacervation were refinements of the Overbeek-Voorn theory. A number of recent theoretical papers deal with the complexation of homogeneously charged spheres and oppositely charged polyelectrolytes [Netz and Joanny, 1999; Nguyen and Shklovskii, 2001]. They could be applied to the complexation of oppositely charged proteins and polyelectrolytes. Recently, de Vries *et al.* (2003) considered the binding of a polyelectrolyte to the surface of a protein by considering the protein as a sphere with random charge patches, explaining the complexation between similarly charged proteins and polyelectrolytes (above the pI of the protein).

Current work in the field reports the influence of various parameters (*e.g.* charge density, pH, ionic strength, and biopolymer concentration) on the electrostatic interactions of polymers [Dubin and Oterie, 1983; Schmitt *et al.*, 1998]. It is now well-known that pH and ionic strength are key parameters that can regulate the strength of the electrostatic interactions. Mattison *et al.* (1995), for example, reported the phase boundaries of protein-polyelectrolyte systems. Using turbidimetric titrations, they determined the pH-induced structural transitions of synthetic polymer complexes. The formation of soluble protein-polyelectrolyte complexes was initiated at pH_c , which preceded the pH of visual phase separation at pH_b [Mattison *et al.*, 1995; Dubin *et al.*,

1987; Kaibara *et al.*, 2000]. These pH-induced transitions were also determined for whey proteins and gum arabic [Weinbreck *et al.*, 2003a; Weinbreck and de Kruif, 2003b]. Gum arabic is a polysaccharide that carries carboxylic groups and can be considered as a weak polyelectrolyte whose charge density is pH-dependent. The electrostatic interactions between whey proteins and gum arabic lead to the formation of coacervates in the pH window between 2.5 and 4.8 [Weinbreck *et al.*, 2003a; Weinbreck and de Kruif, 2003b; Schmitt *et al.*, 1999; Schmitt 2000b].

However, many of the polysaccharides used in food systems are of the strong polyelectrolyte- type, for example, the carrageenans and the exopolysaccharide B40 (EPS B40) from lactic acid bacteria, carrying sulfate and phosphate groups, respectively. The objective of this work was to study the interaction between whey proteins and a phosphated polysaccharide naturally present in yogurt-like products, the exopolysaccharide EPS B40. The EPS B40 is excreted by the lactic acid bacterium *Lactococcus lactis* subsp. *cremoris* NIZO B40 during fermentation and thus acts as a natural thickener in acidified milk products. EPS B40 has already been extensively studied at NIZO food research from a genetic point of view [van Kranenburg, 1999]; the physical properties of the EPS and its role in fermented milks have been studied by van Marle *et al.* (1999) and Ruas-Madiedo *et al.* (2002), and the segregative phase separation between EPS B40 and dairy proteins at neutral pH was studied by Tuinier *et al.* (1999, 2000). Thus, the anionic polysaccharides play an important role in the texture and stability of dairy/food products. Since almost all food products have an acidic pH, it is clear that the complex formation between proteins and polysaccharides is of prime interest. This model study aims to clarify, first, whether pH transitions and soluble/aggregated complexes are formed for a mixture of whey proteins and EPS B40 in acidic conditions at various ionic strengths, using turbidity measurements. The formation of soluble complexes was explored at the molecular level using three different methods (*i.e.* dynamic and static light scattering and viscosity measurement). Finally, the influence of the protein to polysaccharide (Pr:Ps) ratio and the order of polymer mixing allowed more insights into the structure, the properties, and the apparent stoichiometry of the complexes which were previously unknown.

EXPERIMENTAL SECTION

Materials

Bipro is a whey protein (WP) isolate consisting mainly of 75% β -lactoglobulin (β -lg), and 15% α -lactalbumin (α -la) - from Davisco Foods International (Le Sueur, MN). Residual whey protein aggregates were removed by acidification as previously described [Weinbreck *et al.*, 2003a]. The exopolysaccharide EPS B40 was produced and isolated from *Lactococcus lactis* subsp. *cremoris* NIZO B40 at NIZO food research (The Netherlands) as described by Tuinier *et al.* (1999). The freeze-dried powder was stored at 5°C. It contains 63% EPS B40, 18% protein, 8% ash, 6% mannan-rich material and 5% water. The weight-averaged molar mass (M_w) and the average radius of gyration (R_g) were determined with SEC MALLS ($M_w = 1620$ kg/mol and $R_g = 86$ nm). The ionic strength was adjusted by addition of reagent-grade NaCl. Deionized water was used in all experiments. Control measurements with only WP and only EPS B40 were systematically carried out under the same conditions as the mixtures of biopolymers. The zeta-potential of the WP and EPS B40 mixture was measured as a function of pH with a Zetasizer 2000 (Malvern, USA).

Turbidimetric titration under acidification

Mixtures of WP and EPS B40 (initial pH = 7) were acidified by dropwise addition of HCl. The influence of the ionic strength ($[NaCl] = 0 - 1M$), the protein to polysaccharide ratio (Pr:Ps = 1:1 - 25:1 w/w) and the total biopolymer concentration ($C_p = 0.05\% - 0.5\%$) were studied by varying one parameter at a time. The turbidity of each sample was measured as a function of the pH with a Cary 1E spectrophotometer (Varian, The Netherlands) at a wavelength of 514.5 nm (similar to previous measurements [Weinbreck *et al.*, 2003a]). The samples were put in a 1 cm path-length cuvette and the turbidity was then measured as a function of time at 25°C. The turbidity (τ) was defined as:

$$\tau = - \ln (I/I_0),$$

where I is the light intensity that passes through a volume of solution of 1 cm length and I_0 the incident light intensity. (The turbidity corresponds thus to the optical density multiplied by 2.3).

Turbidimetric titration under salt addition

The turbidity of WP / EPS B40 mixtures was followed upon addition of NaCl at pH 3 and pH 4 for $C_p = 0.1\%$ and at a Pr:Ps ratio of 2:1. The initial mixture was adjusted to pH 4 or pH 3. Then, a known amount of NaCl was added in powder form to the mixture and at each salt addition, the turbidity of the mixture was measured. Blanks of mixtures at pH 7, WP at pH 3 and EPS B40 at pH 3 were also titrated in the same way.

Static and dynamic light scattering measurement

The static light scattering (SLS) and dynamic light scattering (DLS) experiments were carried out on mixtures of 0.1% w/w biopolymer concentration at various pH values using a 22 mW HeNe laser with a wavelength of 632.8 nm. The light beam was focused on the axis of the goniometer using mirrors and a lens. The stock solutions of WP and EPS B40 were initially filtered with a 0.45 μm filter separately to avoid the filtration of some initial complexes, and the mixture of WP / EPS B40 was then centrifuged for 30 s to remove all impurities and air bubbles. The sample was placed in the cuvette housing, which was kept at a temperature of 25°C in a toluene bath. The scattering angle was varied from 30° to 150° in 10° steps. The measurement was repeated three times at each angle. The detected intensity was processed by a digital ALV-5000 correlator. From the intensity as a function of angle, the molar mass and the radius of gyration of the particles could be determined as a function of pH.

Viscosity measurement

The viscosity of the WP/EPS B40 mixtures was obtained using a capillary viscosimeter Ubbelohde (Schott Geräte, Germany), using a capillary No. 1c that can contain 20 mL of dispersion. The viscosity measurements were carried out at 25°C on samples containing 0.1% WP/EPS B40 at a Pr:Ps ratio of 2:1, and at $[\text{NaCl}] = 0$ and 25 mM. The samples were acidified with glucono- δ -lactone (GDL), and their viscosity was related to the pH of the sample. Calibration was done with water.

Titration of one polymer by the other

The titration was performed by i) slowly adding under stirring 0.1% WP into 0.1% EPS B40 (titration A) or ii) adding 0.1% EPS B40 into 0.1% WP (titration B). These titrations were done at pH 3 and at pH 4 on mixtures of low ionic strength. The Pr:Ps ratio was then recalculated and at each ratio, the turbidity of the sample was measured.

High-Performance Liquid Chromatography (HPLC) measurements

The amount of residual WP and EPS B40 in the upper phase was followed in time for a mixture of WP / EPS B40 ($C_p = 0.1\%$, Pr:Ps = 4:1, pH = 4). The samples were prepared with titrations A and B and they were left under continuous stirring for 10 days. Every day, a sample was taken out. After 2h of natural phase separation, the amount of β -lg, α -la, and EPS B40 was analyzed by HPLC, using a Biosep Sec 2000 column at a pump flow of 0.7 mL/min. The proteins were detected with the UV at 280 nm (Applied Biosystems) and the EPS B40 was detected by refraction index (RI, Erma-7510, Betron Scientific) and the concentration was extrapolated from a calibration plot.

RESULTS AND DISCUSSION

Behavior of the system as a function of pH and salt

Because the interaction between WP and EPS B40 was expected to be mainly electrostatic in nature, pH and ionic strength would play a key role in the complex formation [Schmitt *et al.*, 1998]. Indeed, pH affects the ionization degree of the amino groups of the protein, and electrostatic complexing will take place below the pI of the protein. If microions are present in the solution, they can interact with the charged groups of the polymers and affect complex formation. Therefore, the influence of pH and ionic strength on the interaction between WP and EPS B40 was first investigated by means of turbidity measurements and macroscopic observations. Figure 3.1 illustrates the turbidity of mixtures titrated with HCl for ionic strengths ranging from 0 to 200 mM.

Under acidification, the mixtures of WP/EPS B40 showed an increase of turbidity, while the turbidity of control samples with only WP or EPS B40 remained constant at a low turbidity over the whole pH range (results not shown here). The turbidity increase of WP / EPS B40 mixtures was attributed to the formation of electrostatically bound protein – polysaccharide complexes, which initially occurred at a pH close to the pI of the protein (pI = 5.2). Specifically, for $[\text{NaCl}] < 75 \text{ mM}$, the turbidity curves increased in two steps. These two pH transitions were designated as pH_c and pH_ϕ . The first increase appeared at pH_c (in the pH window 5.4 – 4.5), and the second at pH_ϕ (between pH 4.5 and pH 3), below which macroscopic phase separation took place. For $[\text{NaCl}] > 75 \text{ mM}$, only one increase in turbidity was recorded (at pH_c) and no macroscopic phase separation occurred.

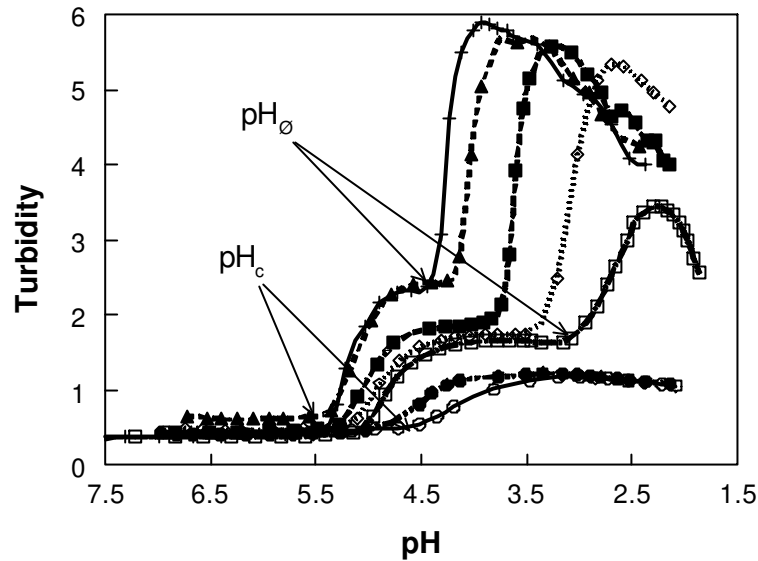


Figure 3.1: HCl titration at various ionic strengths of a mixture of WP / EPS B40, total biopolymer concentration = 0.25%, Pr:Ps ratio = 2:1, temperature = 25°C; (+): [NaCl] = 0 mM; (◻): [NaCl] = 10 mM; (◻): [NaCl] = 25 mM; (◻): [NaCl] = 40 mM; (◻): [NaCl] = 50 mM; (◻): [NaCl] = 100 mM, (◻): [NaCl] = 200 mM.

Figure 3.1 also highlights the strong effect of the addition of salt microions to the mixture. Indeed, the addition of NaCl caused a shift of pH_c and pH_ϕ to more acidic values and the maximum turbidity decreased. Figure 3.2 summarizes the results shown in Figure 3.1 by plotting the values of pH_c and pH_ϕ as a function of the ionic strength. The values of pH_c and pH_ϕ at various C_p values are also reported in the figure ($C_p = 0.05\%$, 0.1% , 0.25% , and 0.5%). The resulting state diagram illustrates that the pH boundaries (pH_c and pH_ϕ) seemed to be independent of the total biopolymer concentration, but they were strongly dependent upon ionic strength.

At $pH > pH_c$, the dispersions were fully transparent; both polymers were negatively charged, which prevented their complexation. At pH_c , the turbidity of the mixture increased, showing that some attraction between the polymers took place. However, no macroscopic phase separation occurred. This result would suggest that the formation of primary complexes between WP and EPS B40 was first induced at pH_c . Then, at pH_ϕ , the turbidity abruptly increased, illustrating further aggregation of the complexes, which will require that they approach a neutrality condition; the mixture became unstable and phase-separated in time. The pH transitions are salt dependent, which is

a well-known phenomenon. The microions screen the charges of the polymers and thus reduce the range of their associative interaction [Bungenberg de Jong, 1949b; Overbeek and Voorn, 1957; Schmitt *et al.*, 1998]. As a result, the polymers interact at a lower pH, where the protein carries more positive charges. If the [NaCl] was high enough (> 50 mM), the charges of the biopolymers were screened and the electrostatic interaction was insufficient to induce electroneutrality of the complexes and thus aggregation. Varying the total biopolymer concentration (C_p) did not seem to affect the interaction between the WP and the EPS B40 (*i.e.* pH_c and pH_ϕ). As demonstrated by Mattison *et al.* (1995), the C_p only influences the amount of complexes formed. And since the charge balance between WP and EPS B40 is not modified by increasing C_p , the phase boundaries will occur at the same pH. These results are in agreement with results previously found for synthetic polymers and other biopolymers, where two pH transitions (pH_c and pH_ϕ) were also reported [Mattison *et al.*, 1995; Weinbreck *et al.*, 2003a; Weinbreck and de Kruif, 2003b].

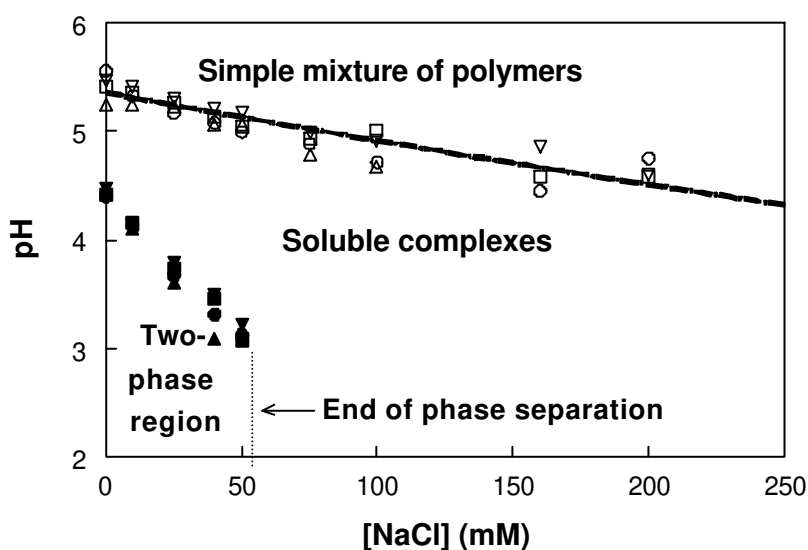


Figure 3.2: State diagram as a function of [NaCl] of a mixture of WP / EPS B40, Pr:Ps ratio = 2:1, temperature = 25°C, for various total biopolymer concentrations (C_p) (/) $C_p = 0.05\%$, (/) $C_p = 0.1\%$, (/) $C_p = 0.25\%$, (∇ /) $C_p = 0.5\%$, open symbols: pH_c and filled symbols: pH_ϕ .

Next, to check whether the aggregated complexes were reversible, the titration upon salt addition was carried out on mixtures of WP / EPS B40 at a pH where aggregation of the complexes already occurred (Figure 3.3). The turbidity of mixtures containing

initially insoluble complexes (at pH 3 and pH 4) was monitored as a function of NaCl concentration. As the ionic strength increased, the turbidity of the mixture dropped to lower turbidity values, which occurred faster at pH 4 than at pH 3 (Figure 3.3). At $[\text{NaCl}] = 200 \text{ mM}$, the turbidity values were similar to the values of the soluble complexes in Figure 3.1. Since the turbidity of the blanks (WP and EPS B40) was low (<0.5), it indicated that the turbidity at high salt concentrations was not due to a salting out of the protein (blanks not shown here). This result would suggest that at high salt concentration, soluble complexes were still present in the mixture, which is consistent with the result of the state diagram (Figure 3.2). The addition of salt weakened the interactions between the biopolymers and the precipitates dispersed spontaneously into soluble complexes. The first breaking point of the turbidity occurred at $[\text{NaCl}] = 20 \text{ mM}$ at pH 4 and $[\text{NaCl}] = 50 \text{ mM}$ at pH 3 for $C_p = 0.25\%$. These values corresponded to the salt concentration at which the phase boundary was crossed in Figure 3.2 (denoted as the point of salt resistance) [Bungenberg de Jong, 1949b]. The formation / dissociation of the aggregated complexes was thus reversible. The soluble complexes remained in solution in the salt concentration range studied.

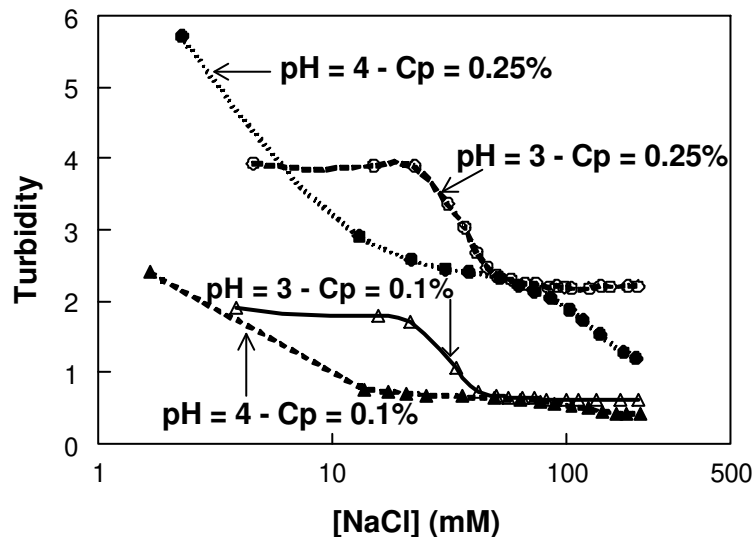


Figure 3.3: Salt titration of WP / EPS B40 mixtures, Pr:Ps = 2:1, temperature = 25°C , (/): $C_p = 0.1\%$, (/): $C_p = 0.25\%$, open symbols: pH 3, filled symbols: pH 4.

The effect of pH on the complex formation arises from the dependence of protein charge density on pH [de Vries *et al.*, 2003; Mattison *et al.*, 1999]. The influence of ionic strength can easily be understood if the complexation is mainly electrostatic in nature. Indeed, by addition of microions, electrostatic screening causes pH_c and pH_ϕ to decrease with increasing ionic strength. In a previous study, the value of the zeta-potential of the protein has been determined as a function of pH (results not shown here). Therefore, another representation of the state diagram would be to convert pH (pH_c and pH_ϕ) to protein zeta-potential and plot it as a function of the square root of the ionic strength (\sqrt{I}) (Figure 3.4).

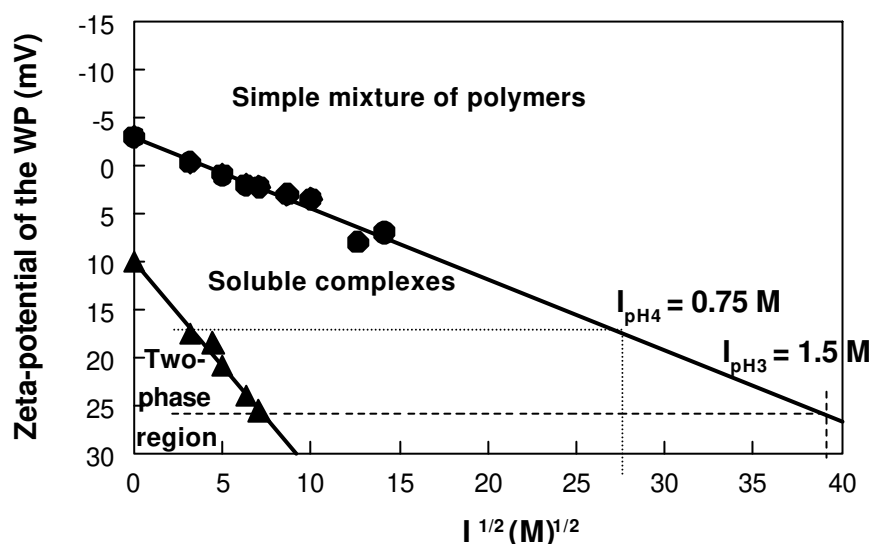


Figure 3.4: Data of Figure 3.2 presented as the zeta-potential of WP as a function of the ionic strength ($I^{1/2}$) for a WP / EPS B40 mixtures, Pr:Ps = 2:1, Temperature = 25°C, (●): Zeta-potential at pH_c (▲): Zeta-potential at pH_ϕ .

Both zeta-potentials at pH_c and pH_ϕ were linear with \sqrt{I} , showing that the critical surface charge density was proportional to the Debye-Hückel parameter ($\hat{\epsilon}, \hat{\epsilon} \sim \sqrt{I}$) and that the system is thus controlled by electrostatic forces. This result is consistent with several theoretical treatments [Muthukumar, 1987, 1995; Evers *et al.*, 1986], and this relation has already experimentally been described for a complexation between proteins and a synthetic strong polyelectrolyte [Mattison *et al.*, 1995]. If the linear relation is extrapolated, the presence of soluble complexes would then be suppressed at $[NaCl] =$

0.75 M at pH 4 and 1.5 M at pH 3. From general properties of the Debye-Hückel term, it is evident that adding salt promotes decomplexation.

Events at the molecular level

To get more insights into the complexation at the molecular level, light scattering experiments (SLS and DLS) were carried out on a mixture of 0.1% WP/EPS B40 at Pr:Ps = 2:1 - and on EPS B40 blanks - as a function of pH. The values of the R_g and M_w of the mixture were normalized to the values of the R_{g0} and M_{w0} of the EPS B40 blank (Figure 3.5).

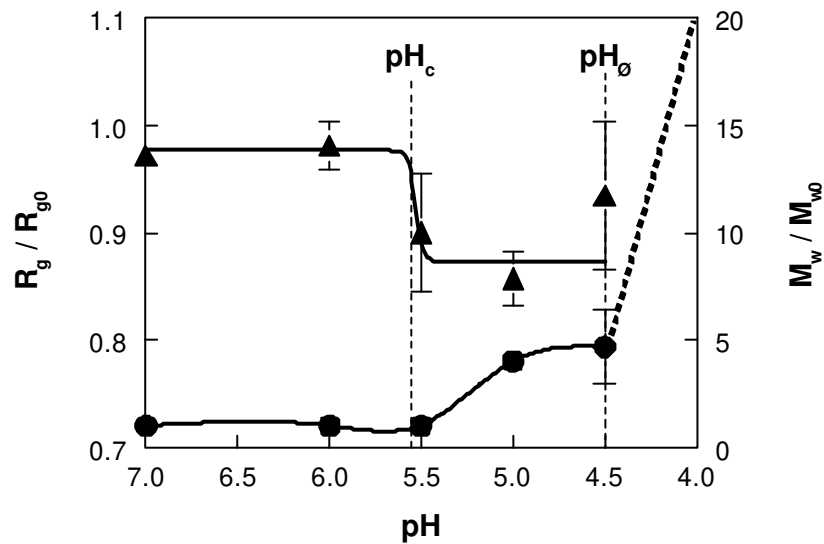


Figure 3.5: Normalized molecular weight (M_w/M_{w0}) and radius of gyration (R_g/R_{g0}) of a mixture of WP / EPS B40 compared to an EPS B40 blank, Pr:Ps = 2:1, total biopolymer concentration = 0.1%, temperature = 25°C; [NaCl] = 0 mM; (Δ): M_w , (\circ): R_g .

At $pH > pH_c$, R_g was close to the value of R_{g0} ($R_g / R_{g0} = 1$) and the M_w in the mixture was equal to the M_{w0} of the EPS B40 blank ($M_w / M_{w0} = 1$). Between pH_c and pH_ϕ , the R_g of the EPS B40 in the mixture decreased by 12% of its initial size and the M_w of the polymer increased by a factor of 4. In view of the fact that Pr:Ps = 2:1, an M_w increase of a factor of 3 would be expected. Indeed, if we estimate that all the WP interacts with the EPS B40 (maximum interaction), the M_w of the complex will be $2 \times M_w + 1 \times M_w$, since the Pr:Ps ratio is expressed in w/w. The experiments showed an increase of a factor of 4, which is, concerning the uncertainties, in good agreement with the

estimation. At pH_ϕ , the M_w strongly increased and the sample was very turbid. Since the experiments were carried out at low salt concentrations, long-range interactions took place in the system and the values of R_g and M_w will therefore be uncertain. Besides, because of the polydispersity of the sample and the difficulty of interpreting light scattering experiments on turbid systems (for $\text{pH} > \text{pH}_\phi$), viscosity measurements were carried out in order to check if the same trend is found as with the light scattering.

Figure 3.6 represents the evolution of the viscosity of a mixture of WP/EPS B40 ($C_p = 0.1\%$, Pr:Ps = 2:1) as a function of pH, compared to a blank of EPS B40, at $[\text{NaCl}] = 0$ and 25 mM. For $[\text{NaCl}] = 0$ mM, the viscosity of the EPS B40 blank was larger than the viscosity of the WP / EPS B40 mixture, which could be explained by the fact that the ionic strength was increased when acid was added to the mixture. The viscosity of the WP / EPS B40 mixture decreased as a function of pH and especially at pH_c and pH_ϕ (determined by turbidity measurements), where two breaking points could be noticed. On the other hand, for $[\text{NaCl}] = 25$ mM, both the viscosity of the blank of EPS B40 and the viscosity of the mixture of WP / EPS B40 remained constant until pH_ϕ , where the viscosity of the mixture of WP / EPS B40 decreased. The viscosity of a dilute polymer mixture is directly related to the size of the particle. Therefore, the viscosity measurement is another means of measurement of the particle size, which is less influenced by the polydispersity (and turbidity) of the sample. Bungenberg de Jong (1949b) used this type of measurement, and he attributed the decrease in the viscosity before and during the actual complexation to a reduction of the amount of liquid occluded inside the complexes. The decrease in viscosity of polyelectrolyte systems has been used to determine the optimum conditions of complexation [Ganz, 1974; Koh and Tucker, 1988a] and it was reported that the low viscosity close to the point of complexation is consistent with intrapolymer condensation [Dubin and Oteric, 1983].

As illustrated in Figures 3.5 and 3.6, the size reduction of the polymer with a simultaneous increase of the molecular weight highlights the complexation of WP molecules to the EPS B40 chain, indicating the formation of soluble complexes. The shrinkage of the EPS B40 molecule, occurring at low ionic strength and not at $[\text{NaCl}] = 25$ mM, could be understood as a reduction of the intramolecular repulsion induced by the interaction of the WP with the phosphate group of the EPS B40. At low ionic strength, this interaction could even occur at a pH above the pI of the protein (pI = 5.2)

because of the presence of positive “patches” on the WP [de Vries *et al.*, 2003; Dubin *et al.*, 1994; Wen and Dubin, 1997]. In this pH window, the mixture did not phase separate; therefore, the complexes are called “soluble complexes”. Furthermore, the increase of turbidity in the soluble complexes region in Figure 3.1 can now be attributed to an increase of the molecular weight of the compounds and not an increase of their size. At pH_ϕ the complexes aggregate together, as shown by the dramatic increase of the molecular weight and the strong decrease of the viscosity due to two-phase flow / phase separation.

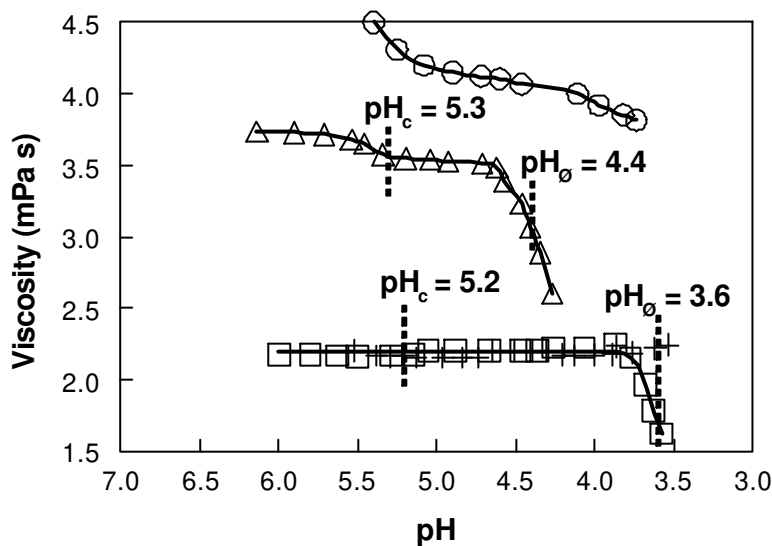


Figure 3.6: Viscosity measurement of (○): a blank of EPS B40, $C_p = 0.03\%$, $[\text{NaCl}] = 0 \text{ mM}$; (△): a mixture of WP / EPS B40, $C_p = 0.1\%$, Pr:Ps ratio =2:1, $[\text{NaCl}] = 0 \text{ mM}$; (+): a blank of EPS B40, $C_p = 0.03\%$, $[\text{NaCl}] = 25 \text{ mM}$; (□): a mixture of WP / EPS B40, $C_p = 0.1\%$, Pr:Ps ratio =2:1, $[\text{NaCl}] = 25 \text{ mM}$; temperature = 25°C.

The results presented here for a strong polyelectrolyte were reminiscent of the results found previously for a weak polyelectrolyte (gum arabic) [Weinbreck *et al.*, 2003a]. The influences of parameters such as pH and salt were similar. However, some soluble complexes were still present at high salt concentrations for WP/EPS B40, which was not the case for WP/gum arabic. The interaction between WP and EPS B40 is stronger than that of WP and gum arabic, because of the higher charge density of the EPS B40.

Protein to polysaccharide ratio and dynamics of complex formation

The influence of the protein to polysaccharide ratio (Pr:Ps) and the order of mixing the biopolymers provided information on the structure, apparent stoichiometry, and dynamics of the complexes.

The state diagram of Figure 3.7 was determined using turbidimetric titration under acidification as a function of the Pr:Ps ratio. It represents the region of stability and instability of a mixture of WP/EPS B40 as a function of the Pr:Ps ratio ($C_p = 0.1\%$ and $[\text{NaCl}] = 0 \text{ mM}$). The pH_c remained constant around $\text{pH } 5.3$ for all Pr:Ps ratios. On the other hand, the pH_ϕ increased as the Pr:Ps ratio increased up to Pr:Ps = 9:1, where the pH_ϕ then stabilized.

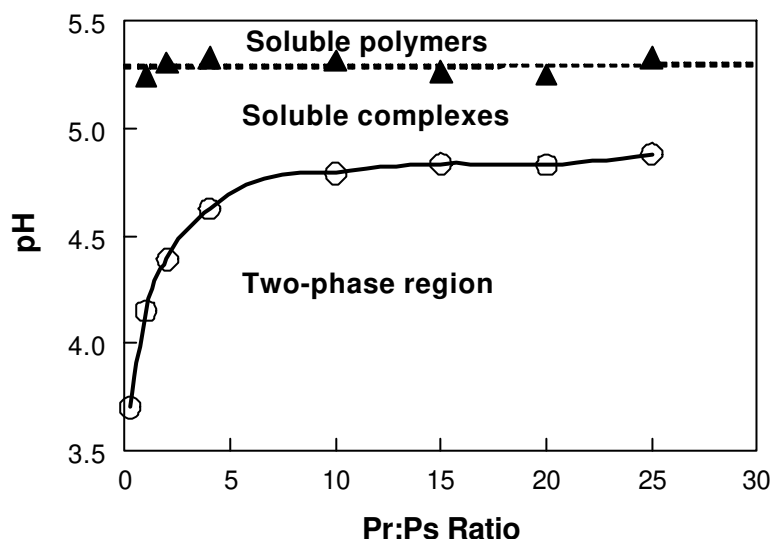


Figure 3.7: State diagram as a function of Pr:Ps ratios of a mixture of WP / EPS B40, total biopolymer concentration = 0.1%, $[\text{NaCl}] = 0 \text{ mM}$, temperature = 25°C , (Δ): pH_c , (\circ): pH_ϕ .

The dependence of pH_ϕ on the Pr:Ps ratio can be explained if phase separation is induced by the neutralization of the soluble complex. If more proteins are available per polysaccharide chain (large Pr:Ps), then phase separation takes place at a higher pH. At a Pr:Ps ratio close to 9:1, the pH_ϕ leveled off (from $\text{pH}_\phi = 4.8$). From zeta-potential measurements performed on WP and EPS B40 (not presented here), the zeta-potential value of the protein at $\text{pH} = 4.8$ was -9 to -10 times smaller than the zeta-potential value of the polysaccharide. This result was in good agreement with the Pr:Ps ratio at

which pH_0 leveled off. The use of zeta-potential measurements for the prediction of complex coacervation was already reported by Burgess *et al.* (1984) in order to determine the optimum pH and ionic strength. They showed that at the electrical equivalence pH (EEP), where the electrophoretic mobility of the complex is zero, the electrophoretic mobility of the separated polyions was inversely related to the composition of the complex. In other words, if the Pr:Ps composition is 9:1, then one will find that the electrophoretic mobility at the EEP is 1:9. A saturated ratio of Pr:Ps = 9:1 (w/w) would correspond to a ratio of 0.5:0.000617 (mol/mol) (with the M_w of EPS B40 = 1620 kg/mol and the M_w of WP = 18 kg/mol). This means that 810 molecules of WP interact with one EPS B40 chain. The EPS B40 consists of 1680 repeating units, which corresponds to a complexation of one protein per two repeating units of EPS B40 [Tuinier *et al.*, 1999]. This situation corresponds to a close packing of the WP on the chain of EPS B40, which is consistent with the hypothesis that the EPS B40 is saturated. The pH_c was not dependent on the Pr:Ps ratio, which could suggest that the formation of soluble complexes was the result of the interaction between a single polysaccharide chain and a defined amount of protein. By comparing these results with some typical pH_c values of WP/gum arabic, it appeared that the pH_c was higher for the WP/EPS B40 system than for WP/gum arabic. The pI of the WP is 5.2 and the soluble complexes were already formed at pH 5.3 because the protein already carried some positive patches [Dubin *et al.*, 1994; Wen and Dubin, 1997]. Furthermore, in the two-phase region, the WP/EPS B40 complexes looked more like a precipitate than a coacervate, unlike WP/gum arabic. The explanation lies in the fact that the charge density of EPS B40 is much higher than that of gum arabic.

Next, the order of biopolymer mixing was studied (Figure 3.8). When the WP was slowly added to a mixture of EPS B40 at pH 3 (titration A), the formation of complexes was instantaneous as indicated by the strong initial increase of turbidity, and phase separation occurred slowly in time. At a Pr:Ps = 1.35:1, the complexes precipitated, which was indicated by a sharp decrease of turbidity due to the high instability of the sample in the cuvette. At pH 4, the initial addition of WP induced a slight increase of the turbidity, which remained constant between a Pr:Ps = 0.3:1 and Pr:Ps = 0.9:1. In this region, the mixture did not phase separate after one week. Then the turbidity increased slowly until a Pr:Ps = 5.3:1, above which precipitation occurred. At Pr:Ps < 5.3:1, the mixture slowly phase separated in the following days. On the other hand, for Pr:Ps >

5.3:1, the mixture precipitated instantaneously. When the EPS B40 was added to the mixture of WP (titration B), the mixtures behaved differently. Indeed, they precipitated immediately, and the complexes stayed as a precipitate even at low Pr:Ps ratios. Experimentally, the turbidity was difficult to measure because of a fast phase separation in the cuvette, the data could, thus, not be plotted in Figure 3.8. From titration A, one can conclude that the interaction is much stronger at pH 3 than at pH 4, which is in agreement with the previous results of Figure 3.3. In Figure 3.3, the salt titration was performed at Pr:Ps = 2:1, which means that the complexes were in a precipitate form at pH 3 but not at pH 4.

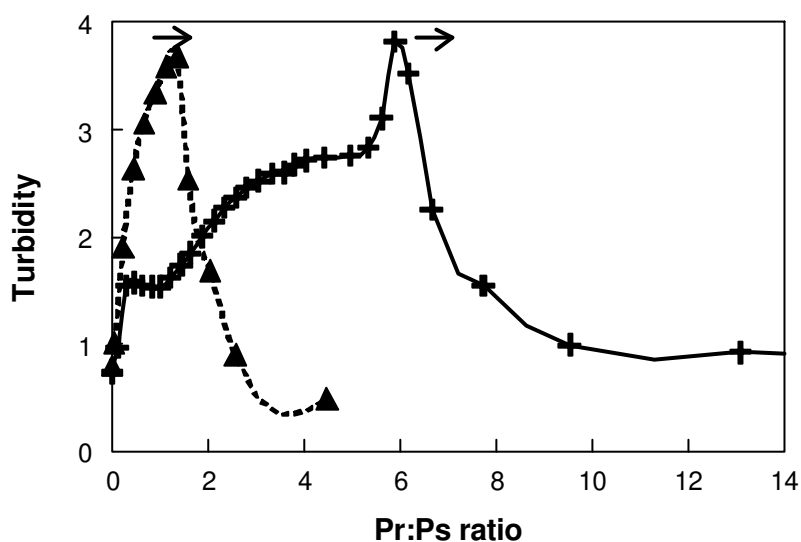


Figure 3.8: Titration of EPS B40 by WP (titration A) (○): pH 3, (+): pH 4. Total biopolymer concentration = 0.1%, [NaCl] = 0 mM, temperature = 25°C.

The results of titration B showed that the complexes formed at high ratios (precipitates) were not reversible upon decreasing the Pr:Ps ratio. The way the complexes were formed seemed to influence their nature. To understand which of the two states would be the most favorable for the complexes, two mixtures were prepared, one with titration A and the other with titration B, at a Pr:Ps ratio of 4:1 and at pH = 4. Under those conditions, the amount of EPS B40 would be in excess compared to the WP. The mixtures were left under continuous stirring for 2 weeks and the behavior of the samples was followed in time. As illustrated in Figure 3.9, the sample prepared with titration A (addition of WP into the EPS B40) was initially turbid, but after 4 days, the

sample contained some precipitates, like the sample made with titration B. It seemed that the system rearranged to form precipitates. To check this hypothesis, the experiment was repeated and the upper phase of the mixtures was taken out every day. After 2 h of phase separation, the upper phase was analyzed by HPLC and the amount of unbound β -lg, α -la, and EPS B40 was determined in time (Figure 3.10). The results were similar for both mixtures (titrations A and B); therefore, only the results of titration A are shown. The concentration of unbound α -la seemed to be unchanged in time. In contrast, the amount of β -lg in the upper phase decreased in the first 4 days and then remained stable. The amount of soluble EPS B40 was reduced in the first 2 days, and then increased. These results support the evidence that the complexes rearranged in time. During the first 4 days, some soluble complexes were still present in the mixture, as indicated by the initial decrease of β -lg and EPS B40. Then, the complexes rearranged to form fully neutralized EPS B40 and some free EPS B40 chains were expelled into the aqueous phase. Besides, the initial amount of α -la before complexation was 0.012%, and the residual amount of unbound α -la after complexation was close to that value. The pH of the mixture was close to the pI of α -la (pI = 4.1), meaning that the α -la was less charged than the β -lg. The complexes were thus mainly formed between EPS B40 and β -lg. These results could be understood if WP binds cooperatively to the EPS B40. The final state of the mixture consisted of neutral complexes and of free EPS B40.

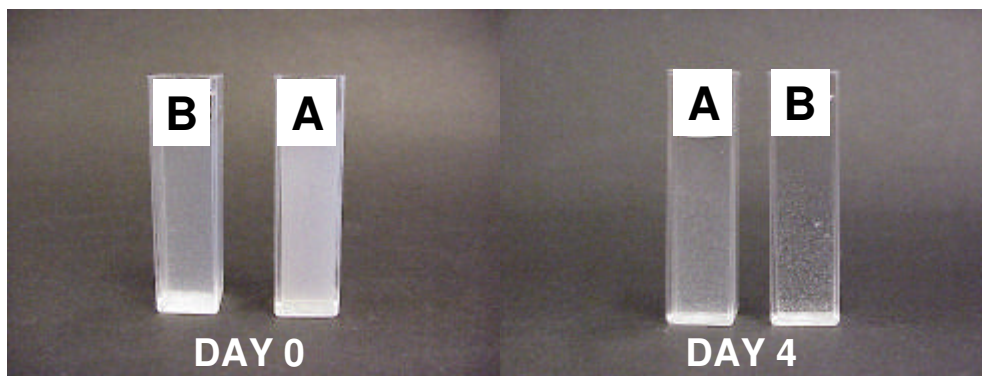


Figure 3.9: Pictures of mixtures of WP / EPS B40, $C_p = 0.1\%$, Pr:Ps = 4:1, [NaCl] = 0 mM, pH = 4; tube A: WP added to EPS B40 (titration A); tube B: EPS B40 added to WP (titration B).

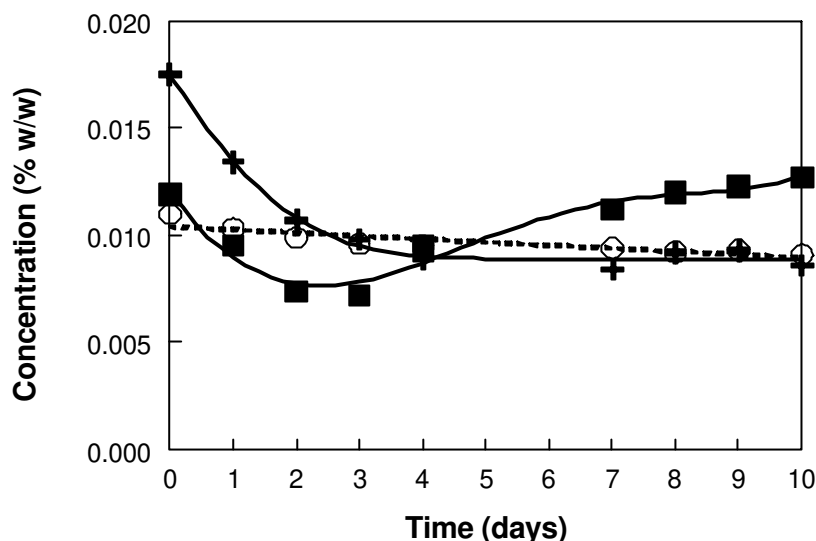


Figure 3.10: Concentration of unbound polymer in the upper phase of a WP / EPS B40 mixture as a function of time (initial $C_p = 0.1\%$, Pr:Ps = 4:1, [NaCl] = 0 mM, pH = 4). (○): α -lactalbumin, (+): β -lactoglobulin, (□): EPS B40.

Considering all the results, a mechanism is proposed to understand the structure and the formation of the complexes formed. When the mixture is slowly acidified from pH 7 to pH 2, the complexes are initially formed by interaction between a certain amount of WP per polysaccharide chain. Indeed, the independence of the pH_c upon the Pr:Ps ratio suggests that soluble complexes are formed between a single polysaccharide chain and a fixed amount of WP. Those complexes could be called homogeneous complexes. Upon further acidification, the WP becomes more charged and progressively saturates the EPS B40 chain that will precipitate. When the compounds are directly mixed at acidic pH, the results can be different. First, if the EPS B40 is added to an excess of WP, one could easily understand that there are enough WP molecules to saturate the polysaccharide chain; therefore, a precipitate is formed immediately. And upon further addition of EPS B40, the WP molecules saturate the EPS B40 one by one and do not redistribute over all EPS B40 chains. However, if the WP is added to the EPS B40 under stirring, the WP will be distributed on all the EPS B40 chains in excess, but with time and under continuous stirring, the WP will more likely be redistributed in order to neutralize one EPS B40 chain at a time. Such an effect can be called cooperative binding [Mattison *et al.*, 1999; Dubin *et al.*, 1990;

Currie *et al.*, 2000; Tolstoguzov *et al.*, 1985; Antonov and Gonçalves, 1999]. Indeed, it seems that if one WP binds to an EPS B40 molecule, the next WP will bind more effectively due to an increasing binding constant. These results are consistent with previous studies of Gurov *et al.* (1977) on the sorption of bovine serum albumin (BSA) by dextran sulfate. When the BSA and the dextran sulfate are mixed under the condition of intense complexing, the complexes obtained hardly dissolve in water. On the contrary, when the mixture is obtained by slow titration, the interaction is gradually increased and the resulting complexes are soluble. The latter complexes correspond to a uniform distribution of protein molecules among the dextran sulfate chain, and when the pH is increased, the distribution becomes nonuniform. This phenomenon is attributed to the cooperative nature of the BSA sorption on the polysaccharide chain [Tolstoguzov *et al.*, 1985; Olins *et al.*, 1967; McGhee and von Hippel, 1974]. Similar results were found for the system WP/EPS B40.

CONCLUSIONS

Electrostatic interactions between EPS B40 and WP led, under appropriate conditions of pH and ionic strength, to the formation of soluble or aggregated complexes. When the mixtures were slowly acidified, instability arose from a two-step process. First, soluble complexes were formed at pH_c and then macroscopic phase separation took place at pH_ϕ . The values of these pH transitions were strongly salt dependent. The addition of microions weakened the interactions between the particles by screening the charges, and this phenomenon depended linearly on \sqrt{I} , that is, the ionic strength. In the pH region where soluble complexes were formed, viscosity and SLS measurement showed that the complexation of the WP with the phosphate groups of the EPS B40 reduced the intramolecular repulsion and the “stiffness” of the molecule, allowing a decrease in particle size. Finally, the order of biopolymer mixing is important to determine the structure and the apparent stoichiometry of the complexes. The rearrangement of the complexes was followed in time, showing that the energetically most favorable state for both biopolymers is to form few neutralized EPS B40 chains rather than distributing the WP over all the EPS B40 chains. In other words, the WP bound cooperatively to EPS B40 in the condition studied (low salt). This work gave a better understanding of the formation and the structure of soluble complexes. The results are consistent with previous studies involving carboxylated polysaccharide. In

the future, the interaction of WP with a sulfated polysaccharide will be studied to test the hypothesis.

ACKNOWLEDGEMENTS

Friesland Coberco Dairy Foods (FCDF) is acknowledged for sponsoring this work. The authors thank Pascale Louis-Louisy, Roelie Holleman and Jan van Riel for their experimental assistance, and Dr. Patricia Ruas Madiedo, Dr. Hans Tromp, and Dr. Renko de Vries for encouraging discussions.

CHAPTER 4

Complexation of Whey Protein with Carrageenan*

ABSTRACT

The formation of electrostatic complexes of whey protein (WP) and a non gelling carrageenan (CG) was investigated as a function of pH, ionic strength, temperature, and protein to polysaccharide (Pr:Ps) ratio. On lowering the pH, the formation of soluble WP / CG complexes was initiated at pH_c , and insoluble complexes at pH_ϕ , below which precipitation occurred. The values of the transition pH varied as a function of the ionic strength. It was shown that at $[NaCl] = 45 \text{ mM}$, the value of pH_ϕ was the highest, showing that the presence of monovalent ions was favorable to the formation of complexes by screening the residual negative charges of the CG. When $CaCl_2$ was added to the mixtures, complexes of WP / CG were formed up to pH 8 via calcium bridging. The electrostatic nature of the primary interaction was confirmed from the slight effect of temperature on the pH_ϕ . Increasing the Pr:Ps ratio led to an increase of the pH_ϕ until a ratio of 30:1 (w/w), at which saturation of the CG chain seemed to be reached. The behavior of WP / CG complexes was investigated at low Pr:Ps ratio, when the biopolymers were mixed directly at low pH. It resulted in an increase of the pH of the mixture, compared to the initial pH of the separate WP and CG solutions. The pH increase was accompanied by a decrease in conductivity. The trapping of protons inside the complex probably resulted from a residual negative charge on the CG. If NaCl was present in the mixture, the complex took up the Na^+ ions instead of the H^+ ions.

*F. Weinbreck, H. Nieuwenhuijse, G. W. Robijn, C. G. de Kruif
Accepted for publication in *Journal of Agriculture and Food Chemistry*

INTRODUCTION

Macromolecules are the main components of formulated food products and the control of structural properties of proteins and polysaccharides is a wide topic of investigation [Tolstoguzov, 2002]. Interactions between food macromolecules can be either repulsive or attractive, underlining two opposite phenomena: biopolymer incompatibility and complex formation [Tolstoguzov, 2003]. Interbiopolymer complexing of positively charged proteins and anionic polysaccharides can lead to the formation of soluble or insoluble complexes [Dubin and Murrel, 1988]. Systematic studies were carried out on the complexation behavior of proteins with synthetic polyelectrolytes and proteins with polysaccharides [Dubin *et al.*, 1994; Kaibara *et al.*, 2000; Mattison *et al.*, 1995, 1998, 1999; Park *et al.*, 1992; Wang *et al.*, 1996; Wen and Dubin, 1997; Xia *et al.*, 1999; Schmitt *et al.*, 1998; Weinbreck *et al.*, 2003a, 2003b, 2003c]. They revealed two pH-induced structural transitions due to increasing attractive interaction and depending on the ionic strength of the system, indicating that complexation was mainly electrostatically driven. The formation of soluble protein / polyelectrolyte complexes was initiated at pH_c on lowering pH, which preceded the pH of macroscopic phase separation at pH_ϕ . Often, soluble complexes were formed at pH values above the isoelectric point (pI) of the protein, *i.e.* the pH at which the protein is overall negatively charged [Dubin *et al.*, 1994; Wen and Dubin, 1997; de Vries *et al.*, 2003]. This phenomenon can be explained by the presence of positively charged patches at the surface of the protein.

Previous work in our group included the study of whey protein and a weak polyelectrolyte [Weinbreck *et al.*, 2003a, 2003b]. The electrostatic interactions between the whey proteins and the carboxylated gum arabic led to the formation of a liquid coacervate in the pH window between 2.5 and 4.8 [Weinbreck *et al.*, 2003a, 2003b; Schmitt *et al.*, 1999, 2000b]. It was also shown that the pH boundaries pH_c and $\text{pH}_{\phi 1}$ were mainly due to the formation of a complex between the β -lactoglobulin and the gum Arabic (the contribution of α -lactalbumin would appear at lower pH values). The interaction of whey proteins with the phosphated exocellular polysaccharide EPS B40 (EPS B40) was studied as well [Weinbreck *et al.*, 2003c]. Now, the interaction between the whey proteins and another strong polyelectrolyte, carrageenan (CG) has been investigated. The two batches used in this study had the commercial name of \ddot{e} -

carrageenan (δ -CG), however, since the amount of pure δ -CG was rather limited in one of the batches, the authors referred to the polysaccharide as carrageenan (CG). CG is an anionic sulfated polysaccharide extracted from red algae [van de Velde, 2002]. It is mainly used as a thickener / viscosity builder. Three main types of CG are used in the food industry, The λ -CG does not present pronounced gelling properties, unlike the other two commercial types of carrageenan (*i.e.* ι and κ). λ -CG carries three sulfate groups, ι -CG two sulfate groups and κ -CG one sulfate group per repeating unit. The two CG batches used in this study are non gelling, the type I is a mixture of different CG types and the type II is a pure λ -CG. CG is highly charged (much more than gum arabic or EPS B40). It is known that the molecular attraction of protein-bound NH_3^+ groups for $-\text{OSO}_3^-$ groups is much stronger than for $-\text{CO}_2^-$ groups [Dickinson, 1998]. CG are added to food products to enhance their textural properties, and since most food products have an acid pH, CG and protein would form complexes and alter the texture and stability of food products. Various studies on proteins / CG have already been carried out, especially on the effect of segregative interactions on the gelling properties of κ -carrageenan [Antonov and Gonçalves, 1999; Bourriot *et al.*, 1999; Capron *et al.*, 1999; Ould Eleya and Turgeon, 2000a, 2000b; Langendorff *et al.*, 1999, 2000]. A beneficial consequence of complexation of proteins with sulfated polysaccharide is the protection afforded against loss of solubility as a result of protein aggregation during heating or following high-pressure treatment [Imeson *et al.*, 1977; Ledward, 1979; Galazka *et al.*, 1997, 1999]. The protective effect is probably due to the blocking of the hydrophobic sites of the protein by the polysaccharide [Dickinson, 1998]. Interactions of casein with CG or pectin are widely used in the control of texture and stability of some dairy products (*e.g.* yoghurt drinks) [Langendorff *et al.*, 1999, 2000; Hansen, 1982; Tuinier *et al.*, 2002; Tromp *et al.*, in press; Parker *et al.*, 1994]. However, very limited work has been done on the electrostatic interaction between whey proteins and CG, especially λ -CG.

This work aims to investigate the complex formation of whey proteins (WP) and CG as a function of pH and ionic strength. Furthermore, an attempt was made to compare the results with those obtained with WP / gum arabic and WP / EPS B40. This comparison allowed us to identify system-specific or generic properties of the complexes. In addition, the results can also be used for practical applications (*e.g.* in dairy products), so as to understand how the formation of WP / CG complexes can be tuned. Interesting

results on the addition of calcium ions to induce complex formation and on the influence of temperature on the pH_{ϕ} allowed a clarification of the phenomenon involved in complexing. Titration experiments revealed the behavior of the complexes as ion traps, which was previously poorly recognized for this type of system.

EXPERIMENTAL SECTION

Materials

Bipro is a whey protein isolate (WP) comprised mainly of α -lactoglobulin (α -lg), and α -lactalbumin (α -la), from Davisco Foods International (Le Sueur, USA). Residual whey protein aggregates were removed by acidification (at $pH = 4.75$) and centrifugation (1h at 33000 rpm with a Beckman L8-70M ultracentrifuge, Beckman Instruments, The Netherlands). The supernatant was then freeze-dried (in a Modulo 4K freeze-dryer from Edwards High Vacuum International, UK). Finally, the resulting powder was stored at $5^{\circ}C$. The final powder contained (w/w) 88.1% protein (N x 6.38), 9.89% moisture, 0.3% fat, and 1.84% ash (0.66% Na^{+} , 0.075% K^{+} , 0.0086% Mg^{2+} , and 0.094% Ca^{2+}). The protein content of the treated Bipro is: 14.9% α -la, 1.5% bovine serum albumin, 74.9% β -lg, and 3.2% immunoglobulin.

Two batches of CG were used. The first batch (type I) is Lambda Carrageenan 3830 Carravisco DLF1 from Ferdiwo (Oudwater, The Netherlands). The powder contains (w/w) 8.7% moisture, 0.64% proteins (Dumas method), and 13.2% ash (0.07% PO_4^{3-} , 0.16% Ca^{2+} , 0.077% Mg^{2+} , 3% K^{+} , 2.2% Na^{+} , 12 mg/kg Fe^{3+} , and 0.32% Cl). The amount of glucose is low (0.9%) and saccharose $< 0.05\%$. The weight-averaged molar mass of the CG type I measured by SEC MALLS is 774 kDa and the weight-average radius 49 nm. The second batch (type II) is GENU[®] lambda carrageenan X-7055 (BRR) from CPKelco (Lille Skensved, Denmark) and is not commercially available. Both CG samples are cold water soluble and do not gel. Stock solutions were prepared by dissolving the powder in deionized water (concentrations were set at 0.10% or 0.25% w/w). Various WP and CG mixtures were obtained by diluting the stock solutions in deionized water at the desired pH and ionic strength (use of NaCl or $CaCl_2$). The concentration of the total biopolymer (Cp) was set at 0.10% or 0.25%, the ratio of WP to CG (Pr:Ps) was varied from 1:1 to 150:1 (w/w), and the salt (NaCl or $CaCl_2$) added to the mixtures from 0 to 1 M.

Characterization of the carrageenan batches

Nuclear magnetic resonance (^1H NMR) experiments were carried out on both CG batches. It was found that the type I contains various types of carrageenan in the following quantities: λ -carrageenan: 9%, κ -carrageenan: 46%, ν -carrageenan: 20%, μ -carrageenan: 1%, and ι -carrageenan: 24%. Moreover, the type I does not contain any other additives. This result surprisingly revealed that the type I powder contains only a rather low amount of λ -carrageenan and therefore was compared to a purer sample. Indeed, the ^1H NMR spectrum of type II CG showed that only λ -carrageenan was present, and a small amount of starch (in the range of 10%) could also be detected. Zetapotential measurements were carried out on both CG mixtures with a Zetasizer 2000 (Malvern, USA). The results showed that the zetapotential of both CG samples was -86 mV.

In most of the experiments, the type I CG was used (the commercial-grade sample), unless otherwise mentioned.

Turbidimetric titration under acidification

Mixtures of WP and CG were acidified by dropwise addition of HCl or by adding glucono- δ -lactone (GDL), which provided a slow acidification. The influence of the ionic strength ($[\text{NaCl}]$ or $[\text{CaCl}_2] = 0 - 1\text{M}$), the protein to polysaccharide ratio (Pr:Ps = 1:1 – 150:1 w/w) and the total biopolymer concentration ($C_p = 0.10\%$ or 0.25% w/w) was studied by varying one parameter at a time. The turbidity of each sample was measured as a function of the pH with a Cary 1E spectrophotometer (Varian, The Netherlands) at a wavelength of 514.5 nm (similar to previous measurements [Weinbreck *et al.*, 2003a]). The samples were put in a 1 cm path-length cuvette and the turbidity was then measured as a function of time at 25°C . The turbidity (τ) was defined as:

$\tau = -\ln(I/I_0)$, where I is the light intensity that passes through a volume of solution of 1 cm length and I_0 is the incident light intensity.

The pH_c (pH where soluble complexes are formed) was determined for some samples; it could be measured using dynamic light scattering (DLS) measurements, with a 22 mW HeNe laser at a wavelength of 632.8 nm. The sample was initially filtered with a 0.45 μm filter and centrifuged for 30 s to remove all impurities and air bubbles. The sample was placed in the cuvette housing, which was kept at a temperature of 25°C in a toluene bath. The goniometer was set at 45° . The detected intensity was processed

by a digital ALV-5000 correlator. Finally, the scattered light intensity was measured and its average was recorded every minute. The averaged intensity was used as the scattering intensity value each minute. The values of pH_c were measured graphically as the intersection point of two tangents to the curve, as described in [Weinbreck *et al.*, 2003c].

Each measurement was at least done in duplicate. Control measurements with only WP and only CG were systematically carried out under the same conditions as the mixtures of biopolymers. From all measurements, a statistical uncertainty of 0.2 pH-units was calculated (Statsoft, Inc. (2001).STATISTICA, version 6).

Titration of one polymer by the other

The titration was performed by slowly adding under stirring 0.25% WP into 0.25% CG (type I). These titrations were done at pH 3 and at pH 4 on mixtures at $[NaCl] = 0$ mM and 45 mM. The Pr:Ps ratio was then recalculated and at each ratio, the turbidity, the pH, and the conductivity of the WP / CG mixture were measured. The conductivity of the WP / CG mixture at each Pr:Ps ratio was then subtracted from the initial conductivity of the CG mixture and plotted as a function of Pr:Ps ratio. Titration curves were reproducible within the uncertainty of 0.5 Pr:Ps ratio and 0.2 pH-units.

Conductivity measurement

The conductivity of the mixtures was systematically measured with a conductivity meter LF 340 and a standard conductivity cell TetraCon[®] 325 (Wissenschaftlich – Technische Werkstätten GmbH, Germany).

RESULTS AND DISCUSSION

Behavior of the system as a function of pH and salt

The interaction between WP and CG is expected to be electrostatic in nature. Indeed, since the pH influences the ionization of the protein charges, electrostatic complexes would be formed in the pH window where WP and CG are oppositely charged. Furthermore, the presence of ions in the solution may screen the charges of the polymer and influence the formation of complexes. Therefore, the two key parameters (*i. e.* pH and ionic strength) influencing the complexation between two oppositely charged polymers were varied systematically. Mixtures of WP and CG were acidified

and the turbidity of the mixtures was measured as a function of pH for various concentrations of NaCl ($C_p = 0.25\%$ and $Pr:Ps = 15:1$).

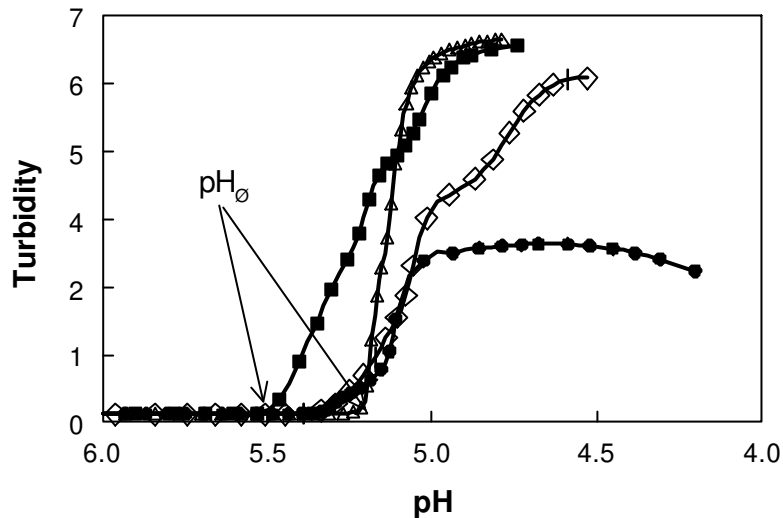


Figure 4.1: HCl titration at various ionic strengths of a mixture of WP / CG, total biopolymer concentration = 0.25%, Pr:Ps ratio = 15:1, Temperature = 25°C; (◇): [NaCl] = 0 mM; (△): [NaCl] = 15 mM; (□): [NaCl] = 45 mM; (●): [NaCl] = 120 mM.

Figure 4.1 shows that the turbidity increased abruptly in the pH range 5.5 – 5.2 for all samples. The blanks of WP or CG remained at a low turbidity over the whole pH range (not shown here). The pH at which the turbidity suddenly increased was defined as pH_0 . For $pH < pH_0$, the mixtures became unstable and the complexes sedimented / precipitated to the bottom of the test tubes. The value of pH_0 varied with the [NaCl]. For $[NaCl] < 45$ mM, pH_0 shifted towards higher pH values and the maximum turbidity increased, showing an increase in number and/or size of the biopolymer complexes. A small addition of salt seemed thus to enhance the formation of complexes. Burgess (1990) mentioned that complexation could be reduced because of an unfavorable extended shape of the molecules at low salt. The result could also be explained if phase separation was a result of the charge compensation of the complexes. Below their pI , the proteins became net-positively charged and bound to the sulfate groups of the CG. However, the charge density of CG is so high that electroneutrality of the complex is not fully achieved by the WP only (possibly because of a spatial packing problem). Therefore, if small microions are present in the solution, they will screen the

residual negative groups of CG and thus effectively reduce repulsion between complexes and allow an effective phase separation. When the concentration of NaCl was higher than 45 mM, the pH_{ϕ} shifted to lower values and for $[NaCl] > 1$ M, no phase separation occurred. The influence of salt as being unfavorable to complexation is a well-known phenomenon and was already reported in the 1940's [Bungenberg de Jong, 1949b]. A large ionic strength is known to reduce electrostatic interactions by screening the charges of the biopolymers. Therefore, at $[NaCl] > 1$ M, the complexes were not formed. Between 45 mM and 1 M, complexes could be formed at more acidic pH_{ϕ} values, corresponding to a pH where the WP carried more charges. The interaction of ions with the complex will be described below.

The type of microion present in the solution was studied by comparing the effect of NaCl and $CaCl_2$ on the complex formation of WP and CG. The valency of the microions had already been reported as an important parameter in biopolymer interactions [Burgess, 1990]. Acid titration was carried out on mixtures of WP / CG at a $C_p = 0.25\%$, Pr:Ps = 15:1 for NaCl and $CaCl_2$ in the range of ionic strength 0 – 400 mM. Two different sources of CG were compared: type I and type II. From the acid titration, the value of pH_{ϕ} was determined (as in Figure 4.1) for each sample (in duplicate). The average value of pH_{ϕ} is plotted in Figure 4.2 for mixtures of WP / type I CG and WP / type II CG at various ionic strengths (using NaCl or $CaCl_2$). The values of pH_{ϕ} varied with the ionic strength but were similar for both CG batches. When NaCl was added, the complexes were formed at pH values near or below the pI of the protein with a slightly higher pH_{ϕ} at $[NaCl] = 45$ mM, as was discussed above. On the other hand, the addition of $CaCl_2$ showed that complexes were formed at pH values higher than the pI. For $[CaCl_2] = 45 - 140$ mM, complexes were formed around pH 8. Blanks with only WP or CG remained clear and stable, showing that the complexes were formed at high pH only in the presence of a mixture of WP / CG. This result suggested that another type of interaction occurred in the presence of $CaCl_2$. It was supposed that ion bridging took place between the divalent calcium ion (Ca^{2+}) and the negatively charged WP and CG molecules. An electrostatic complex at neutral pH occurs between κ -carrageenan and κ -casein in the absence of specific cations [Snoeren *et al.*, 1975]. Complexation also occurs between κ -carrageenan and α_{s1} -casein or β -casein, but in the latter case only in the presence of Ca^{2+} , through the formation of calcium bridges [Skura and Nakai, 1981; Ozawa *et al.*, 1984].

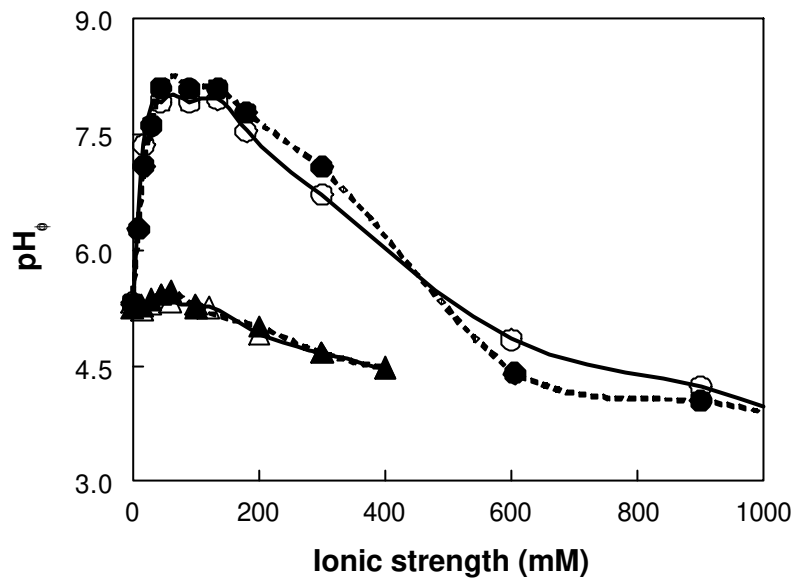


Figure 4.2: State diagram as a function of ionic strength of a mixture of WP / CG, Pr:Ps ratio = 15:1, total biopolymer concentration = 0.25%, Temperature = 25°C, (/): addition of NaCl, (/) addition of CaCl₂, open symbols: type I CG and filled symbols: Type II CG. The mixture shows macroscopic phase separation below the curves.

Temperature

In general, a temperature change will influence the biopolymer / biopolymer interactions by changing the Flory-Huggins interaction energy. If other enthalpic interactions - in addition to the Coulombic interactions - would be involved, the temperature would also have an influence. Low temperatures favor hydrogen bond formation and hydrophobic interactions are enhanced by temperature increase. In this study, the turbidimetric titration was carried out at various temperatures in the range 5 – 50°C for three different samples. The values of pH_{ϕ} are presented as a function of temperature in Figure 4.3. In the range studied, temperature had a small effect on the complex formation. A slight increase of pH_{ϕ} could be noticed at low temperatures. Kaibara *et al.* (2000) studied the effect of temperature on complexation of bovine serum albumin and cationic polyelectrolytes. They found that pH_c (pH at which soluble complexes were formed) and pH_{ϕ} were not temperature dependent. It can be concluded that the primary interaction between WP and CG was thus mainly electrostatic in nature but may include entropy contributions, as described in the Overbeek and Voorn theory, due to the

release of counterions [Overbeek and Voorn, 1957]. Indeed, adding large amounts of salt suppressed the complexation of primary complexes. Recent work by Girard *et al.* (2003) reported that from the binding isotherms of the pectin to the α -lactoglobulin, the formation of two kinds of complexes has been evidenced. The first ones were soluble intrapolymeric complexes, which formation was driven by enthalpy gain (binding stoichiometry of 6-8). The second ones were based on the aggregation of the previous ones and were mostly controlled by entropy (binding stoichiometry of 15-16.5).

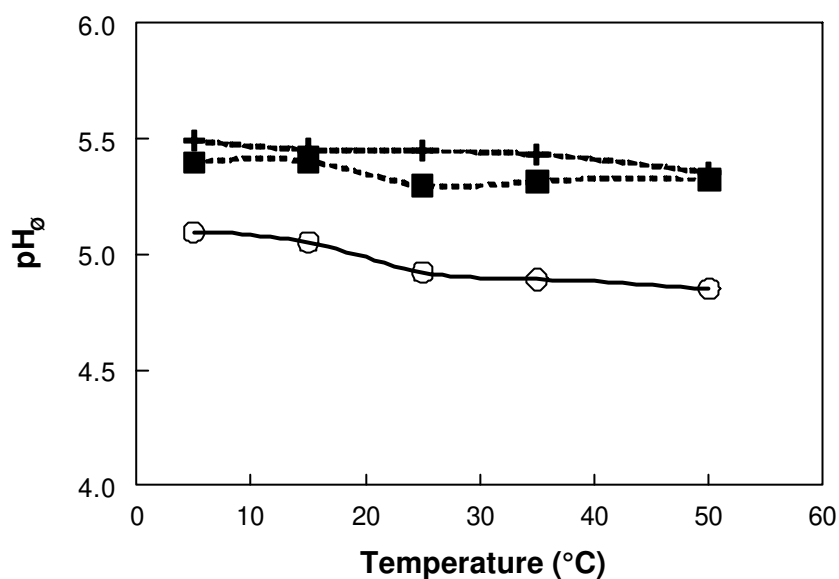


Figure 4.3: State diagram as a function of temperature of a mixture of WP / CG, Pr:Ps = 15:1, (+): Cp = 0.25%, [NaCl] = 45 mM; (◻): Cp = 0.1%, [NaCl] = 45 mM; (○): Cp = 0.1%, [NaCl] = 0mM.

Protein to polysaccharide ratio

The amount of WP molecules available per polysaccharide chain is obviously of importance in the electrostatic complex formation. There is at each pH a specific ratio for which electroneutrality of the complex is reached [Schmitt *et al.*, 1998]. Here, a mixture of WP / CG at Cp = 0.1% and without any addition of NaCl was studied at various Pr:Ps ratios. For each Pr:Ps ratio, acid titration coupled to turbidity and light scattering measurements allowed the determination of pH₀ and pH_c. pH_c was defined as the pH at which soluble complexes were formed. The value of the pH_c could be found by performing light scattering measurements under slow acidification (more sensitive than turbidity measurements). The values of pH_c and pH₀ are plotted in a

state diagram as a function of the Pr:Ps ratio in Figure 4.4. Above pH_c , the polymers were negatively charged and thus did not interact. Already at $\text{pH} > \text{pI}$ of the WP ($\text{pI } \beta\text{-lg} = 5.2$), there was a strong interaction as $\text{pH}_c > \text{pI}$. The probable reason being the presence of positive patches and in addition charge fluctuations of the protein near the pI [Dubin *et al.*, 1988; Wen and Dubin, 1997; de Vries *et al.*, 2003]. Then, below pH_ϕ , insoluble complexes were formed and phase separation occurred. The pH_c remained constant around $\text{pH } 5.5$ for all ratios. This result suggested that the formation of soluble complexes occurred between a single polyelectrolyte chain and a given amount of proteins. On the other hand, pH_ϕ increased up to a Pr:Ps = 30:1, where pH_ϕ then stabilized. The dependence of pH_ϕ on the Pr:Ps ratio could be explained if phase separation was induced by the aggregation of the soluble complexes which reached electroneutrality. Indeed, the charge compensation of the WP / CG occurred at a higher pH if more protein molecules were available per polysaccharide chain (larger Pr:Ps). For Pr:Ps > 30:1, the pH_ϕ remained stable, indicating that saturation of the CG had probably taken place. A saturation ratio of 30:1 (w/w) corresponds to a Pr:Ps ratio of 1300:1 (mol/mol), meaning that 1300 molecules of WP would be complexed to one CG chain at $\text{pH} = 5.1$.

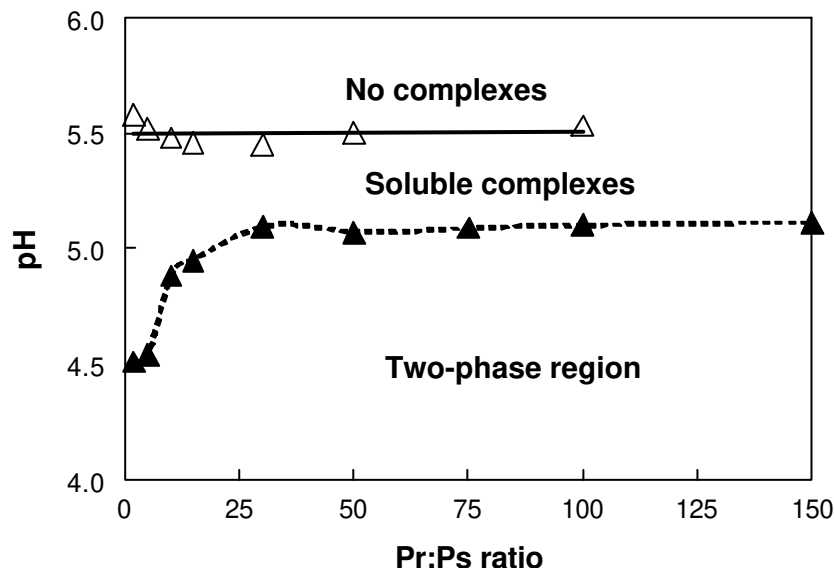


Figure 4.4: State diagram as a function of protein to polysaccharide ratio (Pr:Ps) of a mixture of WP / CG, $[\text{NaCl}] = 0 \text{ mM}$, total biopolymer concentration = 0.1%, Temperature = 25°C , (Δ): pH_c , (\blacktriangle): pH_ϕ .

These results are qualitatively similar to previous results on complex formation of WP/gum arabic and WP/EPS B40 [Weinbreck *et al.*, 2003a, 2003c]. Gum arabic carries carboxylic groups and EPS B40 phosphate groups. The zeta potential of the CG is two times larger than the zeta potential of the EPS B40 and three times larger than the zeta potential of the gum arabic. Indeed, we found that EPS B40 bound less WP than CG and gum Arabic less still. Therefore, the interaction between WP and CG is much stronger than for the other two polysaccharides and pH_c ($pH_c = 5.5$) is also higher than the pH_c of EPS ($pH_c = 5.3$) and gum arabic ($pH_c = 5.2$). Nevertheless, the influence of parameters like ionic strength, Pr:Ps ratio, and pH is qualitatively similar for all the systems studied.

Then, WP / CG complexes were formed differently by adding WP slowly into the CG mixture at pH 3 and pH 4 for $[NaCl] = 0$ mM and $[NaCl] = 45$ mM. The formation of the complexes was monitored by turbidity measurement as a function of the Pr:Ps ratio. Figure 4.5a shows that the turbidity increased faster at pH 3 than at pH 4 and at $[NaCl] = 45$ mM than at $[NaCl] = 0$ mM. These results were very consistent with previous findings. At pH 3, the WP carried more charges and the electrostatic interaction was thus enhanced compared to pH 4. From results described above, it was also demonstrated that a salt concentration of 45 mM enhanced the formation of complexes, shifting the pH_ϕ to higher pH values (see Figures 4.1 and 4.2). However, during the experiment, the pH and the conductivity of the mixtures were monitored in parallel and the results, plotted in Figure 4.5b, were surprising. Indeed, if WP was slowly added into a CG mixture of the same pH, the pH of the mixture increased and the conductivity decreased. The pH increased up to +0.3 pH-units for mixtures at pH_{ini} 3 and +1.4 pH-units at pH_{ini} 4 for mixtures at $[NaCl] = 0$ mM. When NaCl was added to the sample, the pH increase was less dramatic. This experiment revealed that when complexes were formed, in the case of low Pr:Ps, the complexes bound the ions available in the mixture. If NaCl was present, then, Na^+ ions were incorporated in the complexes. But if the amount of positive ions was too limited, the H^+ ions were trapped within the complexes, leading to a pH increase of the mixture. Furthermore, if extra WP were added (higher Pr:Ps ratio), then the complexes incorporated the WP and released the positive ions, the pH slowly decreased and finally reached its initial value, and the conductivity of the sample became close to the conductivity of the WP mixture (corresponding to a change in conductivity of -325 μ S/cm at $[NaCl] = 0$ mM pH 3 and -290 μ S/cm at $[NaCl] = 45$ mM pH 4). The ion uptake seemed to be needed to screen

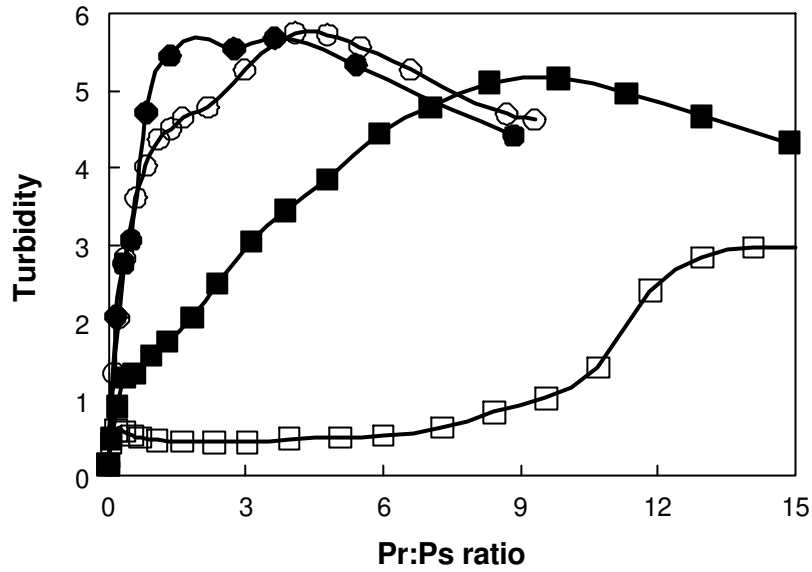


Figure 4.5a: Turbidity of a WP / CG mixtures as a function of Pr:Ps ratio, total biopolymer concentration = 0.25%, Temperature = 25°C. (●): pH 3, [NaCl] = 0 mM ; (○): pH 3, [NaCl] = 45 mM ; (■): pH 4, [NaCl] = 0 mM ; (□): pH 4, [NaCl] = 45 mM.

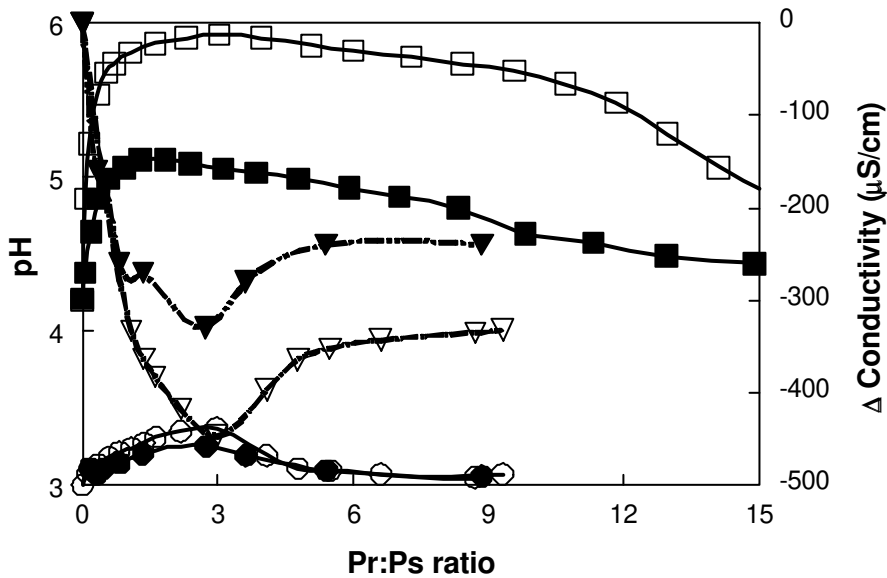


Figure 4.5b: pH and conductivity variation as a function of Pr:Ps ratio, total biopolymer concentration = 0.25%, Temperature = 25°C. (●)(▽): pH_{ini} 3, [NaCl] = 0 mM ; (○)(◊): pH_{ini} 3, [NaCl] = 45 mM ; (■)(▽): pH_{ini} 4, [NaCl] = 0 mM ; (□)(◊): pH_{ini} 4, [NaCl] = 45 mM. (●)(○)(■)(□): evolution of pH. (▽)(◊): evolution of conductivity.

the excess negative charges of the CG. Similar results were already reported in the case of xanthan / chitosan complex gel by Ikeda *et al.* (1995); the main reason of this phenomenon was described as a tendency to increase a number of ionic pairs between reacting polyelectrolytes. In the particular case of WP / CG studied here, it might be possible that the protons were taken up by the WP, as it would lead to an increase of its positive net charge. By adding further WP, the buffer capacity of the mixture was increased, and more WP molecules were able to react with the CG, and the pH returned to its initial value.

CONCLUSIONS

The formation of WP / CG complexes resulted from electrostatic interactions. The slight effect of temperature on the pH formation of insoluble complexes highlighted that the interaction was mainly Coulombic in nature. Whether soluble or insoluble complexes were formed depended on various parameters like pH, ionic strength, and Pr:Ps ratio. In the presence of calcium ions, complexes could be formed up to neutral pH via calcium binding. If the system was supplemented with 45 mM NaCl, the formation of insoluble complexes was enhanced and complexes were formed close to and below the pI of the protein. CG being a highly negatively charged molecule, the presence of microions promoted the formation of electroneutral complexes by screening the residual negative charges of the complex. If salt was present in insufficient quantity, the complexes incorporated the protons, which resulted in a pH increase of the mixture. Comparing the results to previous work done with carboxylated and phosphated polysaccharide, it seems justified to conclude that the intensity of the WP / polysaccharide interaction correlated with the zeta potential of the polysaccharide: CG > EPS B40 > gum Arabic, which paralleled the stoichiometry of the complexes.

ACKNOWLEDGMENTS

Friesland Coberco Dairy Foods (FCDF) is acknowledged for their financial support. The authors would like to thank Agnès Gaven for her experimental assistance on Figures 4.1 and 4.4, Dr. Harry Rollema for the NMR measurements, and Dr. Fred van de Velde for his invaluable advice on carrageenan. Prof. Martien Cohen Stuart and Dr. Renko de Vries are acknowledged for enlightening discussions.

CHAPTER 5

Composition and Structure of Whey Protein / Gum Arabic Coacervates*

ABSTRACT

Complex coacervation in whey protein / gum arabic (WP/GA) mixtures was studied as a function of three main key parameters: pH, initial protein to polysaccharide mixing ratio $(Pr:Ps)_{ini}$, and ionic strength. Previous studies had already revealed under which conditions a coacervate phase was obtained. This study aimed now to understand how these parameters influence the phase separation kinetics, the coacervate composition and the internal coacervate structure. At a defined $(Pr:Ps)_{ini}$, an optimum pH of complex coacervation was found (pH_{opt}), at which the strength of electrostatic interaction was maximum. For $(Pr:Ps)_{ini} = 2:1$, the phase separation occurred the fastest and the final coacervate volume was the largest at $pH_{opt} = 4.0$. The composition of the coacervate phase was determined after 48 h of phase separation and revealed that, at pH_{opt} , the coacervate phase was the most concentrated. Varying the $(Pr:Ps)_{ini}$ shifted the pH_{opt} to higher values when $(Pr:Ps)_{ini}$ was increased, and to lower values when $(Pr:Ps)_{ini}$ was decreased. This phenomenon was due to the level of charge compensation of the WP/GA complexes. Finally, the structure of the coacervate phase was studied with small angle X-ray scattering (SAXS). SAXS data confirmed that at pH_{opt} the coacervate phase was dense and structured. Model calculations revealed that the structure factor of WP induced a peak at $Q = 0.7 \text{ nm}^{-1}$, illustrating that the coacervate phase was more structured, inducing the stronger correlation length of WP molecules. When the pH was changed to more acidic values, the correlation peak faded away, due to a more open structure of the coacervate. A shoulder in the scattering pattern of the coacervates was visible at small Q. This peak was attributed to the presence of residual charges on the GA. The peak intensity was reduced when the strength of interaction was increased, highlighting a greater charge compensation of the polyelectrolyte. Finally, increasing the ionic strength led to a less concentrated, a more heterogeneous, and a less structured coacervate phase, induced by the screening of the electrostatic interactions.

*F. Weinbreck, R. H. Tromp, C. G. de Kruif,
Considered for publication in *Biomacromolecules*

INTRODUCTION

For application of biopolymers (such as proteins and polysaccharides) in the pharmaceutical, cosmetic, and food industries, their interactions are of major relevance in their respective applications. The repulsive and attractive forces between the biopolymers underlie two different phenomena: biopolymer incompatibility and complex formation [Tolstoguzov, 2003]. Complex coacervation is a specific type of complex formation. It is the phase separation which occurs in a mixture of oppositely charged polymer solutions. Insoluble complexes between the polymers are formed and they concentrate in liquid droplets, also called coacervate droplets. The coacervate droplets sediment and fuse to form a coacervate phase. Thus, complex coacervation leads to the formation of two liquid phases: the upper phase, poor in polymers and rich in solvent, and a lower coacervate phase concentrated in polymers [Bungenberg de Jong, 1949a]. Biopolymer coacervates are used as fat replacers or meat analogues, for coatings and for encapsulation of flavors or drugs, and in biomaterials (e.g. edible films and packaging) [Bakker *et al.*, 1994; Burgess, 1994; Luzzi, 1970; Kester and Fennema, 1986].

Most of the studies on complex coacervation have been carried out on the gelatin / gum arabic system, since the pioneering work of Bungenberg de Jong (1949a). The formation of biopolymer complexes arises mainly from electrostatic interactions and is dependent on the ionization degree of the polymers, and thus the pH. The presence of salt can suppress complex coacervation to varying degrees, depending on the nature and concentration of salt [Bungenberg de Jong, 1949a; Overbeek and Voorn, 1957; Schmitt *et al.*, 1998]. The biopolymer concentration is also a critical parameter, and an optimum mixing ratio exists which corresponds to an electrically equivalent amount of each polymer [Burgess and Carless, 1984]. The trend is nowadays to replace gelatin by another protein; that is why whey protein (WP) and gum arabic (GA) were used in the present study. The WP used was a whey protein isolate consisting of 75% β -lactoglobulin (β -lg), which is the main protein responsible for the complex formation with GA [Weinbreck *et al.*, 2003a]. Native β -lg has an iso-electric point (pI) of 5.2 and is thus positively charged below this pI value. Commercial samples of WP always contained some denatured β -lg, which drastically influences the coacervation [Schmitt *et al.*, 2000a; Sanchez and Renard, 2002c]; therefore in this study aggregates of denatured β -lg were removed. GA is a complex polysaccharide exuded from the

African tree *Acacia senegal*. It is an arabinogalactan composed of three distinct fractions with different protein contents and different molecular weights [Osman *et al.*, 1993; Randall *et al.*, 1989]. The composition analysis of GA revealed the presence of a main galactan chain carrying heavily branched galactose/arabinose side chains. The carbohydrate moiety is composed of D-galactose (40% of the residues), L-arabinose (24%), L-rhamnose (13%), and two uronic acids, responsible for the polyanionic character of the gum, D-glucuronic acid (21%) and 4-O-methyl-D-glucuronic acid (2%). The structure of GA is complex and poorly known. GA is negatively charged above pH 2.2, since at low pH (< 2.2) the dissociation of the carboxyl groups is suppressed. GA displays good emulsifying properties and its viscosity is low compared to other polysaccharides of similar molar mass [Sanchez *et al.*, 2002b].

Previous work was carried out on the complex formation of WP and GA as a function of key parameters, such as pH, ionic strength, biopolymer concentration and initial protein to polysaccharide mixing ratio (Pr:Ps)_{ini} [Weinbreck *et al.*, 2003a; Schmitt *et al.*, 1999; Weinbreck and de Kruif, 2003b]. Weinbreck *et al.* (2003a) demonstrated that around the iso-electric point of the WP, soluble complexes of WP/GA were formed (at pH_c), and if the pH was decreased even further (< pH₀₁), complexes associated and phase separated into a coacervate phase. At even lower pH (< pH₀₂), GA became neutral and complex coacervation was prevented. The pH window where complex coacervation occurred shrank with increasing ionic strength due to the screening of the charges by the microions. The structure of the primary soluble WP/GA complexes was proposed to be a GA molecule decorated with WP. Secondary aggregation of the primary soluble WP/GA complexes was scarcely studied and the final microstructure of the coacervate phase remains unknown so far. There is a need to study the structure of coacervating systems [Turgeon *et al.*, 2003]. Studies on synthetic polyelectrolytes reported a sponge-like and hierarchically self-assembled “fractal” network of coacervates as found from electron microscopy [Menger *et al.*, 2000; Menger, 2002]. Recently, Leisner *et al.* (2003) investigated the structure of a poly(glutamic acid) / dendrimer coacervate by light scattering and small-angle X-ray scattering. A first attempt to describe the kinetics of complex coacervation was made with α -lg / GA using diffusing wave spectroscopy (DWS) and confocal scanning laser microscopy (CSLM) [Schmitt *et al.*, 2001a]. Depending on the initial mixing ratio, the DWS patterns were rather complex, combining both coalescence of the particles and sedimentation. Sanchez *et al.* (2002a) continued the study of the phase separation of α -lg / GA mixtures with CSLM and small angle

static light scattering, and they concluded that the aggregation of coacervates leads to the formation of an equilibrated heterogeneous structure whose interfaces were rough. The authors could not describe the phase separation mechanism on the basis of spinodal decomposition or nucleation and growth since the initial stages were too fast to be measured. So far, studies on the structure of equilibrated biopolymer coacervates are still lacking. Since the conditions for WP/GA coacervate formation were known, in this work phase separation *per se* was studied as a function of the key parameters: pH, ionic strength and Pr:Ps ratio. The first goal of this study was to analyze the kinetics of phase separation and the growth of the coacervate phase by determining which parameters influence the sedimentation kinetics and by relating them to the composition of the coacervate phase. Indeed, the coacervate phases were characterized (water content and biopolymer content) as a function of pH, ionic strength and (Pr:Ps)_{ini} ratio. And finally, the internal structure of the coacervate was studied by small angle X-ray scattering (SAXS) in the conditions previously used.

EXPERIMENTAL SECTION

Materials

Bipro from Davisco Foods International (Le Sueur, USA) is an isolate of whey protein (WP) consisting mainly of β -lactoglobulin (β -lg), and α -lactalbumin (α -la). Residual whey protein aggregates were removed by acidification (at pH 4.75) and centrifugation (1 h at 33000 rpm with a Beckman L8-70M ultracentrifuge, Beckman Instruments, The Netherlands). The supernatant was then freeze-dried (in a Modulo 4K freeze-dryer from Edwards High Vacuum International, UK). Finally, the resulting powder was stored at 5°C. The final powder contained (w/w) 88.1% protein (N x 6.38), 9.89% moisture, 0.3% fat and 1.84% ash (0.66% Na⁺, 0.075% K⁺, 0.0086% Mg²⁺, and 0.094 % Ca²⁺). The protein content of the treated Bipro was: 14.9% α -la, 1.5% BSA, 74.9% β -lg, and 3.2% immunoglobulin (IMG).

Gum arabic (GA; IRX 40693) was a gift from Colloides Naturels International (Rouen, France). The powder contained (w/w) 90.17% dry solid, 3.44% moisture, 0.338% nitrogen and 3.39% ash (0.044% Na⁺, 0.76% K⁺, 0.20% Mg²⁺ and 0.666% Ca²⁺). Its weight average molar mass ($M_w = 520\ 000$ g/mol) and its average radius of gyration ($R_g = 24.4$ nm) were determined by size exclusion chromatography followed by multiangle laser light scattering (SEC MALLS). SEC MALLS was carried out using a TSK-Gel

6000 PW + 5000 PW column (Tosoh Corporation, Tokyo, Japan) in combination with a precolumn Guard PW 11. The separation was carried out at 30°C with 0.1 M NaNO₃ as eluent at a flow rate of 1.0 mL min⁻¹.

Stock solutions of 3% (w/w) were prepared by dissolving the powder in deionized water.

The zeta-potential of the 0.1% (w/w) WP and 0.1% (w/w) GA mixtures was measured as a function of pH with a Zetasizer 2000 (Malvern, USA).

Kinetics of phase separation

The stock solutions of 3% (w/w) WP and GA were mixed to obtain a final volume of 30 mL with a defined protein to polysaccharide (Pr:Ps)_{ini} ratio (w/w). The initial pH of the stock solution was 7.0. Sodium azide (0.02% w/w) was added to prevent bacterial growth. At time t_0 , the mixtures were acidified using 0.1 M and 1 M HCl to reach the desired pH value (in the range from 3.0 to 5.0). First, the influence of pH at various (Pr:Ps)_{ini} (1:1, 2:1, 8:1) was investigated. Then, the influence of the ionic strength was studied at (Pr:Ps)_{ini} = 2:1 and pH = 4.0. The ionic strength was adjusted with NaCl in the range 0 – 100 mM. After acidification, the samples were directly placed in a graduated tube at 25°C and the coacervate phase volume was measured as a function of time. Measurements were taken every minute at first, and then every day for 7 days. Each kinetics experiment was repeated at least twice.

Composition of the coacervate phase

WP/GA coacervates were prepared as mentioned above at (Pr:Ps)_{ini} of 1:1, 2:1, or 8:1 at various pH values. WP/GA coacervates were also prepared at (Pr:Ps)_{ini} = 2:1, pH 4.0 for [NaCl] ranging from 0 mM to 100 mM. After acidification to the desired pH value, the mixtures were poured into a decanter and left to phase separate for 48 h. Then, the amount of water contained in each coacervate phase (dense lower phase) was determined at least in duplicate by weighing the coacervate phase before and after freeze-drying. The concentrations of residual WP and GA in the upper phase were determined by HPLC. The main proteins of WP (*i. e.* α -la and β -lg) were detected with a UV detector at 280 nm (Applied Biosystems), whereas the GA was detected by refraction index (RI, Erma-7510, Betron Scientific). The injector was a Waters 717 plus Autosampler. A volume of 25 μ l was injected for each run. The column was a Biosep.

Sec. 2000 (Phenomenex) and the pump was a Waters Associates (Isocratisch) with a flow of 0.7 ml/min.

Small angle X-ray scattering (SAXS) measurements

WP/GA coacervates were prepared as described in the paragraph above. Experiments were carried out on the lower coacervate phase. Small angle X-ray scattering (SAXS) measurements were made at the Dutch-Belgian beam-line (DUBBLE) at the European Synchrotron Radiation Facility (ESRF) in Grenoble (France). The cuvettes contained 19.65 mm³ of sample. The wavelength of the X-rays was $\lambda = 0.93 \text{ \AA}$, the detector was a two-dimensional (512 x 512 pixels) gas-filled detector placed at 5 m distance from the sample. The scattering wave vector (Q) was between 0.1 and 1.7 nm⁻¹ (corresponding to a range of observable length scales between 62.8 nm and 3.7 nm in real space). The temperature of the samples was kept at 25°C.

RESULTS AND DISCUSSION

Kinetics of phase separation

The study aimed to characterize the influence of various factors such as pH, initial protein to polysaccharide ratio $(Pr:Ps)_{ini}$, and ionic strength, on the complex coacervation of whey proteins (WP) and gum arabic (GA). Coacervation of a WP/GA mixture occurred in a specific pH range [Weinbreck *et al.*, 2003a]. Insoluble complexes of WP and GA concentrated into coacervate droplets that coalesced and accumulated with time at the bottom of a graduated tube [Sanchez *et al.*, 2002a]. The volume of the bottom coacervate layer could thus be measured as a function of time. The phase separation of the complex coacervation process can be divided into several stages. This work aimed to probe the sedimentation kinetics of the coacervate droplets (referred to as phase separation kinetics) by measuring the volume of the coacervate phase as a function of time (from minutes to days). A picture of the system with well separated phases is given in Figure 5.1 (photo A). After phase separation the coacervate phase remained liquid-like (Figure 5.1, photo B).

Mixtures of WP/GA were prepared at various pH values (3.0; 3.5; 3.8; 4.0; 4.2; 4.35; 4.5), the initial volume of each mixture being 30 mL, with a total biopolymer concentration (C_p) of 3% (w/w), a $(Pr:Ps)_{ini}$ of 2:1, and a low ionic strength (no NaCl added). The fraction of the coacervate phase (percentage of total volume) is plotted for

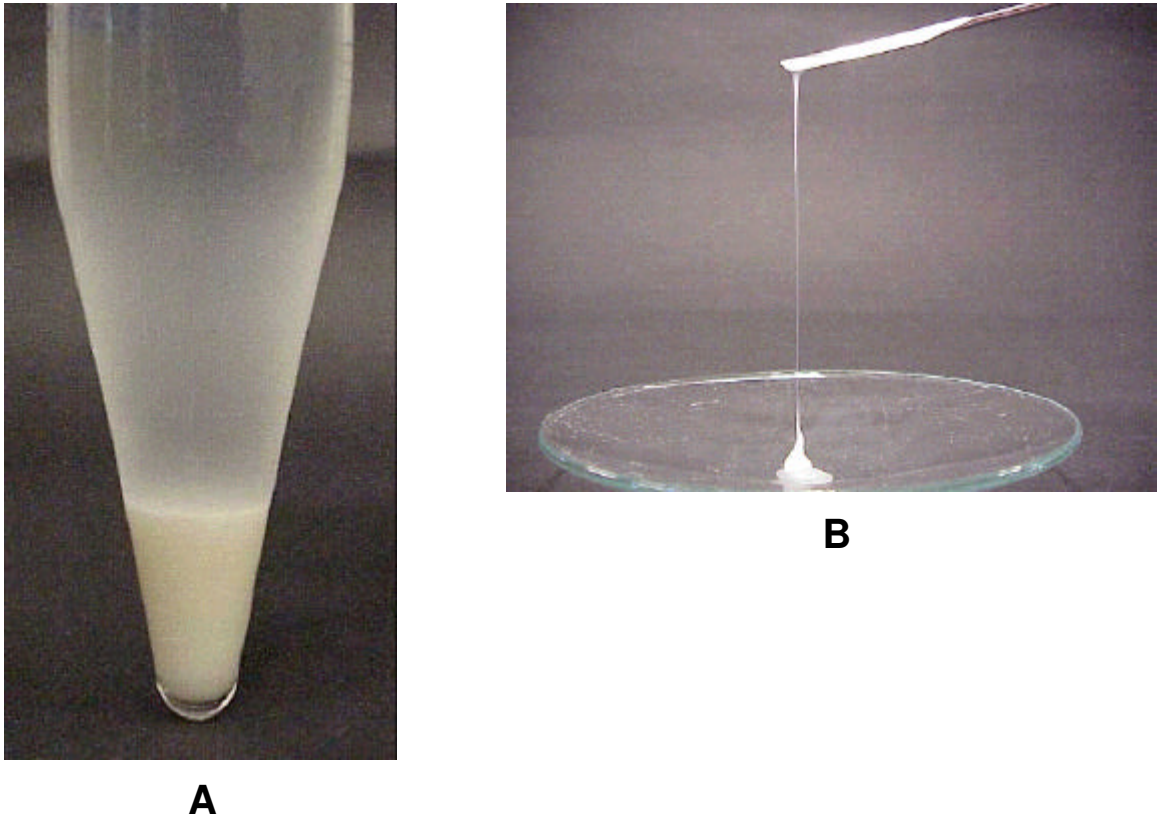


Figure 5.1: Pictures of (A): a phase separated mixture of WP/GA after 1 week of phase separation; the lower phase is the coacervate phase; (B): WP/GA coacervate phase poured with a spatula.

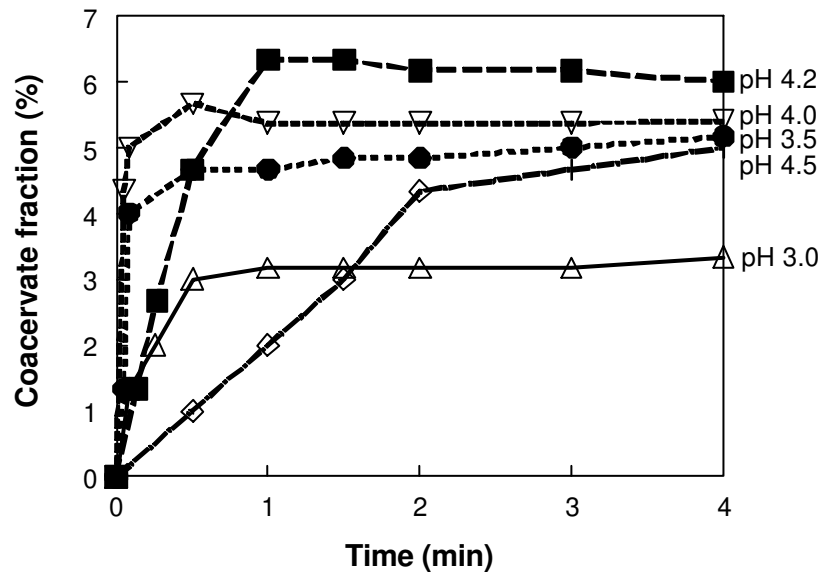


Figure 5.2: Fraction of WP/GA coacervate phase (% of total volume) as a function of time, $C_p = 3\%$, $(Pr:Ps)_{ini} = 2:1$, $[NaCl] = 0$ mM. (\square): pH 3.0; (\circ): pH 3.5; (∇): pH 4.0; (\blacksquare): pH 4.2; (\diamond): pH 4.5.

various pH values as a function of time in Figure 5.2. The volume of the coacervate phase increased very rapidly during the first 4 min. After 24 h, the volume of the coacervate phase was stable at every pH value, except at pH 4.5, where the volume decreased slightly during 3 days. This phenomenon could be due to a slow rearrangement of the coacervate phase. Indeed, if the charge compensation was not completely achieved (GA in excess in this case), then the coalescence of the coacervate droplets would take more time and water would be slowly expelled from the coacervate phase. The kinetics of formation of the coacervate phase seemed to be pH dependent and could be measured from the initial slope of the kinetics curves. In Figure 5.3, the kinetics of the growth of the coacervate phase highlighted the pH dependence of the phase separation. At pH 4.0, the phase separation was at its fastest. The strength of the electrostatic interaction was estimated by calculating the absolute value of the product of the measured zeta potentials of the WP and of the GA molecules as a function of pH. The result is also plotted in Figure 5.3. It showed that the shapes of both curves (kinetics of phase separation and zeta potential product) were similar. It could therefore be hypothesized that the kinetics of phase separation was related to the strength of the electrostatic interaction between WP and GA molecules. Thus, the stronger the electrostatic interaction was, the faster the phase separation. The phase separation and the formation of the coacervate phase arose from the formation of insoluble WP/GA complexes that concentrated into coacervate droplets of various sizes. These coacervate droplets coalesced into a phase separated layer at the bottom of the tube. If the coacervate droplets were fully charge balanced, they would coalesce faster than if some residual charges were present. As mentioned by Sanchez *et al.* (2002a), when the proteins were in insufficient quantity, they could not totally compensate the negative charges of the GA. As a result, a surface layer of GA stabilized the coacervates, inhibiting the interactions between coacervate droplets. In these conditions, rearrangement of the coacervate was needed and the coacervate droplets settled very slowly. These results were confirmed in a recent work where the diffusivity of the WP and the GA within their coacervate phase was studied by the means of several techniques [Weinbreck *et al.*, 2004c]. One of the technique used was fluorescence recovery after photobleaching (FRAP) in combination with confocal scanning light microscope (CSLM). It appeared that most of the coacervate phases prepared at various pH values were rather homogeneous (with sometimes some water inclusion), except at pH 4.5 where even though some coacervate droplets were

coalescing slowly, after two days of phase separation, some non coalesced droplets were still visible.

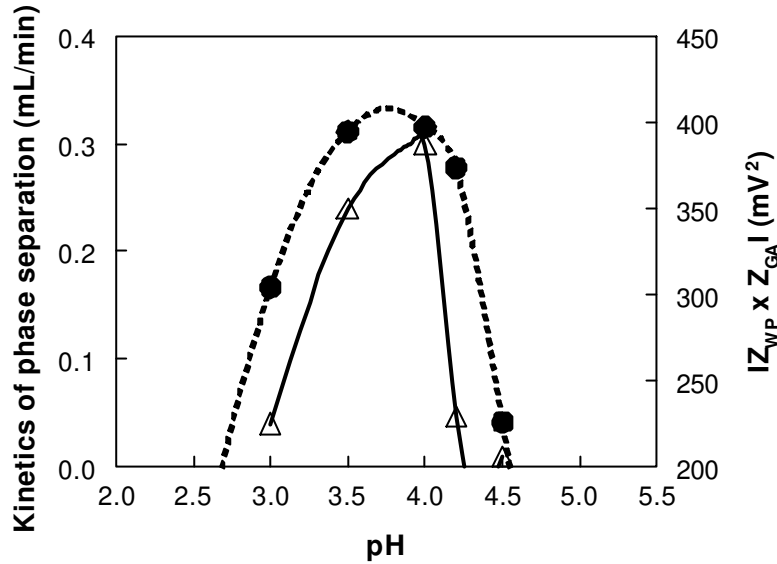


Figure 5.3: (●): Kinetics of phase separation of WP/GA coacervate as a function of pH, $C_p = 3\%$, $(Pr:Ps)_{ini} = 2:1$, $[NaCl] = 0$ mM. (△): Product of zeta potential of WP and GA as a function of pH.

The same experiment as above was then carried out for $(Pr:Ps)_{ini} = 1:1$ and $8:1$. The final volume (percentage of total volume) of the coacervate phase after 7 days is plotted as a function of pH in Figure 5.4. As illustrated in this figure, complex coacervation occurred in a specific pH range depending on the $(Pr:Ps)_{ini}$ ratio. For pH values close to the iso-electric point of the WP ($pI = 5.2$) and close to the pH at which GA became neutral ($pH = 2.0$), no coacervation took place because of the neutrality of one of the polymers. The maximum volume of coacervate was close to 7% of the total volume of the solution. This result was in good agreement with previous work of Burgess and Carless (1984), who reported a maximum (gelatin/GA) coacervate phase volume corresponding to 8% of the total volume. The pH at which the maximum volume of coacervate was obtained ($pH_{Vol-max}$) increased when $(Pr:Ps)_{ini}$ increased. Indeed, for a $(Pr:Ps)_{ini} = 8:1$, $pH_{Vol-max} = 4.8$, whereas $pH_{Vol-max}$ was between 4.0 and 4.2 for $(Pr:Ps)_{ini} = 2:1$, and between 3.0 and 3.5 for $(Pr:Ps)_{ini} = 1:1$. This shift of $pH_{Vol-max}$ to lower values when the $(Pr:Ps)_{ini}$ decreased was understandable since fewer protein molecules were available per polysaccharide chain and a more acidic pH was

necessary to get more positive charges on the WP, which would then be sufficient to compensate the negative charges of the GA. Furthermore, the final volume of coacervate was smaller at $(Pr:Ps)_{ini} = 8:1$ than at $(Pr:Ps)_{ini} = 2:1$ and $1:1$. This phenomenon could easily be understood, since at $(Pr:Ps)_{ini} = 8:1$, the concentration of GA was lower than at the other ratios (same C_p but higher $Pr:Ps$). The voluminosity of the coacervate phase was mainly due to the voluminosity of the GA (which is a larger molecule than the WP molecules). These results were in agreement with previous studies, where Sanchez *et al.* (2002a) mentioned that changing the \hat{a} -lg to GA ratio (from 1:1 to 2:1) altered the coarsening kinetics as well as the structure and morphology of coacervates.

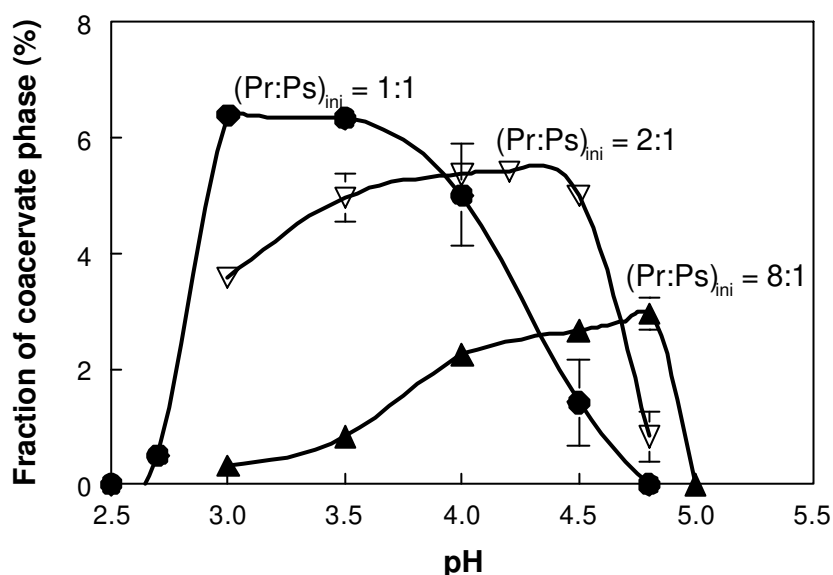


Figure 5.4: Fraction of WP/GA coacervate phase (% of total volume) as a function of pH after 7 days of phase separation. (●): $(Pr:Ps)_{ini} = 1:1$; (▽): $(Pr:Ps)_{ini} = 2:1$; (▲): $(Pr:Ps)_{ini} = 8:1$.

Composition of the coacervate phase after 48h of phase separation

Effect of pH and Pr:Ps ratio

After 48h of phase separation, the amount of water contained in the coacervate phase was measured by weighing the coacervate before and after freeze-drying. From this measurement, the total biopolymer concentration (C_p) in the WP/GA coacervates could be deduced, and it is plotted in Figure 5.5a. All the coacervates were very concentrated

in biopolymer, C_p varying from 11% (w/w) up to 33% (w/w). The results indicated that, for each $(Pr:Ps)_{ini}$, there was a pH at which the C_p was the largest (pH_{Cp-max}). On either side of the pH_{Cp-max} , C_p decreased, highlighting that fewer polymers were involved in the complex formation. Thus, at pH_{Cp-max} , the optimum conditions for coacervation were reached. For $(Pr:Ps)_{ini} = 1:1$, the $pH_{Cp-max} = 3.5$, for $(Pr:Ps)_{ini} = 2:1$, $pH_{Cp-max} = 4.0$, and for $(Pr:Ps)_{ini} = 8:1$, $pH_{Cp-max} = 4.5$. The values of the pH_{Cp-max} shifted to lower values when the $(Pr:Ps)_{ini}$ was reduced. The explanation of this phenomenon was the same as described above. Indeed, by decreasing the amount of WP available per GA chain, the pH at which charge compensation occurs shifted to lower pH values, at which the WP became sufficiently charged. It is important to note that the $pH_{Vol-max}$ corresponded to the pH_{Cp-max} , meaning that at the optimum pH of coacervation, a large volume of highly concentrated polymers was obtained. It seemed that if more biopolymers were present in the mixture, the volume of the coacervate phase was also increased. For $(Pr:Ps)_{ini} = 2:1$, both biopolymer concentration and coacervate volume were maximum at pH = 4.0. Furthermore, as depicted in Figure 5.3, for $(Pr:Ps)_{ini} = 2:1$, pH 4.0 was also the pH at which the fastest kinetics of phase separation was obtained, like the pH of the maximum strength of electrostatic interaction.

From HPLC measurements carried out on the dilute upper phase of the WP/GA mixtures, the residual amount of unbound WP and GA could be determined. From this value, the ratio of WP and GA (Pr:Ps) in the coacervate phase could be calculated by taking into account the volume of the coacervate phase. The results are presented in Figure 5.5b for various $(Pr:Ps)_{ini}$ (*i.e.* 1:1, 2:1, 8:1) as a function of pH. The general trend was similar for all $(Pr:Ps)_{ini}$ studied. Increasing pH led to an increase of the Pr:Ps in the coacervate phase. This result could easily be understood by considering the charge density of the WP and the GA. Indeed, the zeta potential of WP is obviously strongly pH-dependent, and since GA is a weak polyelectrolyte, its zeta potential decreased in the pH window studied ($Z_{GA, pH5} = -28$ mV; $Z_{GA, pH3.5} = -17$ mV; $Z_{GA, pH2} = 0$ mV). By calculating the zeta potential ratio between WP and GA ($Z_{WP}:Z_{GA}$) as a function of pH, it was clear that more proteins were needed at higher pH to compensate the negative charges of the GA. At acidic pH, the WP became more charged and the GA less charged, which would explain that fewer proteins were necessary to compensate the charges of the carboxylic groups of the GA. For $(Pr:Ps)_{ini} = 1:1$, GA was in excess in the upper phase, and for $(Pr:Ps)_{ini} = 8:1$, WP was in excess. At pH_{Cp-max} , the Pr:Ps in the coacervate phase were rather similar to their respective $(Pr:Ps)_{ini}$ of 1:1 and 2:1. For

$(\text{Pr:Ps})_{\text{ini}} = 8:1$, the Pr:Ps ratio in the coacervate phase was 4:1 at $\text{pH}_{\text{Cp-max}} = 4.5$. Since the kinetics of phase separation was slow as compared to the other ratio it is possible that the equilibrium was not yet obtained for this ratio. Furthermore, the surprising result lay in the observed difference of the final values of Pr:Ps in the coacervate depending on the $(\text{Pr:Ps})_{\text{ini}}$. This result was unexpected since if the complexes were charge balanced at each pH, the amount of WP bound per GA would not be dependent on the initial Pr:Ps ratio. And here, the higher the $(\text{Pr:Ps})_{\text{ini}}$, the higher the Pr:Ps in the coacervate phase. This result was already found by Schmitt *et al.* (1999) for a system of pure $\hat{\alpha}$ -lg and GA. It appeared that there was still a mass action effect which led to the phase separation of more WP if the initial WP concentration was larger. Therefore, one could conclude that there was a charge adjustment of the polymers, where the pK of dissociation of the charged groups would shift to maintain the overall charge balance of the system. Thus, it seemed that the coacervate is a very flexible system that adapts to external parameters, by shifting its charge distribution and / or its chain conformation. This finding supports the fact that, when charge compensation was not instantaneously obtained, the coacervate droplets rearranged by adjusting their charges to form a charge balanced coacervate phase.

Effect of pH and ionic strength

A way to weaken the electrostatic interaction is addition of NaCl to the mixture. The increase of the ionic strength reduces the pH range where complex coacervation takes place, and above a critical $[\text{NaCl}]$, complex coacervation is suppressed [Weinbreck *et al.*, 2003a]. The influence of the ionic strength was studied as a function of pH for a mixture of WP/GA with a $(\text{Pr:Ps})_{\text{ini}} = 2:1$ at pH 4.0 (these conditions were chosen since it was found that they correspond to the optimum coacervation conditions). Increasing amounts of NaCl were added to the mixture, ranging from 0 mM to 100 mM. The final volume of the coacervate phase obtained after 48 h of phase separation is plotted in Figure 5.6 together with the final C_p in the coacervate (determined from water content as described above). The results showed that increasing ionic strength led to a decrease of the coacervate volume, and above 60 mM of NaCl, no coacervate phase was obtained: coacervation was inhibited. It is also worth noting that the kinetics of phase separation decreased upon salt addition (not shown here). The Pr:Ps in the coacervate phase (determined by HPLC) remained constant, independent of the ionic strength. Furthermore, addition of NaCl led to a more watery coacervate phase, less

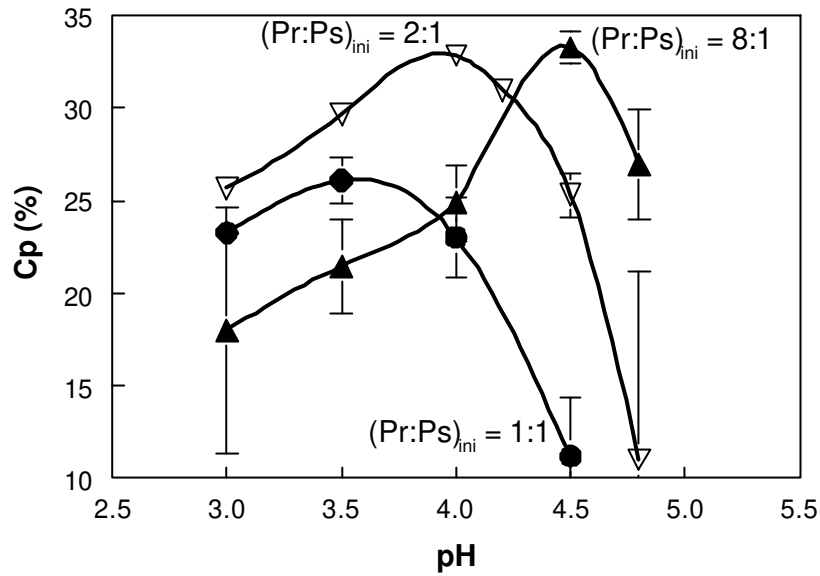


Figure 5.5a: Total biopolymer concentration (C_p) in the WP/GA coacervate phase as a function of pH after 48h of phase separation. (●): $(Pr:Ps)_{ini} = 1:1$; (▽): $(Pr:Ps)_{ini} = 2:1$; (▲): $(Pr:Ps)_{ini} = 8:1$.

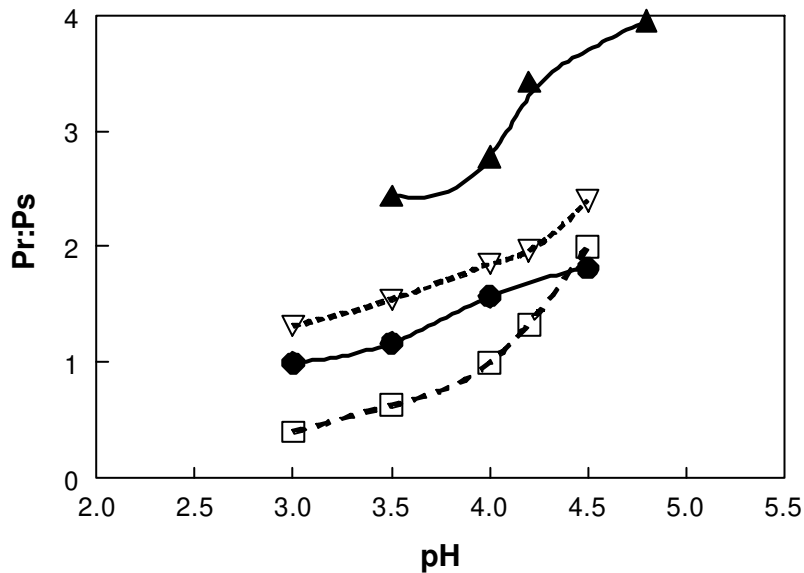


Figure 5.5b: Same system as in Figure 5.5a. Final Pr:Ps in the WP/GA coacervate phase as a function of pH after 48h of phase separation. (●): $(Pr:Ps)_{ini} = 1:1$; (▽): $(Pr:Ps)_{ini} = 2:1$; (▲): $(Pr:Ps)_{ini} = 8:1$; (□): Zetapotential of WP / Zetapotential of GA ($Z_{WP}:Z_{GA}$).

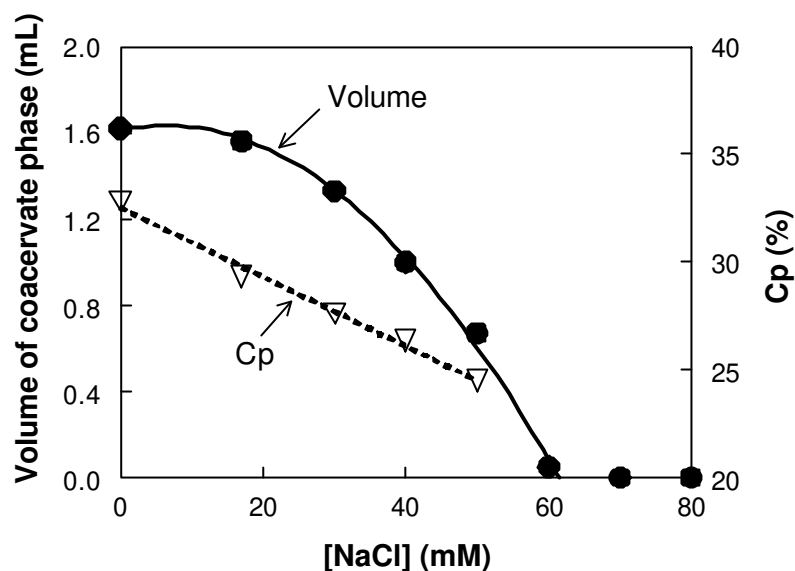


Figure 5.6: Composition of WP/GA coacervate phase as a function of the ionic strength after 48h of phase separation, $(Pr:Ps)_{ini} = 2:1$, $pH = 4.0$. (●): volume of the coacervate phase; (▽): total biopolymer concentration (C_p) in the coacervate phase.

concentrated in polymer, as described by the linear decrease of C_p as a function of $[NaCl]$. These results highlighted once more that the addition of microions in the mixture screened the charges of the polymers and decreased the complex formation [Bungenberg de Jong, 1949a; Weinbreck *et al.*, 2003a]. As described in the theory of Overbeek and Voorn (1957), below a critical salt concentration and a critical initial polymer concentration, the mixtures demixed into a polymer-rich phase and an aqueous phase poor in polymers. The composition of the two phases became closer when the concentration of microions was increased and finally reached a critical point, beyond which phase separation no longer occurred. As illustrated in Figure 5.6, the concentration of polymer in the coacervate phase decreased upon increasing the $[NaCl]$. The critical salt concentration was 60 mM in this case, which led to a critical C_p of 22%. Thus, if WP and GA were mixed at an initial $C_p > 22\%$, no phase separation would occur. This experiment was already carried out in a previous study, where a phase diagram of mixtures of WP/GA was determined for $Pr:Ps = 2:1$ and at $pH 3.5$ [Weinbreck *et al.*, 2003a]. At $pH = 3.5$, the critical concentration was measured at 15% of WP and GA ($Pr:Ps = 2:1$). Here, the experiments were carried out at $pH 4.0$, the pH

at which the strongest electrostatic interactions took place; thus the critical concentration would be expected to be somewhat higher.

Small angle X-ray scattering (SAXS) measurements

Effect of pH

WP/GA coacervates were collected at various pH values as described above. Small angle X-ray scattering (SAXS) measurements were performed on each coacervate phase (fixed pH, fixed $(Pr:Ps)_{ini}$ ratio). The scattering pattern was represented by plotting the product of the scattered intensity and the wave vector ($I(Q) \times Q$) versus the scattering wave vector Q (Holtzer plot).

Figure 5.7a shows the pattern of coacervate phases prepared at $(Pr:Ps)_{ini} = 2:1$ and at various pH values (3.0, 3.5, 4.0, 4.2, 4.5). The scattering intensity of the initial mixture at pH 7.0 (before coacervation took place) was low and rather flat compared to the coacervated samples because of a lower polymer concentration and the absence of phase separation. The low and flat scattering pattern of the initial mixture highlighted that the system was not structured at pH 7.0. On the contrary, the scattering patterns of the coacervate phases presented characteristics features. Comparing the values of the scattered intensity in Figure 5.7a showed that the intensity decreased in the order: pH 4.5, pH 3.0, pH 3.5, pH 4.2, and pH 4.0 (c.f. inset). In Figure 5.7b the scattering patterns of the coacervate were shifted in order to compare their shapes more easily. A peak was measured at $Q \sim 0.3 \text{ nm}^{-1}$ for all the coacervate samples. The peak in the scattering pattern at $Q \sim 0.3 \text{ nm}^{-1}$ was attributed to the presence of GA. Indeed, when a (weak) polyelectrolyte like GA is present in a mixture, a peak appears corresponding to the repulsion between the charged groups of the molecule. This assumption is backed up by previous neutron scattering experiments of a GA mixture which showed a similar scattering behavior with a peak at $Q = 0.2 \text{ nm}^{-1}$. By increasing the ionic strength, the polyelectrolyte peak was reduced due to the screening of the carboxylic groups [unpublished result]. At pH 4.0 the concentration of GA in the coacervate phase was higher than at pH 4.2 and 4.5, as illustrated in Figure 5.5a and 5.5b, and a shift of the polyelectrolyte peak was noticeable from $Q = 0.30 \text{ nm}^{-1}$ at pH 4.5 (lower [GA]) to $Q = 0.37 \text{ nm}^{-1}$ at pH 4.0 (c.f. inset). This result was in good agreement with what one would expect for a polyelectrolyte solution. A shoulder at $Q = 0.7 \text{ nm}^{-1}$ was more or less pronounced depending on the pH value of the coacervate phase. It could be attributed

to a distribution of the WP structurally arranged in a compact manner. The position of the maximum of the shoulder was indeed independent of the WP concentration and of the pH, indicating an excluded volume type of interaction. The shoulder was the most pronounced at pH 4.0 and 4.2 (pH of maximum interaction). For pH 3.0 and 3.5, the peak faded away. This result suggested that at pH 4.0 and 4.2, the coacervate phase was more structured, thus inducing a stronger correlation between the WP molecules. To confirm this hypothesis, an attempt was made to use model calculations to predict the scattering intensity behavior of a WP/GA mixture and check whether the presence of the two peaks were really due to the GA molecules at $Q \sim 0.3 \text{ nm}^{-1}$ and WP molecules at $Q = 0.7 \text{ nm}^{-1}$. The scattering pattern of a WP / GA mixture was calculated from the individual scattering patterns of each biopolymer. The form factor $P(Q)$ of GA was approximated by calculating the scattering function of a charged polymer chain with excluded volume of the segments [Poetschke *et al.*, 2000]. WP are mainly composed of $\hat{\alpha}$ -lg. The hard sphere model (radius of $\hat{\alpha}$ -lg = 3 nm) was used to calculate the form factor $P(Q)$ and the structure factor $S(Q)$ of the $\hat{\alpha}$ -lg [McQuarrie, 1973]. This approximation was very simplified but the main features of the scattering pattern were recovered. In this model, it was hypothesized that the scattering patterns of the WP and GA were independent of each other. The scattering curve model of the coacervate was therefore obtained by adding the scattering intensities calculated for $\hat{\alpha}$ -lg and GA in the proportion as present in the coacervate phase at pH 4.0: 1.85 $\hat{\alpha}$ -lg per 1 GA. The model calculation was compared to the experimental data in Figure 5.7c for a coacervate at pH 4.0 and showed the qualitative features of the experimental data, especially for the position of the a peak at $Q = 0.7 \text{ nm}^{-1}$, corresponding to the structure factor of the protein, which confirmed the distribution of the WP as in a hard sphere liquid (*i.e.* WP distributed in a compact manner). Thus, one could tentatively conclude that WP served as macroions that controlled the degree of swelling of the GA molecules, especially at pH = 4.0. If the pH was decreased, the WP molecules were less numerous in the coacervate and the correlation peak was less pronounced (shoulder at $Q = 0.7 \text{ nm}^{-1}$ less pronounced) and if the electrostatic force was reduced (at pH < 4.0 or pH > 4.0), the GA molecules were less compact (peak shifting from 0.37 to 0.30 nm^{-1}), leading to a more open structure of the coacervate phase.

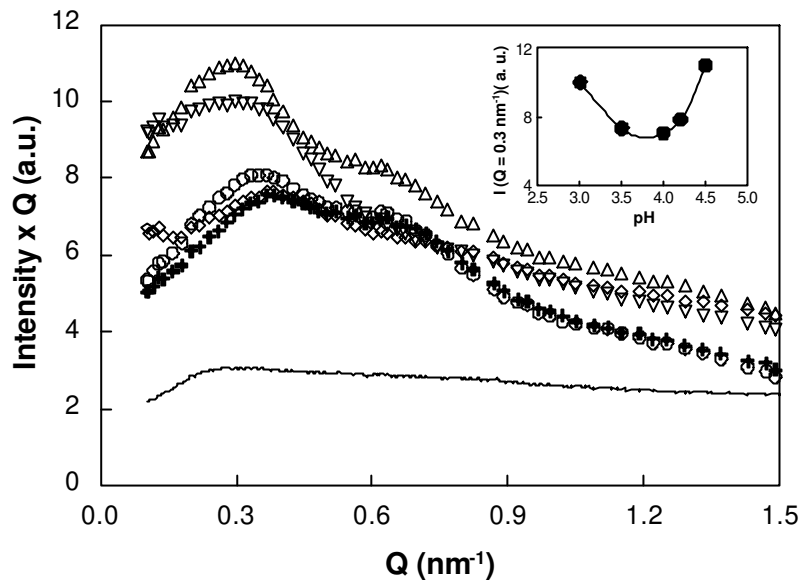


Figure 5.7a: SAXS data of WP/GA coacervate phase, $(Pr:Ps)_{ini} = 2:1$. (○): pH 4.5; (□): pH 4.2; (+): pH 4.0; (◇): pH 3.5; (▽): pH 3.0; (—): mixture of 3% WP/GA at pH 7.0. In the inset, the value of the scattering intensity at $Q = 0.3$ nm⁻¹ is plotted as a function of pH.

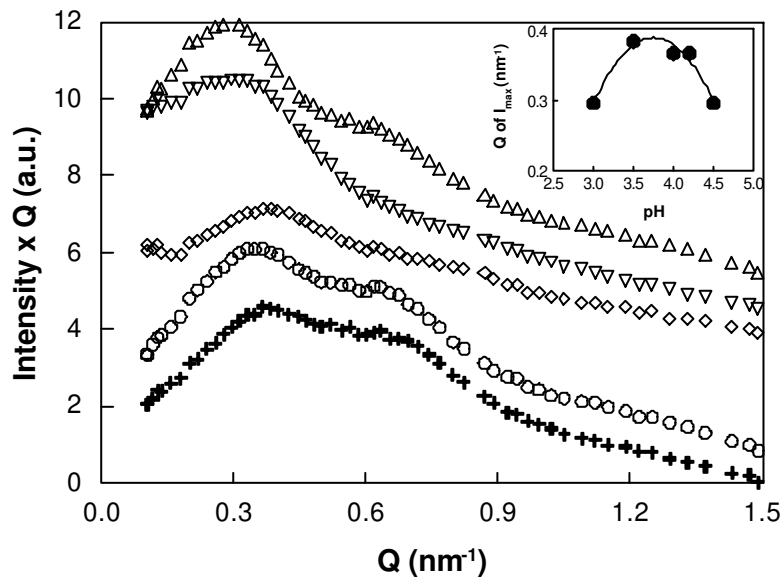


Figure 5.7b: SAXS data of WP/GA coacervate phase, $(Pr:Ps)_{ini} = 2:1$. Same values as Figure 5.7a, but shifted for better clarity. (○): pH 4.5; (□): pH 4.2; (+): pH 4.0; (◇): pH 3.5; (▽): pH 3.0. In the inset, the Q value corresponding to the maximum intensity is plotted as a function of pH.

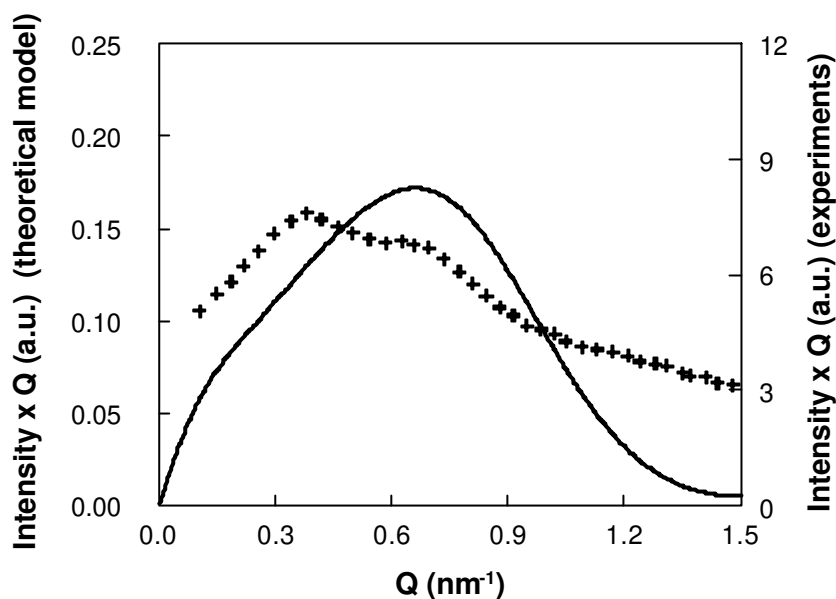


Figure 5.7c: (+): SAXS data of WP/GA coacervate, $(\text{Pr:Ps})_{\text{ini}} = 2:1$, pH 4.0; (—): Theoretical calculation.

Effect of Pr:Ps

SAXS measurements were carried out on coacervates prepared at $(\text{Pr:Ps})_{\text{ini}} = 1:1$, $2:1$ and $8:1$ for various pH values. The scattering patterns of coacervate prepared at pH 4.0 for the three different $(\text{Pr:Ps})_{\text{ini}}$ values is shown in Figure 5.8. For all the $(\text{Pr:Ps})_{\text{ini}}$ values studied, a peak was measured at $Q = 0.7 \text{ nm}^{-1}$, corresponding to the specific length scale in the WP distribution. The height of the polyelectrolyte peak at Q around 0.3 nm^{-1} decreased by increasing $(\text{Pr:Ps})_{\text{ini}}$. Indeed, the amount of WP in the coacervate phase increased by increasing $(\text{Pr:Ps})_{\text{ini}}$ as depicted in Figure 5.5b, and thus WP molecules might act as a screener of the polyelectrolyte interaction, reducing the intensity of the polyelectrolyte charge correlation peak. The scattering patterns were also compared for the three $(\text{Pr:Ps})_{\text{ini}}$ values but at the $\text{pH}_{\text{Cp-max}}$ determined in Figure 5.5a. The results are presented in Figure 5.9. The scattering patterns followed the expected trend. The amount of GA in the coacervate phase was maximum at $(\text{Pr:Ps})_{\text{ini}} = 1:1$ (cf. Figures 5.5a and 5.5b). The peak at $Q = 0.3 \text{ nm}^{-1}$ was thus more pronounced for $(\text{Pr:Ps})_{\text{ini}} = 1:1$. The amount of WP being maximum for $(\text{Pr:Ps})_{\text{ini}} = 8:1$, the peak at $Q = 0.7 \text{ nm}^{-1}$ was more pronounced at this ratio. Overall, the scattering patterns depicted in Figure 5.9 were more similar to each other than the scattering patterns in Figure 5.8, showing that the structures of the coacervate were comparable at their optimum pH.

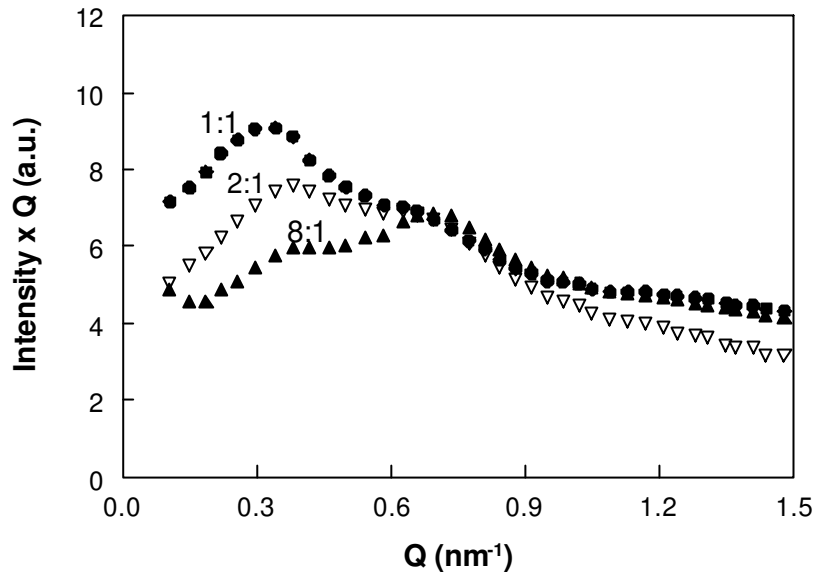


Figure 5.8: SAXS data of WP/GA coacervate phase, pH 4.0. (●): (Pr:Ps)_{ini} = 1:1; (▽): (Pr:Ps)_{ini} = 2:1; (▲): (Pr:Ps)_{ini} = 8:1.

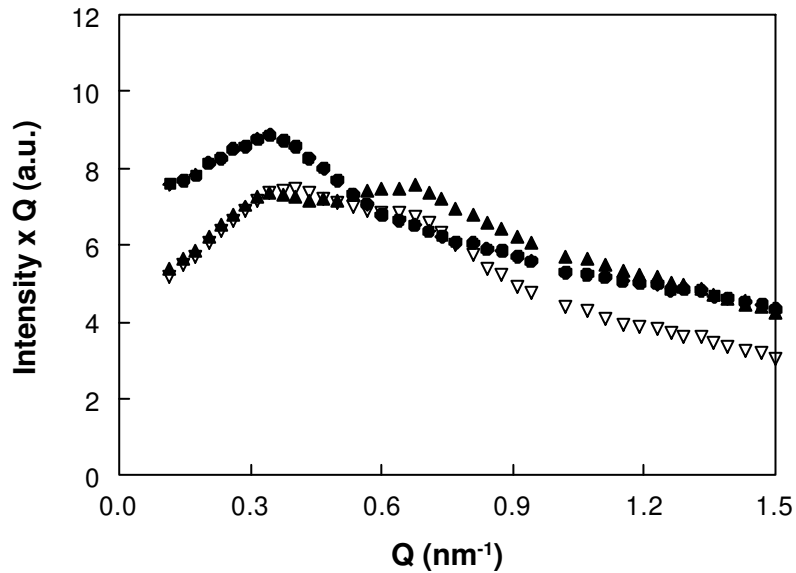


Figure 5.9: SAXS data of WP/GA coacervate phase, pH_{Cp-max}. (●): (Pr:Ps)_{ini} = 1:1, pH_{Cp-max} = 3.5; (▽): (Pr:Ps)_{ini} = 2:1, pH_{Cp-max} = 4.0; (▲): (Pr:Ps)_{ini} = 8:1, pH_{Cp-max} = 4.5.

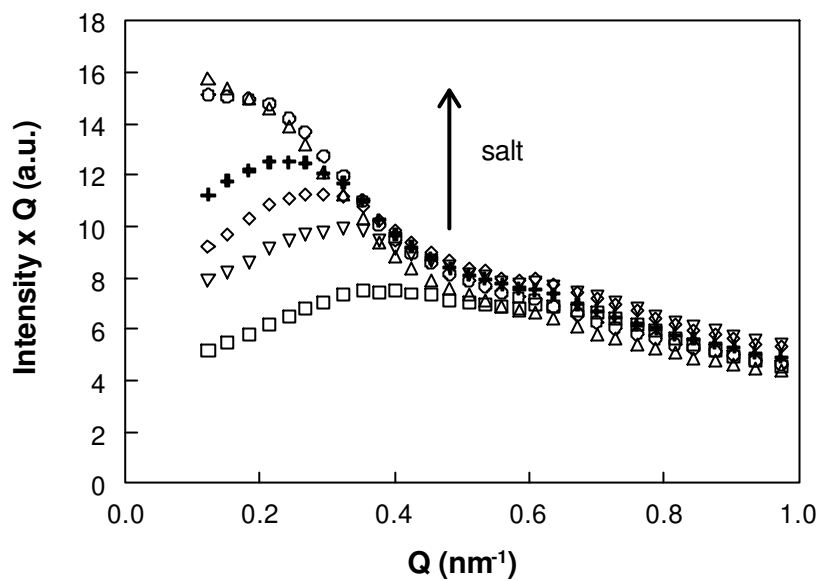


Figure 5.10a: SAXS data of WP/GA coacervate phase, $(Pr:Ps)_{ini} = 2:1$, pH 4.0, various $[NaCl]$. (○): 55 mM; (□): 50 mM; (+): 40 mM; (△): 30 mM; (▽): 20 mM; (◇): 0 mM.

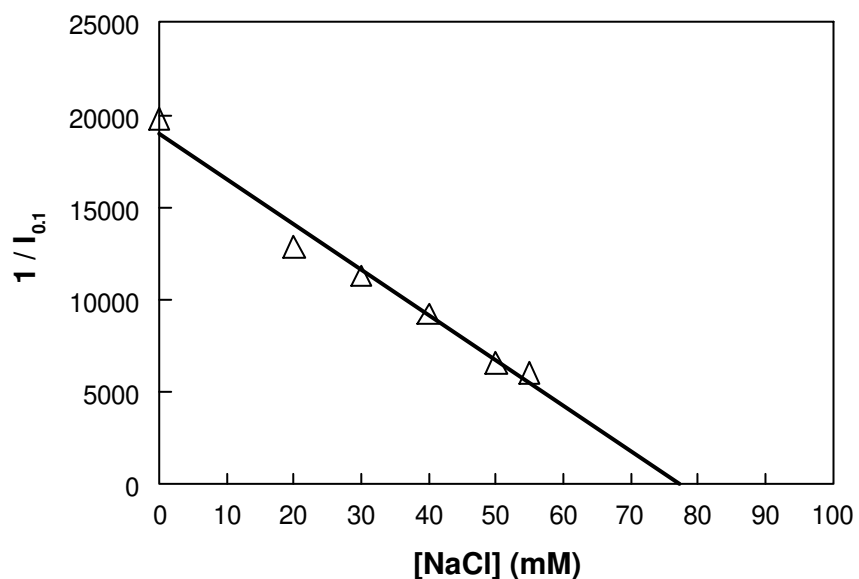


Figure 5.10b: $1/|b_{0.1}|$ versus $[NaCl]$. $b_{0.1}$ was measured from plot 9a.

Effect of the ionic strength

WP/GA coacervates were prepared at $(\text{Pr:Ps})_{\text{ini}} = 2:1$ at pH 4.0, and at various ionic strengths (ranging from $[\text{NaCl}] = 0 \text{ mM} - 55 \text{ mM}$). SAXS measurements were carried out on the coacervate phase and the scattering patterns are presented in Figure 5.10a. The results indicated that the addition of salt increased the scattered intensity, despite the fact that the polymer concentration decreased. When the ionic strength was increased, the strength of electrostatic interaction decreased as explained in the previous section. The structure of the coacervate also changed; the coacervate phase became less structured. By increasing $[\text{NaCl}]$, the position of the polyelectrolyte peak moved towards lower Q values and its intensity increased, indicating a more heterogeneous and more open coacervate structure. The scattering intensity at $Q = 0 \text{ nm}^{-1}$ is proportional to the osmotic compressibility of the system [McQuarrie, 1973]. Closer to the critical point, the osmotic compressibility tends to infinity. Experimentally, the values at $Q = 0 \text{ nm}^{-1}$ were not measurable, so the inverse of the scattering intensity at $Q = 0.1 \text{ nm}^{-1}$ ($1/l_{0.1}$) is plotted as a function of NaCl concentration in Figure 5.10b. The system was moved closer to the critical point when the ionic strength was increased [Weinbreck *et al.*, 2003a]. Therefore, the compressibility was increased, as indicated by the decrease of the term $1/l_{0.1}$. The extrapolation of $1/l_{0.1} = 0$ (corresponding to the critical point) gave a value of $[\text{NaCl}] = 77 \text{ mM}$, which could be interpreted as the critical NaCl concentration above which no complexation occurred. In Figure 5.6, it was found that coacervation was inhibited at $[\text{NaCl}] = 60 \text{ mM}$. Considering the rough approximation of $l_{0.1}$ as the compressibility under equilibrium, the agreement was fair.

CONCLUSIONS

The formation of complex coacervates was optimum at a specific pH value. For a $(\text{Pr:Ps})_{\text{ini}} = 2:1$, the optimum pH (pH_{opt}) was pH 4.0. At this particular pH, where the strength of the interaction was maximum, the volume and the density of coacervate phase were also the highest (Figures 5.4 and 5.5a) and phase separation occurred the fastest (Figure 5.3). SAXS data confirmed that, at pH_{opt} , the coacervate was dense and structured, as depicted in Figure 5.7a. From model calculation, a typical size of WP of 3 nm induced a peak at $Q = 0.7 \text{ nm}^{-1}$, meaning that WP behaved as in a hard sphere liquid in the coacervate phase. The structure of the coacervate phase should be seen

as a network of compact GA molecules whose degree of shrinkage depended on the amount of electrostatically bound WP. When the pH was decreased, fewer protein molecules were included in the coacervate phase and the correlation peak at $Q = 0.7 \text{ nm}^{-1}$ was almost undetectable, GA molecules were less compact and the coacervate less structured. Varying $(\text{Pr:Ps})_{\text{ini}}$ shifted the pH_{opt} to higher values when $(\text{Pr:Ps})_{\text{ini}}$ was increased and to lower values when $(\text{Pr:Ps})_{\text{ini}}$ was decreased. This phenomenon was due to the level of charge balance between WP and GA, which controlled the kinetics of phase separation and the structure of the coacervates, as already mentioned by Sanchez *et al.* (2002a). Another way of tuning the structure of the coacervate was by increasing the ionic strength. In doing so, the electrostatic interactions were screened and the coacervates became more watery (Figure 5.6). SAXS measurements also showed that the structure of coacervates was more heterogeneous and less structured when salt was added to the system, *i.e.* closer to the critical point (Figure 5.10a and 5.10b).

Denser or more open structures of WP/GA coacervates could be obtained by changing parameters like pH, Pr:Ps, or ionic strength. The diffusion properties and the barrier properties will be very dependent on this structure, which can be very useful for using the coacervates as barriers in encapsulation applications for instance. The diffusion of WP and GA within the coacervate phase is described in Chapter 7 [Weinbreck *et al.*, 2004c].

ACKNOWLEDGMENTS

Friesland Coberco Dairy Foods (FCDF) is acknowledged for their financial support. The authors would like to thank Vincent Gervaise and Frédérique Sanzey for their experimental assistance, Ab van der Linde for his help with the Zetasizer, and Dr. Igor Bodnár for enlightening discussions. Dr. Sven Hoffmann and Dr. Wim Bras are thanked for their technical assistance at DUBBLE (ESRF, Grenoble, France). The Netherlands Organization for the Advancement of Research (NWO) is acknowledged for providing the possibility and financial support for performing measurements at DUBBLE.

CHAPTER 6

Rheological Properties of Whey Protein / Gum Arabic Coacervates*

ABSTRACT

Complex coacervation in whey protein (WP) / gum arabic (GA) mixtures occurred in a specific pH window between 2.5 and 4.8. After phase separation, a concentrated polymer (also called coacervate) phase was obtained, whose visco-elastic properties were studied at various pH values. The viscosity of the WP/GA coacervate exhibited a surprisingly low shear-rate dependence, especially at pH 4.0, from 0.3 s^{-1} to 30 s^{-1} and a shear thinning above 30 s^{-1} , indicating a structural change. Hysteresis in the flow curve was measured at the pH values at which the electrostatic interactions were the strongest. Hysteresis was due to a slow structural rearrangement of the coacervate phase and, with time, the initial viscosity was completely recovered, showing that structural changes were reversible. In frequency sweep experiments, the values of G'' were up to 10 times higher than the values of G' , indicating the highly viscous character of the coacervates. pH 4.0 appeared to be the pH at which the coacervate phase was the most concentrated in biopolymer ($C_p = 32\%$), and at which the highest viscosity was measured. By decoupling the effect of biopolymer concentration and electrostatic interactions, it appeared that the high viscosity of the WP/GA coacervates was mainly due to the strong electrostatic interactions at low pH. The weaker the electrostatic interaction was, the lower the viscosity, especially at pH 4.5 and 3.0. The viscous behavior of the coacervates showed parallels with that of concentrated latex dispersions. WP/GA particles would consist of a GA polymer chain (as in latex) but now cross-linked by the electrostatic interactions with WP.

*F. Weinbreck, R. H. W. Wientjes, H. Nieuwenhuijse, G. W. Robijn, C. G. de Kruif
Submitted for publication

INTRODUCTION

Complex coacervation is a spontaneous liquid / liquid phase separation that occurs when two oppositely charged polymers (e.g. protein and polysaccharide) are mixed in aqueous media, leading to a separation into two phases. The lower phase is called the (complex) coacervate and is very concentrated in both polymers, and the upper phase, called the supernatant or equilibrium phase, is a dilute polymer solution. Complex coacervation finds applications in various fields [Schmitt *et al.*, 1998]. The most important industrial application of complex coacervation is microencapsulation. Microcapsules result from the ability of the coacervate to form a coating around sensitive materials [see for example: Burgess, 1994; Daniels and Mittermaier, 1995; Luzzi, 1970]. Complex coacervation is also a cheap and easy method for purification of macromolecules [Serov *et al.*, 1985; Wang *et al.*, 1996]. Coacervates are used as food ingredients (e.g. fat replacers or meat analogues) [Bakker *et al.*, 1994; Dziezak, 1989; Tolstoguzov *et al.*, 1974] or biomaterials (e.g. edible films, packaging) [Kester and Fennema, 1986]. This broad range of application of protein / polysaccharide complex coacervation is probably due to the fact that these ingredients are from a biological source and are entirely biodegradable, and possess high nutritional and functional properties. Burgess (1994) mentioned that the high viscosity of the albumin / gum arabic coacervate led to capsules that were more stable against coalescence, although no cross-linking agent was used, and Gurov *et al.* (1986) hypothesized that the complex formation of bovine serum albumin and dextran sulfate caused an effect on the mechanical properties of the interfacial films, which were more elastic. Thomassin and Merkle (1997) pointed out that the visco-elastic properties of the coacervate phase influenced the encapsulation process.

As mentioned in a recent review on protein – polysaccharide interaction, the understanding of coacervating systems remains scarce [Turgeon *et al.*, 2003]. Although there are several indications from the literature cited above that the rheology of the coacervate phase is an important parameter, literature on the visco-elasticity of a coacervate system is rather limited. Sánchez *et al.* (1995) determined the viscosity of dispersions of soy proteins – polysaccharide complexes, and found that the viscosity of a soy protein mixed with guar or xanthan was respectively 140 times and 2.4 times higher than the viscosity of the unmixed biopolymer solutions. Mann and Malik (1996) also showed that the viscosity of whey proteins (WP) – carboxymethylcellulose (CMC)

complexes depended on the complex concentration. As polysaccharide dispersions display generally higher viscosity than protein dispersions, it is rather expected that the protein to polysaccharide ratio modifies the viscosity of complex mixtures, as described for protein-starch based fat replacers [Tarr and Bixby, 1995]. Furthermore, the interaction between the polymers will influence the visco-elasticity of the system. The role of electrostatic interactions inducing an increase in viscosity has been reported in various studies. Stronger gels of protein / carrageenan were formed due to electrostatic interaction between the polymers [Baeza *et al.*, 2002; Ould Eleya and Turgeon, 2000b]. Arnedo and Benoit (1987) hypothesized that a stronger ionic interaction of sodium alginate with gelatin was responsible for a higher viscosity measured for this system as compared to a gelatin / gum arabic system.

From this overview, it becomes clear that the relation between macroscopic visco-elasticity and mesoscopic parameters is rather limited. Also a better physical understanding is required to optimize practical applications like encapsulation. Therefore, the scope of this study was to obtain insights into the structure of the coacervate phase via the study of the flow behavior and visco-elastic properties of whey protein / gum arabic (WP/GA) coacervates. Previous studies showed that complex coacervation between WP and GA occurred in a specific pH window (between pH_{ϕ_1} and pH_{ϕ_2}) [Weinbreck *et al.*, 2003a]. Under acidic conditions, WP and GA were oppositely charged and formed an electrostatic complex. If the required conditions were met, the WP/GA complexes phase separated and concentrated in coacervate droplets that subsequently sedimented and coalesced at the bottom of the tube to form a homogeneous coacervate layer. The phase-ordering kinetics of α -lactoglobulin/GA complex coacervation was recently studied using small-angle static light scattering [Sanchez *et al.*, 2002a]. No definite conclusion on the occurrence of spinodal decomposition or nucleation and growth was possible. In addition, an attempt was made to understand the structure of α -lactoglobulin/GA coacervates. Depending on the protein to polysaccharide ratio, the internal structure of the coacervate droplets appeared vesicular to sponge-like, exhibiting numerous inclusions of water [Schmitt *et al.*, 2001a]. The occurrence of vacuoles was explained by the presence, at the interface of coacervate droplets, of GA that was not electrostatically neutralizing α -lactoglobulin, so that water was entrapped [Sanchez *et al.*, 2002a]. In time, neutralization proceeded, leading to rearrangements within the coacervates, and the vacuoles disappeared. Thus, in this study, rheological measurements were done on the coacervate phase

after 48 h of phase separation. The strength of the electrostatic interaction between WP and GA varied as a function of pH, and, since the formation of WP/GA complexes arose from the charge compensation, the stoichiometry and composition of the coacervate phase will differ at each pH. Existing theoretical models describing the process of complex coacervation are only approximate [Overbeek and Voorn, 1957; Tainaka, 1979; Veis and Aranyi, 1960]. As far as we know, there are no theories or models describing the rheology. Hopefully, the experimental results presented here may lead to new ideas and models. The goal of the present work was, firstly, to investigate the composition of the coacervate phase in WP and GA at various pH values and, secondly, to study the rheological properties of the coacervates at each specific pH. These unique results will aid the understanding of the structure of a coacervate phase.

EXPERIMENTAL SECTION

Materials

Bipro is a whey protein isolate (WP) consisting mainly of α -lactoglobulin (α -lg), and α -lactalbumin (α -la) - from Davisco Foods International (Le Sueur, USA). Residual whey protein aggregates were removed by acidification (at pH 4.75) and centrifugation (1 h at 33000 rpm with a Beckman L8-70M ultracentrifuge, Beckman Instruments, The Netherlands). The supernatant was then freeze-dried (in a Modulo 4K freeze-dryer from Edwards High Vacuum International, UK). Finally, the resulting powder was stored at 5°C. The final powder contained (w/w) 88.1% protein (N x 6.38), 9.89% moisture, 0.3% fat and 1.84% ash (0.66% Na⁺, 0.075% K⁺, 0.0086% Mg²⁺, and 0.094% Ca²⁺). The protein content of the treated Bipro is: 14.9% α -la, 1.5% BSA, 74.9% β -lg, and 3.2% immunoglobulin (IMG).

Gum arabic (GA; IRX 40693) was a gift from Colloides Naturels International (Rouen, France). The powder contained (w/w) 90.17% dry solid, 3.44% moisture, 0.338% nitrogen and 3.39% ash (0.044% Na⁺, 0.76% K⁺, 0.20% Mg²⁺ and 0.666% Ca²⁺). Its weight average molar mass ($M_w = 520\ 000$ g/mol) and its average radius of gyration ($R_g = 24.4$ nm) were determined by size exclusion chromatography followed by multiangle laser light scattering (SEC MALLS). SEC MALLS was carried out using a TSK-Gel 6000 PW + 5000 PW column (Tosoh Corporation, Tokyo, Japan) in combination with a

precolumn Guard PW 11. The separation was carried out at 30°C with 0.1 M NaNO₃ as eluent at a flow rate of 1.0 mL min⁻¹.

Stock solutions of 3% (w/w) were prepared by dissolving the powder in deionized water.

The zeta-potential of the WP and GA mixtures was measured as a function of pH with a Zetasizer 2000 (Malvern, USA).

Preparation of the coacervates

The stock solutions of 3% (w/w) WP and GA were mixed at a protein to polysaccharide (Pr:Ps) ratio of 2:1. Sodium azide (0.02% w/w) was added to prevent bacterial growth. The pH of the mixtures was set precisely (± 0.05 pH-units) at various values: 3.0, 3.5, 3.8, 4.0, 4.2, 4.35, 4.5. The samples were placed in a decanter at 25°C for 48 h to allow complete phase separation. The experiments were carried out on the lower (coacervate) phase.

Composition of the coacervate phase

The amount of water contained in the coacervates at each pH was determined at least in duplicate by weighing the sample before and after freeze-drying. The concentrations and composition of WP and GA in the coacervates were determined by measuring the residual polymers in the upper phase by HPLC.

Nuclear Magnetic Resonance (NMR)

NMR measurements were carried out on the WP/GA coacervate phase (prepared in D₂O instead of deionized water) at pH 4.0 in order to determine the diffusion coefficient of the GA within the coacervate phase. DOSY (Diffusion Ordered SpectroscopY) spectra were taken on a Bruker DRX500 spectrometer operating at 500.13 MHz. A pulse sequence, using stimulated echo, longitudinal eddy current delay and bipolar gradient pulses, was applied. The experiment was performed at 22°C. Typical values for the parameters were: 8 s for the relaxation delay, 400 ms for diffusion time (Δ) and 3 ms for the gradient pulse length (δ). The gradient strength was varied linearly from 10 to 500 mT/m. Gradient calibration was based on a solution of SDS, glucose and ATP in D₂O [Morris and Johnson, 1993]. Processing of the data was carried out using the DOSY module of the XWinNMR software.

Rheological measurements

The rheological measurements were done using a Carri-med Rheometer, type CSL² 500 A/G H/R, with a cone-plate geometry (diameter 6 cm, angle 2°) (TA Instruments Benelux, Belgium). The temperature was controlled at 25°C by using a Peltier element. For each sample, flow curves were measured at increasing shear rate (from 0.3 s⁻¹ to 100 s⁻¹) followed by a reverse flow at decreasing shear rate (from 100 s⁻¹ to 0.3 s⁻¹). The ramp mode was logarithmic and the time between two measurements was 30 s. For Figure 6.2c, the same flow measurement was carried out as previously described, but an extra time step was added at a shear rate of 10 s⁻¹ on the first flow curve (A) and reverse flow curve (B), where the viscosity was monitored every 5 s during 20 min for A and 30 min for B. Frequency sweeps (0.1 – 40 Hz) were carried out as well for a strain of 1.0%, which was in the linear regime (as checked by strain sweep measurements). During the measurements, all samples were covered with paraffin oil to avoid drying. Blanks of the same composition as the coacervates were measured at pH 7.0. Measurements were done at least in triplicate in order to get good statistics on the results.

RESULTS AND DISCUSSION

This study aimed to give more insights into the structure and rheology of WP/GA coacervates. In a first part of the study, the WP/GA coacervates were analyzed and characterized by determining their polymer concentration. Then, flow measurements were made to study the influence of pH on the viscosity of the coacervate. Frequency sweep measurements were carried out on the same samples and the influence of the electrostatic interactions on the rheological and visco-elastic properties of the coacervates was estimated from zeta-potential measurements. Finally, the results were discussed in terms of structural properties of the coacervates.

Composition of the coacervate phase

Complex coacervates of whey proteins (WP) and gum arabic (GA) were prepared at various pH values. The initial composition of the mixture was identical for all samples; the total biopolymer concentration (C_p) was set at 3% and the protein to polysaccharide ratio (Pr:Ps) at 2:1. After acidification to the desired pH, the samples were left at 25°C for 48 h to reach complete phase separation. A coacervate phase

consisting of WP/GA complexes was formed at the bottom of the decanter. The coacervate phase was taken out and freeze-dried to determine the amount of water. The amount of residual WP and GA in the upper phase was also measured by HPLC. Thus, the final composition of the coacervate, *i.e.* the concentration in biopolymer (C_p) and the final Pr:Ps, was determined and plotted for each pH in Figure 6.1. Increasing the pH from pH 3.0 to pH 4.5 led to an increase of the Pr:Ps in the coacervate phase from 1.3 to 2.6. The WP used in this study mainly consisted of β -lg (>75%), which had an iso-electric point (pI) of 5.2. Thus, by increasing the pH from 3.0 to 4.5, the charge density of the protein decreased. This result was in line with previous work and could be understood since at higher pH, more proteins will bind to the GA to compensate its negative charges [Weinbreck *et al.*, 2003b]. On the other hand, at pH 3.0, the protein was much more charged than at higher pH, and the GA less negatively charged, and thus fewer proteins were needed to obtain a neutral complex. Furthermore, the amount of total biopolymer showed a maximum ($C_p = 32.8\%$) at pH 4.0, which indicated that at this pH the maximum degree of coacervation was reached. The composition and the formation of the WP/GA coacervates showed a strong pH dependence.

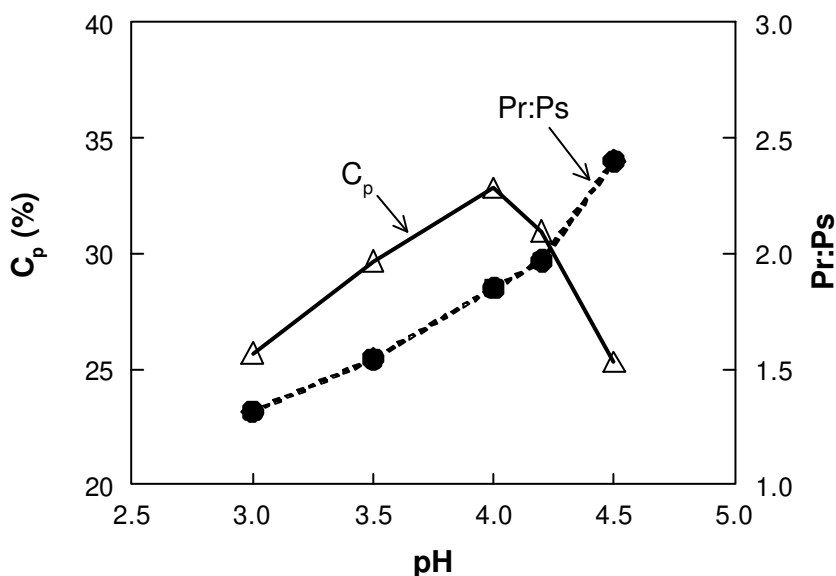


Figure 6.1: (Δ): Total biopolymer concentration and (\bullet): Protein to polysaccharide ratio in the WP / GA coacervate phase as a function of pH.

Flow experiments

The viscosity (η) of the WP/GA coacervates was determined by carrying out flow experiments for samples prepared at various pH values. The results are presented in Figures 6.2a and 6.2b for pH 4.0 and pH 3.0 respectively, upon increasing and decreasing shear rate. A blank was also measured in both cases. The blanks had the same composition as the coacervate phase (same Cp and Pr:Ps as depicted in Figure 6.1), but they were prepared at pH 7.0, a pH at which no attractive electrostatic interactions between WP and GA occurred.

As illustrated in Figure 6.2a, the viscosity of the coacervate at pH 4.0 was much higher than the viscosity of the blank at pH 7.0, although the concentration of biopolymer was similar, which implied that electrostatics caused the high viscosity of the coacervate. Besides, at pH 4.0, the viscosity of the coacervate decreased slightly (from 5 to 2.5 Pa.s) with increasing shear rate from 0.1 to 30 s⁻¹, which highlighted the very limited shear thinning behavior of the coacervate. The blank showed more shear thinning (almost over one decade) than the coacervate. The result was striking since most concentrated biopolymer mixtures are shear thinning due to the polysaccharide relaxations. Recently, Sanchez *et al.* (2002b) studied the rheological properties of acacia gum dispersions and they reported that the viscosity of a 12% GA solution decreased from ~ 0.025 Pa.s to 0.013 Pa.s as the shear rate increased from 0.08 s⁻¹ to 100 s⁻¹. The blank in Figure 6.2a was composed of 11.5% GA and 21.3% WP (see Figure 6.1), and it behaved similarly to the samples described by Sanchez *et al.* (2002b). GA was, as expected, the main molecule responsible for inducing a shear thinning viscosity. At a shear rate of 30 s⁻¹, a kink in the flow curve of the coacervate at pH 4.0 was visible with a local slope of about -2. For conventional concentrated polymer systems, theory predicts a slope between 0 and -1 [Macosko, 1993]. The observation of higher slopes indicated the existence of an additional mechanism besides the alignment of the polymers due to the shear rate of 30 s⁻¹. A possible additional mechanism would be the breakdown of structures due to the breakup of physical bonds at high shear. This hypothesis was supported by the fact that the sample showed hysteresis between increasing and decreasing flow rate. Indeed, a gap between the flow curves was clearly visible, although the initial viscosity at low shear rates was recovered. This result showed that at pH 4.0, the coacervate phase contained structures which needed time to reform after a deformation. This structure

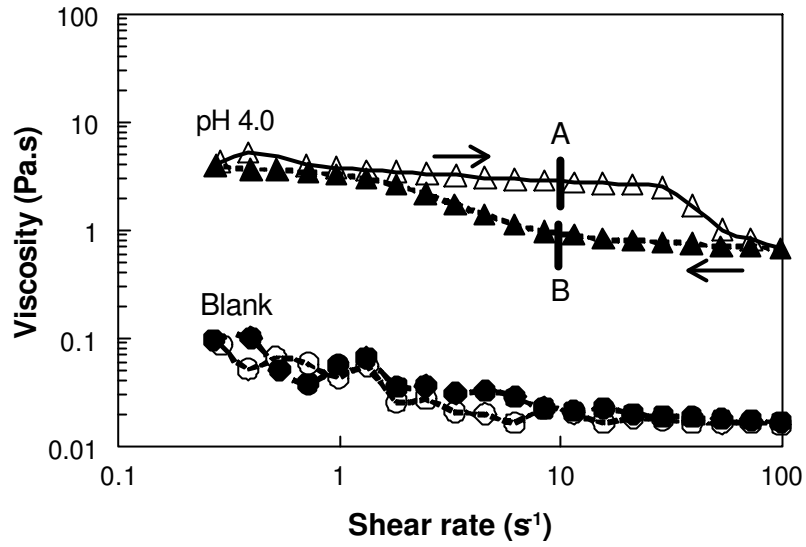


Figure 6.2a: Viscosity of WP/GA coacervates as a function of shear rate, Temperature = 25°C; (/): pH 4.0 and (/): blank at pH 7.0, open symbols: first flow and filled symbols: reverse flow.

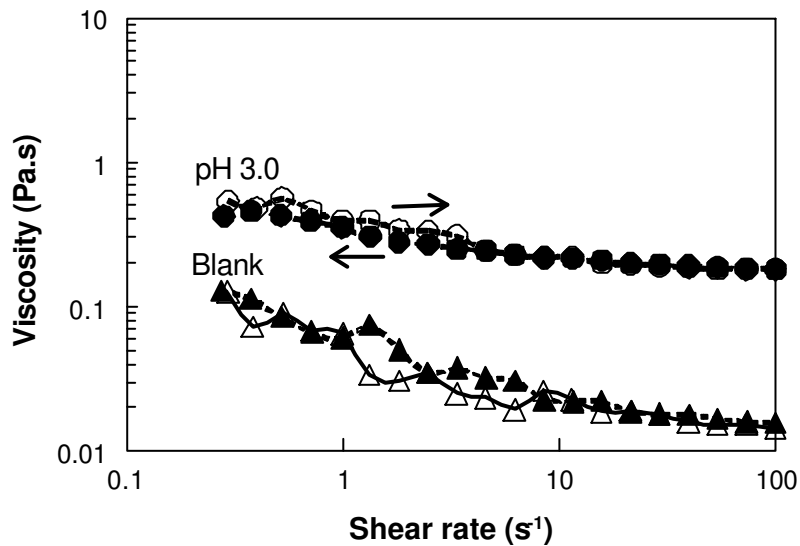


Figure 6.2b: Viscosity of WP/GA coacervates as a function of shear rate, Temperature = 25°C; (/): pH 3.0 and (/): blank at pH 7.0, open symbols: first flow and filled symbols: reverse flow.

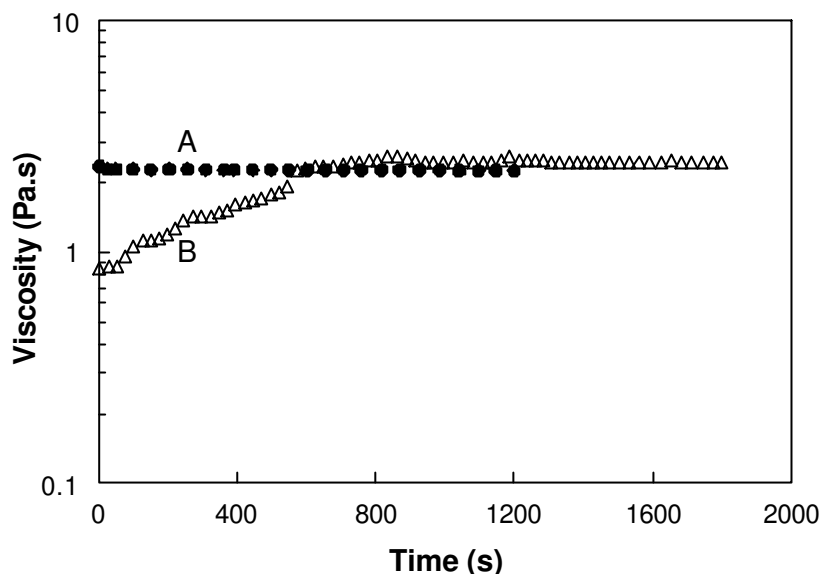


Figure 6.2c: Viscosity of WP / GA coacervates as a function of time for the points A and B in figure 6.2a, pH = 4.0, shear rate = 10 s^{-1} , Temperature = 25°C ; (\bullet): point A (first flow), (\triangle): point B (reverse flow).

was most probably due to the electrostatic interactions between WP and GA. The presence of electrostatic interactions at pH 4.0 would lead to an attraction of the WP to the GA chain, which might disturb the deformation of the polysaccharide. Indeed, when no attractive interaction took place, such as in the blank at pH 7.0, the shear thinning behavior was more pronounced but no hysteresis was measured.

In Figure 6.2b, the viscosity of the coacervate at pH 3.0 and the viscosity of the blank made of the same composition as the coacervate, but at pH 7, are plotted as a function of shear rate. The viscosity of the coacervate was lower at pH 3.0 than at pH 4.0, although it still remained higher than the viscosity of the blank. The coacervate at pH 3.0 was more shear thinning than at pH 4.0. Limited hysteresis was measured and no clear structure breakdown was noticeable as compared to the sample at pH 4.0.

The hypothesis that the hysteresis appearing at pH 4.0 was due a slow structural rearrangement was checked by an extra experiment. The same experiment as in Figure 6.2a was repeated but an extra step was added at a shear rate of 10 s^{-1} ; the viscosity was measured as a function of time in the first and reverse flow (point A and B respectively, cf Figures 6.2a and 6.2c). The results are presented in Figure 6.2c. At point A, the viscosity of the coacervate at a constant shear rate of 10 s^{-1} did not change

with time, showing that the sample was in a dynamic equilibrium state during the increasing flow rate measurement. In contrast, in the reverse flow curve, at point B, the viscosity of the coacervates slowly increased from a low initial viscosity ($\eta = 0.85 \text{ Pa}\cdot\text{s}$) up to the same viscosity as the viscosity measured at the point A ($\eta = 2.4 \text{ Pa}\cdot\text{s}$). Then, the viscosity measured at point B remained constant at this value. This experiment showed that the coacervate structures were disrupted at high shear (30 s^{-1}) and needed time to be reformed. Indeed, in Figure 6.2a, the reverse flow curve was measured with one measurement every 30 s, and from Figure 6.2c, it seemed that the sample at point B reached a constant value after 11 min. Thus, the hysteresis measured in Figure 6.2a was mainly due to a slow recovery of the initial coacervate structure; this structure was fully reversible even after a breakdown.

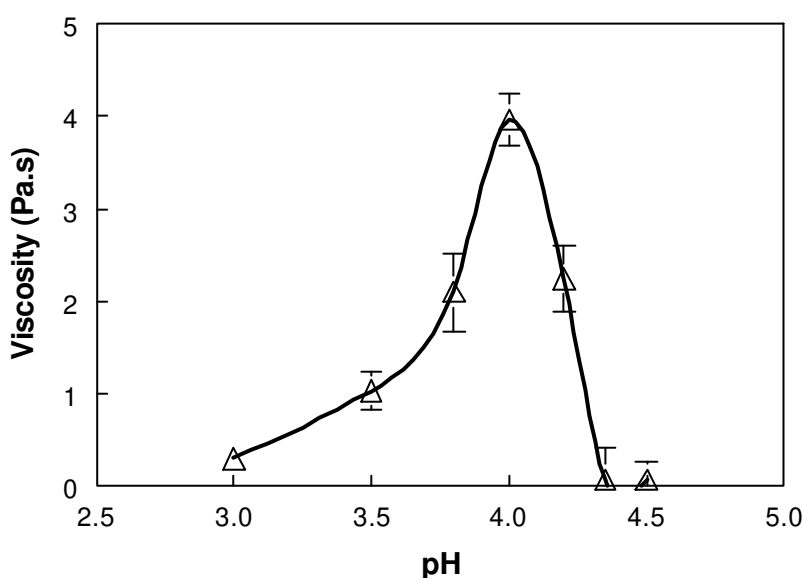


Figure 6.3: Averaged viscosity of WP / GA coacervates at various pH values, shear rate = 0.5 s^{-1} , Temperature = 25°C . Error bars represent the standard deviation based on triplicate measurements.

In order to give a broader overview of the influence of pH, flow experiments were carried out at various pH values and the viscosity at a shear rate of 0.5 s^{-1} was plotted as a function of pH (Figure 6.3). The values of viscosity showed a maximum at pH 4.0 but were asymmetrical on either side of this value. From pH 3.0 to pH 4.0, the viscosity increased smoothly, and from pH 4.0 to 4.5, the viscosity of the coacervates decreased sharply. Furthermore, coacervates prepared at pH 3.8, 4.0, and 4.2 presented some

hysteresis. This result showed that the viscosity of coacervates was clearly pH-dependent and pH 4.0 was the pH of maximum coacervation (highest C_p and η).

Frequency sweeps

The dynamic moduli G' and G'' were measured with frequency sweep experiments at a constant strain of 1%, which was checked as being in the linear regime. The values of G'' were typically 3 to 7 times higher than the values of G' , and because of the highly viscous behavior of the coacervates, the values of G' were not reliable. Results of G'' versus frequency are plotted for various pH values in Figure 6.4. For blanks (not shown here), the ratio of G''/G' was around 0.4 at 0.5 Hz, showing that the viscous properties of the coacervates appeared only when the electrostatic attractive interactions took place. In 6% GA dispersions, Sanchez *et al.* (2002b) showed that G''/G' could reach values around 0.3 – 0.4; these results were in good agreement with the values of $G''/G' = 0.4$ found here for the blanks. Concerning the coacervate sample at acidic pH values, the slopes of G'' versus frequency were between 0.92 and 0.99 (except for pH 4.5), which was close to the theoretical limits of +1 for completely relaxed polymer mixtures [Macosko, 1993].

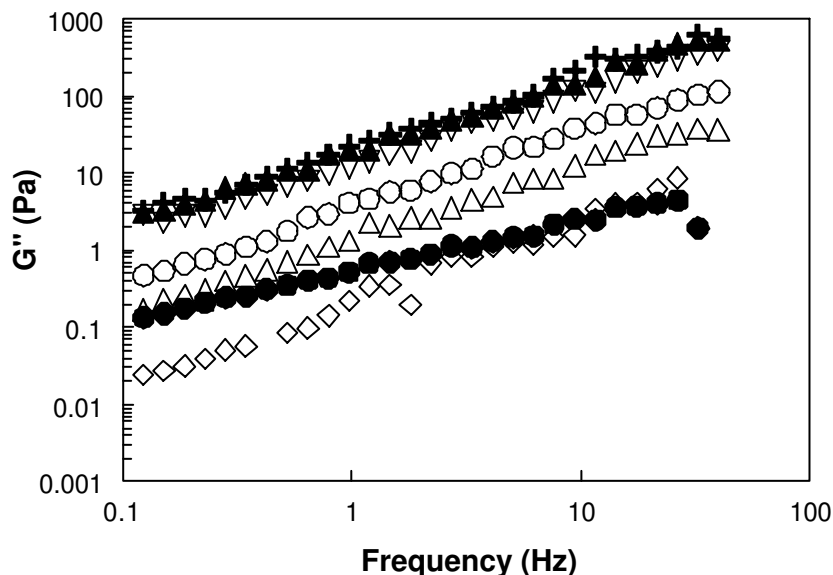


Figure 6.4: Viscous modulus (G'') of WP/GA coacervates as a function of the oscillation frequency, constant strain of 1%, Temperature = 25°C.; (○): pH 3.0; (□): pH 3.5; (▽): pH 3.8; (+): pH 4.0; (△): pH 4.2; (◇): pH 4.35; (●): pH 4.5.

The Cox Merz rule states that the shear dependence of the steady state viscosity (η) is equal to the frequency dependence of the linear visco-elastic viscosity η^* ($\eta^* = \sqrt{(\eta'{}^2 + \eta''{}^2)}$), for a shear rate equal to the angular frequency ($\dot{\gamma}$) [Macosko, 1993]. Applying the Cox Merz rule in this particular case would correspond to compare η to η' since G' ($G' = \eta' / \dot{\gamma}$) was small compared to G'' ($G'' = \eta'' / \dot{\gamma}$). The pH-averaged ratio of η' / η equaled 1.20 with a standard deviation of 0.67 (for G'' at 0.1 Hz and η at 0.6 s⁻¹). The Cox Merz rule held fairly well for this system at low deformation. Here, it should be emphasized that no structure breakdown was visible in the frequency sweeps, indicating that the structure of the coacervates was in dynamic equilibrium during the frequency sweep measurement. Finally, the maximal value of G'' was found at pH 4.0, as for the flow experiments. More detailed experiments were then carried out to understand the influence of pH on the viscosity.

Influence of the electrostatic interactions

The rheological measurements showed that the viscosity of the coacervates was highly pH dependent. However, it was reported that at each pH, the composition of the coacervate phase with respect to concentration was different (Figure 6.1), since the charge density of the protein and the polysaccharide varies as a function of pH. From these results, it seemed obvious that the composition of the coacervates might influence their viscosity. For that reason blanks were made at the same WP and GA concentration as the coacervate (for each pH) but at pH 7.0, where no attractive electrostatic interaction were present. Flow experiments were carried out on those blank samples. The viscosity of the coacervates was then divided by the viscosity of the blank to eliminate the influence of the different polymer concentrations; the results are shown in Figure 6.5. A strong maximum was clearly obtained at pH 4. The value of the viscosity of the coacervate was 45 times larger than the viscosity of the blank at pH 7. For lower and higher pH, this ratio was less extreme, and for pH 4.5, the ratio was close to 1. It could be concluded that the high viscosity of the coacervates was mainly due to the attractive electrostatic interactions between WP and GA. An attempt was made to quantify the strength of the interaction by calculating the absolute product of the individual zeta-potentials of the WP and the GA ($Z_{WP} \times Z_{GA}$) as a function of pH. The calculation showed that the $Z_{WP} \times Z_{GA}$ was maximum at pH 4.0, meaning that the electrostatic interaction between WP and GA was the strongest at this pH. In Figure 6.6, $\eta_{\text{coacervates}} / \eta_{\text{blanks}}$ was plotted as a function of the product of the zeta-potential of

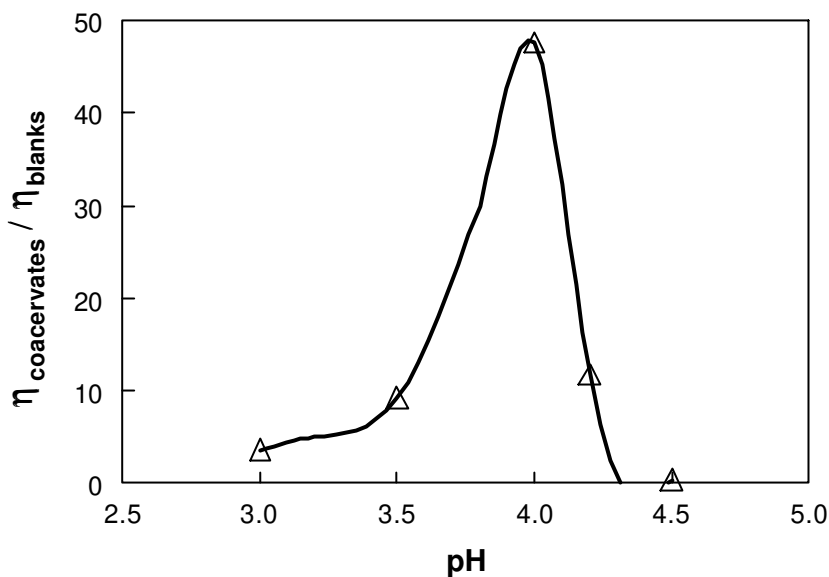


Figure 6.5: Viscosity of coacervates normalized by the viscosity of the blank as a function of pH. For each pH a blank corresponding to the same composition (Cp and Pr:Ps) of the coacervate was made, but at pH 7.0.

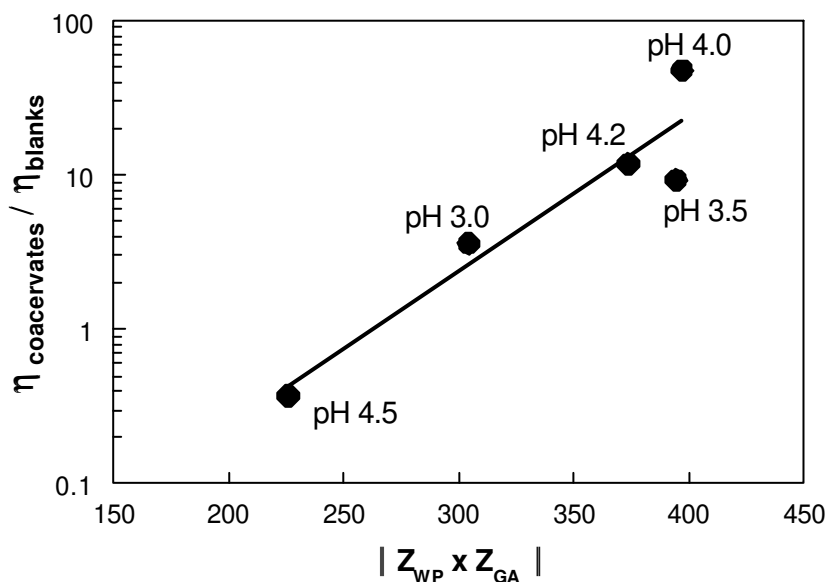


Figure 6.6: Viscosity of coacervates normalized by the viscosity of the blank as a function of the product of the zeta-potentials of WP and GA.

the individual polymers ($Z_{WP} \times Z_{GA}$). The higher the zeta-potential product was, the higher the viscosity of the coacervates. The results highlighted once more that the strength of the electrostatic interaction was the main factor responsible for the high viscosity of the coacervates.

Discussion on the structure of the coacervate phase

This study presents one of the first results on the viscosity of WP/GA coacervates as a function of pH. It was found that the viscosity was strongly pH-dependent and the highest viscosity was observed at pH 4.0. The flow experiments (viscosity versus shear rate) at pH 4.0 indicated that shear thinning occurred at a shear rate of 30 s^{-1} . For concentrated polymer systems, shear thinning behavior is related to diffusion processes of the polymers within the system. However, the observed viscosity decrease at 30 s^{-1} was stronger than expected from diffusion only. Therefore, the decrease indicated a structure change, as evidenced by Figure 6.2c, in which it is shown that after a high shear the system needed 11 min to obtain the full recovery of the initial viscosity. The diffusion coefficient of GA (D_{GA}) in the coacervate was measured by NMR. At pH 4.0, $D_{GA} = 3.82 \times 10^{-12} \text{ m}^2 \text{ s}^{-1}$. The characteristic time scale (τ_{GA}) over which GA diffused in the coacervate could be estimated from the diffusion coefficient using:

$$\tau_{GA} = a^2 / D_{GA} \quad (\text{Eq.1})$$

where a is the radius of the GA molecule. By using $a = R_g = 24 \text{ nm}$, the time scale corresponding to the diffusion of the GA was estimated as 0.15 ms. The viscosity decrease appeared at a shear rate of 30 s^{-1} , which corresponds to a time scale of 33 ms. This difference in time scale thus indicated that the diffusional relaxation of GA was not at the origin of the shear thinning. One can argue that, since the observed time scale over which the viscosity decreases is higher than τ_{GA} , also the typical length scale had to be larger than R_g . By using Eq. (1) backwards, this typical length scale would then be of the order of 0.4 μm . Such a length scale would be in line with the fact that the coacervate phase was optically turbid. This turbidity arose from a length scale in the micrometer range. If the coacervate phase was made of a homogeneous structure of polymers on the nanometer scale, it would look transparent, which was the case for the blanks. Obviously, heterogeneities on a micrometer scale were formed. Leisner *et al.* (2003) explained the structure of poly(glutamic acid) / anionic dendrimer coacervates also by assuming an initial aggregation of intermolecular clusters which

led to compact microgel heterogeneities. Although this result is in good agreement with the hypothesis raised here, the nature of the aggregation is still poorly understood. From previous experiments, it was found that the WP / GA complexes could be viewed as a GA chain decorated with WP molecules (like a pearl necklace) [Weinbreck *et al.*, 2003a]. This polymer chain was, however, not extended, but collapsed as appeared from combined dynamic and static light scattering experiments on the soluble complexes in the one phase region. Thus, the WP/GA complexes could be viewed as dense particles still having a mutual attractive interaction. In such a dispersion, the viscosity would scale with the volume fraction (ϕ) and the strength of the attractive interaction. As shown by Russel (1984) for a (semidilute) dispersion of adhesive hard spheres, the ϕ^2 – term is an exponential function of the interaction potential. Therefore, in the present work, one would expect that viscosity would scale with the exponent of the interaction potential. In order to examine this hypothesis, in Figure 6.6, $\ln(\eta_{\text{coacervates}} / \eta_{\text{blanks}})$ was plotted against the electrostatic interaction $Z_{\text{WP}} \times Z_{\text{GA}}$ and a clear linear dependence was observed.

Summarizing, we can explain the behavior of WP/GA coacervates by assuming that the system consists of dense particles with a mutual attractive interaction. This would be in line with the observation that the system is much more viscous than elastic. An analogy could be made with latex particles. Latex particles are internally covalently cross-linked which rheological behavior is rather similar to the behavior observed for the coacervate system at pH 4.0 [de Rooij, 1994]. In the case of the coacervate system, GA will be electrostatically “cross-linked” with WP. The stronger the electrostatic interaction is, the denser the complexes. Furthermore, since electrostatic interactions do have a physical origin, also a structure recovery as observed in Figure 6.2c can be expected.

CONCLUSIONS

pH played a major role in the composition and properties of WP/GA complex coacervates. At pH 4.0, the viscosity of the coacervate was maximum and so were the biopolymer concentration and the strength of the interaction. In the pH range between 3.0 and 4.5, the coacervate did not present a shear thinning onset (below 20 s^{-1}). At a shear rate of 30 s^{-1} , for pH 4.0, a sharp viscosity decrease occurred. Hysteresis upon increasing and decreasing shear rate could be measured for pH 3.8, 4.0, and 4.2 (pH where the electrostatic interactions were the strongest). It was shown that hysteresis

was related to a slow structural rearrangement of the coacervates after shearing. Rheological measurements on the coacervate phase have not been carried out before (as far as we know) and they brought new insights into the structure of the coacervate. By decoupling the effect of concentration and electrostatic forces, it seemed that the binding of the WP to the GA was responsible for the highly viscous behavior of the coacervates. The results could thus be understood by regarding the coacervate as a liquid phase whose structure could be deformed and reformed in a reversible process. The WP/GA complexes could be seen as a concentrated dispersion of GA chains electrostatically “cross-linked” with WP. Future measurements, such as diffusion measurements of the WP and the GA, X-ray scattering, and diffusing wave spectroscopy will be carried out to validate this hypothesis.

ACKNOWLEDGMENTS

Friesland Coberco Dairy Foods (FCDF) is acknowledged for their financial support. The authors would like to thank Vincent Gervaise for his experimental assistance and Dr. Harry Rollema for carrying out the NMR experiments. Special thanks to Prof. Jorrit Mellema for a critical reading of the manuscript.

CHAPTER 7

Diffusivity of Whey Protein and Gum Arabic in their Coacervates*

ABSTRACT

Structural properties of whey protein (WP) / gum arabic (GA) coacervates were investigated by measuring the diffusivity of WP and GA in their coacervate phase as a function of pH by means of three different complementary techniques. The combination of these measurements revealed new insights into the structure of coacervates. Nuclear magnetic resonance (NMR) measured the self-diffusion coefficient of the GA in the coacervate phase prepared at various pH values. Fluorescence recovery after photobleaching (FRAP) was measured using a confocal scanning laser microscope (CSLM). The WP and GA were covalently labeled with two different dyes. The time of fluorescence recovery, related to the inverse of the diffusion coefficient, was evaluated from the measurements and the diffusivity of the WP and GA on a long time scale could be individually estimated at each pH value. Diffusing wave spectroscopy (DWS) combined with transmission measurement was carried out in the coacervate phase and the diffusion coefficient corresponding to the averaged diffusion coefficient of all particles that scattered in the system was calculated as a function of pH. Independently of the technique used, the results showed that the diffusion of the WP and GA within the coacervate phase was reduced as compared to a diluted biopolymer mixture. NMR, DWS and FRAP measurements gave similar results, indicating that the biopolymers moved the slowest in the coacervate matrix at pH 4.0 - 4.2. It is assumed that the diffusion of the WP and GA is reduced because of a higher electrostatic interaction between the biopolymers. Furthermore, FRAP results showed that in the coacervate phase WP molecules diffused 10 times faster than GA molecules. This result is very relevant as it shows that WP and GA move independently in the liquid coacervate phase. Finally, DWS measurements revealed that the coacervate phase rearranged with time, as evidenced by a decrease of the diffusion coefficient and a loss of the turbidity of the sample. A more homogeneous transparent coacervate phase was obtained after few days / weeks. Faster rearrangement was obtained at pH 3.0 and 3.5 than at higher pH values.

*F. Weinbreck, H. S. Rollema, R. H. Tromp, C. G. de Kruif
Considered for publication in *Langmuir*

INTRODUCTION

Coacervation is a term used to describe an associative liquid / liquid colloidal phase separation. The phase separation leads to the formation of a phase rich in the colloids, called coacervate, and a remaining phase which is poor in colloids [Bungenberg de Jong, 1949a, 1949b; Schmitt *et al.*, 1998; Turgeon *et al.*, 2003]. In the case of complex coacervation, the coacervate is obtained due to the ability of two attracting molecules to form a complex, *e.g.* two oppositely charged polymers. The complexes concentrate into coacervate droplets that will sediment and coalesce to form a separate phase. The coacervate phase exhibits specific properties that distinguish it from the original solution. It is usually more viscous and more concentrated than the initial polymer solution [Nairn, 1995]. Complex coacervation was first discovered by Tiebackx (1911). Later, Bungenberg de Jong (1949a, 1949b) collected a large amount of data on the complex coacervation of gelatin / gum arabic systems. Based on their experimental work, Overbeek and Voorn (1957) developed a first theoretical model for complex coacervation.

From a biological point of view, complex coacervation is a very interesting phenomenon. Oparin (1953) suggested that coacervates could play a role in the appearance of life on earth. The nature, formation and structure of coacervate systems can help to understand the mechanism of biological processes. Furthermore, due to their particular properties, coacervates are applied in foods, cosmetics, pharmaceutical and medicines [Schmitt *et al.*, 1998]. The main application of complex coacervation, used in industry since the 1950's, is microencapsulation. Insoluble materials (*e.g.* flavors, drugs) can be coated by a layer of coacervate [Burgess, 1994; Chilvers and Morris, 1987; Daniels and Mittermaier, 1995; Ijichi, 1997; Luzzi, 1970]. Coacervates are also used as fat replacers or meat analogues in food products, or biopackaging [Tolstoguzov, 1974; Soucie and Chen, 1986; Kester and Fennema, 1986; Shih, 1994]. From both a fundamental and an applied point of view, there is a need to a better understanding of coacervate systems. The formation of the electrostatic complexes between two polymers can be influenced by many physico-chemical parameters. Indeed, pH and ionic strength play a key role in the strength of the electrostatic interaction [Bungenberg de Jong, 1949b; Overbeek and Voorn, 1957]. Studies revealed that complexation appeared as a two-step process upon pH changes: first

intrapolymeric soluble complexes are formed and then the occurrence of interpolymeric complexes and insoluble complexes leads to macroscopic phase separation [Dubin *et al.*, 1994; Kaibara *et al.*, 2000; Mattison *et al.*, 1995; Girard *et al.*, 2002; Weinbreck *et al.*, 2003a]. Recent work from Leisner and Imae (2003) showed that the poly(glutamic acid) / dendrimer coacervates are randomly branched gels with a sponge-like morphology and compact inhomogeneities larger than 20 nm. The structure of the α -lactoglobulin / gum arabic system was studied by confocal scanning laser microscopy (CSLM) and it appeared that the coacervate contained vacuoles of entrapped solvent [Schmitt *et al.*, 2001a]. Sanchez *et al.* (2002a) explained that the presence of the solvent vacuoles might be due to the presence of residual uncharged gum arabic at the interface of the coacervate droplets, which facilitates the entrapment of solvent when the droplets coalesce into a coacervate phase. In a purely synthetic system of zwitterionic Gemini surfactants in water, Menger *et al.* (2000; 2002) reported the structure of coacervates as sponge-like vesicles. These recent studies already give new insights into the complexity of coacervate systems and more work is necessary to understand the structure of coacervates.

In this work, complex coacervation of whey protein / gum arabic (WP/GA) was investigated. Previous results indicated under which conditions coacervates are obtained, *i.e.* pH, ionic strength, protein to polysaccharide (Pr:Ps) ratio [Weinbreck *et al.*, 2003a; Schmitt *et al.*, 1999]. The content in WP, GA, and water of the coacervate phase was found to be very much dependent on these physico-chemical parameters; the stronger the electrostatic interaction, the more concentrated the coacervate phase in biopolymers was [Weinbreck *et al.*, 2004a]. The strength of the electrostatic interactions was estimated from the absolute product of the measured zeta potential of the WP and the GA, and it appeared to be maximum at pH 4.0. Investigations of the structural properties of the coacervate phase were carried out by small angle X-ray scattering (SAXS) and it appeared that, for a Pr:Ps = 2:1, the coacervate phase was the most structured at pH 4.0, the pH at which the strength of the electrostatic interaction and the concentration of the polymer in the coacervate phase were maximal [Weinbreck *et al.*, 2004a]. Furthermore, rheological measurements on the WP/GA coacervate phase indicated that the highest viscosity was obtained at pH 4.0 [Weinbreck *et al.*, 2004b]. The viscosity of the coacervate was 45 times higher than the viscosity of a blank prepared at the same biopolymer concentration (C_p), but at a pH

where no electrostatic interaction took place (pH 7). On the other hand, for other pH values, on either side of pH 4.0, the viscosity of the coacervate phase was between 1 and 15 times higher than their respective blanks (same C_p , pH 7). The high viscosity was just not only due to a higher C_p in the coacervate phase, but it was mainly due to a stronger attractive interaction between WP and GA. Taken together, the results show that at the pH of optimum coacervation (pH 4.0 for Pr:Ps = 2:1), the strength of electrostatic interaction is the strongest, giving rise to a very dense concentrated and viscous coacervate phase. It is thus expected that the mobility and the diffusion of WP and GA would be limited under those conditions. The focus of this study was on the diffusivity of WP and GA within their coacervate phase prepared at various pH values. The diffusion of WP and GA was monitored individually in order to investigate whether the WP and GA diffused together or individually in the coacervate phase. Finally, the long-time behavior of the coacervate phase was investigated by following the evolution of the diffusion coefficient during several days. In order to fulfill these goals, three different techniques were used. Nuclear magnetic resonance (NMR) was used to measure the diffusion coefficient of GA within the coacervate phase. Fluorescence recovery after photobleaching (FRAP) measurements were carried out with a CSLM, and the diffusion of the labeled WP and labeled GA could be individually estimated. Finally, diffusing wave spectroscopy (DWS), combined with transmission measurements, was used to obtain quantitative values of the diffusion coefficient corresponding to the averaged diffusion of all particles that scattered in the system. The three techniques measure translational diffusion coefficients. NMR and FRAP measurements monitor long-time diffusion, whereas DWS monitors short-time diffusion. NMR, FRAP and DWS measurements were found to be very suitable methods for the investigation of highly concentrated systems. Each technique used here had its advantages and limitations. Thus, the use of three independent techniques would give complementary results on the structure of the WP/GA coacervates as a function of pH.

EXPERIMENTAL SECTION

Materials

Bipro is a whey protein isolate (WP) consisting mainly of α -lactoglobulin (α -lg), and α -lactalbumin (α -la) - from Davisco Foods International (Le Sueur, USA). Residual whey protein aggregates were removed by acidification (at pH 4.75) and centrifugation (1 h at 33000 rpm with a Beckman L8-70M ultracentrifuge, Beckman instruments, The Netherlands). The supernatant was then freeze-dried (in a Modulo 4K freeze-dryer from Edwards High Vacuum International, UK). Finally, the resulting powder was stored at 5°C. The final powder contained (w/w) 88.1% protein (N x 6.38), 9.89% moisture, 0.3% fat and 1.84% ash (0.66% Na⁺, 0.075% K⁺, 0.0086% Mg²⁺, and 0.094 % Ca²⁺). The protein content of the treated Bipro is: 14.9% α -la, 1.5% BSA, 74.9% β -lg, and 3.2% immunoglobulin (IMG).

Gum arabic (GA; IRX 40693) was a gift from Colloides Naturels International (Rouen, France). The powder contained (w/w) 90.17% dry solid, 3.44% moisture, 0.338% nitrogen, 0.044% Na⁺, 0.76% K⁺, 0.20% Mg²⁺ and 0.666% Ca²⁺. Its weight average molar mass ($M_w = 520\ 000$ g/mol) and its average radius of gyration ($R_g = 24.4$ nm) were determined by size exclusion chromatography followed by multiangle laser light scattering (SEC MALLS). SEC MALLS was carried out using a TSK-Gel 6000 PW + 5000 PW column (Tosoh Corporation, Tokyo, Japan) in combination with a precolumn Guard PW 11. The separation was carried out at 30°C with 0.1 M NaNO₃ as eluent at a flow rate of 1.0 mL min⁻¹.

Stock solutions of 3% (w/w) were prepared by dissolving the powder in deionized water.

Fluorescent labels, namely fluorescein-5-isothiocyanate (FITC) and 5- (and 6-) carboxylfluorescein succinimidyl ester (FAM-SE) were purchased from Molecular Probes (Leiden, The Netherlands) and deuterium oxide (D₂O) from Aldrich Chemical Company Inc. (Milwaukee, USA).

Preparation of the coacervates

The stock solutions of 3% (w/w) WP and GA were mixed at a protein to polysaccharide (Pr:Ps) ratio of 2:1 (w/w). Sodium azide (0.02% w/w) was added to prevent bacterial growth. The pH of the mixtures was set (± 0.05 pH-unit) at the desired value (pH range between 3.0 and 4.5) using 0.1 M and 1 M HCl. After acidification, the samples were

placed in a separatory funnel at 25°C. All the experiments were carried out on the coacervate (lower) phase that was collected after 24h of phase separation.

Nuclear magnetic resonance (NMR)

1D-NMR and DOSY (Diffusion Ordered Spectroscopy) spectra were taken on a Bruker DRX500 spectrometer operating at 500.13 MHz for the DOSY experiments. A pulse sequence, using stimulated echo, longitudinal eddy current delay and bipolar gradient pulses, was applied. All experiments were performed at 22°C. Typical values for the parameters were: 8 s for the relaxation delay, 400 ms for diffusion time (Δ) and 3 ms for the gradient pulse length (δ). The gradient strength was varied linearly from 10 to 500 mT/m. Gradient calibration was based on a solution of SDS, glucose and ATP in D₂O [Morris and Johnson, 1993]. Processing of the data was carried out using the DOSY module of the XWinNMR software.

The coacervate samples were prepared as described above, except that D₂O was used as a solvent instead of deionized water. The pH was adjusted with DCl and NaOD. The pH values were taken from the reading of the pH meter and were not corrected for the influence of the D₂O. NMR measurements were carried out on the WP/GA coacervate phase at pH 4.5, 4.2, 4.0, and 3.8 in order to determine the diffusion coefficient of the GA within the coacervate phase. It was not possible to determine the diffusion coefficient of the WP because of severe signal broadening.

Fluorescence recovery after photobleaching (FRAP)

Labeling procedure

WP (5% w/w at pH 7.0) was covalently labeled with FITC (1 μ mol / g WP) and GA (5% w/w at pH 8.0) with FAM-SE (4 μ mol / g GA). Both mixtures were left overnight under stirring in the dark. The mixtures were then freeze dried after removal of the free label by exhaustive dialysis against deionized water. Fluorescein was the fluorophore of choice because it readily photolyzes under relatively low illumination intensities [Gibbon and Hardingham, 1998; Chen *et al.*, 1995]. Turbidity experiments as described in a previous paper were carried out with the labeled polymers and it was found that the pH at which complex coacervation occurred was not affected by the labeling procedure [Weinbreck *et al.*, 2003a]. Coacervates with labeled-WP/GA and WP/labeled-GA were prepared as described above. FRAP measurements were carried

out on the labeled-WP/GA coacervates at pH 4.3, 4.2, 4.0, 3.8, 3.6, 3.5, and on the WP/labeled-GA coacervates at pH 4.0, 3.8, 3.6, 3.5.

Equipment

Photobleaching experiments were carried out at on a LEICA TCS SP confocal scanning laser microscope (CSLM), equipped with an inverted microscope (model Leica DM IRBE), used in the single photon mode with an Ar/Kr visible light laser. The following Leica objective was used: 63x/UV/1.25NA/water immersion/PL APO (63w). The laser emitted at 488 nm, within the excitation spectrum of FITC and FAM-SE. 1 mL of sample was poured into a spherical cavity microscope slide covered by Parafilm and a coverslip to avoid drying. Digital images files were acquired in 1024 x 1024 pixels resolution. A prebleached image of dimension 80 x 80 μm was taken with a reduced laser intensity (about 40% of the maximum laser power). Then a block of dimensions 20 x 20 μm with a height of approximately 1 μm , centered on the observed region and selected by the zoom control of the instrument, was bleached at maximum laser intensity for 30 s (laser power 9 mW). For fluorescence recovery, time series were collected in 2 dimensions (1 image per minute) at the reduced laser intensity that was used for the prebleached image.

Data analysis

The intensity of the fluorescence of an area was represented by the average value of the pixels in this area. Fluorescent recovery curves were obtained by plotting the intensity of the bleached area divided by the intensity of the background as a function of time. Normalization on the background intensity was necessary because of fluctuations in the laser power. The recovery curves have an exponential shape according to the following equation:

$$\frac{I_{norm}(\infty) - I_{norm}(t)}{I_{norm}(\infty) - I_{norm}(t_0)} = e^{-\frac{t}{\tau}} \quad \text{Eq.(1)}$$

in which $I_{norm}(t) = \frac{I_{bleachedarea}(t)}{I_{backgroundarea}(t)}$ and τ is the time constant of the system and is inversely proportional to the diffusion coefficient (D). The values of τ were calculated at various pH values for the labeled-WP and the labeled-GA. All measurements were repeated at least 4 times. The values reported in this study are the averaged values and their respective standard deviation. The averaged τ values at various pH values

were compared by doing a Scheffe test with significant marked differences at $p < 0.05$ (Statsoft, Inc. (2001).STATISTICA, version 6).

The diffusion coefficient of the molecule (D) in one direction is related to the $\hat{\delta}$ value and can be expressed as:

$$D = \frac{a^2}{2\tau} \quad \text{Eq.(2)}$$

where a^2 corresponds to the mean squared displacement in one direction (which depends on the size of the bleached area).

Diffusing wave spectroscopy (DWS)

DWS measurements were carried out on an experimental setup. The expanded laser source was an NEC Corp. 50 mW He/Ne laser emitting at wavelength $\lambda = 633$ nm through an optical fiber. Coacervate samples were prepared as described above at various pH values and were poured into a 0.5 cm optical path length cuvette and covered by Parafilm to avoid drying of the samples. The samples were stored at room temperature and were measured every day for 22 days. The temperature was controlled at 25°C. The measurements were carried out in the transmission mode. The scattered light intensity was processed with 50R Flex Instruments software, and the intensity autocorrelation function $g_2(t)$ of each sample was collected. The field autocorrelation function $g_1(t)$ is defined as [Weitz and Pine, 1993]:

$$g_2(t) \equiv |g_1(t)|^2 \quad \text{Eq.(3)}$$

The field autocorrelation function $g_1(t)$ can also be defined as [Weitz and Pine, 1993]:

$$g_1(t) = \frac{\left(\frac{L}{l^*} + \frac{4}{3}\right)\sqrt{\frac{6t}{\tau_0}}}{\left(1 + \frac{8t}{3\tau_0}\right)\sinh\left(\frac{L}{l^*}\sqrt{\frac{6t}{\tau_0}}\right) + \left(\frac{4}{3}\sqrt{\frac{6t}{\tau_0}}\cosh\left(\frac{L}{l^*}\sqrt{\frac{6t}{\tau_0}}\right)\right)} \quad \text{Eq.(4)}$$

where L is the sample width ($L = 0.5$ cm), l^* is the transport mean free path of a photon, $\hat{\delta}_0$ is defined as:

$$\tau_0 = (D \times k_0^2)^{-1} \quad \text{Eq.(5)}$$

where D is the diffusion coefficient and k_0 is defined as:

$$k_0 = \frac{2\pi}{\lambda} \quad \text{Eq.(6)}$$

and λ is defined as:

$$\lambda = \frac{\lambda_{laser}}{n} \quad \text{Eq.(7)}$$

where λ_{laser} is the wave length of the laser light in vacuum, n is the refractive index of the medium and for water $n = 1.33$.

Transmission measurements

Transmission measurements were carried out on each coacervate sample with a CARY 4000 spectrophotometer (Varian, The Netherlands) in order to obtain I^* . The same cuvettes as for DWS measurements were used.

I^* was calculated from transmission (T) measurements according to [Kaplan *et al.*, 1993]:

$$T = \frac{\frac{5 I^*}{3 L}}{1 + \frac{4 I^*}{3 L}} \quad \text{Eq.(8)}$$

Thus, from the fit of the data of the correlation function ($g_1(t)$) given in Eq. (4) using the transmission data, a value of the diffusion coefficient D could be calculated.

RESULTS AND DISCUSSION

The main purpose of this work was to get more insights into the structure of the whey protein (WP) / gum arabic (GA) coacervate phase by monitoring the diffusion of the WP and the GA within the coacervate itself. As previous results showed, the coacervate phase is very viscous and very concentrated in polymer (up to 20 – 30% w/w) [Weinbreck *et al.*, 2004a, 2004b]. Various techniques were used and results were compared.

Nuclear Magnetic Resonance (NMR)

Translational diffusion of molecules was studied by means of pulsed field gradient NMR techniques. A magnetic field gradient was applied in combination with a spin-echo pulse sequence. If diffusion occurs, the NMR signal is reduced depending on the value of the diffusion coefficient and the strength of the field gradient. With diffusion-ordered 2D NMR (DOSY) experiments, usually the strength of the magnetic field gradient is varied. A 2D spectrum was obtained with the chemical shift on the abscissa and the self-diffusion coefficient on the ordinate [Morris and Johnson, 1993].

From an analysis of 1D-NMR spectra of a WP sample, a GA sample and a WP/GA coacervate sample, the signals characteristic for WP and GA could be assigned. GA showed a sharp peak at 1.27 ppm and a characteristic envelope around 3.9 ppm (Figure 7.1). WP in the absence of GA showed characteristic signals at 0.9 ppm (-CH₃ groups) and in the aromatic region from 6 to 11 ppm. In the coacervate phase the signals of WP were strongly broadened and could not be monitored in the DOSY experiment. The signals of GA were broadened too but were still clearly detectable in the DOSY spectra. Consequently, for WP/GA coacervates prepared at pH 4.5, 4.2, 4.0, and 3.8 only the self-diffusion of the GA could be determined.

The results of the diffusion coefficients of GA as a function of pH are presented in Figure 7.2. The diffusion coefficient of the GA in a dilute system at pH 7 ($D_{\text{pH}7} = 10.8 \times 10^{-12} \text{ m}^2\text{s}^{-1}$) was higher than the diffusion coefficient of GA in the coacervate, since GA molecules were electrostatically bound to WP in a very concentrated biopolymer phase. The diffusion coefficient of GA in the coacervate was pH-dependent and showed a minimum close to the pH range 4.0 – 4.2. The use of D₂O as a solvent might induce some changes in the behavior of the coacervate phase as compared to a coacervate prepared in H₂O. Hydrophobic interactions are enhanced in D₂O, but the dielectric constant remains the same. However, the pK_a values of glutamine residues shifts +0.1 unit in D₂O and since $\text{pD} = \text{pH} (\text{meter reading}) + 0.4 - \text{pK}_a$, the dissociation would shift as well [Bundi and Wüthrich, 1979]. Therefore, the exact position of the minimum in the

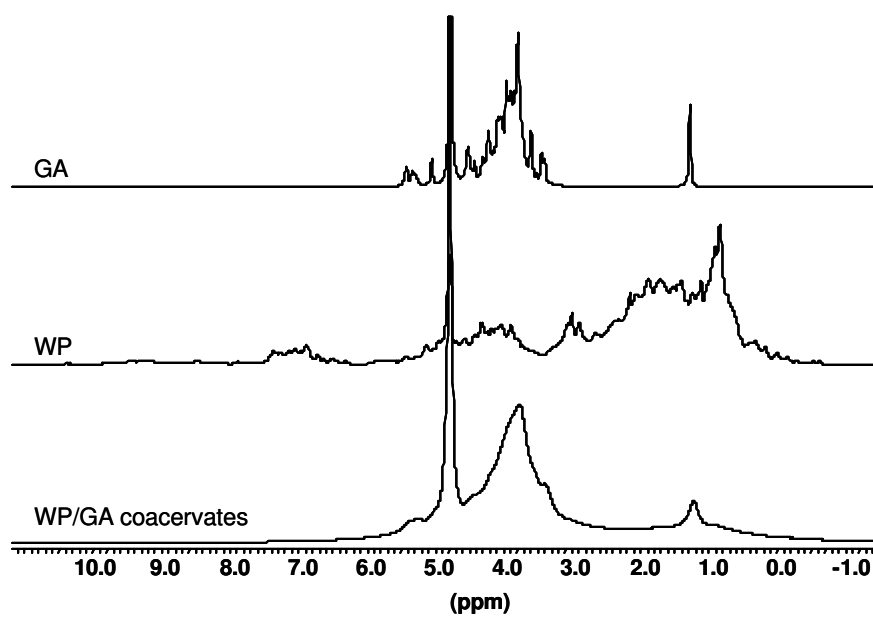


Figure 7.1: ¹H-NMR spectra of GA sample, WP sample, and WP/GA coacervate sample at pH 4.0.

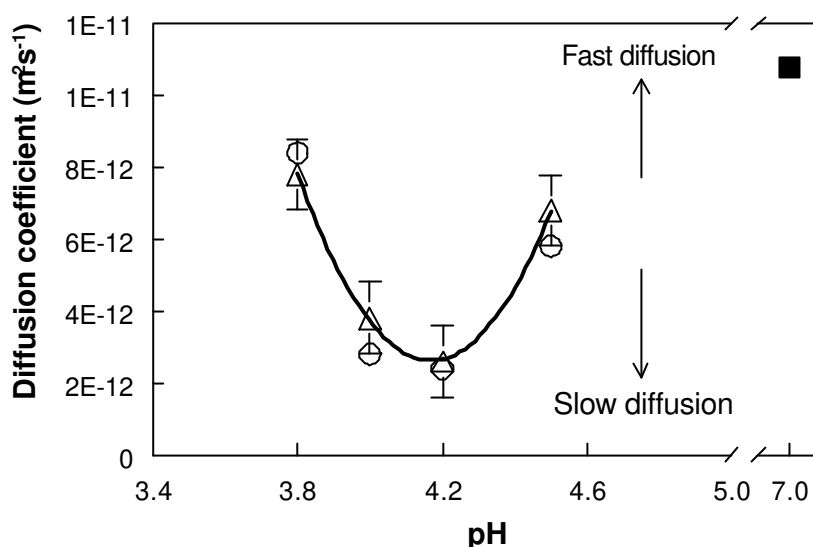


Figure 7.2: Diffusion coefficient of GA in a WP/GA coacervate as a function of pH, as measured by pulsed field gradient NMR. (): signal at 3.9 ppm; (): signal at 1.27 ppm; (): blank of diluted 3% GA dispersion. Error bars correspond to standard deviations.

diffusion coefficient of GA within the coacervate phase may not exactly coincide with that in H₂O. It might shift the maximum 0.2 – 0.3 units towards more acidic pH values if H₂O is used as a solvent. From previous measurements, it was found that pH 4.0 corresponded to the pH at which the strength of interaction, the viscosity, and the concentration in polymer were all at maximum [Weinbreck *et al.*, 2004a, 2004b]. Thus, it is expected that the diffusion of polymers is slowest around this pH value.

The diffusion of WP could unfortunately not be determined from NMR measurements. Another method, fluorescence recovery after photo bleaching (FRAP), was therefore used to measure independently the diffusion of WP and GA.

Fluorescence recovery after photo bleaching (FRAP)

FRAP is a technique used to investigate molecular mobility within cells and membranes systems in situ. In this study, a confocal scanning laser microscope (CSLM) was used to study diffusion of labeled-WP and labeled-GA in the coacervate phase.

Diffusion of labeled-GA

GA molecules were labeled with FAM-SE on the proteic part present in the GA molecules. Because the amount of protein in the GA sample is low (2%), a stronger fluorescein label was used (FAM-SE) in a higher concentration than that used for the labeling of WP with FITC. Coacervates containing WP (non labeled) and labeled-GA were prepared at pH 4.0. Pictures of the sample were taken at 1 min intervals for at least 1.5 h. A characteristic FRAP time series is presented in Figure 7.3. Even before bleaching, the coacervate phase appeared heterogeneous in the partition of GA. Indeed, some bright yellow spots indicated that large aggregates of GA were present in the sample. As reported by Sanchez *et al.* (2002a), these aggregates are known to be always present in GA samples. Some round black spots were also visible on the pictures, probably inclusion of solvent droplets entrapped in the coacervate. After photo bleaching, a black square appeared on the picture fading away with time. The intensity profile of the background area ($I_{\text{background}}$) and the bleached area ($I_{\text{bleached area}}$) was monitored with time. The intensity of the bleached area was initially low and then increased to reach the same intensity as the background because of the diffusion of GA. Overall variations in intensity were due to fluctuations in the laser power.

Diffusion of labeled-WP

WP molecules were labeled with FITC and a coacervate at pH 4.0 was prepared using labeled WP and (non labeled) GA. The same bleaching procedure was used as for the above sample. Figure 7.4 illustrates the time series pictures taken by CSLM. Before bleaching, the WP looked homogeneously distributed in the coacervate phase. Some dark spots corresponding to entrapped solvent were also visible. After 20 min, the bleached square had disappeared. The recovery of the bleached area seemed to be much faster than when GA was labeled, showing qualitatively that the diffusion of WP was faster than the diffusion of GA.

Quantification

The intensities of the bleached area and the background were monitored as a function of time. The recovery curve could be obtained by plotting $\ln \frac{I_{\text{norm}}(\infty) - I_{\text{norm}}(t)}{I_{\text{norm}}(\infty) - I_{\text{norm}}(t_0)} \equiv \ln X$ as a function of time, and it is expected to be a straight line which slope = $-1/\delta$. The recovery curves of the samples presented in Figures 7.3 and 7.4 are shown in Figure

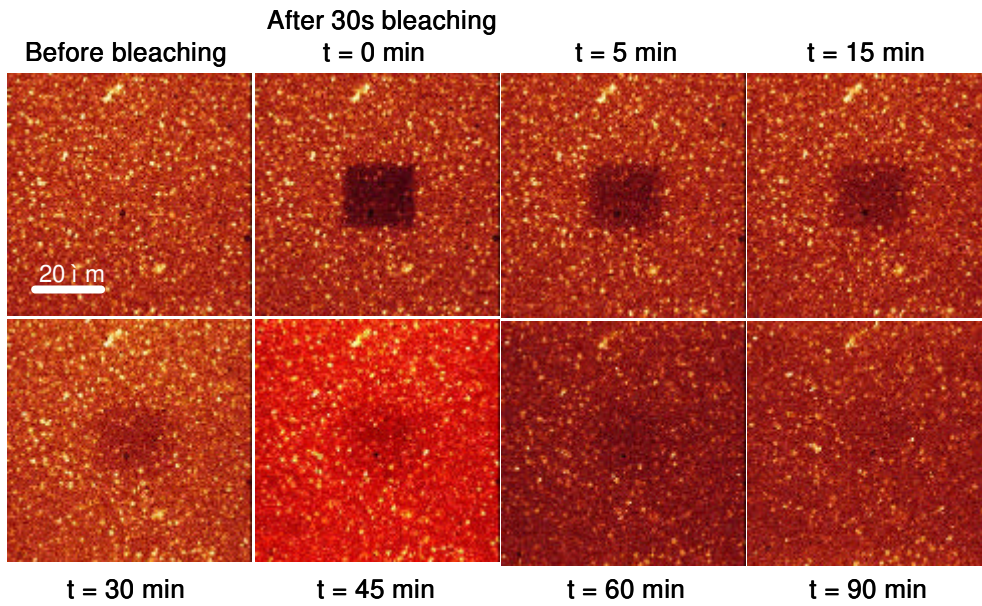


Figure 7.3: CSLM micrographs of a WP/labeled-GA coacervate prepared at pH 4.0 at different times. The black rectangle corresponds to the bleached area. GA is labeled with FAM-SE.

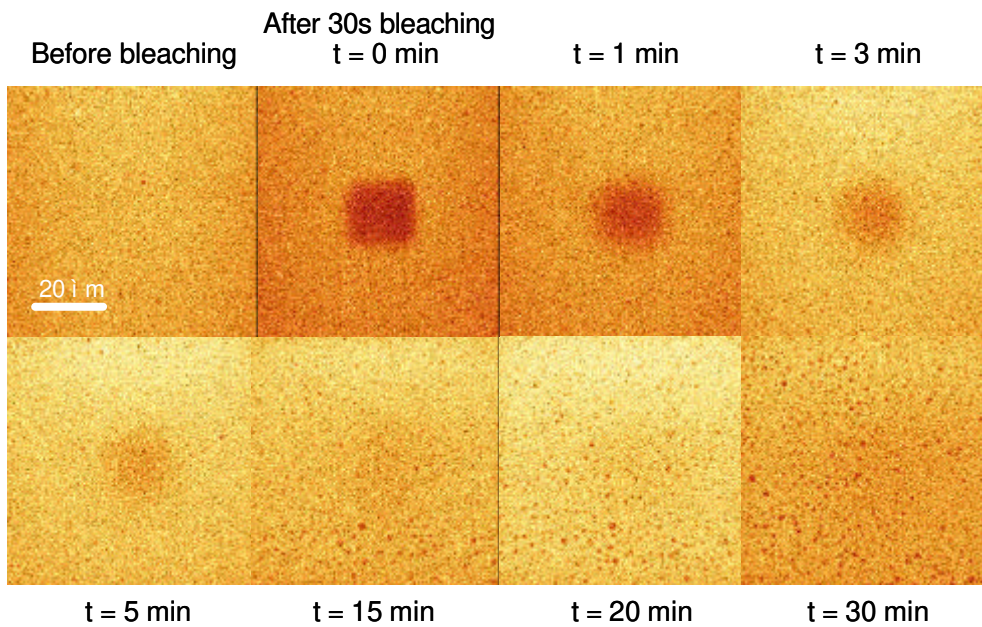


Figure 7.4: CSLM micrographs of a labeled-WP/GA coacervate prepared at pH 4.0 at different times. The black rectangle corresponds to the bleached area. WP is labeled with FITC.

7.5. The recovery curve of the WP appeared to be a straight line which gave a $\hat{\delta} = 9 \text{ min}^{-1}$. The slope corresponding to the recovery of GA was less steep, and $\hat{\delta} = 53 \text{ min}^{-1}$. However, it should be noted that in some cases the recovery curves of the GA deviated slightly from the straight line, probably because of the heterogeneities in the GA mixtures, but the $\hat{\delta}$ values of GA were always much larger than the WP values.

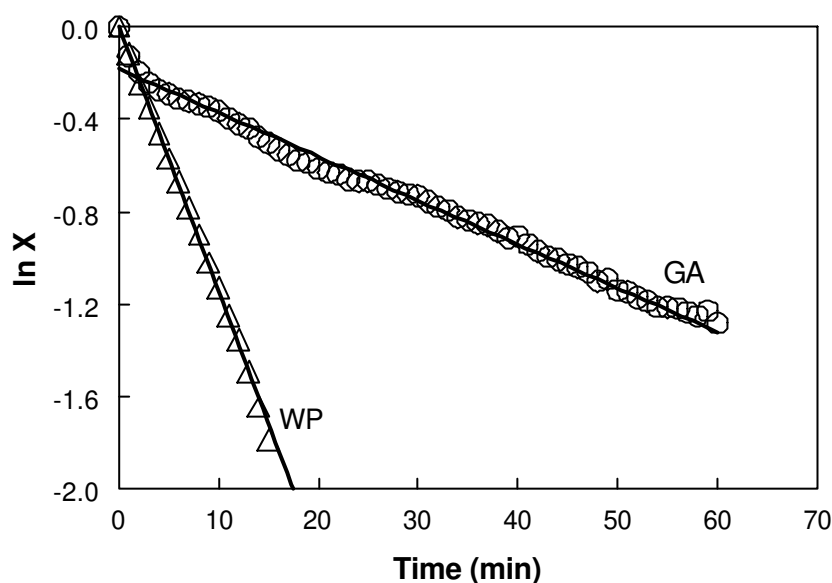


Figure 7.5: Recovery curves of the fluorescence with time from Figures 7.3 and 7.4, based on Eq. (1). Samples correspond to a coacervate of (): labeled-WP/GA and (): WP/labeled-GA.

The values of $\hat{\delta}$ were calculated for a range of pH values for coacervates with labeled-WP and labeled-GA. In Figure 7.6a, the values of $\hat{\delta}$ corresponding to the diffusion of WP are plotted as a function of pH. Considering statistical analysis, it seemed that diffusivity was lowest at around pH 4.0 and 4.2 and faster on either side of these values. Indeed, at pH 4.0 the viscosity and the strength of the electrostatic interactions were at maximum, paralleled by a slower diffusion of the molecules. For pH > 4.4, the coacervate phase did not appear as a homogeneous phase but some large coacervate droplets were still present, showing that phase separation was incomplete. FRAP experiments could thus not be carried out at pH > 4.4. On the other hand, for pH values below 3.5, the diffusion was so fast that most of the recovery of the fluorescence occurred during the bleaching step; quantitative analysis could thus not be performed

at pH < 3.5. The values of $\hat{\delta}$ for GA were compared to the values of $\hat{\delta}$ for WP in Figure 7.6b. The values of $\hat{\delta}$ for GA were more difficult to calculate because of the heterogeneities in the sample, and reproducibility of the results was limited. However, even if the standard deviations were rather large, the values of $\hat{\delta}$ of GA are significantly larger than the values of $\hat{\delta}$ for WP, illustrating quantitatively that the diffusion of WP in the coacervate was faster than the diffusion of GA. Diffusion of the GA was also too fast at pH < 3.5 and could not be quantified by FRAP. Furthermore, at pH > 4.1, the samples containing labeled-GA showed a poor phase separation and coacervate droplets did not coalesce into a homogeneous phase. This limiting pH value was lower than the limiting value corresponding to samples prepared with labeled-WP. Although it was checked that the labeling did not influence the pH of complex formation, it remains possible that the fluorescent markers changed the interfacial properties of the coacervate droplets and thus their coalescence. Indeed, fluoresceins (FITC and FAM-SE) are hydrophobic molecules that are positively charged at pH below 6.4. It was already reported that FITC molecules were present at the gelatin / dextran interface [Edelman, 2003]. In the case of the coacervates prepared with labeled-GA, the concentration of FAM-SE label was higher than the concentration of FITC for labeled-WP, which would then enhance this interfacial phenomenon. Furthermore, it was also reported by Sanchez *et al.* (2002a) that the interface of the coacervate droplets was mainly made of GA molecules. In that case, the FAM-SE marker would also be located at the interface, preventing coalescence of the coacervate droplets.

FRAP measurements give information on the diffusion of the molecules on a long time scale. Under these conditions, the diffusion of both WP and GA could be measured, and the main conclusion was that WP and GA move independently in the coacervate phase. From Eq. (2), the diffusion coefficients of WP and GA could be calculated. However, since diffusion occurs in three dimensions, the molecules would be expected to diffuse on a horizontal plane (the plane of the bleached square, 20 x 20 μm) but also - and mostly - in the vertical direction. Since the height of the bleached block is

approximately 1 μm , this value was taken for a and $D = \frac{a^2}{2\tau}$. Under those conditions the

diffusion coefficients were comprised between $1.1 \times 10^{-11} \text{ m}^2\text{s}^{-1}$ and $3.4 \times 10^{-12} \text{ m}^2\text{s}^{-1}$ for WP and between $7.8 \times 10^{-12} \text{ m}^2\text{s}^{-1}$ and $2.6 \times 10^{-12} \text{ m}^2\text{s}^{-1}$ for GA. Considering that the diffusion coefficients measured by FRAP were an approximation (because of the uncertainty of a), the values were in good agreement with the NMR results. Finally, a

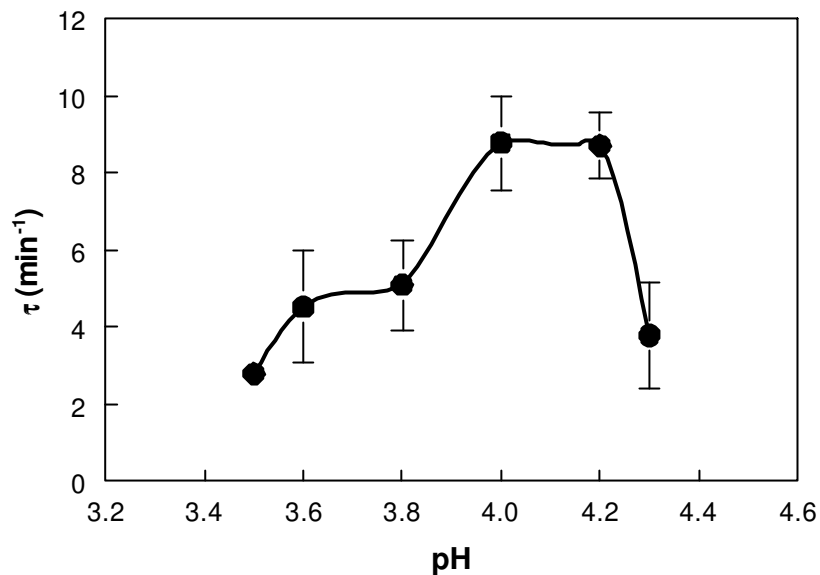


Figure 7.6a: Averaged $\hat{\delta}$ of WP as a function of pH, as calculated from the recovery curves for a labeled-WP/GA coacervate. Error bars represent standard deviations.

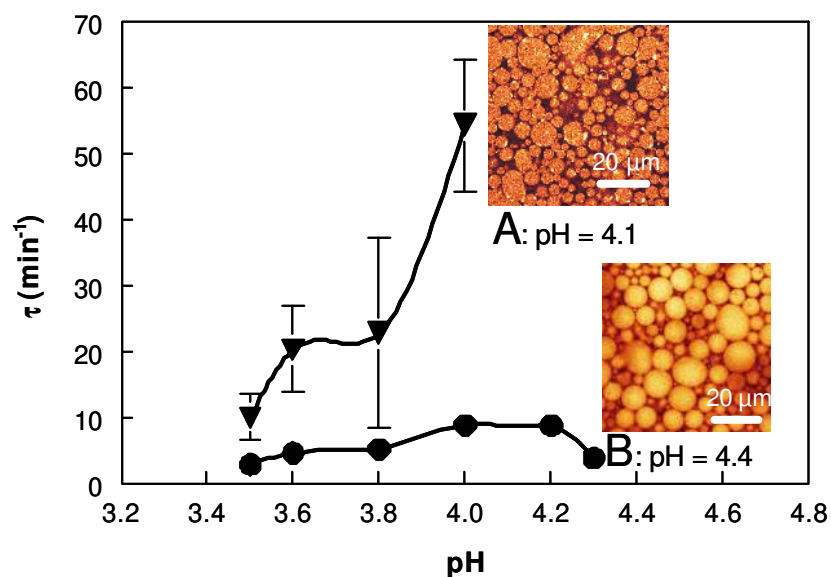


Figure 7.6b: Averaged $\hat{\delta}$ of WP and GA as a function of pH, as calculated from the recovery curves for a WP/labeled-GA coacervate. (●): $\hat{\delta}_{WP}$; (▲): $\hat{\delta}_{GA}$. Error bars represent standard deviations. (A): CSLM micrograph of the WP/GA coacervate phase with GA labeled with FAM-SE at pH = 4.1; (B): CSLM micrograph of the WP/GA coacervate phase with WP labeled with FITC at pH = 4.4.

third method was used for monitoring mobility in order to determine the diffusion of all scattering molecular species: diffusing wave spectroscopy (DWS).

Diffusing wave spectroscopy (DWS)

Quantification of the diffusion coefficient

The passage of multiply scattered photons in a turbid medium can be treated as a (diffusive) random walk. The multiple scattering process is modulated by the diffusive motion of the colloidal particles. As a result, intensity fluctuations in the scattered light reflect the diffusivity of the colloids as in traditional dynamic light scattering [Weitz and Pine, 1993]. DWS measurements were carried out on the coacervate samples obtained after 24h of phase separation (*i.e.* at the same conditions as for FRAP and NMR measurements described above). For each sample a correlation function was monitored, as depicted in Figure 7.7. By increasing the pH from 3.0 to 4.5, the decay of the correlation function was shifted to shorter times. For each sample, a curve fitting allowed determination of the values of the parameters of the correlation function described in Eq. (4). However, the mobility of the particles in the coacervate phase could not be directly compared for the different pH values because the turbidity of the coacervate was different for each sample. Thus, transmission measurements were carried out with a spectrophotometer; the results are reported in Table 1. For pH values 3.0 and 3.5, the transmission of the coacervates was higher, showing that the samples were more transparent and that the scattering intensities would be different from the other pH values. The calculation of I^*/L from Eq. (8) reveals that I^*/L was always smaller than 0.1 (multiple scattering mode) for all samples, which is the main requirement for the use of DWS. From the values of I^*/L and the curve fitting, the diffusion coefficient could be calculated for all the coacervate samples. The results are given in Figure 7.8 and are compared quantitatively to the previous diffusion measurements obtained by NMR and FRAP. The diffusion coefficients obtained by DWS measurements corresponded to the averaged diffusion of all particles that scattered in the coacervate, *i.e.* WP and GA. DWS preferentially measured the particles that scattered more and thus the largest particles. The values obtained by DWS are in very good agreement with previous NMR and FRAP results. A minimum in the diffusion coefficient was found around pH 4.0 and 4.2. On either side of this pH range, the molecules diffused faster.

pH	T (%)	I*/L
4.5	0.23	0.001404
4.2	0.22	0.001286
4.0	0.27	0.001632
3.5	0.55	0.003328
3.0	1.69	0.010231

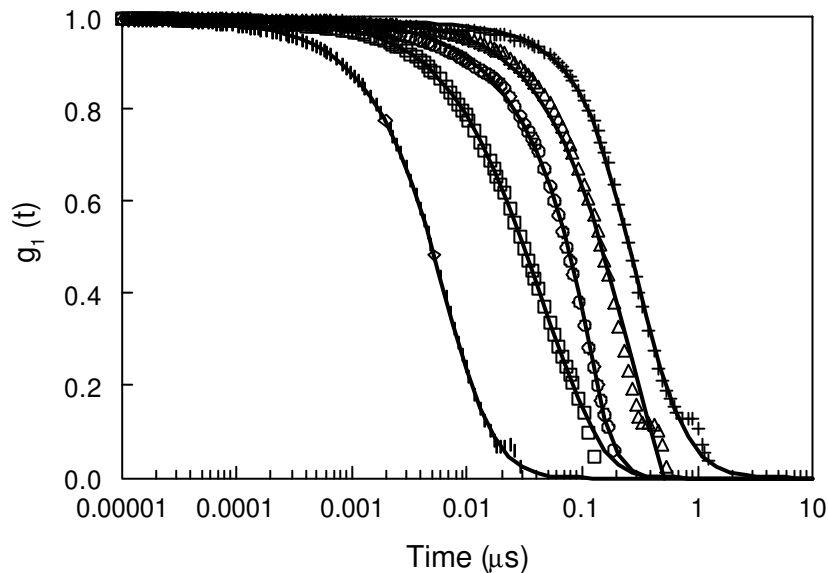


Figure 7.7: Field autocorrelation function $g_1(t)$ of WP/GA coacervates prepared at various pH values: (○): pH 4.5; (□): pH 4.2; (△): pH 4.0; (◇): pH 3.5; (+): pH 3.0. The lines correspond to curve fitting using Eq. (4).

Rearrangement with time

Transmission and DWS measurements are non-invasive techniques which were used to follow samples for 22 days. Transmission of the coacervate at various pH values is plotted as a function of time in Figure 7.9. The samples at pH 3.0 and 3.5 turned from opaque to almost transparent in 2 to 5 days. In those conditions, DWS could not be carried out, since multiple scattering no longer occurred. At the other pH values, the

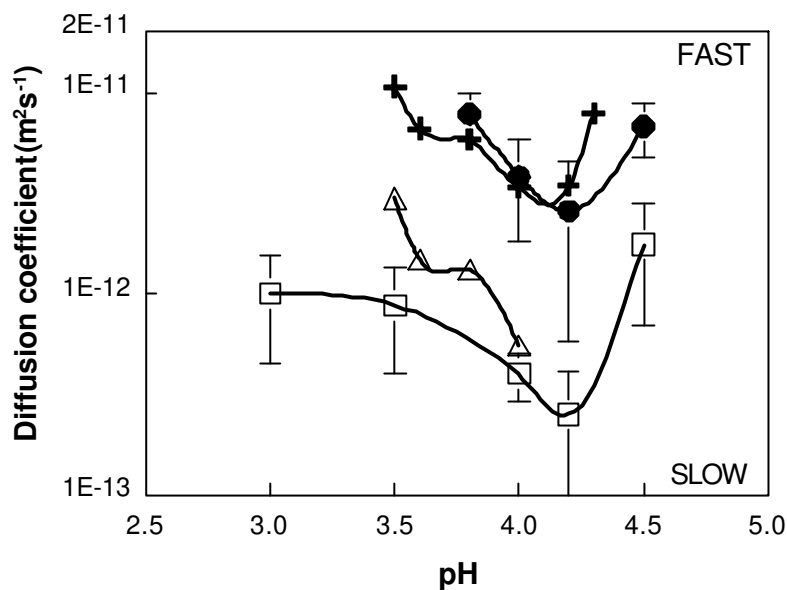


Figure 7.8: Diffusion coefficients in WP/GA coacervate after 24h of phase separation, using: (○): NMR (diffusion of GA); (□): DWS (diffusion of WP+GA); (+) FRAP (diffusion of WP); (△): FRAP (diffusion of GA). Error bars correspond to standard deviations.

transmission increased slightly but remained at values below 0.4%, which was still in the multiple scattering mode. This change in turbidity as a function of time meant that rearrangement occurred in the samples. The coacervates became transparent, and thus more homogeneous, since the initial turbidity of dispersions was due to the presence of entities in the range of micrometer size. One could hypothesize that the rearrangement was due to the expulsion / redistribution of entrapped solvent. Because of the high viscosity of the mixtures, the rearrangement of the coacervate phase is a slow process. And since the viscosity was lower and the diffusion coefficient was larger at pH 3.0 and 3.5, the rearrangement occurred faster than at pH 4.0 and 4.2. For pH 4.5, it is possible that some residual unbalanced charges at the surface of the droplets prevented the coalescence, as depicted by CSLM in Figure 7.5b. Thus, rearrangement was slower. The rearrangement of the molecules within the coacervate phase had an impact on the diffusion coefficient. Indeed, as depicted in Figure 7.10, the diffusion of the molecules was slower after one week for all the pH values that could be measured. This result was another sign of the rearrangement of the coacervates with time. These results proved that the phase equilibrium of the coacervates was achieved very slowly. This factor needs to be taken into account in further studies on complex coacervation.

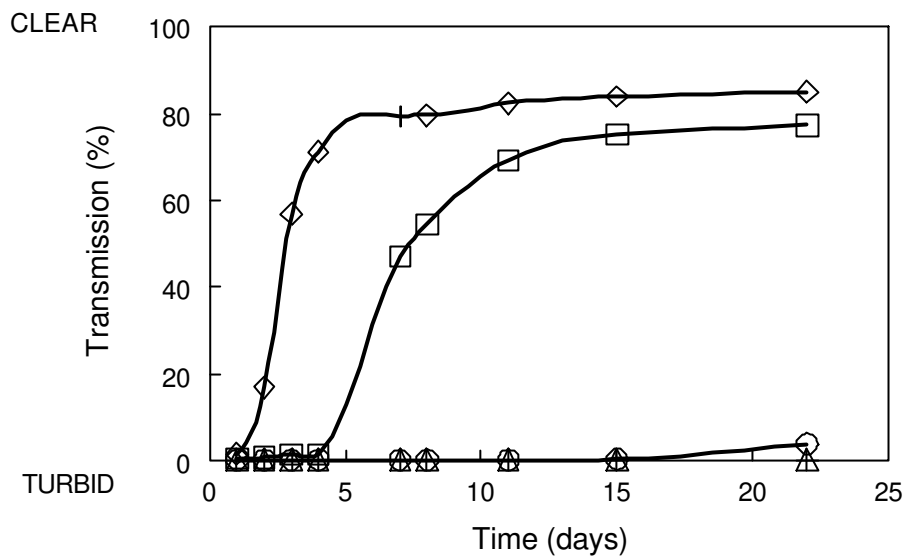


Figure 7.9: Transmission measurements of the WP/GA coacervate phases with time. (\diamond): pH 3.0; (\square): pH 3.5; (\triangle): pH 4.0; (\circ): pH 4.2; (+): pH 4.5.

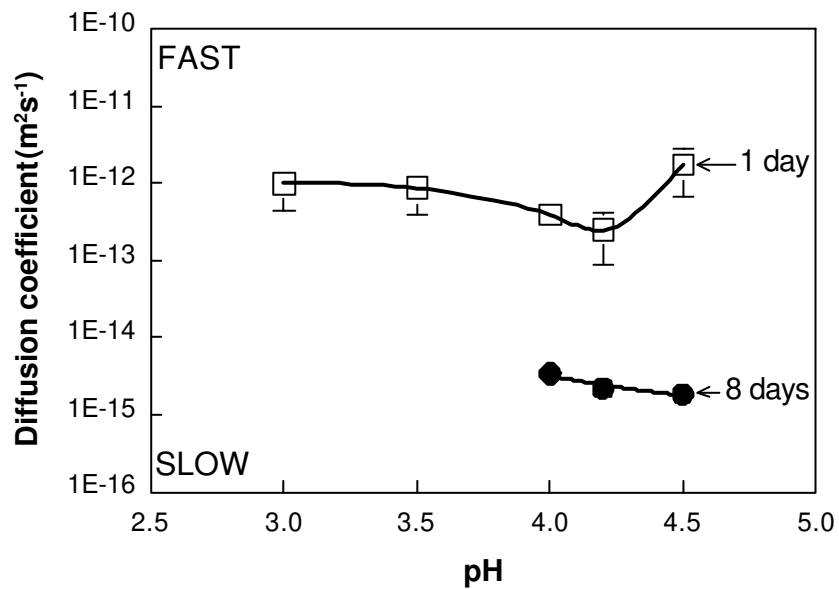


Figure 7.10: Diffusion coefficients of WP/GA coacervate using DWS: (\square): after 24h of phase separation (\circ): after 8 days of storing at room temperature. Error bars correspond to standard deviations.

CONCLUSIONS

The complementary results for diffusivity of the biopolymers in a coacervate phase were obtained from three different techniques (*i.e.* NMR, FRAP, and DWS). All results were in good agreement with each other. The diffusion of WP and GA in the coacervate phase was much slower than in a dilute system. Because of the high concentration of polymers in the coacervate phase (20 – 30 % w/w) and because of the presence of electrostatic interactions at acidic pH, the diffusion of the biopolymers in the coacervate phase would be reduced. All the results indicated that the diffusion of the WP and GA was at minimum around pH 4.0 and 4.2, since it corresponds to the pH at which both the strength of the electrostatic interaction and the viscosity were maximum [Weinbreck *et al.*, 2004b]. Furthermore, FRAP data showed that the diffusion of the WP in the coacervate was 10 times faster than the diffusion of the GA. It was concluded that WP and GA moved independently in the coacervate phase. This result is very relevant for the understanding of the structure of the coacervate, meaning that electrostatic bonds between WP and GA continually break and re-form, in a reversible way, and that WP can move along the GA chain. Finally, using DWS measurements, the behavior of the coacervate could be followed for several days and it was found that the coacervate phase slowly rearranged with time, as evidenced by the loss of turbidity of the samples and by the lower diffusion coefficient. Rearrangement occurred faster at pH 3.0 and 3.5; the samples looked transparent after a few days, preventing the use of DWS for further quantification. Thus, rearrangement of the coacervate phase occurs in order to form a more homogeneous transparent phase as a result of the diffusion of the polymers within the coacervate. This result opens new insights into the relatively unexplored field of coacervate structure.

ACKNOWLEDGMENTS

Friesland Coberco Dairy Foods (FCDF) is acknowledged for their financial support. The authors would like to thank Vincent Gervaise and Frédérique Sanzey for their contribution to the experimental work.

CHAPTER 8

Microencapsulation of Oils using Whey Protein / Gum Arabic Coacervates*

ABSTRACT

Microencapsulating sunflower oil, lemon and orange oil flavor was investigated using complex coacervation of whey protein / gum arabic. At pH 3.0 – 4.5, the WP/GA complexes formed electrostatic complexes that could be successfully used for microencapsulation purposes. The formation of a smooth biopolymer shell around the oil droplets was achieved at a specific pH (close to 4.0) and the payload of oil (*i. e.* amount of oil in the capsule) was higher than 80%. Small droplets were easier to encapsulate within a coacervate matrix than large ones, which were present in a typical shell / core structure. The stability of the emulsion made of oil droplets covered with coacervates was strongly pH-dependent. At pH 4.0, the creaming rate of the emulsion was much higher than at other pH values. This phenomenon was investigated by carrying out zeta potential measurements on the mixtures. It seemed that at this specific pH, the zeta potential was close to zero, highlighting the presence of neutral coacervate at the oil / water interface. The influence of pH on the capsule formation was in accordance with previous results on coacervation of whey proteins and gum arabic, *i.e.* WP/GA coacervates were formed in the same pH window with and without oil, and the pH where the encapsulation seemed to be optimum corresponded to the pH at which the coacervate was the most viscous. Finally, to illustrate the applicability of these new coacervates, the release of flavored capsules incorporated within Gouda cheese showed that large capsules gave stronger release, and the covalently cross-linked capsules showed the lowest release, probably because of a tough dense biopolymer wall which was difficult to break by chewing.

*F. Weinbreck, M. Minor, C. G. de Kruif
Submitted for publication

INTRODUCTION

Microencapsulation techniques are used in food and pharmaceuticals for the protection of enzymes or health ingredients, the taste masking of encapsulated drugs, controlled release, the encapsulation of flavors for food and drinks, and in home and personal care products [see reviews on the subject by: Luzzi, 1970; Dziezak, 1988; Shahidi and Han, 1993; Magdassi and Vinetsky, 1997; Gibbs *et al.*, 1999; Sparks, 1999]. One of the microencapsulation methods is coacervation – phase separation technology, which has been used as a physicochemical procedure for the preparation of polymeric capsules [Deasy, 1984; Arshady, 1990; Ijichi, 1997]. Coacervation was first investigated by Bungenberg de Jong and Kruyt (1929) and was classified into two systems: simple and complex coacervation. The term coacervation is derived from the Latin *acervus*, meaning “heap” and the prefix *co* (=together) to indicate gathering of the colloidal particles. Complex coacervation is based on the formation of a complex (coacervate) between oppositely charged polymers, usually proteins and polysaccharides. If the required conditions are met, the polysaccharide and the protein form a complex which may form a film / coating around the target material that needs to be encapsulated [Nairn, 1995]. Traditionally, gelatin is used in combination with gum arabic in numerous studies. The first commercial application was in 1954, when Green and associates of the National Cash Register Company researched the coacervation process for producing carbonless copy paper [Green, 1956]. Since then, this system was applied in many investigations [see for example: Luzzi and Gerraughty, 1964, 1967; Madan *et al.*, 1972, 1974; Newton *et al.*, 1977; Nixon and Nouh, 1978; Takenaka *et al.*, 1980; Takeda *et al.*, 1981; Flores *et al.*, 1992; Jizomoto *et al.*, 1993; Palmieri *et al.*, 1996,1999; Ijichi, 1997; Lamprecht *et al.*, 2000a, 2000b, 2001]. However, nowadays, there is a need to replace gelatin for health and religious reasons. Replacing gelatin by whey protein (WP) and using it in combination with gum arabic (GA) would lead to various advantages. For example, the encapsulation processes with WP/GA coacervation could be carried out at room temperature (or low temperatures $> 0^{\circ}\text{C}$), which is not possible to achieve with gelatin ($T_{\text{gelation}} \sim 40^{\circ}\text{C}$). The encapsulation of temperature - sensitive compounds (*e.g.* volatile flavors) should be improved with the WP/GA system. Basic studies were already performed on the complex coacervation of WP and GA [Schmitt *et al.*, 1999; Weinbreck *et al.*, 2003a, 2003b] and the conditions under which coacervates are formed are now well known and understood. Renard *et al.*

(2002) mentioned the WP/GA system for application in controlled release and encapsulation of drugs, but so far no experimental results on the use of WP/GA coacervates are available. The goal of this work was thus to show that the WP/GA coacervates could be used for encapsulation of oil droplets and flavors. Various conditions influencing the formation of coacervates were studied (pH and biopolymer concentration) and compared to previous results. The stability of the encapsulated emulsion was then investigated as a function of pH. Finally, merely to illustrate the possibilities of the WP/GA coacervates, capsules of lemon oil were incorporated into Gouda cheese and the flavor release was measured in time.

EXPERIMENTAL SECTION

Materials

Bipro is a whey protein isolate (WP) comprised mainly of α -lactoglobulin (α -lg), and α -lactalbumin (α -la) - from Davisco Foods International (Le Sueur, USA). Residual whey protein aggregates were removed by acidification (at pH = 4.75) and centrifugation (1 h at 33000 rpm with a Beckman L8-70M ultracentrifuge, Beckman instruments, The Netherlands). The supernatant was then freeze-dried (in a Modulo 4K freeze-dryer from Edwards High Vacuum International, UK). Finally, the resulting powder was stored at 5°C and it contained (w/w) 88.1% protein (N x 6.38), 9.89% moisture, 0.3% fat and 1.84% ash (0.66% Na⁺, 0.075% K⁺, 0.0086% Mg²⁺ and 0.094%Ca²⁺). The protein content of the treated Bipro is: 14.9% α -la, 1.5% bovine serum albumin (BSA), 74.9% β -lg, and 3.2% immunoglobulin (IMG).

Gum arabic (GA; IRX 40693) was a gift from Colloides Naturels International (Rouen, France). The powder contained (w/w) 90.17% dry solid, 3.44% moisture, 0.338% nitrogen and 3.39% ash (0.044% Na⁺, 0.76% K⁺, 0.20 Mg²⁺ and 0.666% Ca²⁺). Its weight average molar mass ($M_w = 520\ 000\text{g/mol}$) and its average radius of gyration ($R_g = 24.4\ \text{nm}$) were determined by size exclusion chromatography followed by multiangle laser light scattering (SEC MALLS). SEC MALLS was carried out using a TSK-Gel 6000 PW + 5000 PW column (Tosoh Corporation, Tokyo, Japan) in combination with a precolumn Guard PW 11. The separation was carried out at 30°C with 0.1 M NaNO₃ as eluent at a flow rate of 1.0 mL min⁻¹.

Stock solutions were prepared by dissolving the powder in deionized water. The pH was adjusted with HCl and NaOH. Three types of oil were used: orange oil flavor from

RC Treatt & Co (Suffolk, England), sunflower oil (Reddy oil) and lemon juice flavor from Givaudan (Dubendorf, Switzerland). Glutaraldehyde grade II 25% was purchased from Sigma.

Preparation of the capsules

The capsules were always prepared in the same way at room temperature, independently of the type of oil used. First, an oil in water (O/W) emulsion was prepared by dispersing the oil into a stock solution of WP at pH 7. Then, a stock solution of GA (at pH 7) was poured into the O/W emulsion and stirred for 30 min. The final concentration of oil was 5% (w/w) in all experiments (after the addition of the GA solution). The ratio of WP to GA (Pr:Ps) was kept constant at 2:1 (w/w), since most of the previous work was done at this ratio [Weinbreck *et al.*, 2003a]. The pH of the mixtures was adjusted to the desired value and the mixture was left under slow stirring overnight.

Influence of physico-chemical parameters (pH, biopolymer concentration, droplet size)

Encapsulated orange oil was prepared as described above. The influence of various parameters on the encapsulation of oil was investigated: pH, total biopolymer concentration (Cp) and droplet size. Various pH values were studied (from 2.0 to 5.0 in 0.5 steps and at pH 7.0) for Cp = 1%. Cp was varied from 0.05 % to 3.0 % (w/w) at pH = 4.0. The oil droplet size was varied by dispersing the oil with a blender (Polytron, Kinematica, Switzerland) at speed 4 for 5 min, or with a magnetic stirrer (Cp = 1% and pH = 4.0). The size of the oil droplets was measured with a Mastersizer X (Malvern, UK). The size of large droplets (prepared with a magnetic stirrer) was very polydisperse and varied from 50 μm to 1000 μm . Emulsions prepared with the blender had a size between 5 μm and 50 μm . The capsules were visualized under a light microscope (Leica, Rijswijk, The Netherlands).

Emulsion stability and zeta potential

Encapsulated sunflower oil was prepared as described above (Cp = 1%), except that after emulsifying the oil with a blender, the emulsion was homogenized at 200 bar with a Rannie homogenizer (type 8.30 H) to obtain a stable emulsion at pH 7. The droplet size measured with the Mastersizer X was around 1.5 μm . The pH of the emulsion was

varied from pH 2.0 to 7.0. The turbidity of the emulsion was measured several times per day with a Turbiscan (Formulation, France) during 5 days. This instrument measures the intensity of the back-scattered light along the height of the 1 cm diameter glass tubes containing the emulsions. The creaming rate of the emulsion could thus be determined by following in time the leveling off of the interface between the lower clear layer and the upper cream layer.

The zeta potential of the homogenized emulsion of encapsulated sunflower oil ($C_p = 1\%$, 5% sunflower oil, and pressure = 200 bar) was measured as a function of pH. The titration was carried out with 1 M HNO_3 from pH 7 to pH 2. Two blanks consisting of an emulsion homogenized only with WP and an emulsion homogenized only with GA were prepared and their zeta potential was also measured as a function of pH. The measurements were made with an Acoustisizer (Matec Applied Sciences Inc., Hokinton, USA) at Philips Natlab in Eindhoven, The Netherlands.

Encapsulated lemon oil in Gouda cheese

Lemon flavor was encapsulated following the same procedure as used for encapsulated sunflower oil (described above), but the process was carried out at 5°C to limit flavor evaporation. The amount of oil was set at 6.67%, $C_p = 1\%$, pH = 4.0. One batch was made by dispersing the oil with a blender (small droplets) and another one with a magnetic stirrer (large droplets). From each batch, blanks of the emulsion were prepared at pH 7.0. At that pH, no coacervation occurred and the oil was not encapsulated. From the encapsulated batch (at pH 4.0), one part was not cross-linked and the other part was cross-linked by slowly adding concentrated glutaraldehyde to the mixture with stirring, in order to reach a final glutaraldehyde concentration of 0.1%. The mixtures were then mixed for 45 min; the capsules were washed to get rid off the residual glutaraldehyde and filtered. The slurry was redispersed in deionized water to reach the initial volume of the mixture. The capsules were added to Gouda cheese during the cheese process at NIZO food research. 5 ml of each mixture (blank, non-cross-linked capsules and cross-linked capsules – small and large capsules) were added to 1800 g of curd and the curd was mixed by hand for 1 min. Afterwards, the curd was pressed into four identical cheeses of 250 g each, brined (4 h), and graded for one month. After one month, the cheeses were tasted in duplicate by five panelists with the MS Nose. The panelists were instructed to chew the cheese regularly for 30 s without swallowing, then to swallow the entire piece of cheese, and after swallowing, to

continue chewing for 60 s. The order of the samples was randomized. While panelists were eating the cheese, the nose space concentration of limonene (main component of lemon oil) was monitored by sampling the airflow from one nostril over a 1.5 min period. A full description of the apparatus is available in Weel *et al.* (2002). An average of the limonene intensity from all panelists' results was calculated for the six cheeses and plotted as a function of time.

RESULTS AND DISCUSSION

Influence of physico-chemical parameters (pH, biopolymer concentration, droplet size)

Microencapsulation of oil droplets by the complex coacervation method is known to be strongly influenced by many parameters, such as pH, biopolymer concentration (Cp), and droplet size [Madan *et al.*, 1972, 1974; Nixon and Nouh, 1978; Takenaka *et al.*, 1980; Burgess and Carless, 1985; Arshady, 1990; Burgess, 1994; Ijichi *et al.*, 1997; Thimma and Tammishetti, 2003]. Since the formation of complex coacervates arises from electrostatic interactions between the positively charged WP and the negatively charged GA, coacervates can be formed in the pH range 2.5 – 4.8 [Weinbreck *et al.*, 2003a]. Orange oil droplets were encapsulated with WP/GA coacervates following the method described above. The microcapsules were made at various pH values and were observed under the light microscope to see if a coacervate wall was visible around the oil droplets (Figure 8.1). It appeared that at pH > 5.0, no encapsulation took place. In the pH region 4.5 – 3.0, a layer of coacervate was noticeable around the oil droplets and the capsules formed had the tendency to stick together in the absence of shear. At pH 4.5, coacervates were visible in the mixture encapsulating partially some oil droplets and partially in the bulk solution. At pH 4.0, a smooth coacervate layer homogeneously enveloped the oil and the capsules formed clusters when stirring was stopped. At pH 3.5, the oil was still well encapsulated but the coacervate layer seemed less homogeneous. At lower pH (below 3.0), the oil droplets were not encapsulated. These results were in good agreement with previous studies [Weinbreck *et al.*, 2003a]. From that work, it was found that complex coacervation between WP and GA occurred in a specific pH window, which was the same when oil was added to the mixture. The viscosity of the coacervate layer was previously investigated and was found to be very much pH-dependent [Weinbreck *et al.*, 2004b]. Here, the best capsules were formed

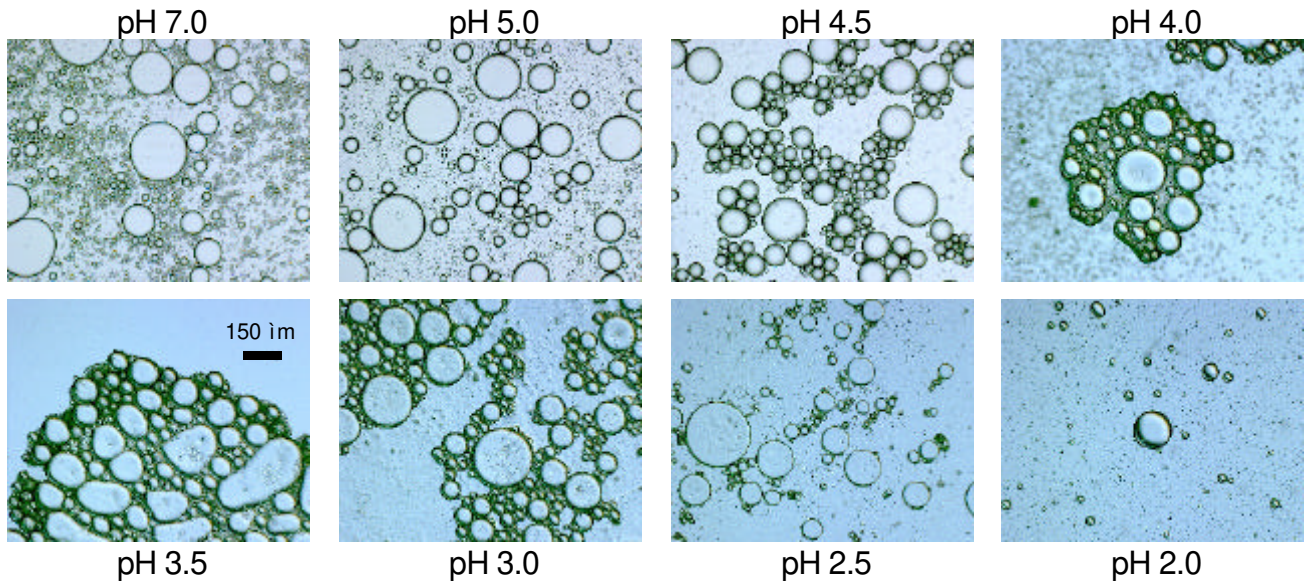


Figure 8.1: Encapsulated orange flavor with WP / GA coacervates at various pH values, 5% oil, $C_p = 1\%$, Pr:Ps = 2:1. The scale bar represents 150 μm .

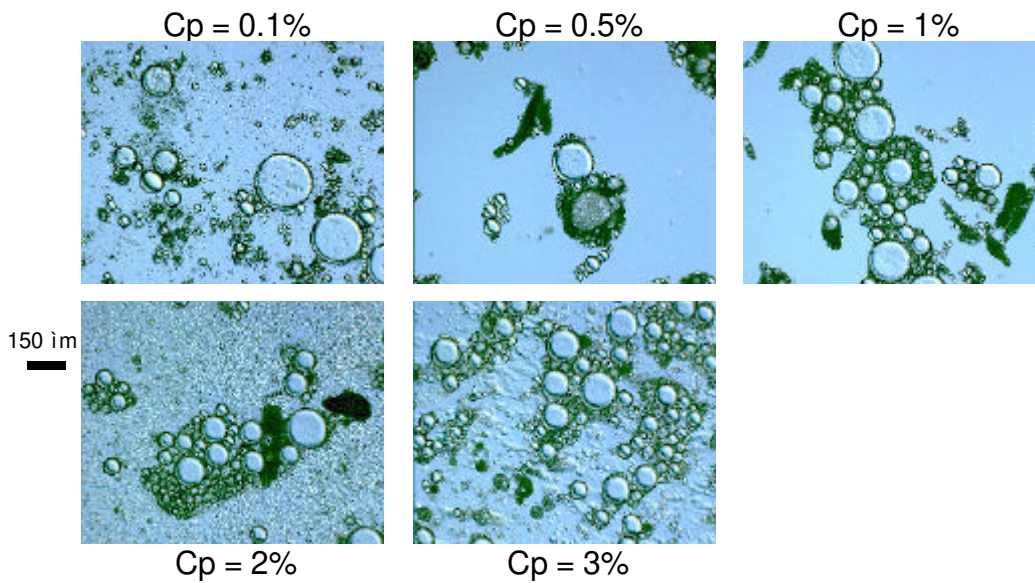


Figure 8.2: Encapsulated orange flavor with WP / GA coacervates at various C_p , 5% oil, pH = 4.0, Pr:Ps = 2:1. The scale bar represents 150 μm .

at pH 4.0, at which the viscosity of the coacervate was the highest and at which most polymers were present in a coacervate form [Weinbreck *et al.*, 2004b]. Burgess (1994) reported previously that a high viscosity of the coacervate resulted in more stable capsules, but if the viscosity was too high, then encapsulation could be impaired. Each biopolymer combination needs to be investigated to obtain the optimum conditions for encapsulation. For WP/GA, pH = 4.0 seemed to give the best results at a Pr:Ps of 2:1.

If the ratio of protein to polysaccharide is changed, then the optimum pH would also be shifted [Weinbreck *et al.*, 2003b].

The influence of total biopolymer concentration was studied on a 5% oil in water (O/W) emulsion. The C_p was varied from 0.1% to 3.0% and the pH was set at 4.0. The samples were visualized under the microscope (Figure 8.2). A thin and homogeneous coacervate layer was observed around the oil droplets at $C_p > 0.5\%$. For $C_p > 1\%$, the coacervate layer was thicker and free coacervates were found in solution. A C_p between 0.5% and 1% seemed to be sufficient to encapsulate 5% of oil. The payload of oil: polymer would be between 90% and 80%. This high payload is a major advantage of encapsulation using complex coacervation and is in the same range if gelatin is used [Luzzi, 1970; Dziezak, 1988]. For $C_p > 8\%$, one would expect a reduction of the amount of coacervate because of a self-suppression on coacervation at high concentrations [Burgess and Carless, 1985; Burgess, 1994; Weinbreck *et al.*, 2003a].

Various oil droplet sizes could be achieved, depending on the way the emulsion was prepared. Small droplets ($D_{[3;2]} = 5 - 50 \mu\text{m}$) were made by using a blender and large droplets ($D_{[3;2]} = 50 - 200 \mu\text{m}$) by dispersing the oil with a magnetic stirrer. In both cases, the emulsions were very polydisperse. From microscopic observations, it was found that small droplets were easily encapsulated whereas some large droplets were only partially or not at all encapsulated. The capsules also looked different depending on the size of the oil droplets. Large droplets were individually surrounded by a thin coacervate layer, whereas small droplets were encapsulated in a matrix of coacervate as shown in Figure 8.3. It has already been reported that oil droplets larger than $250 \mu\text{m}$

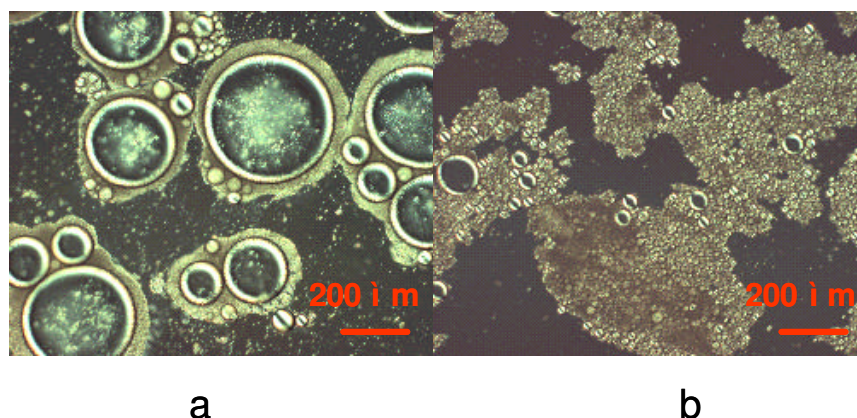


Figure 8.3: Encapsulated orange flavor with WP / GA coacervates, 5% oil, $C_p = 1\%$, pH = 4.0, Pr:Ps = 2:1. (a): large droplets prepared with magnetic stirrer; (b): small droplets prepared with a blender. The scale bar represents $200 \mu\text{m}$.

were difficult to encapsulate [Madan *et al.*, 1972; Ijichi *et al.*, 1997]. This difference might be attributed to a different encapsulation mechanism for small and large droplets. Upon pH decrease, coacervate droplets are initially formed in the bulk, and then they migrate, wet the surface of the oil and spread [Madan *et al.*, 1972; Ijichi *et al.*, 1997]. The wetting and spreading of the coacervate has a major impact on the encapsulation [Madan *et al.*, 1972; Newton *et al.*, 1977; Ijichi *et al.*, 1997; Thomassin *et al.*, 1997]. Good wetting properties of the coacervate are required and the viscosity of the coacervate should be high enough to form a resistant barrier around the oil droplets but not so high as to prevent spreading on the surface. The encapsulation of large droplets requires the aggregation and the partial coalescence of a great amount of coacervate droplets. On the other hand, for encapsulation of small droplets, entrapment of the substance in one coacervate droplet is more likely to occur and requires less rearrangement than wetting and spreading, which involves a change of shape of the coacervate.

Stability of the encapsulated emulsion

When oil droplets were encapsulated by complex coacervation of WP and GA, it was noticed that the emulsion was highly unstable against creaming. The stability of a homogenized emulsion ($D_{[3,2]} = 1.5 \mu\text{m}$) for $C_p = 1\%$ was investigated as a function of pH. Creaming of the oil droplets was measured with the Turbiscan. The interface between the clear lower phase and the cream layer was sharp and evolved in time. A sample at pH 7 was taken as a reference. Only after 5 days a small cream layer was measurable. From these measurements, the volume of the clear layer could be plotted as a function of time, and the initial slope gave the velocity of creaming (s). The creaming velocity at pH 7.0 (s_0) was very low, $s_0 = 0.0002 \text{ mm}\cdot\text{min}^{-1}$. In Figure 8.4, the relative velocities (s/s_0) of all samples are plotted as a function of pH. The instability of the emulsion was strongly pH-dependent. For pH 6.0, no creaming was observed after 2 days ($s/s_0 = 1$). By decreasing the pH from 6.0 to 3.6, the creaming rate increased and a maximum was measured at pH 3.6, where the creaming was 400 times faster than at pH 7. Below pH 3.6, s/s_0 decreased. Since the electrostatic interaction between WP and GA is strongly pH-dependent, the formation of a WP/GA complex at the oil / water interface decreased and the repulsion between droplets and creaming was enhanced. Zeta potentials of the emulsion stabilized with WP and GA were measured as a function of pH in order to quantify the charge profile of the oil

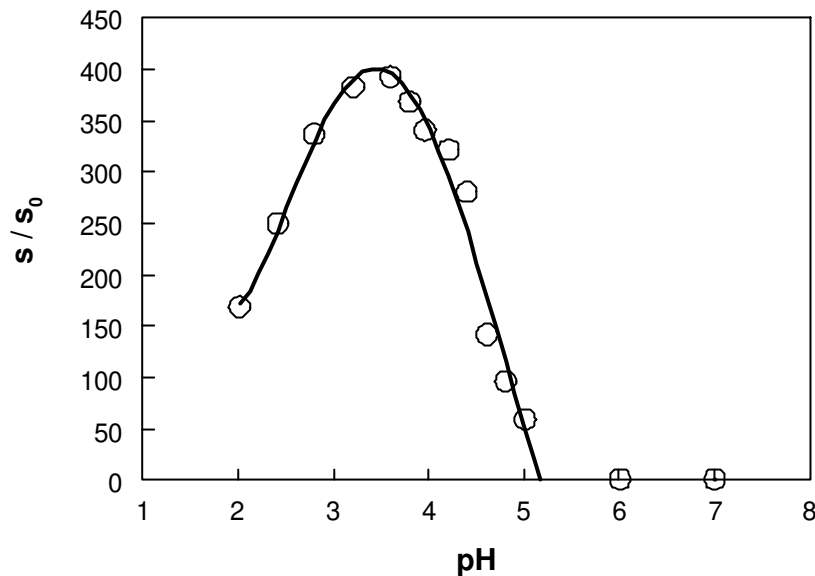


Figure 8.4: Relative creaming velocity (s/s_0) of a sunflower oil emulsion stabilized with WP and GA at various pH; 5% oil, $C_p = 1\%$, Pr:Ps = 2:1, $D_{[3:2]} = 1.5 \mu\text{m}$.

droplets. Blanks of emulsions stabilized only with WP or only with GA were also carried out. The results are shown in Figure 8.5. The emulsion stabilized with only GA had a negative Helmholtz - Smoluchowski potential from pH 7.0 until pH 2.5 and the emulsion stabilized with only WP had a negative potential above its pI (= 5.2) and a positive potential below. The results of the blanks were as expected. Indeed, the pI of β -lg (the main protein present in WP) is known to be around this value [Weinbreck *et al.*, 2003a]. GA is a weak polyelectrolyte and its charge density decreases at low pH, as was already measured in a bulk solution [Burgess and Carless, 1984; Schmitt *et al.*, 1999] or as an emulsifier [Jayme *et al.*, 1999]. The Helmholtz - Smoluchowski potential was then measured for an emulsion stabilized with WP and GA as a function of pH. For $pH > 5.3$, the zeta potential of the emulsion was negative, as for an emulsion emulsified only with WP. At pH 5.0, the potential of the emulsion decreased to the same value as the potential of the emulsion made only with GA. From pH 5.0 to pH 3.0, the potential of the mixed emulsion was very close to zero. At pH 2.7 and below, the potential of the mixed emulsion increased drastically to reach high positive values. The results of the zeta potential measurements were in good agreement with the values of the emulsion stability and with the previous results on the behavior of WP/GA as a function of pH

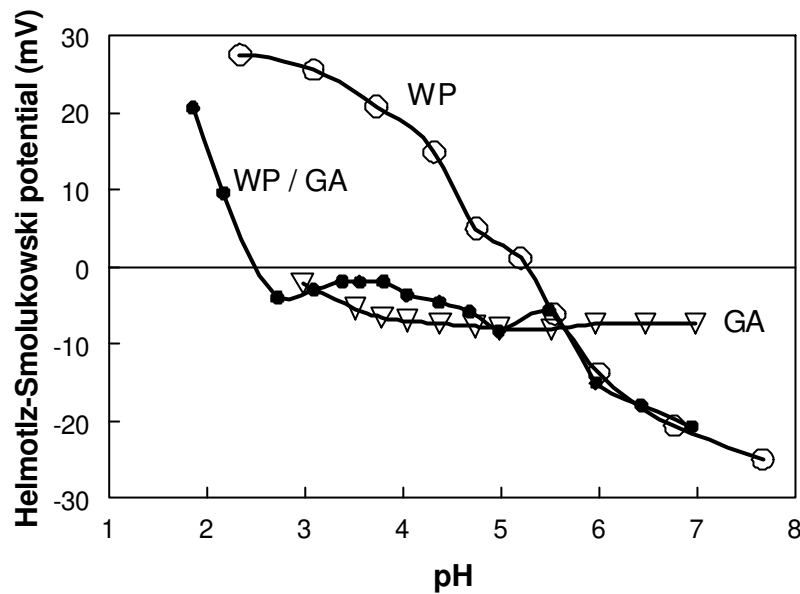


Figure 8.5: Helmholtz - Smoluchowski potential of a 5% sunflower oil emulsion as a function of pH; (○): emulsion stabilized with WP; (▽): emulsion stabilized with GA; (●): emulsion stabilized with WP/GA.

[Weinbreck *et al.*, 2003a]. Since WP was negatively charged above pH 5.2, GA (also negatively charged) did not interact with the WP, repulsion occurred between the oil droplets and the emulsion remained stable. Just below pH 5.2, the WP became positive and interacted with the GA present in the mixture. It has already been shown in previous studies that soluble complexes of WP / GA were formed in the pH region 5.2 – 4.8 [Weinbreck *et al.*, 2003a]. As a result, the zeta potential of the emulsion was similar to the zeta potential of the blank emulsion homogenized with GA. Between pH 4.8 and 2.5, coacervates were formed as shown by Weinbreck *et al.* (2003a) and a coacervate layer was formed around the oil droplets (c.f. Figure 8.1). The coacervate layer being a quasi-neutral phase, the zeta potential measured was close to zero, and a strong attraction between oil droplets occurred, which was responsible for a fast creaming rate of the emulsion (cf Figure 8.4). Then, below pH 2.5, GA, being a weak polyelectrolyte, lost its charge and reached neutrality. As a consequence, the coacervates were disrupted and the oil / water interface was probably composed of some neutral GA and certainly composed of positive WP, as indicated by the positive zeta potential of the emulsion and the decrease of creaming rate. For preparing good encapsulated material, it is thus very important to maintain stirring during the whole process to avoid

phase separation. To avoid the clotting and creaming of the encapsulated droplets, the coacervate layer can be cross-linked chemically (e.g. glutaraldehyde) or enzymatically (e.g. transglutaminase). The coacervation then becomes irreversible, WP and GA being covalently cross-linked, the pH of the mixture can then be varied (above pH 6.0) and repulsion between droplets occurs without breaking the coacervate layer.

Encapsulated lemon oil in cheese

Large capsules (size ~ 50 – 1000 μm) and small capsules (size ~ 5 – 50 μm) of lemon oil were prepared by complex coacervation of WP/GA. One batch was cross-linked with 0.1% glutaraldehyde and the other batch was not cross-linked. Blanks were made of the same emulsion of lemon oil with WP and GA but at pH 7 (where no capsules were formed) and they were compared to the capsules. The capsules were put in a Gouda cheese, by incorporating them into the curd during the cheese process. The cheeses were graded for one month and the release of the flavor was monitored with the MS Nose. The six cheese samples containing the capsules were tasted by five panelists and the amount of limonene released was measured in real time. The average flavor

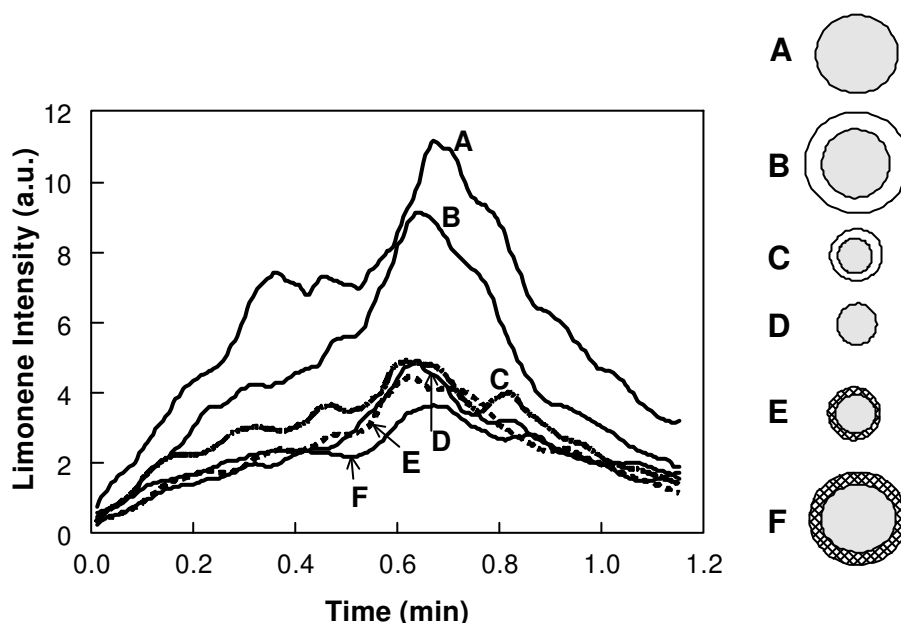


Figure 8.6: Average flavor release, MS Nose curves from cheeses containing limonene capsules. (A): Large capsule, blank pH 7; (B): Large capsule, encapsulated in WP/GA pH 4, not cross-linked; (C): Small capsule, encapsulated in WP/GA pH 4, not cross-linked; (D): Small capsule, blank pH 7; (E): Small capsule, encapsulated in WP/GA pH 4, cross-linked; (F): Large capsule, encapsulated in WP/GA pH 4, cross-linked.

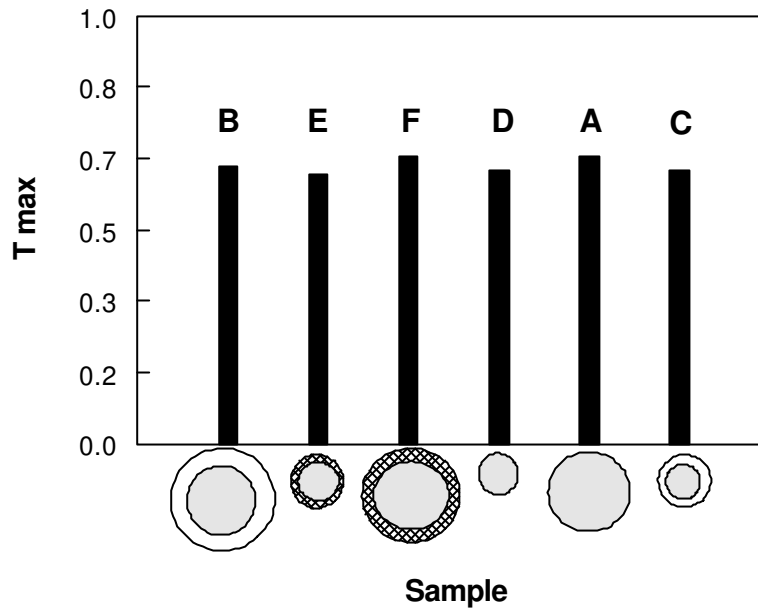


Figure 8.7: Time of maximum intensity for cheese containing limonene capsules. (A): Large capsule, blank pH 7; (B): Large capsule, encapsulated in WP/GA pH 4, not cross-linked; (C): Small capsule, encapsulated in WP/GA pH 4, not cross-linked; (D): Small capsule, blank pH 7; (E): Small capsule, encapsulated in WP/GA pH 4, cross-linked; (F): Large capsule, encapsulated in WP/GA pH 4, cross-linked.

release was plotted in Figure 8.6. All panelists' results were similar. The larger capsules (blank and non-cross-linked) gave the strongest flavor release. The cross-linked batches (small and large capsules) gave the lowest release intensity. The time at which the maximum intensity was detected is plotted in Figure 8.7. The maximum intensity was reached at approximately the same time for all samples, just after swallowing took place ($t_{\text{swallowing}} = 0.5$ min). The largest capsules gave the strongest release, probably because it was easier to break them upon chewing compared to the small capsules. The fact that the cross-linked capsules gave a low release could be explained if not all capsules were broken upon chewing, the cross-linking giving very strong capsule walls. However, it should be mentioned that the preparation of cross-linked capsules included an extra washing step, in which part of the flavor could have been washed away, but it is believed that this effect is very small. Preliminary studies on the degree of flavor evaporation by gas chromatography showed that the evaporation was delayed by a factor of 4 for non-cross-linked (large) capsules and by a factor of 10 for cross-linked capsules. The amount of limonene in the capsules and its oxidation products should be studied in more detail in further shelf-life experiments in order to get a more quantitative

description. So far, it has been shown that encapsulation with WP/GA is feasible. To improve the release of flavor in a product, a large droplet size is preferred and the degree of cross-linking should be carefully balanced between a well-encapsulated material and a high release.

CONCLUSIONS

Capsules containing oil (*e.g.* flavors) could successfully be prepared using complex coacervation of WP and GA under specific conditions. Parameters such as pH, polymer concentration and capsule size were investigated and the results were in very good agreement with previous basic work. Capsules prepared at pH 4.0 showed a smooth shell of WP/GA coacervate around the oil droplets. pH 4.0 corresponds to the pH at which all WP and GA reacted to form a coacervate. Furthermore, at this pH, the strength of the electrostatic interaction and the viscosity of the coacervates were at maximum. A high payload (up to 90%) of oil versus polymer could be achieved. Small oil droplets (< 50 μm) could be encapsulated into a coacervate matrix more easily than large droplets. Large oil droplets (> 200 μm) were formed by a typical core / shell mechanism and were occasionally only partially encapsulated. For preparation of the capsules at pH between 4.5 and 3.0, it was very important to use continuous stirring. Indeed, emulsions stabilized with WP/GA coacervates were highly unstable against creaming at pH < 5.0. The fastest creaming rate was obtained at pH 3.6 and corresponded to a surface charge that was close to zero. As an example, various capsules of lemon oil were prepared and introduced into a cheese. After one month, the flavor release was higher for large capsules, which were easier to chew, than small ones. The degree of cross-linking should be carefully tuned since cross-linked capsules gave a lower flavor release than the non-cross-linked batch. These results showed that a matrix of WP / GA can be successfully used for encapsulation purposes. However, more work is needed to check the barrier properties of these coacervates against water, flavor, and oxygen diffusion.

ACKNOWLEDGMENTS

Friesland Coberco Dairy Foods (FCDF) is acknowledged for their financial support. The authors would like to thank Annemiek Pul, Mauritz Burgering, Marjet Laats and Bertus

Damman for their experimental assistance. Philips Natlab in Eindhoven is acknowledged for lending their Acoustizer equipment. Prof. Martien Cohen Stuart and Dr. Renko de Vries are acknowledged for useful discussions.

REFERENCES

- Akinshina, A.; Linse, P. Monte Carlo simulations of polyion – macroion complexes. 1. Equal absolute polyion and macroion charges. *Macromolecules* **2002**, *35*, 5183-5193.
- Alberstsson, P.- . *Partition of cell particles and macromolecules*; Wiley Interscience: New York, 1971, 2nd edition.
- Andelman, D.; Joanny, J. F. On the adsorption of polymer-solutions on random surfaces – The annealed case. *Macromolecules* **1991**, *24*, 6040-6042.
- Antonov, Yu. A.; Gonçalves, M. P. Phase separation in aqueous gelatin – κ carrageenan systems. *Food Hydrocolloids* **1999**, *13*, 517-524.
- Arnedo, C.; Benoit, J.-P. Characterization of complex coacervates used to form microencapsulation. *Polymeric Material Science and Engineering* **1987**, *57*, 255-259.
- Arshady, R. Microspheres and microcapsules, a survey of manufacturing techniques Part II: Coacervation. *Polym. Eng. Sci.* **1990**, *31*, 905-914.
- Arvanitoyannis, I.; Psomiadov, E.; Nakayama, A. Edible films made from sodium caseinate, starches, sugar or glycerol. I. *Carbohydr. Polym.* **1996**, *31*, 179-192.
- Baeza, R. I.; Carp, D. J.; Pérez, O. E.; Pilosof, A. M. R. κ -carrageenan - protein interactions : effect of proteins on polysaccharide gelling and textural properties. *Lebensm.-Wiss. U.-Technol.* **2002**, *35*, 741-747.
- Bakker, M. A. E.; Koning, M. M. G.; Visser, J. Fatty ingredients, WO Patent Application 94/14334, Unilever, 1994.
- Ball, V.; Winterhalter, M.; Schwinte, P.; Lavallo, P.; Voegel, J. C.; Schaaf, P. Complexation mechanism of bovine serum albumin and poly(allylamine hydrocolloid). *J. Phys. Chem.* **2002**, *106*, 2357-2364.
- Bourriot, S.; Garnier, C.; Doublier, J.-L. Micellar-casein - κ -carrageenan mixtures. I. Phase separation and ultrastructure. *Carbohydrate Polymers* **1999**, *40*, 145-157.
- Bundi, A.; Wüthrich, K. ¹H-NMR parameters of the common amino acid residues in aqueous solutions of the linear tetrapeptides H-Gly-Gly-X-L-Ala-OH. *Biopolymers* **1979**, *18*, 285-297.
- Bungenberg de Jong, H. G.; Kruyt, H. R. Coacervation (Partial miscibility in colloid systems). *Proc. Koninkl. Med. Akad. Wetenschap.* **1929**, *32*, 849-856.
- Bungenberg de Jong, H. G. Crystallisation- Coacervation- Flocculation. In *Colloid Science*; Kruyt H. R., Ed.; Elsevier Publishing Company: Amsterdam, 1949a, Vol. II, Chapter VIII, p. 232-258.
- Bungenberg de Jong, H. G. Complex colloid systems. In *Colloid Science*; Kruyt H. R., Ed.; Elsevier Publishing Company: Amsterdam, 1949b, Vol. II, Chapter X, p. 335-432.
- Bungenberg de Jong, H. G. Morphology of coacervates. In *Colloid Science*; Kruyt H. R., Ed.; Elsevier Publishing Company: Amsterdam, 1949c, Vol. II, Chapter XI, p. 433-480.
- Burgess, D. J.; Carless, J. E. Microelectrophoretic studies of gelatin and acacia for the prediction of complex coacervation. *Journal of Colloid and Interface Science* **1984**, *98* (1), 1-8.
- Burgess, D. J.; Carless, J. E. Manufacture of gelatin/gelatin coacervate microcapsules. *International Journal of Pharmaceutics* **1985**, *27*, 61-70.
- Burgess, D. J.; Carless, J. E. Complex coacervate formation between acid- and alkaline-processed gelatins. In *Coulombic interactions in macromolecular systems*; Eisenberg A.,

- Bailey F. E., Eds.; ACS Symposium Series 302, American Chemical Society: Washington DC, 1986, Chapter 21, p.251-260.
- Burgess, D. J. Practical analysis of complex coacervate systems. *Journal of Colloid and Interface Science* **1990**, *140*, 227-238.
- Burgess, D. J.; Kwok, K. K.; Megremis, P. T. Characterization of albumin – acacia complex coacervation. *J. Pharm. Pharmacol.* **1991**, *43*, 232-236.
- Burgess, D. J. Complex coacervation: microcapsule formation. In *Macromolecular complexes in chemistry and biology*; Dubin, Bock, Davis, Schulz, Thies, Eds.; Springer Verlag: Berlin, 1994, Chapter 17, p. 285-300.
- Burova, T. V.; Varfolomeeva, E. P.; Grinberg, Vya E.P.; Haertlé, T.; Tolstoguzov, V. B. Effect of polysaccharides on the stability and denaturation of soybean trypsin (Kunitz) inhibitor. *Macromol. Biosci.* **2002**, *2*, 286-292.
- Capron, I.; Nicolai, T.; Durand, D. Heat induced aggregation and gelation of β -lactoglobulin in the presence of κ -carrageenan. *Food Hydrocolloids* **1999**, *13*, 1-5.
- Carlsson, F.; Linse, P.; Malmsten, M. Monte Carlo simulation of polyelectrolyte-protein complexation. *J. Phys. Chem. B* **2001**, *105*, 9040-9049.
- Chen, H.; Swedlow, J. R.; Grote, M.; Sedat, J. W.; Agard, D. A. The collection, processing, and display of digital three-dimensional images of biological specimens. In *Handbook of biological confocal microscopy*; Pawley J. B. Ed.; Plenum Press: New York, 1995, p. 197-210.
- Chen, W.-S.; Henry, G. A.; Gaud, S. M.; Miller, M. S.; Kaiser, J. M.; Balmadeca, E. A.; Morgan, R. G.; Baer, C. C.; Borwankar, R. P.; Hellgeth, L. C.; Strandholm, J. J.; Hasenheuttl, G. L.; Kerwin, P. J.; Chen, C. C.; Kratochvil, J. F.; Lloyd, W. L. Microfragmented ionic polysaccharide / protein complex dispersions, European Patent Application, 0,340,035,A2, Kraft General Foods Inc., 1989.
- Chilvers, G. R.; Morris, V. J. Coacervation of gelatin – gellan gum mixtures and their use in microencapsulation. *Carbohydrate Polymers* **1987**, *7* (2), 111-120.
- Currie, E. P. K.; Cohen Stuart, M. A.; Fleer, G. J.; Borisov, O. V. Brushes with annealed excluded-volume interactions. *Eur. Phys. J. E.* **2000**, *1*, 27-40.
- Daniels, R.; Mittermaier, E. M. Influence of pH adjustment on microcapsules obtained from complex coacervation of gelatin and acacia. *J. Microencapsulation* **1995**, *12* (6), 591-599.
- Dautzenberg, H. Polyelectrolyte complex formation a highly aggregated systems: methodical aspects and general tendencies. In *Physical chemistry of polyelectrolytes. Surfactant sciences*; Radeva T., Ed.; Marcel Dekker: New York, 2001, Vol. 99, p.743-792.
- Deasy, P.B. *Microencapsulation and related drug processes*; Marcel Dekker: New York, 1984, p. 61-95.
- Dickinson, E. Stability and rheological implications of electrostatic milk protein-polysaccharide interactions. *Trends in Food Science and Technology* **1998**, *9*, 347-354.
- Doublier, J.-L.; Garnier, C.; Renard, D.; Sanchez, C. Protein-polysaccharide interactions. *Current Opinion in Colloid & Interface Science* **2000**, *5*, 202-214.
- Dubin, P. L.; Oterie, R. Association of polyelectrolytes with oppositely charged micelles. *J. Colloid Interface Sci.* **1983**, *95*, 453-461.
- Dubin, P. L.; Ross, T. D.; Sharma, I.; Yegerlehner, B. E. Coacervation of polyelectrolyte – protein complexes. In *Ordered media in chemical separations*; Hinze W. L., Armstrong D. W., Eds.; American Chemical Society: Washington, DC, 1987; Chapter 8, p. 162-169.
- Dubin, P. L.; Murrel, J. M. Size distribution of complexes formed between poly (dimethyldiallylammonium chloride) and bovine serum albumin. *Macromolecules* **1988**, *21*, 2291-2293.
- Dubin, P. L.; Vea, M. E. Y.; Fallon, M. A.; Thé, S. S.; Rigsbee, D. R.; Gan, L. M. Higher order association in polyelectrolyte-Micelle complexes. *Langmuir* **1990**, *6*, 1422-1427.

- Dubin, P. L.; Gao, J.; Mattison, K. Protein purification by selective phase separation with polyelectrolytes. *Separation and Purification Methods* **1994**, *23* (1), 1-16.
- Dziezak, J. D. Microencapsulation and encapsulated ingredients. *Food Technol.* **1988**, *4*, 136-157.
- Dziezak, J. D. Fat, oils, and fat substitutes. *Food Technol.* **1989**, *7*, 66-74.
- Easton, I. A.; Gorham, S. D. Protein / polysaccharide complexes, US Patent Application 4,614,794, Johnson and Johnson, 1986.
- Edelman, M. W. *Segregative phase separation in aqueous mixtures of polydisperse biopolymers*. Ph.D. Thesis, Wageningen University, Wageningen, The Netherlands, 2003.
- Ellis, D. L.; Yannas, I. V. Recent advances in tissue synthesis *in vivo* by use of collagen-glycosaminoglycan copolymers. *Biomaterials* **1996**, *17* (3), 291-299.
- Ellis, M.; Kong, C. Y.; Muthukumar, M. Polyelectrolyte adsorption on heterogeneously charged surfaces. *J. Chem. Phys.* **2000**, *112* (19), 8723-8729.
- Evers, O. A.; Fleer, G. J.; Scheutjens, J. M. H. M.; Lyklema, J. Adsorption of weak polyelectrolytes from aqueous solution. *J. Colloid Interface Sci.* **1986**, *111*, 446-454.
- Flores, R. J.; Wall, M. D.; Carnahan, D. W.; Orofino, T. A. An investigation of internal phase losses during the microencapsulation of fragrances. *J. Microencapsulation* **1992**, *9* (3), 287-307.
- Fogolari, F.; Ragona, L.; Licciardi, S.; Romagnoli, S.; Michelutti, R.; Ugolini, R.; Molinari, H. Electrostatic properties of bovine beta-lactoglobulin. *Proteins: Struct., Func., Genet.*, **2000**, *39*, 317-330.
- Galazka, V. B.; Ledward, D. A.; Sumner, I. G.; Dickinson, E. Influence of high pressure on bovine serum albumin and its complex with dextran sulfate. *J. Agric. Food Chem.* **1997**, *45*, 3465-3471.
- Galazka, V. B.; Smith, D.; Ledward, D. A.; Dickinson, E. Complexes of bovine serum albumin with sulfated polysaccharides: effects of pH, ionic strength and high pressure treatment. *Food Chem.* **1999**, *64*, 303-310.
- Ganz, A. J. How cellulose gum reacts with proteins. *Food Eng.* **1974**, *46*, 67-69.
- Gibbs, B. F.; Kermasha, S.; Alli, I.; Mulligan, C. N. Encapsulation in food industry: a review. *International Journal of Food Sciences and Nutrition* **1999**, *50*, 213-224.
- Girard, M.; Turgeon, S. L.; Gauthier, S. F. Interbiopolymer complexing between α -lactoglobulin and low- and high- methylated pectin measured by potentiometric titration and centrifugation. *Food Hydrocolloids* **2002**, *16*, 585-591.
- Girard, M.; Turgeon, S. L.; Gauthier, S. F. Thermodynamic parameters of α -lactoglobulin – pectin complexes assessed by isothermal titration calorimetry. *J. Agric. Food Chem.* **2003**, *51*, 4450-4455.
- Green, B. K.; Schleicher, L. Manifold Record Material, US Patent Application 2 730 456, The National Cash Register Company, 1956.
- Green, B. K.; Schleicher, L. Oil-containing Microscopic capsules and method of making them, US Patent Application 2 800 457, The National Cash Register Company, 1957.
- Gribbon, P.; Hardingham, T. E. Macromolecular diffusion of biological polymers measured by confocal fluorescence recovery after photobleaching. *Biophysical Journal* **1998**, *75*, 1032-1039.
- Grymonpré, K. R.; Staggemeier, B. A.; Dubin, P. L.; Mattison, K. W. Identification by integrated computer modeling and light scattering studies of an electrostatic serum albumin-hyaluronic acid binding site. *Biomacromolecules* **2001**, *2*, 422-429.
- Gurov, A. N.; Wajnerman, E. S.; Tolstoguzov, V. B. Interaction of proteins with dextransulfate in aqueous medium. *Stärke* **1977**, *29* (6), 186-190.
- Gurov, A. N.; Gurova, N. V.; Tolstoguzov, V. B. Protein – polysaccharide complexes as surfactants. *Die Nahrung* **1986**, *30* (3-4), 349-353.

References

- Hansen, P. M. T. Hydrocolloid-protein interactions: relationship to stabilization of fluid milk products. A review. *Prog. Food Nutr. Sci.* **1982**, *6*, 127-138.
- Hayashi, Y.; Ullner, M.; Linse, P. Complex formation in solutions of oppositely charged polyelectrolytes at different polyion compositions and salt content. *J. Phys. Chem. B* **2003**, *107*, 8198-8207.
- Heilbrunn, L. V. *The colloid chemistry of protoplasma*. Gebr. Borntraeger: Berlin, 1928, p. 233-255.
- Hidalgo J.; Hansen, P. M. T. Selective precipitation of whey proteins with carboxymethylcellulose. *J. Dairy Sci.* **1971**, *54* (9), 1270-1274.
- Ijichi, K.; Yoshizawa, H.; Uemura, Y.; Hatate, Y. Multi-layered gelatin/Acacia microcapsules by complex coacervation. *Journal of Chemical Engineering of Japan* **1997**, *30* (5), 793-798.
- Ikeda, S.; Kumagai, H.; Sakiyama, T.; Chu, C.-H.; Nakamura, K. Method for analyzing pH-sensitive swelling of amphoteric hydrogels – application to a polyelectrolyte complex gel prepared from xanthan and chitosan. *Biosci. Biotech. Biochem.* **1995**, *59* (8), 1422-1427.
- Imeson, A. P.; Ledward, D. A.; Mitchell, J. R. On the nature of the interaction between some anionic polysaccharides and proteins. *J. Sci. Food Agric.* **1977**, *28*, 661-667.
- Islam, A. M.; Phillips, G. O.; Sljivo, A.; Snowden, M. J.; Williams, P. A. A review of recent developments on the regulatory, structural and functional aspects of gum arabic. *Food Hydrocolloids* **1997**, *11* (4), 493-505.
- Ivinova, O. N.; Izumdurov, V. A.; Munoretz, V. I.; Galaev, Iy V. I.; Mattiasson, B. Influence of complexing polyions on the thermostability of basic proteins. *Acromol. Biosci.* **2003**, *3*, 210-215.
- Jayme, M. L.; Dunstan, D. E.; Gee, M. L. Zeta potentials of gum arabic stabilised oil in water emulsions. *Food Hydrocolloids* **1999**, *13*, 459-465.
- Jizomoto, H.; Kanaoka, E.; Sugita, K.; Hirano, K. Gelatin-Acacia microcapsules for trapping micro oil droplets containing lipophilic drugs and ready disintegration in the gastrointestinal tract. *Pharmaceutical Research* **1993**, *10* (8), 1115-1122.
- Kaibara, K.; Okazaki, T.; Bohidar, H. B.; Dubin, P. L. pH-induced coacervation in complexes of bovine serum albumine and cationic polyelectrolytes. *Biomacromolecules* **2000**, *1*, 100-107.
- Kaplan, P.D.; Kao, M. H.; Yodh, A. G.; Pline, D. Geometric constraints for the design of diffusing-wave spectroscopy experiments. *J. Applied Optics* **1993**, *32* (21), 3828-3836.
- Kester, J. J.; Fennema, O. R. Edible films and coatings: a review. *Food Technol.* **1986**, *40* (12), 47-59.
- Koh, G. L.; Tucker, I. G. Characterisation of sodium carboxymethylcellulose-gelatine complex coacervation by viscosity, turbidity, and coacervate wet weight and volume measurement. *J. Pharm. Pharmacol.* **1988a**, *40*, 233-236.
- Koh, G. L.; Tucker, I. G., Characterisation of sodium carboxymethylcellulose – gelatine complex coacervation by chemical analysis of the coacervate and equilibrium fluid phases. *J. Pharm. Pharmacol.* **1988b**, *40*, 309-312.
- (van) Kranenburg, R. *Exopolysaccharide biosynthesis in Lactococcus lactis; A molecular characterisation*, Ph.D. Thesis, Wageningen University, Wageningen, The Netherlands, 1999.
- (de) Kruif, C. G. Skim milk acidification. *J. Colloid Interface Sci.* **1997**, *185*, 19-25.
- (de) Kruif C. G.; Tuinier R. Polysaccharide protein interactions. *Food Hydrocolloids* **2001**, *15*, 555-563.
- Lamprecht, A.; Schäfer, U. F.; Lehr, C.-M. Visualisation and quantification of polymer distribution in microcapsules by confocal laser scanning microscopy (CSLM). *International Journal of Pharmaceutics* **2000a**, *196*, 223-226.
- Lamprecht, A.; Schäfer, U. F.; Lehr, C.-M. Characterization of microcapsules by confocal laser scanning microscopy: structure, capsule wall composition and encapsulation rate. *Europ. J. Pharm. Biopharm.* **2000b**, *49*, 1-9.

- Lamprecht, A.; Schäfer, U. F.; Lehr, C.-M. Influences of process parameters on preparation of microparticle used as a carrier system for $\dot{U} - 3$ unsaturated fatty acid ethyl esters used in supplementary nutrition. *J. Microencapsulation* **2001**, *18* (3), 347-357.
- Langendorff, V.; Cuvelier, G.; Launay, B.; Michon, C.; Parker, A.; de Kruif, C. G. Casein micelle / iota carrageenan interactions in milk: influence of temperature. *Food Hydrocolloids* **1999**, *13*, 211-218.
- Langendorff, V.; Cuvelier, G.; Michon, C.; Launay, B.; Parker, A.; de Kruif, C. G. Effects of carrageenan type on the behaviour of carrageenan / milk mixtures. *Food Hydrocolloids* **2000**, *14*, 273-280.
- Ledward, D. A. Protein-polysaccharide interactions. In *Polysaccharides in Food*. Blanchard J.M.V., Mitchell J.R., Eds.; Butterworths: London, United Kingdom, 1979; p. 205-217.
- Leisner, D.; Imae, T. Interpolyelectrolyte complex and coacervate formation of poly(glutamic acid) with a dendrimer studied by light scattering and SAXS. *J. Phys. Chem. B* **2003**, *107*, 8078-8087.
- Lepeschkin, W. *Kolloidchemie des Protoplasmas*; Julius Springer: Berlin, 1924, p. 142.
- Luzzi, L. A.; Gerraughty, R. J. Effects of selected variables on the extractability of oils from coacervate capsules. *J. Pharm. Sci.* **1964**, *53* (4), 429-431.
- Luzzi, L. A.; Gerraughty, R. J.; Effects of selected variables on the microencapsulation of solids. *J. Pharm. Sci.* **1967**, *56*, 634-638.
- Luzzi, L. A. Microencapsulation. *J. Pharm. Sci.* **1970**, *59* (10), 1367-1376.
- Macosko, C. W. *Rheology: principles, measurements and applications Vol. 1*; John Wiley & Sons Inc.: New York, 1993.
- Madan, P.L.; Luzzi, L.A.; Price, J.C. Factors influencing microencapsulation of a waxy solid by complex coacervation. *J. Pharma. Sci.* **1972**, *61*, 1586-1588.
- Madan, P.L.; Luzzi, L.A.; Price, J.C. Microencapsulation of a waxy solid: wall thickness and surface appearance studies. *J. Pharma. Sci.* **1974**, *63*, 280-284.
- Magdassi, S.; Vinetsky, Y. Microencapsulation: methods and industrial applications. In *Microencapsulation of oil-in-water emulsions by proteins*; Benita S., Ed.; Marcel Dekker Inc.: New York, 1997, p. 21-33.
- Mann, B.; Malik, R. C. Studies on some functional characteristics of whey proteins – polysaccharide complex. *J. Food Sci. Technol.* **1996**, *33* (3), 202-206.
- (van) Marle, M. E.; van den Ende, D.; de Kruif, C. G.; Mellema, J. Steady shear viscosity of stirred yoghurts with varying ropiness. *J. Rheol.* **1999**, *43* (6), 1643-1662.
- Mattison, K. W.; Brittain, I. J.; Dubin, P. L. Protein-polyelectrolyte phase boundaries. *Biotechnol. Prog.* **1995**, *11*, 632-637.
- Mattison, K. W.; Dubin, P. L.; Brittain, I. J. Complex formation between bovine serum albumin and strong polyelectrolytes: effect of polymer charge density. *J. Phys. Chem. B* **1998**, *102*, 3830-3836.
- Mattison, K. W.; Wang, Y.; Grymonpré, K.; Dubin, P.L. Micro- and macro- phase behaviour in protein-polyelectrolytes systems. *Macromol. Symp.* **1999**, *140*, 53-76.
- McGhee, J. D.; von Hippel, P. H. Theoretical aspects of DNA-protein interactions: co-operative and non-co-operative binding of large ligands to a one-dimensional homogeneous lattice. *J. Mol. Biol.* **1974**, *86*, 469-489.
- McMullen, J. N.; Newton, D. W.; Becker, C. H., Pectin-gelatine complex coacervates I: Determinants of microglobule size, morphology, and recovery as water-dispersible powders. *J. Pharm. Sci.* **1982**, *71*, 628-633.
- McQuarrie, D. A. *Statistical mechanics*; Woods J. A., Cato R., Eds.; Harper and Row: London, 1973.
- Menger, F. M.; Peresyphkin, A. V.; Caran, K. L.; Apkarian, R. P. A sponge morphology in an elementary coacervate. *Langmuir* **2000**, *16*, 9113-9116.
- Menger, F. M. Supramolecular chemistry and self-assembly. *PNAS* **2002**, *99*, 4818-4822.

- Morris, K. F.; Johnson Jr., C. S. Resolution of discrete and continuous molecular size distributions by means of diffusion-ordered 2D NMR spectroscopy. *J. Am. Chem. Soc.* **1993**, *115*, 4291-4299.
- Muthukumar, M. Adsorption of a polyelectrolyte chain to a charge surface. *J. Chem. Phys.* **1987**, *86*, 7230-7235.
- Muthukumar, M. Pattern recognition by polyelectrolytes. *J. Chem. Phys.* **1995**, *103*, 4723-4731.
- Nairn, J. G. Coacervation-phase separation technology. In *Advances in Pharmaceutical Science*; Gauderton B., Jones T., McGinity J., Eds.; 1995, p. 93-219.
- Nakajima, A.; Sato, H. Phase relationships of an equivalent mixture of sulfated polyvinyl alcohol and aminoacetylated polyvinyl alcohol in microsalt aqueous solution. *Biopolymers* **1972**, *10*, 1345-1355.
- Netz, R. R.; Joanny, J.-F. Complexation between a semiflexible polyelectrolyte and an oppositely charged sphere. *Macromolecules* **1999**, *32*, 9026-9040.
- Newton, D. W.; McMullen, J. N.; Becker, C. H. Characteristics of medicated and unmedicated microglobules recovered from complex coacervates of gelatin – acacia. *J. Pharm. Sci.* **1977**, *66*, 1327-1330.
- Nguyen, T. T.; Shklovskii, B. I. Complexation of a polyelectrolyte with oppositely charged spherical macroions: Giant inversion of charge. *J. Chem. Phys.* **2001**, *114*, 5905-5916.
- Nixon, J. R.; Nouh, A. The effect of microcapsule size on the oxidative decomposition of core material. *J. Pharm. Pharmac.* **1978**, *30*, 533-537.
- O'Brien, F. J.; Harley, B. A.; Yannas, I. V.; Gibson, L. Influence of freezing rate on pore structure in freeze-dried collagen-GAG scaffolds. *Biomaterials* **2004**, *25* (6), 1077-1086.
- Odijk, T. Adsorption of a polymer to a randomly interacting surface. *Macromolecules* **1990**, *23*, 1875-1876.
- Olins, D. E.; Olins, A. L.; von Hippel, P. H. Model nucleoprotein complexes: studies on the interaction of cationic homopolypeptides with DNA. *J. Mol. Biol.* **1967**, *24*, 157-176.
- Oparin, A. I. *The origin of life*; Dover Publications, Inc.: New York, 1953.
- Osman, M.E.; Williams, P.A.; Menzies, A.R.; Phillips, G.O. Characterization of commercial samples of gum arabic. *J. Agr. Food Chem.* **1993**, *41* (1), 71-77.
- Ould Eleya, M. M.; Turgeon, S. L. Rheology of κ -carrageenan and β -lactoglobulin mixed gels. *Food Hydrocolloids*. **2000a**, *14*, 29-40.
- Ould Eleya, M. M.; Turgeon, S. L. The effects of pH on the rheology of β -lactoglobulin / κ -carrageenan mixed gels. *Food Hydrocolloids* **2000b**, *14*, 245-251.
- Overbeek, J. T. G.; Voorn, M. J. Phase separation in polyelectrolyte solutions. Theory of Complex Coacervation. *J. Cell. Comp. Physiol.* **1957**, *49* (1), 7-26.
- Ozawa, K.; Niki, R.; Arima, S. Interaction of α -casein and κ -carrageenan. I. Viscosity and turbidity under non-gelling conditions. *Agric. Biol. Chem.* **1984**, *48* (3), 627-632.
- Palmieri, G. F.; Martell, S.; Lauri, D.; Wehrle, P. Gelatin – Acacia complex coacervation as a method for ketoprofen microencapsulation. *Drug Development and Industrial Pharmacy* **1996**, *22* (9-10), 951-957.
- Palmieri, G. F.; Lauri, D.; Martelli, S.; Wehrle, P. Methoxybutyrate microencapsulation by gelatin – acacia complex coacervation. *Drug Development and Industrial Pharmacy* **1999**, *25* (4), 399-407.
- Park, J. M.; Muhoberac, B. B.; Dubin, P. L.; Xia, J. Effects of protein charge heterogeneity in protein-polyelectrolyte complexation. *Macromolecules* **1992**, *25*, 290-295.
- Parker, A.; Boulenger, P.; Kravtchenko, T. P. Effect of the addition of high methoxyl pectin on the rheology and colloidal stability of acid milk drinks. In *Food Hydrocolloids: Structure, Properties and Functions*; Nishinari K., Doi E., Eds.; Plenum Press: New York, 1994; p. 307-312.
- Plashchina, I. G.; Mrachkovskaya, T. A. ; Danilenko, A. N.; Kozhevnikov, G. O.; Starodubrovskaya, N. Yu.; Braudo, E. E.; Schwenke, K. D. Complex formation of Faba

- bean legumin with chitosan: surface activity and emulsion properties of complexes. In *Food Colloids, fundamentals and formulation*; Dickinson E., Miller R., Eds.; Royal Society of Chemistry: Cambridge, 2001, p. 293-303.
- Poetschke, D.; Hickl, P.; Ballauf, M.; Pederson, J. S. *Macromol. Theory Simul.* **2000**, *9*, 345-353.
- Poon, W.; Pusey, P.; Lekkerkerker, H. Colloids in suspense. *Phys. World*, April **1996**.
- Pouchayret, F.; Fasan, G.; Grandgeorge, M.; Vigneron, C.; Menu, P.; Dellacherie, E. A potential blood substitute from carboxylic dextran and oxyhemoglobin. I. Preparation, purification and characterization. *Biomat. Art. Cells Immob. Biotech.* **1992**, *20* (2-4), 319-322.
- Randall, R.C.; Phillips, G.O.; Williams, P.A. Fractionation and characterization of gum from *Acacia Senegal*. *Food Hydrocolloids*, **1989**, *3* (1), 65-75.
- Renard, D.; Robert, P.; Lavenant, L.; Melcion, D.; Popineau, Y.; Guéguen, J.; Duclairoir, C.; Nakache, E.; Sanchez, C.; Schmitt, C. Biopolymeric colloidal carriers for encapsulation or controlled release applications. *International Journal of Pharmaceutics* **2002**, *242*, 163-166.
- (de) Rooij, R. *Rheology of weakly aggregating polystyrene latex dispersions*, Ph.D. Thesis, Twente University, Enschede, The Netherlands, 1994.
- Ruas-Madiedo, P.; Tuinier, R.; Kanning, M.; Zoon, P. Role of exopolysaccharides produced by *Lactococcus lactis* subsp. *Cremoris* on the viscosity of fermented milks. *Int. Dairy J.* **2002**, *12*, 689-695.
- Russel, W. B. The Huggins coefficient as a means for characterizing suspended particles. *J. Chem. Soc. Faraday Trans.* **1984**, *80*, 31-41.
- Samuel, R. E.; Lee, C. R.; Ghivizzani, S. C.; Evans, C. H.; Yannas, I. V.; Olsen, B. I.; Spector, M. Delivery of plasmid DNA to articular chondrocytes via novel collagen – glycosaminoglycan matrices. *Hum. Gene Ther.* **2002**, *13* (7), 791 – 802.
- Sanchez, C.; Paquin, P. S. Protein and protein-polysaccharide microparticles. In *Food proteins and their applications*; Damoran S., Paraf A., Eds.; Marcel Dekker: New York: 1997; Chapter 17.
- Sanchez, C.; Mekhloufi, G.; Schmitt, C.; Renard, D.; Robert, P.; Lehr, C.-M.; Lamprecht, A.; Hardy, J. Self-assembly of α -lactoglobulin and acacia gum in aqueous solvent : structure and phase-ordering kinetics. *Langmuir* **2002a**, *18*, 10323-10333.
- Sanchez, C.; Renard, D.; Robert, P.; Schmitt, C.; Lefebvre, J. Structure and rheological properties of acacia gum dispersions. *Food Hydrocolloids* **2002b**, *16*, 257-267.
- Sanchez, C.; Renard, D. Stability and structure of protein – polysaccharide coacervates in the presence of protein aggregates. *International Journal of Pharmaceutics* **2002c**, *242*, 319-324.
- Sánchez, V. B.; Bartholomai, G. B.; Pilosof, A. M. R. Rheological properties of food gums as related to water binding capacity and soy protein interaction. *Lebensm. Wiss. U. Technol.* **1995**, *28* (4), 380-385.
- Schmitt, C.; Sanchez, C.; Desobry-Banon, S.; Hardy, J. Structure and technofunctional properties of protein-polysaccharide cComplexes: a review. *Critical Review in Food Science and Nutrition* **1998**, *38* (8), 689-753.
- Schmitt, C.; Sanchez, C.; Thomas, F.; Hardy, J. Complex coacervation between α -lactoglobulin and acacia gum in aqueous media. *Food Hydrocolloids* **1999**, *13*, 483-496.
- Schmitt, C.; Sanchez, C.; Despond, S.; Renard, D.; Thomas, F.; Hardy, J. Effect of protein aggregates on the complex coacervation between α -lactoglobulin and acacia gum at pH 4.2. *Food Hydrocolloids*, **2000a**, *14*, 403-413.
- Schmitt, C. Etude de la coacervation complexe entre la β -lactoglobuline et la gomme d'acacia en solution aqueuse. Thèse de Doctorat, Institut National Polytechnique de Lorraine, France, 2000b.

- Schmitt, C.; Sanchez, C.; Lamprecht, A.; Renard, D.; Lehr, C.-M.; de Kruif, C. G.; Hardy, J. Study of α -lactoglobulin / acacia gum complex coacervation by diffusing-wave spectroscopy and confocal scanning laser microscopy. *Colloids and Surfaces B: Biointerfaces* **2001a**, *20*, 267-280.
- Schmitt, C.; Sanchez, C.; Despond, S.; Renard, D.; Robert, P.; Hardy, J. Structural modification of α -lactoglobulin as induced by complex coacervation with acacia gum. In *Food Colloids 2000 – Fundamentals of formulation*; Dickinson E., Miller R., Eds.; Royal Society of Chemistry: Cambridge, 2001b, p. 323-331.
- Serov, A. V.; Antonov, Yu. A.; Tolstoguzov, V. B. Isolation of lactic whey proteins in the form of complexes with apple pectin. *Nahrung* **1985**, *1*, 19-30.
- Shahidi, F.; Han, X.-Q. Encapsulation of food ingredients. *Critical reviews in food science and nutrition* **1993**, *33* (6), 501-547.
- Shih, F. F. Interaction of soy isolate with polysaccharide and its effect on film properties. *JAOCs* **1994**, *71* (11), 1281-1285.
- Singh, O. N.; Burgess, D. J. Characterisation of albumin-alginic acid complex coacervation. *J. Pharm. Pharmacol.* **1989**, *41*, 670-673.
- Skepö, M.; Linse, P. Complexation, Phase separation, and redissolution in polyelectrolyte-macroion solutions. *Macromolecules* **2003**, *36*, 508-519.
- Skura, B. J.; Nakai, S. Stabilization of α_1 -casein by κ -carrageenan in the presence of calcium. *Can. Inst. Food Sci. Technol. J.* **1981**, *14*, 59-63.
- Snoeren, T. H. M.; Payens, T. A. J.; Jevnink, J.; Both, P. Electrostatic interaction between kappa-carrageenan and kappa-casein. *Milchwissenschaft* **1975**, *30*, 393-395.
- Soucie, W. G.; Chen, W. S. Edible xanthan gum – protein fibrous complexes, US Patent Application 4, 563, 360, Kraft Inc., 1986.
- Sparks, R. E.; Jacobs, I. C.; Mason, N. S. Microencapsulation. In *Pharmaceutical unit operations – coating, drug manufacturing technology series*; Avis K. E., Shula A.J., Chang R.-K., Eds.; Interpharm. press Inc.: Buffalo Grove, Illinois, U.S.A., 1999, Vol. 3.
- Stoll, S.; Chodanowski, P. Polyelectrolyte adsorption on an oppositely charged spherical particle. Chain rigidity effects. *Macromolecules* **2002**, *35*, 9556-9562.
- Strege, M. A.; Dubin, P. L.; West, J. S.; Flinta, C. D. Protein separation via polyelectrolyte complexation. In *Protein purification: from molecular mechanisms to large scale process*; Ladisch M., Wilson R. C., Painton C. C., Builder S. E., Eds.; American Chemical Society Symposium Series 427, 1990, Chapter 5, 66-79.
- Stupp, S. I.; Braun, P. V. Molecular manipulation of microstructures: biomaterials, ceramics, and semiconductors. *Science* **1997**, *277*, 1242-1248.
- Tainaka, K. Study of complex coacervation in low concentration by virial expansion method. I. salt free systems. *Journal of the Physical Society of Japan* **1979**, *46* (6), 1899-1906.
- Tainaka, K. Effect of counterions on complex coacervation. *Biopolymers* **1980**, *19*, 1289-1298.
- Takeda, Y.; Nambu, N.; Nagai, T. Microencapsulation and bioavailability in beagle dogs of indomethacin. *Chem. Pharm. Bull.* **1981**, *29* (1), 264-267.
- Takenaka, H.; Kawashima, Y.; Lin, S. Y. Micromeritic properties of sulfamethoxazole microcapsules prepared by gelatin – acacia coacervation. *J. Pharm. Sci.* **1980**, *69* (5), 513-516.
- Takenaka, H.; Kawashima, Y.; Lin, S. Y. Electrophoretic properties of sulfamethoxazole microcapsules and gelatin – acacia coacervates. *J. Pharm. Sci.* **1981**, *70*, 302-305.
- Taravel M. N.; Domard, A. Collagen and its interaction with chitosan, II influence of the physicochemical characteristics of collagen. *Biomaterials* **1995**, *16* (11), 865-871.
- Taravel M. N.; Domard, A. Collagen and its interaction with chitosan, III some biological and mechanical properties. *Biomaterials* **1996**, *17* (4), 451-455.
- Tarr, B. D.; Bixby, S. H. Fat substitute, US Patent Application 5,393,550, Nurture Inc., 1995.

- Thimma, R. T.; Tammishetti, S. Study of complex coacervation of gelatin with sodium carboxymethyl guar gum: microencapsulation of clove oil and sulphamethoxazole. *J. Microencapsulation* **2003**, *20* (2), 203-210.
- Thomassin, C.; Merkle, H. P.; Gander, B. A. Physico – chemical parameters governing protein microencapsulation into biodegradable polyesters by coacervation. *International Journal of Pharmaceutics* **1997**, *147*, 173-186.
- Tiebackx, F. W. Z. Gleichzeitige Ausflockung zweier Kolloide. *Chem. Ind. Kolloide* **1911**, *8*, 198-201.
- Tolstoguzov, V. B.; Izjumov, D. B.; Grinberg, V. Y.; Marusova, A. N.; Chekhovskaya, V. T. Method of making protein-containing foodstuffs resembling minced meat, US Patent Application 3,829,587, 1974.
- Tolstoguzov, V. B.; Grinberg, V. Y.; Gurov, A. N. Some physicochemical approaches to the problem of protein texturization. *J. Agric. Food Chem.* **1985**, *33* (2), 151-159.
- Tolstoguzov, V. B. Functional properties of food proteins and role of protein – polysaccharide interaction. *Food Hydrocolloids* **1991**, *4* (6), 429-468.
- Tolstoguzov, V. B. Structure-property relationships in foods. In *Macromolecular interactions in food technology*; Parris N., Kato A., Creamer L. K., Pierce J., Eds.; ACS symposium series 650; American Chemical Society: Washington DC, 1996; p. 2-14.
- Tolstoguzov, V.B. Thermodynamic aspects of biopolymer functionality in biological systems, foods, and beverages. *Critical Reviews in Biotechnology* **2002**, *22* (2), 89-174.
- Tolstoguzov, V. Some thermodynamic considerations in food formulation. *Food Hydrocolloids* **2003**, *17*, 1-23.
- Tromp, R. H.; de Kruif, C. G.; van Eijk, M.; Rolin, C. On the mechanism of stabilisation of acidified milk drinks by pectin. *Food Hydrocolloids*, in press.
- Tuinier, R., Zoon, P., Olieman, C., Cohen Stuart, M. A., Flerer, G.J., de Kruif, C.G. Isolation and physical characterization of an exocellular polysaccharide. *Biopolymers* **1999**, *49*, 1-9.
- Tuinier, R.; Dhont, J. K. G.; de Kruif, C. G. Depletion-induced phase separation of aggregated whey proteins colloids by an exocellular polysaccharide. *Langmuir* **2000**, *16*, 1497-1507.
- Tuinier, R.; Rolin, C.; de Kruif, C. G. Electrosorption of pectin onto casein micelles. *Biomacromolecules* **2002**, *3*, 632-638.
- Turgeon, S. L.; Beaulieu, M.; Schmitt, C.; Sanchez, C. Protein – polysaccharide interactions: phase-ordering kinetics, thermodynamic and structural aspects. *Current opinion in colloid and interface science* **2003**, *8* (4-5), 401-414.
- Truong-Le, V. L.; August, J. T.; Leong, K. W. Controlled gene delivery by DNA-gelatin nanospheres. *Human Gene Therapy* **1998**, *9*, 1709-1717.
- Vasbinder, A. J. *Casein – whey protein interactions in heated milk*, Ph.D. Thesis, Utrecht University, Utrecht, The Netherlands, 2002.
- Veis, A.; Aranyi, C. Phase separation in polyelectrolyte systems. I. Complex coacervates of gelatine. *J. Phys. Chem.* **1960**, *64*, 1203-1210.
- Veis, A. Phase separation in polyelectrolyte solutions. II. Interaction effects. *J. Phys. Chem.* **1961**, *65*, 1798-1803.
- Veis, A. Phase separation in polyelectrolyte systems. III. Effect of aggregation and molecular weight heterogeneity. *J. Phys. Chem.* **1963**, *67*, 1960-1964.
- Veis, A.; Bodor, E.; Mussell, S. Molecular weight fractionation and the self-suppression of complex coacervation. *Biopolymers* **1967**, *5*, 37-59.
- (van de) Velde, F.; de Ruiter, G.A. Carrageenan. In *Biopolymers: Polysaccharides II: Polysaccharides from Eucaryotes*; Steinbüchel A., de Baets S., Vandamme E. J., Eds.; Wiley-VCH: Weinheim, Germany, 2002; Vol. 6., pp. 245-274.
- Verheul, M.; Pedersen, J. S.; Roefs, S. P. F. M.; de Kruif, K. G. Association behavior of native α -lactoglobulin. *Biopolymers* **1999**, *49*, 11-20.

- (de) Vries, R. Flexible polymer-induced condensation and bundle formation of DNA and F-actin filaments. *Biophys J.* **2001**, *80* 1186-1194.
- (de) Vries, R.; Weinbreck, F.; de Kruif, C. G. Theory of polyelectrolyte adsorption on heterogeneously charged surfaces applied to soluble protein – polyelectrolyte complexes. *J. Phys. Chem.* **2003**, *118*, 4649-4659.
- Wang, Y-f.; Gao, J. Y.; Dubin, P. L. Protein separation via polyelectrolyte coacervation: selectivity and efficiency. *Biotechnol. Prog.* **1996**, *12*, 356-362.
- Wang, Y.; Kimura, K.; Huang, Q.; Dubin, P. L.; Jaeger, W. Polyelectrolyte-micelle coacervation: effects of micelle surface charge density, polymer molecular weight, and polymer/surfactant ratio. *Macromolecules* **2000**, *33*, 3324-3331.
- Weel, K. G. C.; Boelrijk, A. E. M.; Alting, A. C.; van Mil, P. J. J. M.; Burger, J. J.; Gruppen, H.; Voragen, A. G. J.; Smit, G. Flavor release and perception of flavored whey protein gels: perception is determined by texture rather than by release. *J. Agric. Food Chem.* **2002**, *50*, 5149-5155.
- Weinbreck, F.; de Vries, R.; Schrooyen, P.; de Kruif, C. G. Complex coacervation of whey proteins and gum arabic. *Biomacromolecules* **2003a**, *4* (2), 293-303. (Chapter 2 of this thesis)
- Weinbreck, F.; de Kruif, C. G. Complex coacervation of globular proteins and gum Arabic. In *Food Colloids Biopolymers and Materials*; Dickinson E.; van Vliet T., Eds.; Royal Society of Chemistry: Cambridge, U.K., 2003b; p. 337-344.
- Weinbreck F.; Nieuwenhuijse, H.; Robijn, G. W.; De Kruif C.G. Complex formation of whey proteins – exocellular polysaccharide EPS B40. *Langmuir* **2003c**, *19*, 9404-9410. (Chapter 3 of this thesis)
- Weinbreck, F.; Tromp, R. H.; de Kruif, C. G. Composition and structure of whey protein / gum arabic coacervates. Considered for publication in *Biomacromolecules* **2004a**. (Chapter 5 of this thesis)
- Weinbreck, F.; Wientjes, R. H. W.; Nieuwenhuijse, H.; Robijn, G. W.; de Kruif, C. G. Rheological properties of whey protein / gum arabic coacervates. *Submitted for publication* **2004b**. (Chapter 6 of this thesis)
- Weinbreck, F.; Rollema, H. S.; Tromp, R. H.; de Kruif, C. G. Diffusivity of whey protein and gum arabic in their coacervates. Considered for publication in *Langmuir* **2004c** (Chapter 7 of this thesis)
- Weitz, D. A.; Pine, D. J. Diffusing wave spectroscopy. In *Dynamic light scattering*; Brown W., Ed.; Clarendon Press: Oxford, 1993, Chapter 16, p. 652-720.
- Wen, Y-p.; Dubin, P. L. Potentiometric studies of the interactions of bovine serum albumin and poly(dimethyldiallylammonium chloride). *Macromolecules* **1997**, *30*, 7856-7861.
- Xia, J.; Dubin, P. L.; Kokufuta, E.; Havel, H.; Muhoberac, B. B. Light scattering, CD, and ligand binding studies of ferrihemoglobin-polyelectrolyte complexes. *Biopolymers* **1999**, *50*, 153-161.
- Yan, X-L; Khor, E.; Lim, L-Y. Chitosan – alginate films prepared with chitosan at different molecular weights. *J. Biomed. Mater. Res.* **2001**, *58* (4), 358-365.
- Yannas, I. V. Biologically active analogues of extracellular matrix: artificial skin and nerves. *Angew. Chem. Int. Ed. Engl.* **1990**, *29* (1), 20-35.
- Yannas, I. V. Applications of ECM analogs in surgery. *J. Cell. Biochem.* **1994**, *56*, 188-191.
- Yannas, I. V. *In vivo* synthesis of tissue and organs. In *Principles of tissue engineering*; Lanza R., Langer R., Chick, W., Eds.; Austin: Landes Company, 1997, Chapter 12.
- Zaleskas, J. M.; Kinner, B.; Freyman, T. M.; Yannas, I. V.; Gibson, L. J.; Spector, M. Growth factor regulation of smooth muscle actin expression: contraction of human articular chondrocytes and meniscal cells in a collagen-GAG matrix. *Exp Cell Res.* **2001**, *270* (1), 21-31.

SUMMARY

Milk proteins and polysaccharides are ingredients used in food products and pharmaceutical products. The main motivation of this research was to better understand and control the interactions of ingredients within food products. This thesis aimed to investigate the behavior of protein / polysaccharide mixtures under mildly acid conditions, as in food products. Then, usually the protein is positively charged and the polysaccharide negatively charged and can form an electrostatic complex.

In **Chapter 1**, an introduction to the behavior of protein / polysaccharide mixtures is given. Emphasis is put on aggregative phase separation and complex coacervation in particular. Complex coacervation is the term used for the liquid / liquid phase separation arising from the formation of a coacervate layer composed of highly concentrated protein / polysaccharide complexes. Few theoretical descriptions were developed from the 1930's until today and an overview of the current status of research is given. Complex coacervates and protein / polysaccharide complexes in general find application in the field of purification of macromolecules. Also coacervates are applied as new food ingredients like fat replacers and meat analogues, or as new biomaterials in medicine (*e.g.* wound dressing, protheses). The most important industrial application is the use of complex coacervates in microencapsulation, where the liquid coacervate is used as a coating around sensitive materials. Traditionally complex coacervation of gelatine and gum arabic is mainly used industrially. Nowadays, there is, however, a need to replace gelatine for health and religious reasons, and that is the reason why whey proteins (WP) were chosen as the proteins of interest in this thesis. WP (mainly α -lactoglobulin – iso electric point $pI = 5.2$) is a protein present in milk. In the first part of the thesis three different polysaccharides were used in combination with WP, *i.e.* gum Arabic (GA), the exopolysaccharide EPS B40 (EPS B40) and carrageenan (CG). These polysaccharides carry different charged groups; GA bears carboxyl groups, EPS B40, phosphate groups, and CG sulfate groups. The physicochemical conditions for the formation of an electrostatic complex were investigated and compared for each WP/polysaccharide system (Chapters 2-4). The following chapters (Chapters 5-7) deal exclusively with the WP/GA system. An attempt is made to understand the structure of

the WP/GA coacervate which is poorly understood so far. A direct application of this system was tested by encapsulating oil with WP/GA complex coacervates (Chapter 8). In **Chapter 2**, it was shown that WP/GA mixtures form an electrostatic complex in a specific pH range. By slowly acidifying the mixture with glucono- δ -lactone (GDL), various pH boundaries were determined. Soluble WP/GA complexes were formed at pH_c , close to the iso electric point (pI) of the β -lactoglobulin (β -lg). On lowering even further the pH, macroscopic phase separation (complex coacervation) took place at a pH designated as pH_{δ_1} . Finally, at pH_{δ_2} , complexation was suppressed because GA tends to neutrality. It was also shown that β -lg was the main complex forming protein (as compared to α -lactalbumin). In the region of soluble complexes (between pH_c and pH_{δ_1}), and at low ionic strength, the GA molecule shrunk when WP interacted with the molecule, due to a reduction of the intramolecular repulsion. Increasing ionic strength in the system led to a shift of the pH boundaries to more acidic pH values, which was summarized in a state diagram and could be understood from a newly developed theory. Finally, a phase diagram was made, which showed the influence of the total biopolymer concentration (C_p) on the stability of the complexes. The resulting phase diagram has a similar shape as the phase diagram derived in the Overbeek and Voorn theory for $C_p < 12\%$. However, a 'metastable' region appeared at high C_p .

In **Chapter 3**, the exopolysaccharide EPS B40 was used instead of GA and the behavior of WP/EPS B40 complexes was studied as a function of pH, ionic strength and protein to polysaccharide (Pr:Ps) ratio. EPS B40 is a natural thickener in yoghurt-like products and carries phosphate groups. Here again, soluble complexes were formed at pH_c , and phase separation (precipitation) took place at pH_{δ} . The strength of the interaction was strongly pH- and salt- dependent. Light scattering and viscosity measurements showed that at low salt concentration the compaction of EPS B40 was induced by the interaction of WP with the polysaccharide, leading to a reduction of the hydrodynamic radius of the EPS B40 molecule and an increase of the molar mass. Varying Pr:Ps ratio showed that phase separation was a consequence of charge neutralization of the complex and that the apparent stoichiometry of the complexes depended on the order of mixing the compounds. In time, rearrangement of the WP/EPS B40 complexes occurred to form fully neutralized complexes and free EPS B40 (cooperative binding).

In **Chapter 4**, the interaction between WP and a sulfated polysaccharide, *i.e.* a non gelling carrageenan (CG), was studied as a function of pH, ionic strength, temperature,

and Pr:Ps ratio. The pH boundaries pH_c and pH_0 were also determined. Below pH_0 precipitation occurred. The values of pH_c and pH_0 were salt dependent; the presence of 45 mM of NaCl was favorable for the complex formation by screening the residual negative charges of CG. In the presence of $CaCl_2$, WP/CG complexes could be formed up to pH 8, which was well above the *pI* of the WP, highlighting the involvement of calcium bridges. The pH boundaries pH_c and pH_0 were slightly affected by temperature changes. Saturation of the CG seemed to occur at Pr:Ps = 30:1. At lower Pr:Ps ratio, when WP and CG were mixed at low pH, the pH of the mixture increased. The WP/CG complexes entrapped protons as a result of the residual negative charge on the CG.

In Chapters 2-4, it appeared that complex coacervation occurred only in the case of WP/GA system. For WP/EPS B40 and WP/CG, precipitation took place. Comparing the results, it seemed fair to conclude that the intensity of the WP / polysaccharide interaction correlated with the zeta potential of the polysaccharide: CG > EPS B40 > GA, which paralleled the stoichiometry of the complexes. The interaction between WP and CG was much stronger than for the other two polysaccharides and pH_c ($pH_c = 5.5$) was also higher than the pH_c of EPS ($pH_c = 5.3$) and gum arabic ($pH_c = 5.2$). Nevertheless, the influence of parameters like ionic strength, Pr:Ps ratio, and pH was qualitatively similar for all the systems studied. In general, an understanding of the biopolymer interactions enables the control and adjustment of the properties of food dispersions.

The second part of the thesis focused on the WP/GA coacervate phase and its characteristics. In **Chapter 5**, the influence of previously studied parameters (pH, ionic strength, Pr:Ps) on the velocity of phase separation was studied. The composition of the coacervate phase in water content and biopolymer concentration was also determined and the internal structure of the coacervate was analyzed by small angle X-ray scattering (SAXS). At a defined Pr:Ps, an optimum pH (pH_{opt}) was found, at which the strength of interaction, the kinetics of phase separation, the volume of coacervate phase, and the concentration in biopolymer were maximum. SAXS measurements also revealed that at pH_{opt} the coacervate phase was dense and structured. A specific correlation length was measured at $Q = 0.7 \text{ nm}^{-1}$ which was attributed to the structure factor of the WP. The stronger the electrostatic interaction was (*i.e.* the closer to pH_{opt}), the more pronounced the peak was. At small Q , a peak due to the presence of the charged GA was visible. Increasing the WP/GA electrostatic interaction led to a reduction of the peak intensity because of a greater neutralization of the GA molecule.

When salt was added to the system, the coacervate phase became less concentrated, less homogeneous and less structured because of the screening of the electrostatic interactions.

In **Chapter 6** the viscoelastic properties of the WP/GA coacervate phase was investigated as a function of pH. The coacervate phase was much more viscous than elastic in the pH range 3.0 – 4.5. In the pH range between 3.0 and 4.5, the coacervate did not have a strong shear thinning behavior at low shear rates (below 20 s^{-1}). At a shear rate of 30 s^{-1} , for pH_{opt} , a sharp viscosity decrease occurred. Hysteresis (thexotropy) upon increasing and decreasing shear rate could be measured around pH_{opt} . It was shown that hysteresis was due to a slow structure buildup of the coacervates and in time, the equilibrium coacervate structure could be fully recovered. By decoupling the effect of biopolymer concentration and electrostatic interactions, it appeared that the highly viscous behavior was mainly due to the strong electrostatic interactions.

In **Chapter 7**, the diffusivity of WP and GA was measured in their coacervate phase by means of nuclear magnetic resonance (NMR), fluorescence recovery after photobleaching (FRAP), and diffusing wave spectroscopy (DWS). Independently of the technique used, the results showed that the diffusion of WP and GA within the coacervate phase was slowest at pH_{opt} because of strongest electrostatic interactions. Furthermore, FRAP results showed that WP molecules diffused 10 times faster than GA molecules, which proved that WP and GA moved independently in the coacervate phase. Finally, DWS measurements revealed that the coacervate phase rearranged in time (days to weeks) leading to a loss of the turbidity of the coacervate phase and a decrease of the diffusion coefficient.

The last chapter of this thesis (**Chapter 8**) presents a direct application of the WP/GA system studied in Chapters 2, 5, 6, 7. The WP/GA coacervates were used for encapsulation of flavors and oils. A smooth biopolymer shell around the oil droplets was achieved at pH_{opt} with a payload (*i.e.* amount of oil in the capsules) up to 80%. The emulsions made of oil droplets encapsulated with WP/GA coacervates were highly unstable and their creaming rate was maximal at pH_{opt} . Around pH_{opt} the zeta potential was close to zero because of the presence of a neutral coacervate phase at the oil / water interface. Finally, encapsulated lemon oil droplets were incorporated into Gouda cheese and the flavor release was monitored by mass spectrometry (MS Nose). The results described in Chapter 8 were in good agreement with previous results reported

in Chapters 2, 5, 6, 7. This indicates that the efficiency of the WP/GA coacervates as a biopolymer coating can be predicted from their properties in the bulk solution. At pH_{opt} the coacervates are the most viscous and the most homogeneous and it leads to the formation of the best capsules. The results show how a fundamental understanding of the WP/GA interactions and of the WP/GA coacervate structure could lead to the prediction of the characteristics of the encapsulated product.

SAMENVATTING

Melkeiwitten en polysachariden worden als ingrediënten gebruikt in voedingsmiddelen en farmaceutische producten. Het belangrijkste doel van het onderzoek beschreven in dit proefschrift is het beter begrijpen en beheersen van de interacties van deze ingrediënten. Het onderzoek is erop gericht het gedrag van eiwit/polysacharidemengsels onder mild-zure condities, zoals in voedingsmiddelen, te onderzoeken. Onder deze condities is het melkeiwit gewoonlijk positief en het polysacharide negatief geladen en kunnen ze een elektrostatisch complex vormen, hetgeen van belang is voor de structuur en eigenschappen van producten.

Hoofdstuk 1 is een inleiding waarin het gedrag van eiwit/polysacharidemengsels wordt beschreven. De nadruk ligt op aggregatieve fasenscheiding en complex-coacervatie in het bijzonder. Complex-coacervatie is de term die wordt gebruikt voor de vloeistof/vloeistoffasenscheiding gepaard gaande met de vorming van een coacervaatlaag van sterk geconcentreerde eiwit/polysacharidecomplexen. Vanaf de jaren dertig tot op heden is er een beperkt aantal theoretische beschrijvingen gepubliceerd; in dit hoofdstuk wordt een overzicht gegeven van de huidige stand van zaken op het gebied van complex coacervatie. Complex-coacervaten, en eiwit/polysacharidecomplexen in het algemeen, worden bijvoorbeeld toegepast bij de zuivering van macromoleculen. Ook worden ze gebruikt als nieuwe voedingsingrediënten zoals vetvervangers en vleesvervangers, of als nieuwe biomaterialen in de geneeskunde (bijvoorbeeld wondbedekking en prothesen). De belangrijkste industriële toepassing is het gebruik van complex-coacervaten bij micro-encapsulatie, waarbij het vloeibare coacervaat wordt gebruikt als coating van gevoelige materialen. Complex-coacervatie van gelatine en Arabische gom wordt sinds de veertiger jaren industrieel toegepast. Tegenwoordig is er echter om gezondheids en religieuze redenen behoefte aan vervanging van gelatine, en daarom werden in dit proefschrift wei-eiwitten (WE) gekozen als onderwerp van studie. Wei-eiwitten (voornamelijk β -lactoglobuline met een iso-elektrisch punt pI van 5,2, en daarnaast ook α -lactalbimine) zijn afkomstig uit melk. In het eerste deel van het proefschrift werden drie verschillende polysachariden gebruikt in combinatie met WE, nl. Arabische gom

(AG), het exopolysacharide EPS B40 (EPS B40) en carrageen (CG). Deze polysachariden bevatten verschillende geladen groepen: AG bevat carboxylgroepen, EPS B40 fosfaatgroepen, en CG sulfaatgroepen. Voor elk WE/polysacharidesysteem zijn de fysisch-chemische condities voor de vorming van een elektrostatisch complex onderzocht en vergeleken (Hoofdstukken 2-4). De volgende hoofdstukken (Hoofdstukken 5-7) behandelen uitsluitend het WE/AG-systeem. Getracht is inzicht te krijgen in de structuur van het WE/AG-coacervaat, dat tot nu toe slecht begrepen is. Een directe toepassing van dit systeem werd gerealiseerd door olie te encapsuleren met WE/AG-complex-coacervaten (Hoofdstuk 8).

In **Hoofdstuk 2** wordt aangetoond dat WE/AG-mengsels een elektrostatisch complex vormen onder zekere pH en zoutcondities. Door het mengsel langzaam aan te zuren met glucono- α -lacton (GDL) werden de grenzen van het pH gebied bepaald. Oplosbare WE/AG-mengsels werden gevormd bij pH_c , dicht bij het iso-elektrische punt (pI) van het $\hat{\alpha}$ -lactoglobuline ($\hat{\alpha}$ -lg). Als de pH nog verder werd verlaagd, vond macroscopische fasenscheiding (complex-coacervatie) plaats bij een pH aangeduid als $pH_{\hat{O}1}$. Ten slotte werd bij $pH_{\hat{O}2}$ de complexering onderdrukt omdat AG ongeladen wordt. Ook werd aangetoond dat $\hat{\alpha}$ -lg het belangrijkste complexvormende eiwit is (in vergelijking met α -lactalbumine). In het gebied van oplosbare complexen (tussen pH_c en $pH_{\hat{O}1}$) en bij lage ionsterkte werd het hydrodynamisch volume van het AG-molecuul bij interactie met WE kleiner, ten gevolge van een vermindering van de intramoleculaire afstoting. Verhoging van de ionsterkte in het systeem leidde tot een verschuiving van de pH-grenzen naar lagere pH-waarden, hetgeen is samengevat in een toestandsdiagram en kan worden verklaard uit een nieuw ontwikkelde theorie door de Vries. Ten slotte werd er een fasendiagram opgesteld dat de invloed van de totale biopolymeerconcentratie (C_p) op de stabiliteit van de complexen weergeeft. Het gemeten fasendiagram heeft een zelfde vorm als het fasendiagram in de theorie van Overbeek en Voorn voor $C_p < 12\%$. Bij hoge C_p werd er echter een 'metastabiel' gebied waargenomen.

In **Hoofdstuk 3** wordt het exopolysacharide EPS B40 gebruikt in plaats van AG en het gedrag van WE/EBS-B40-complexen werd bestudeerd als functie van pH, ionsterkte en eiwit/polysacharideverhouding ($Pr:Ps$). EPS B40 is een natuurlijk verdikkingsmiddel in yoghurtachtige producten en bevat fosfaatgroepen. Ook nu werden oplosbare complexen gevormd bij pH_c en vond fasenscheiding (precipitatie) plaats bij $pH_{\hat{O}}$. De mate van interactie was sterk pH- en zoutafhankelijk. Lichtverstrooiings- en viscositeitsmetingen toonden aan dat de compactheid van EPS B40 bij laag

zoutgehalte werd veroorzaakt door de interactie van WE met het polysacharide, met als gevolg een verkleining van de hydrodynamische straal van het EPS-B40-molecuul en een toename van de molaire massa. Door de Pr:Ps-verhouding te variëren werd aangetoond dat fasenscheiding een gevolg was van neutralisering van de lading van het complex en dat de schijnbare stoichiometrie van de complexen afhing van de volgorde waarin de bestanddelen werden gemengd. Na verloop van tijd trad herverdeling in de WE/EPS-B40-complexen op waarbij volledig geneutraliseerde complexen en vrij EPS B40 werden gevormd (coöperatieve binding).

In **Hoofdstuk 4** wordt de interactie tussen WE en een gesulfateerd polysacharide, nl. een niet-gelerend carrageen (CG), bestudeerd als functie van pH, ionsterkte, temperatuur en Pr:Ps-verhouding. Ook werden de pH-grenzen pH_c en pH_0 bepaald. Onder pH_0 trad precipitatie op. De waarden van deze pH-overgangen waren zoutafhankelijk en de aanwezigheid van 45 mM NaCl bevorderde de complexvorming doordat de resterende negatieve ladingen van CG werden afgeschermd. In aanwezigheid van $CaCl_2$ konden WE/CG-complexen worden gevormd tot maximaal pH 8, hetgeen aanmerkelijk hoger was dan het pl van de WE, waaruit de rol van calciumbruggen_bleek. De waarden van pH_c en pH_0 vertoonden een geringe temperatuurafhankelijkheid. Bij Pr:Ps = 30:1 leek verzadiging van het CG op te treden. Bij lagere Pr:Ps waarden, werd bij mengen van WE en CG bij $pH < pH_0$ een pH stijging waargenomen. De WE/CG-complexen binden protonen als gevolg van de resterende negatieve lading op het CG.

In de Hoofdstukken 2-4 is gebleken dat complex-coacervatie alleen optreedt in het geval van het WE/AG-systeem. Bij WE/EPS B40 en WE/CG vond precipitatie plaats en geen vloeistof/vloeistoffasenscheiding. Na vergelijking van de resultaten leek de conclusie gerechtvaardigd dat de intensiteit van de WE/polysacharideinteractie correleert met de zeta-potentiaal van het polysacharide: $CG > EPS\ B40 > AG$, wat correspondeerde met de stoichiometrie van de complexen. De interactie tussen WE en CG was veel sterker dan die tussen WE en de twee andere polysachariden, en de pH_c van CG ($pH_c = 5,5$) was ook hoger dan de pH_c van EPS ($pH_c = 5,3$) en Arabische gom ($pH_c = 5,2$). Niettemin kwam de invloed van parameters als ionsterkte, Pr:Ps-verhouding en pH bij alle onderzochte systemen kwalitatief overeen. Inzicht in de biopolymeerinteracties maakt het mogelijk de eigenschappen van voedingsdispersies te voorspellen.

Het tweede deel van het proefschrift concentreerde zich op de WE/AG-coacervaatfase en de eigenschappen hiervan. In **Hoofdstuk 5** wordt de invloed van eerder bestudeerde parameters (pH, ionsterkte, Pr:Ps) op de snelheid van de fasenscheiding onderzocht. Ook werden het vochtgehalte en de biopolymerconcentraties van de coacervaatfase bepaald. De interne structuur van het coacervaat werd geanalyseerd met kleine-hoek-Röntgenverstrooiing (SAXS). Bij een bepaalde Pr:Ps werd een optimale pH (pH_{opt}) gevonden waarbij de interactiesterkte, de mate van fasenscheiding, het volume van de coacervaatfase en de concentratie aan biopolymeer maximaal waren. SAXS-metingen lieten zien dat de coacervaatfase bij pH_{opt} dicht en gestructureerd was. Een specifieke correlatiepiek werd gemeten bij $Q = 0,7 \text{ nm}^{-1}$; dit kan toegeschreven worden aan de verdeling van de WE in de coacervatefase. Hoe sterker de elektrostatistische interactie was (d.w.z. hoe dicht bij pH_{opt}), hoe meer uitgesproken de piek was. Bij een kleine Q was een piek ten gevolge van de aanwezigheid van geladen AG zichtbaar. Versterking van de elektrostatistische interactie tussen WE en AG leidde tot een verlaging van de piekhoogte vanwege een lagere nettolading van het complex. Toevoeging van zout leidde tot een minder geconcentreerde, minder homogene en minder gestructureerde coacervaatfase als gevolg van de afscherming van de elektrostatistische interacties.

In **Hoofdstuk 6** worden de visko-elastische eigenschappen van de WE/AG-coacervaatfase onderzocht als functie van de pH. In het pH-gebied 3,0 – 4,5 was de coacervaatfase veel meer viskeus dan elastisch. In dit pH-gebied vertoonde het coacervaat bij lage afschuifsnellheden (onder 20 s^{-1}) geen sterke verlaging van de viscositeit als functie van de afschuivingsnelheid. Bij een afschuifsnelheid van 30 s^{-1} trad bij pH_{opt} een scherpe viscositeitsdaling op. Hysterese (thixotropie) na verhoging en verlaging van de afschuifsnelheid kon worden gemeten rond pH_{opt} . Aangevoond werd dat de hysteresis het gevolg was van langzame structuuropbouw van de coacervaten, en na verloop van tijd kon de evenwichtsstructuur van het coacervaat volledig worden hersteld. Ontkoppeling van het effect van de biopolymeerconcentratie en dat van de elektrostatistische interacties liet zien dat het hoogviskeuze gedrag voornamelijk het gevolg was van de sterke elektrostatistische interacties.

In **Hoofdstuk 7** wordt de diffusiesnelheid van WE en AG in de coacervaatfase gemeten met behulp van kernspin resonantie (NMR), fluorescentie herstel na lichtbleking (FRAP) en diffusie wave spectroscopy (DWS). Onafhankelijk van de gebruikte techniek lieten de resultaten zien dat de diffusie van WE en AG binnen de

coacervaatfase het langzaamst was bij pH_{opt} omdat dan de elektrostatische interacties het sterkst zijn. Verder bleek uit de FRAP-resultaten dat WE-moleculen tienmaal sneller diffunderen dan AG-moleculen, hetgeen aantoonde dat WE en AG zich onafhankelijk in de coacervaatfase bewegen. Ten slotte bleek uit DWS-metingen dat de coacervaatfase zich na verloop van tijd (van dagen tot weken) herordent, met als gevolg het verlies van turbiditeit van de coacervaatfase en de verlaging van de diffusiecoëfficiënt.

Het laatste hoofdstuk van dit proefschrift (**Hoofdstuk 8**) beschrijft een directe toepassing van het WE/AG-systeem dat in de Hoofdstukken 2, 5, 6 en 7 is onderzocht. De WE/AG-coacervaten werden gebruikt voor de encapsulatie van smaakstoffen en oliën. Een homogene biopolymeerlaag rond de oliedruppels werd bereikt bij pH_{opt} met een belading (d.w.z. hoeveelheid olie in de capsules) tot max. 80%. De emulsies die waren gemaakt van oliedruppels geëncapsuleerd met WE/AG-coacervaten, waren zeer onstabiel en hun opromingssnelheid was maximaal bij pH_{opt} . Rond pH_{opt} was de zeta-potentiaal bijna nul vanwege de aanwezigheid van een neutrale coacervaatfase in het olie/water-tussengrensvlak. Ten slotte werden geëncapsuleerde druppels citroenolie ingesloten in Goudse kaas en werd het vrijkomen van de smaak gevolgd met behulp van massaspectrometrie (MS Nose[®]). De resultaten beschreven in Hoofdstuk 8 kwamen goed overeen met de eerdere resultaten bereikt in de Hoofdstukken 2, 5, 6 en 7. Dit wees erop dat de efficiëntie van WE/AG-coacervaten als biopolymeercoating kon worden voorspeld uit hun eigenschappen in de bulkoplossing. Bij pH_{opt} waren de coacervaten het meest viskeus en het meest homogeen, en werden de beste capsules gevormd. De resultaten laten zien hoe fundamenteel inzicht in de WE/AG-interacties en in de structuur van WE/AG-coacervaat kan leiden tot de voorspelling van de kenmerken van het geëncapsuleerde product.

RÉSUMÉ

Les protéines laitières et les polysaccharides sont des ingrédients très largement utilisés dans les industries alimentaires. Il est donc important de mieux comprendre et de contrôler les interactions entre ces ingrédients dans les produits de consommation. Cette thèse vise à étudier le comportement de mélanges de protéines et de polysaccharides en conditions acides que l'on rencontre dans la plupart des produits alimentaires. Dans ces mélanges, les protéines sont généralement chargées positivement tandis que les polysaccharides sont chargés négativement. Par conséquent, un complexe électrostatique peut être formé.

Le **chapitre 1** est essentiellement consacré à une introduction sur le comportement des mélanges protéines / polysaccharides. L'accent est mis sur la séparation de phase de type associative et sur la "coacervation complexe" en particulier. "Coacervation complexe" est le terme employé pour décrire le mécanisme de séparation de phase de type liquide / liquide, résultant de la formation de complexes électrostatiques entre les biopolymères (*i.e.* les protéines et les polysaccharides). Ces complexes s'agrègent et forment des gouttelettes liquides appelées coacervats. Les coacervats soumis à la pesanteur flocculent et coalescent pour aboutir à la formation d'une phase inférieure concentrée, en équilibre avec une phase supérieure diluée. Différents modèles théoriques ont été développés depuis les années 1930 jusqu'à aujourd'hui. Une présentation générale de ces théories en est donnée dans le chapitre 1. Les coacervats - et les complexes de protéines / polysaccharides en général - trouvent des applications dans le domaine de purification des macromolécules. On s'en sert aussi en tant que nouveaux ingrédients, substitut de matière grasse, ou comme biomatériaux en médecine (prothèse, pansement). La plus importante application industrielle des coacervats reste la microencapsulation de principes actifs, où le coacervat liquide enrobe un composé sensible. Le système d'encapsulation le plus souvent employé est constitué du couple gélatine / gomme arabique. Pourtant, de nos jours, il existe une grande demande de la part du consommateur de remplacer la gélatine pour des raisons sanitaires et religieuses. C'est pourquoi les protéines du lactosérum (PL) ont été choisies pour cette étude. Les protéines du lactosérum (principalement composées

de la β -lactoglobuline (β -lg) - point isoélectrique = 5.2) sont des protéines laitières présentes dans le lait. Dans la première partie de ce travail, trois différents polysaccharides ont été utilisés en combinaison avec les PL: la gomme arabique (GA), le polysaccharide exocellulaire EPS B40 (EPS B40), et un carraghénane (CG). Ces polysaccharides sont tous chargés négativement mais leurs groupements chimiques diffèrent; la gomme arabique possède des groupements carboxyliques, l'EPS B40 des groupements phosphates, et le CG des groupements sulfates. Les conditions physico-chimiques nécessaires à la formation d'un complexe électrostatique ont été étudiées et comparées pour chaque système PL / polysaccharide (chapitres 2-4). Les chapitres suivants (chapitres 5-7) traitent exclusivement du système PL/GA. L'accent est mis sur la compréhension de la structure des coacervats PL/GA et de la phase concentrée qui reste jusqu'à présent peu décrite. Une application directe de ce système a été testée en encapsulant une huile par des coacervats de PL/GA (chapitre 8).

Dans le **chapitre 2**, il a été démontré qu'en mélangeant les PL et la GA dans une certaine gamme de pH, des complexes PL/GA se forment. En acidifiant lentement le mélange avec de la glucono- δ -lactone (GDL), plusieurs valeurs de pH de transition ont été déterminées. Des complexes solubles sont formés à pH_c , proche du point isoélectrique de la protéine β -lg. En poursuivant l'acidification, la séparation de phase macroscopique (coacervation complexe) est initiée pour un pH qualifié de $pH_{\delta 1}$. Finalement, à $pH_{\delta 2}$ ($< pH_{\delta 1}$), la coacervation est supprimée puisque la GA devient électriquement neutre. Il semble que la β -lg soit la protéine du mélange qui réagisse principalement avec la GA (comparée à l' α -lactalbumine). Dans la région de formation des complexes solubles (entre pH_c et $pH_{\delta 1}$), et à de faibles forces ioniques, les PL réagissent avec la GA et induisent une réduction des répulsions intramoléculaires de la molécule de GA qui devient alors plus compacte. Une augmentation de la force ionique du système conduit à un déplacement des pH de transition vers des valeurs plus acides. L'ensemble de ces résultats est concilié dans un diagramme d'état et comparé à une nouvelle théorie. Enfin, un diagramme de phase a été élaboré. Il présente l'influence de la concentration totale en biopolymères (C_p) sur la stabilité des complexes. Ce diagramme de phase a la même forme que celui qui est dérivé de la théorie de Voorn et Overbeek pour $C_p < 12\%$. Cependant, une région "métastable" apparaît pour de fortes C_p .

Le **chapitre 3** concerne l'étude du comportement des mélanges de PL et d'EPS B40 en fonction du pH, de la force ionique, et du rapport massique protéine: polysaccharide

(Pr:Ps). L'EPS B40 est un polysaccharide phosphaté qui est un épaississant naturel utilisé dans les produits laitiers. Pour ce système des complexes solubles sont également formés à pH_c , et la séparation de phase macroscopique (précipitation) apparaît à pH_0 . La force des interactions électrostatiques est très fortement dépendante du pH et de la force ionique. Pour de faibles forces ioniques, des expériences de diffusion de la lumière et de viscosité montrent une réduction du rayon hydrodynamique de la molécule d'EPS B40 et une augmentation de sa masse molaire. Ce phénomène de compaction de la molécule d'EPS B40 est provoqué par l'interaction des PL avec l'EPS B40. En variant le Pr:Ps, il apparaît que la séparation de phase est une conséquence de la neutralisation du complexe et que la stœchiométrie apparente des complexes dépend de l'ordre dans lequel les biopolymères sont mélangés. De plus, les complexes PL/EPS B40 se réarrangent au cours du temps pour former préférentiellement deux types d'entités distinctes: des complexes de PL/EPS B40 totalement neutres et des molécules d'EPS B40 seules (liaison de type coopérative).

Dans le **chapitre 4**, les interactions entre les PL et un polysaccharide sulfaté, un carraghénane non gélifiant (CG), ont été étudiées en fonction du pH, de la force ionique, de la température, et du rapport massique Pr:Ps. Les valeurs des pH de transition pH_c et pH_0 ont été déterminées en fonction de la force ionique. Lorsque le pH a une valeur inférieure au pH_0 , les complexes PL/CG précipitent. La présence de 45 mM de NaCl semble favorable à la formation de complexes grâce à l'écrantage par les ions des charges négatives résiduelles du CG. En présence de $CaCl_2$, des complexes de PL/CG peuvent être formés jusqu'à pH 8, valeur largement supérieure au point isoélectrique de la α -lg, soulignant la participation de ponts calciques. Les pH de transition pH_c et pH_0 ne sont que très peu affectés par la température. Il semble que la saturation en protéines des molécules de carraghénane apparaît à un rapport massique Pr:Ps = 30:1. A de plus faibles rapports (et faible force ionique), lorsque les PL et le CG sont directement mélangés à un pH acide donné, le pH du mélange augmente, les complexes PL/CG prenant au piège des protons afin d'écranter les charges négatives résiduelles du CG.

Ainsi, le contenu des chapitres 2 à 4 montre que la coacervation complexe (séparation de phase liquide/liquide) se produit uniquement dans le cas du système PL/GA. Les complexes PL/EPS B40 et PL/CG se présentent sous forme de précipités. La comparaison de ces résultats a permis de mettre en évidence que l'intensité des interactions PL/polysaccharide est en corrélation avec le potentiel zêta du

polysaccharide (CG > EPS B40 > GA) et avec la stœchiométrie des complexes. Les interactions entre les PL et le CG sont plus fortes qu'entre les PL et les autres polysaccharides (EPS B40 et GA). En effet, dans le cas des complexes PL/CG, le pH_c ($pH_c = 5.5$) est aussi plus élevé que les pH_c des complexes à base d'EPS B40 ($pH_c = 5.3$) et de la GA ($pH_c = 5.2$). Néanmoins, l'influence de paramètres comme la force ionique, le rapport massique Pr:Ps, et le pH est qualitativement similaire pour tous les systèmes étudiés. De manière générale, la compréhension de la formation des complexes protéines/polysaccharides permet d'ajuster et de mieux comprendre les propriétés des produits alimentaires contenant ces ingrédients.

La seconde partie de cette thèse s'attache à considérer plus particulièrement la phase concentrée du système PL/GA et ses caractéristiques. Dans le **chapitre 5**, l'influence des paramètres précédemment étudiés (pH, force ionique, Pr:Ps) sur la vitesse de séparation de phase est approfondie. La composition en eau et la concentration en biopolymères de la phase concentrée sont déterminées. La structure interne des coacervats est également analysée par diffusion de rayons X aux petits angles (SAXS). Pour un rapport Pr:Ps donné, un pH optimum (pH_{opt}) est déterminé, pH auquel la force d'interaction, la vitesse de séparation de phase, le volume de la phase concentrée et la concentration en biopolymères sont à leur maximum. Les mesures aux rayons X révèlent aussi qu'au pH_{opt} la phase concentrée est dense et structurée. Une distance de corrélation est mesurée à $Q = 0.7 \text{ nm}^{-1}$, et est attribuée au facteur de structure des PL. Plus l'interaction électrostatique est forte (proche du pH_{opt}), plus le pic de corrélation est prononcé. A des petites valeurs de Q, un pic apparaît dû à la présence de charges résiduelles de la GA. Une augmentation de la force électrostatique conduit à une réduction de l'intensité du pic due à une plus grande neutralisation des molécules de GA. Lorsque la force ionique du système augmente, la phase concentrée devient moins homogène, moins structurée, et moins concentrée en biopolymères. Ceci serait principalement dû à l'écrantage des interactions électrostatiques.

Dans le **chapitre 6**, les propriétés viscoélastiques de la phase concentrée obtenue pour un système de PL/GA sont examinées en fonction du pH. La phase concentrée est beaucoup plus visqueuse qu'élastique ($G'' > G'$) dans la gamme de pH comprise entre 3.0 et 4.5. Dans ce domaine et à des vitesses de cisaillement inférieures à 20 s^{-1} , la phase concentrée ne présente pas de propriétés thixotropes. En revanche, pour des vitesses de cisaillement supérieures à 30 s^{-1} et au pH_{opt} , la viscosité diminue fortement. Une hystérésis (thixotropie) est mesurée sous cisaillement près du pH_{opt} . Cette

hystérésis est due à la lente restructuration des coacervats, et après un temps de repos, la structure du coacervat peut être complètement récupérée. Il a aussi été mis en évidence que la forte viscosité du système pouvait principalement être attribuée à la forte interaction électrostatique et en moindre mesure à la présence de concentration élevée en biopolymères.

Dans le **chapitre 7**, la diffusion des PL et de la GA est mesurée dans la phase concentrée par résonance magnétique nucléaire (RMN), par récupération de fluorescence après photoblanchiment (RFAP), et par diffusion dynamique de la lumière en milieu turbide (aussi appelée “diffusing wave spectroscopy”, DWS). Indépendamment de la technique utilisée, les résultats montrent tous que la diffusion des PL et de la GA dans la phase concentrée est la plus lente près du pH_{opt} , à cause de la forte interaction électrostatique. En outre, les résultats de RFAP indiquent que les PL diffusent 10 fois plus vite que la GA, ce qui prouve que les PL et que la GA se déplacent de façon indépendante dans la phase concentrée. Enfin, les mesures de DWS révèlent que la phase concentrée se réarrange au cours du temps (durant des jours, parfois des semaines), conduisant à une perte de sa turbidité et à une diminution du coefficient de diffusion des biopolymères.

Le dernier chapitre de cette thèse (**chapitre 8**) présente une application directe du système PL/GA étudié dans les chapitres 2, 5, 6, 7. Les coacervats de PL/GA sont utilisés pour encapsuler des arômes et des huiles. Une couche régulière de coacervats enrobe des gouttelettes d’huile, ce qui forme des capsules qui peuvent contenir jusqu’à 80% d’huile. Les émulsions faites de gouttelettes d’huile encapsulées par une couche de coacervats sont très instables et la vitesse de crémage est maximale au pH_{opt} . Autour du pH_{opt} , le potentiel zêta des capsules est proche de zéro du fait de la présence de coacervats neutres à l’interface huile / eau. Enfin, un arôme de citron est encapsulé par coacervation complexe puis incorporé dans du fromage (Gouda) au cours de sa fabrication. La libération de l’arôme est détectée par un spectromètre de masse (MS nose). Les résultats obtenus dans le chapitre 8 sont en accord avec les précédents résultats trouvés dans les chapitres 2, 5, 6, 7. Cela indique que l’efficacité des coacervats de PL/GA comme matériel d’encapsulation peut être anticipée à partir des propriétés des coacervats en solution. Au pH_{opt} la phase concentrée est la plus visqueuse et la plus homogène, aussi c’est à ce pH que les meilleures capsules sont obtenues. Ces résultats montrent comment l’acquisition de données fondamentales sur les interactions entre protéines et polysaccharides et sur la structure des coacervats

Résumé

permet de prédire les caractéristiques des capsules obtenues par coacervation complexe.

ACKNOWLEDGEMENTS

In four exciting years working on complex coacervation at NIZO food research, I learned a lot in the field of science and I owe it to a lot of people. This work couldn't be achieved without the help and support of a great amount of people to whom I wish to express my sincere gratitude:

- Kees, my promotor, for giving me the opportunity to do a challenging PhD research, for his guidance, his perpetual enthusiasm and his trust during these years.
- All my colleagues of the Product Technology department, for helping me out when I had questions and doubts, but essentially for the good time I had during my PhD. In particular, I would like to thank my (ex-)roommates Charles, Astrid and Joanke with whom I had a lot of fun and who helped me an innumerable amount of times for translation and advices; the PhD group also called AAFJE (Astrid, Arno, Fanny, Joanke) and who became at the end JFK (Joanke, Fanny, Kees). It was very fruitful to have regular meetings among each other to discuss science and day-to-day problems; the "club" for the presents I found on my desk to celebrate special occasions. A lot of people have helped me: thanks to Bertus and Wim for preparing the Gouda cheese; Els for the light scattering experiments and FRAP; Fred for the advices on carrageenan and labeling (among many other things); Gerhard for introducing me to the world of customers; Hans for the SAXS experiments in Grenoble and for your critical reading of my manuscripts (it is/was very useful); Harry for the NMR experiments, your comments on my manuscripts and your everlasting availability; Igor pour nos petites conversations en français, pour tes bons conseils et pour l'intérêt que tu as montré à mes coacervats; Esther, Marja, Jan and Marijke for the great amount of times that you have saved me from tricky situations in the lab, or in front of my computer (Jan), and for the nice horse riding tours (Marijke); Cees for your advices on analytical issues; Jeroen for helping me out with the fluidized bed coating and spray chilling; Marcel for the zeta potential measurements and your knowledge on encapsulation; Marjet, for the collaboration on encapsulation projects and the good memories from our trip in Germany; Martin

for dealing with my structured plans and the collaboration in several projects; Nel as the account manager of my PhD project; René for your advices on cross-linking; Roelie and Jan van Riel for struggling with the HPLC and the SEC MALLS for the good sake of my experiments; Roland for increasing drastically my knowledge in rheology and DWS; Saskia for your patience in explaining how to handle the Carri-Med and for carrying out the last minute experiment; Heidi for helping me with the administrative documents.

- My other NIZO colleagues, and especially the southern ones: José Escher and Gert van den Hoven for all the hours spent in the traffic jams between NIZO and Wijchen. Carpooling with you was very nice and entertaining! The team of FNI who helped me with MS Nose and flavors, special thanks to Mauritz and Rita. Thanks to Cornelia for the nice front page of this thesis and to my colleagues from the library and the magazijn!
- I would like to acknowledge Friesland Coberco Dairy Foods (FCDF) for the financing of the last two years of my PhD project. Special thanks to Gerard Robijn, Hans Nieuwenhuijse, Christel Timmer, and Miranda Huisman for showing so much interest in my work and for our regular meetings.
- The Softlink team from Wageningen University: Renko de Vries, Martien Cohen-Stuart, Erik van de Linden, and Luben Arnaudov. We met almost every month for interesting scientific discussions.
- My ex-trainees: Pascale Louis-Louis, Agnès Gaven, Annemiek Pul-Hootsen, Vincent Gervaise, and Frédérique Sanzey who worked hard during their training period and who contributed to this thesis. I consider myself very lucky to have worked with so motivated and friendly people as you! This PhD would not have been the same without you. Thanks!
- My paranimfen: Erika Silletti and Joanke Graveland-Bikker: thanks for being by my side for the final test.
- The French team: Christian Sanchez, Christophe Schmitt, and Denis Renard. Merci beaucoup pour votre aide au cours de ces 4 dernières années. Au delà même de nos conversations scientifiques, j'ai beaucoup apprécié votre gentillesse. Christian, Denis, je garde aussi d'excellents souvenirs de nos 24 h à Grenoble! Christophe, merci de ton aide pour mon résumé.
- Remco Tuinier, everything started with you! Thanks for the nice training period I had at NIZO. I am very grateful for your help, trust, advices, and mainly friendship! Peter

Schrooyen, thanks for being my co-promotor during the first year of my PhD and for introducing me to the exciting world of encapsulation, for your trust and support. Unfortunately you had to leave, but it turned out fine for both of us at the end!

- The AIO's of Wageningen University for the fun AIO trip in England; Ab van der Linde from Wageningen University for his help with the zetasizer; Paul Dubin and Christophe Tribet for the interesting and friendly scientific discussions; Thierry Kravtchenko and Colloides Naturels International for providing me with the gum arabic; Prof. Dr. Jorrit Mellema for his advices on rheology.
- The foreign guests who spent some time at NIZO and among them my dear friend Patricia!! Thanks for the good time we spent together!
- My friends who always supported me even if they didn't (and probably still don't) understand what I was doing during these last 4 years! Merci H el ene d'avoir relu mon r esum e.
- My family, especially my parents and Thomas & Sophie. Merci de votre support perp etuel et de votre confiance, m eme si vous ne comprenez pas toujours ce sur quoi je travaille!
- And most of all my fianc e Rui Paulo. You were by my side during all these years and I would like to thank you for the interest you have always shown in my PhD, for the patience with which you listened to my stories, and above all, for your love. I am looking forward to our happy future together! *Aimer savoir est humain, savoir aimer est divin.* [Joseph Roux].

Fanny

CURRICULUM VITAE

Fanny Weinbreck was born on the 22nd February 1977 in Saint-Quentin, France. She finished her high school in June 1994, and in September 1994 she started her 5-year Engineering study at the Université de Technologie de Compiègne (U. T. C.) in France. During her studies, she carried out two training periods. The first one took place in the department Product Technology at NIZO food research (Ede, The Netherlands) from September 1997 until February 1998. Then, from September 1998 until February 1999 she also had the opportunity to follow the Erasmus exchange program at the Instituto Superior Técnico (I. S. T.) in Lisbon (Portugal). And finally, she carried out her second training period at the Department of Product Principles at Unilever Research Vlaardingen (The Netherlands) from March until August 1999. In October 1999 she obtained her degree in Biological Engineering. In March 2000 she started as a junior scientist at NIZO food research for a period of 4 years, at the end of which she could defend her PhD thesis. The subject of the research regarded the understanding of the structure and dynamics of complex coacervates. The last two years of the project was financed by Friesland Coberco Dairy Foods (FCDF). The PhD project was supervised by Prof. C. G. de Kruif, head of the Product Technology department at NIZO food research and part-time professor at the department of Physical and Colloid Chemistry of the University of Utrecht.

LIST OF PUBLICATIONS

This thesis is based on the following publications:

Weinbreck, F.; de Vries, R.; Schrooyen, P.; de Kruif, C. G. Complex coacervation of whey proteins and gum arabic. *Biomacromolecules* **2003**, *4* (2), 293-303. (Chapter 2)

Weinbreck, F.; Nieuwenhuijse, H.; Robijn, G. W.; de Kruif, C. G. Complex formation of whey proteins – exocellular polysaccharide EPS B40. *Langmuir* **2003**, *19*, 9404-9410. (Chapter 3)

Weinbreck, F.; Nieuwenhuijse, H.; Robijn, G. W.; de Kruif, C. G. Complexation of whey proteins with carrageenan. Accepted for publication in *Journal of Agriculture and Food Chemistry*. (Chapter 4)

Weinbreck, F.; Tromp, R. H.; de Kruif, C. G. Composition and structure of whey protein / gum arabic coacervates. Considered for publication in *Biomacromolecules*. (Chapter 5)

Weinbreck, F.; Wientjes, R. H. W.; Nieuwenhuijse, H.; Robijn, G. W.; de Kruif, C. G. Rheological properties of whey protein / gum arabic coacervates. *Submitted for publication*. (Chapter 6)

Weinbreck, F.; Rollema, H. S.; Tromp, R. H.; de Kruif, C. G. Diffusivity of whey protein and gum arabic in their coacervates. Considered for publication in *Langmuir*. (Chapter 7)

Weinbreck, F.; Minor, M.; de Kruif, C. G. Microencapsulation using whey protein / gum arabic coacervates. *Submitted for publication*. (Chapter 8)

Other publications:

van de Velde, F.; Weinbreck, F.; Edelman, M. W.; Tromp, R. H. Visualisation of biopolymer mixtures using Confocal Scanning Laser Microscopy (CSLM) and covalent labelling techniques. *Colloids and Surfaces B: Biointerfaces* **2003**, 31 (1-4), 159-168.

de Vries, R.; Weinbreck, F.; de Kruif, C. G. Theory of polyelectrolyte adsorption on heterogeneously charged surfaces applied to soluble protein-polyelectrolyte complexes. *Journal of Chemical Physics* **2003**, 118, 4649-4659.

Weinbreck, F.; de Kruif, C. G. Complex coacervation of globular proteins and gum arabic. In *Food Colloids Biopolymers and Materials*; Dickinson, E.; van Vliet, T., Eds.; Royal Society of Chemistry: Cambridge, U.K., 2003; pp. 337-344.

Weinbreck, F.; de Kruif, C. G.; Schrooyen, P. Complex coacervates containing whey proteins. Patent WO 03/106014 A1 (24/12/2003).

Weinbreck, F.; de Kruif, C. G. Nieuwe generatie encapsulaten. In *Voedingsmiddelentechnologie*, No 21, pp 14-16, 10 October 2003.

Minor, M.; Weinbreck, F.; de Kruif, C. G. Innovations in encapsulation of food ingredients. In *Innovations in Food Technology*, No. 14, pp 76-77, 1, 2002.